Functionalization of carbonaceous materials for photovoltaic devices

By

Messai Adenew Mamo, MSc.

A dissertation submitted in fulfillment of the requirements for the degree of

Doctor of Philosophy in the Faculty of Science

School of Chemistry

University of the Witwatersrand

Private Bag X03

WITS

2050

Supervisors: Professor Neil J. Coville

Professor Willem A. L. van Otterlo

Declaration

I declare that "Functionalization of carbonaceous materials for photovoltaic devices" is my own, unaided work submitted for the degree of Doctor of Philosophy at the University of Witwatersrand, Johannesburg. It has not been submitted for any degree or examination in any other University, and all sources I have used or quoted have been indicated and acknowledged by means of complete references.

Name: Messai Adenew Mamo (Mr.) Date……..2010

Signature:.....

Acknowledgements

First and foremost I would like to give special thanks to my supervisors, Professor Neil J. Coville and Professor Willem A. L. van Otterlo, for their outstanding help and guidance during the course of this research project.

I would also like to thank Miss Zikhona N. Tetana, Mr. Roy P. Forbes, Mr. Robert Black, Miss Ellen Kwenda, Miss Manoko Maubane, whom I co-supervised in their research projects, Dr. Sabelo D. Mhlanga, and the rest of the CATOMAT group for providing a great working environment.

I also thank Professor Michael J. Witcomb, Mr. Rudolph M. Erasmus, Mr. Richard Mampa, Mr. T. A. van der Merwe, and Dr. Manuel A. Fernandes for their assistance with TEM, Raman spectroscopy, nuclear magnetic resonance spectroscopy, mass spectroscopy and X-ray diffraction analysis, respectively.

I would also like to acknowledge the assistance of the following people during my research visit at Instituto de Química, Universidade Estadual de Campinas, SP, Brazil: Professor Ana Flávia for her kind advice and discussions, and members of LNES Lab João, Agnaldo, César, Lucas especially Flávio, Giovanni and Jilian who helped me a lot as well as others occupants of the laboratory.

I also thank Mr. Basil Chassoulas, Mr. Steve Gannon, Mr. Barry Fairbrother, Mr. David Moloto and Mr. Elias Valoyi, for their technical support. I also thank the School of Chemistry, University of the Witwatersrand, for giving me the opportunity to conduct this research on their premises.

The financial support for this work by the DST/NRF Centre of Excellence in Strong Materials for a scholarship and India-Brazil-South Africa (IBSA), South Africa and Brazil for a research visit to Brazil, are gratefully acknowledged.

List of publications

The following publications originated from different parts the work presented in this thesis:

M. A. Mamo, F. S. Freitas, J. N. de Freitas, W. A. L. van Otterlo, A. F. Nogueira, N. J. Coville, "Poly(3-hexylthiophene) covalently linked to fullerene for use in hybrid solar cells" *submitted to New J. Chem.*

M. A. Mamo, F. S. Freitas, J. N. de Freitas, W. A. L. van Otterlo, A. F. Nogueira, N. J. Coville, "Application of 3-hexylthiophene functionalized CNTs in photovoltaic devices" *to be submitted*

M. A. Mamo, R. P. Forbes, N. J. Coville, W. A. L. van Otterlo, "Ring-opening metathesis co-polymerization of a C_{60}-cyclopentadiene cycloadduct and *N*-(cycloheptyl)-*endo*-norbornene-5,6-dicarboximide" *to be submitted*

M. A. Mamo, N. J. Coville, W. A. L. van Otterlo, "Ring-opening Metathesis Co-polymerization of a C60-cyclopentadiene Cycloadduct and Norbornene with the Grubbs Second-generation Catalyst" *Fullerenes, Nanotubes, and Carbon Nanostructures*, **2007,** 15, 341.

Research visit

From November 2008 to April 2009 research visit at Instituto de Química, Universidade Estadual de Campinas, SP, Brazil.

Presentation at conferences and seminars

Date	Name and place	Type of presentation
July 2007	SACI, Inorganic, Cape town	Poster
August 2007	CATOMAT seminar, Room C509 Humphrey Raikes Building, Wits University.	Oral
February 2008	DST/NRF Centre of Excellence in Strong Materials' Seminar, Room C6 Humphrey Raikes Building, Wits University.	Oral
July 2008	CATOMAT seminar, Room C509 Humphrey Raikes Building, Wits University.	Oral
January 2009	Instituto de Química, Universidade Estadual de Campinas, seminar room, SP, Brazil	Oral
March 2009	Instituto de Química, Universidade Estadual de Campinas, seminar room, SP, Brazil	Oral
May 2009	CATOMAT seminar, Room C509 Humphrey Raikes Building, Wits University.	Oral
June 2009	DST/NRF Centre of Excellence in Strong Materials' Seminar, Room C6 Humphrey Raikes Building, Wits University.	Oral
September 2009	IBSA Meeting on Nanotechnology, Curitiba, Brazil.	Oral
October 2009	SACI Young Chemists Symposium –Gauteng Region, Potchefstroom Campus of the North-west University, Ou Senaatsaal (Building F4) Building, Wits University	Oral
October 2009	School of Chemistry departmental seminar, PhD thesis - final, Room C6 Humphrey Raikes Building, Wits University.	Oral

Note: CATOMAT = catalysis-organometallics-materials research group
IBSA India, Brazil and South Africa

Abstract

A C_{60}-cyclopentadiene cycloadduct was readily synthesized, by a Diels-Alder reaction between C_{60} and freshly cracked cyclopentadiene. The functionalized C_{60} and norbornene were then pre-mixed in varying molar ratios and co-polymerized using a ROMP approach with catalytic amounts of Grubbs second generation catalyst. A series of C_{60}-containing polymers were also synthesized by the co-polymerization of a C_{60}-cyclopentadiene cycloadduct and *N*-(cycloheptyl)-*exo*-norbornene-5,6-dicarboximide in varying ratios using similar procedures. The polymerization was facilitated by use of a catalytic amount of Grubbs second generation catalyst. The C_{60} co-polymers formed were investigated by FT-IR, UV-visible, ^{1}H NMR and ^{13}C NMR spectroscopy, mass spectrometry, differential scanning calorimetry (DSC) and thermal gravimetric analysis (TGA).

Functionalization of C_{60} was achieved by using a 1,3-dipolar addition of azomethine ylides to C_{60} that resulted in fulleropyrrolidines containing 2- and 3-thiophenecarboxaldehyde. Finally, the two C_{60} derivatives, together with different ratios of either thiophene or 3-hexylthiophene, were oxidatively copolymerized using $FeCl_3$ as catalyst.

Either nitrogen-doped or undoped carbon nanotubes were synthesized from ferrocene, pyridine and toluene and decomposition of acetylene over a catalyst respectively, were functionalized using azomethine ylides from the thermal condensation of *N*-methylglycine and 5-norbornene-2-carboxaldehyde. The polymerization from the side walls of the carbon nanotubes using bicyclo[2.2.1]hept-2-ene as a monomer was achieved using the Grubbs' second generation catalyst. The synthesised CNTs and polymer-attached carbon nanotubes were subsequently characterised.

The attachment of different organic functional groups to the carbon nanotubes from the thermal condensation of *N*-methylglycine and 2-thiophenecarboxaldehyde was achieved. The functionalized carbon nanotubes, and either thiophene or 3-hexylthiophene were used in copolymerization reactions by oxidative polymerization, using $FeCl_3$ as catalyst. The copolymers containing the nanotubes, were found to be more regioregular than pure poly(3-hexylthiophene). The synthesised CNTs and polymer-attached carbon nanotubes were then characterised.

The thiophene-based C_{60}-copolymers and thiophene polymer-attached CNTs, with and without TiO_2, were deposited on the surface of TiO_2 paste with, and without, dye impregnation. A sandwich-type cell made from a TiO_2 thin film electrode with, and without, dye impregnation, ionic liquid electrolytes and a Pt-coated fluoride tin oxide (FTO) counter electrode was prepared. Both organic and dye sensitized solar cells (DSSC) were subsequently assembled. The efficiency, current densities, open circuit voltages and fill factors were found to decrease as the concentration of C_{60} derivative in the copolymer decreased. Furthermore, pre-mixing the copolymers with TiO_2 nanoparticles improved the overall performance of the photo cell. In addition, the polymer-attached N-doped CNTs performed better in the photo cells than polymer-attached undoped CNTs.

Table of contents

Title **Page Number**

Acknowledgements ..... **iii**

List of Figures ..... **xv**

Introduction **1**

1.1 Background and rationale 1

1.2 Objectives 4

1.3 Thesis outline 5

1.4 References 7

Literature review **10**

2.0 General 10

2.1 Carbon nanotubes, fullerene (C_{60}) and other carbonaceous materials 10

2.2 Chemistry of fullerene (C_{60}) 11

2.2.1 General introduction to fullerenes (C_{60}) 11

2.2.2 Reactions of fullerene (C_{60}) 14

2.2.3 [2+2] Cycloadditions 14

2.2.4 [3+2] Cycloadditions 15

2.2.5 [4+2] Cycloadditions 16

2.2.6 Other types of reactions on Fullerenes (C_{60}) 17

2.2.7 Application in polymers 19

2.3 Chemistry of carbon nanotubes (CNTs) 21

2.3.1 General introduction 21

2.3.2 Covalent functionalization of carbon nanotubes 21

2.3.3 Sidewall halogenation of CNTs 21

2.3.4 Hydrogenation 23

2.3.5 Cycloadditions 23

2.3.6 Amidation/Esterification Reactions 26

2.3.7 Grafting of Polymers 27
2.3.8 Other reactions 29
2.3.9 Mechanochemical functionalization 30
2.4 The application of fullerene (C_{60}) and carbon nanotubes in solar cells 30
2.4.1 General introduction 30
2.4.2 C_{60} fullerene in photo cells 35
2.4.3 Carbon nanotubes in solar cells 40
2.5 References 42
Chapter 3.. 57
Ring-opening co-polymerization of a C_{60}-cyclopentadiene cycloadduct and norbornene with the Grubbs second generation catalyst* 57
3.1 Introduction 57
3.2 Experimental 59
3.2.1 General procedure 59
3.2.2 Synthesis of the C_{60}-cyclopentadiene cycloadduct 59
3.2.3 Polymerization of Polynorbornene 3.4 59
3.2.4 Co-polymerization of 3.3 and norbornene 3.4 60
3.3 Results and Discussion 60
3.3.1 Synthesis of copolymers 60
3.3.2 Spectroscopic Studies of synthesized materials 62
3.3.2.1 FTIR studies of synthesized materials 62
3.3.2.2 UV-visible absorption spectroscopic studies of synthesized materials 63
3.3.3 Thermal Degradation Studies of synthesized materials 65
3.3.3.1 Differential scanning calorimetry (DSC) 65
3.3.3.2 Thermogravimetric analysis (TGA) 67
3.5 References 69

Chapter 4.. 71

Ring-opening metathesis co-polymerization of a C_{60}-cyclopentadiene cycloadduct and *N*-(cycloheptyl)-endo-norbornene-5,6-dicarboximide 71

4.1 Introduction 71

4.2 Experimental 72

4.2.1 General procedures 72

4.2.2 Synthesis of C_{60}-cyclopentadiene cycloadduct 4.7 72

4.2.3 Synthesis of *N*-(cycloheptyl)-endo-norbornene-5,6-dicarboximide 4.4 72

4.2.4 Polymerization of *N*-(cycloheptyl)-endo-norbornene-5,6-dicarboximide 4.4 to afford 4.9A 73

4.2.5 Co-polymerization of C_{60}-cyclopentadiene 4.7 and *N*-(cycloheptyl)-endo-norbornene-5,6-dicarboximide 4.4 73

4.3 Results and Discussion 74

4.3.1 Synthesis of 4.4 and copolymers 74

4.3.2 Spectroscopic Studies of the synthesized materials 77

4.3.2.1 FTIR studies of synthesized materials 77

4.3.2.2 UV-visible absorption spectroscopic studies of synthesized materials 78

4.3.3 Thermal Degradation Studies 80

4.3.3.1 Differential scanning calorimetry (DSC) 80

4.3.3.2 Thermogravimetric analysis (TGA) 82

4.4 Conclusion 83

4.5 References 84

Chapter 5.. 87

Polymerization of a C_{60} derivative with thiophene in the presence of $FeCl_3$ 87

5.1 Introduction 87

5.2 Experimental 89

5.2.1 General procedures 89

5.2.2 Functionalization of C_{60} 89

5.2.3 Polymerization reactions 90
5.2.3.1 Polymerization reactions to synthesize polythiophene 5.4 and poly(3-hexylthiophene) 5.5 [] 90
5.2.3.2 Copolymerization reactions 91
5.2.3.3 Copolymerization reactions to form polymers 5.6 and 5.7 91
5.2.3.4 Copolymerization reactions to form polymers 5.8a, 5.8b and 5.8c 91
5.2.3.5 Copolymerization reaction to form polymer 5.9 92
5.3 Results and discussion 92
5.3.1 Synthesis of 5.2, 5.3 and copolymers 92
5.3.2 Polymerization reactions of the synthesised materials 93
5.3.3 Characterization of the synthesized copolymer 95
5.3.3.1 ^{1}H NMR spectroscopy of the synthesized copolymers 95
5.3.3.2 FTIR spectroscopy of the synthesized copolymers 97
5.3.3.3 UV-visible spectroscopy of the synthesized copolymers 102
5.3.3.4 Thermogravimetric analysis (TGA) 103
5.4 Conclusion 106
5.5 References 107
Chapter 6.. 112
Functionalization of nitrogen doped and undoped carbon nanotubes using ring opening metathesis polymerization with norbornene 112
6.1 Introduction 112
6.2 Experimental 115
6.2.1 General procedures 115
6.2.2 Synthesis of carbon nanotubes 115
6.2.2.1 Catalyst preparation for CNT synthesis 115
6.2.2.2 Carbon nanotube synthesis 116
6.2.2.3 Nitrogen doped multiwall carbon nanotubes 116

6.2.3 Purification of carbon nanotubes 117
6.2.4 Functionalisation and polymerization of carbon nanotubes 117
6.2.4.1 Functionalisation of carbon nanotubes 117
6.2.4.2 Ring opening metathesis and functionalization of CNTs with norbornene 117
6.3 Results and discussion 118
6.3.1 Synthesis of CNTs 118
6.3.2 Functionalization reactions of CNTs 118
6.3.3 Polymerization reactions of functionalized CNTs 119
6.3.4 Characterization of the synthesised products 120
6.3.4.1 Raman Spectroscopy of the synthesised products 120
6.3.4.2 Transmission electron microscopy (TEM) 122
6.3.4.3 Spectroscopic studies on the copolymers synthesized 124
6.3.5.1 Thermogravimetric Analysis (TGA) of the synthesized materials 129
6.3.5.2 Differential scanning calorimetry studies (DSC) of synthesized copolymers 131
6.4 Conclusion 132
6.5 References 133
Chapter 7.. 138
Synthesis of polythiophene covalently liked to nitrogen doped and undoped carbon nanotubes.. 138
7.1 Introduction 138
7.2 Experimental 140
7.2.1 General procedures 140
7.2.2 Synthesis and purification of carbon nanotubes 140
7.2.3 Functionalization of 7.1 and 7.3 [18] 140
7.2.4 Polymerization reactions 140
7.2.4.1 Preparation of copolymers 7.5 and 7.6 140
7.2.4.2 Preparation of copolymers 7.7 and 7.8 141

7.2.4.3 Preparation of 7.11 141
7.2.4.4 Preparation of 7.9 and 7.10 [] 141
7.3 Results and discussion 142
7.3.1 Functionalization reactions of CNTs 142
7.3.2 Polymerization reactions 143
7.3.3 Characterization of functionalized CNTs and copolymers 143
7.3.3.1 Raman Spectroscopy of functionalized CNTs 143
7.3.3.2 Transmission Electron Microscopy (TEM) 145
7.3.3.2.1 Poly(3-hexylthiophene)/CNT composite 146
7.3.3.2.2 Polythiophene/CNT composite 147
7.3.3.3 ^{1}H NMR spectroscopic studies of the synthesized materials 149
7.3.3.4 FT-IR studies of the synthesized materials 151
7.3.3.5 UV-visible and photoluminescence spectra of the synthesized materials 154
7.3.4.1 Thermogravimentric analysis (TGA) 157
7.3.4.2 Differential scanning calorimetry studies 159
7.4 Conclusions 160
7.5 References 162
Chapter 8.. 165
Application of 3-hexylthiophene functionalized C_{60} and carbon nanotubes in solar cells. 165
8.1 Introduction 165
8.2 Experimental 168
8.2.1 Assembly of the DSSC 168
8.2.2 Assembly of the organic solar cell 168
8.3 Results and discussion 169
8.3.2 Application of copolymers in dye-sensitized solar cells (DSSCs) 171
8.3.2.1 Current-Voltage Characteristics 171
8.3.2.1.1 C_{60}-copolymers 5.3a, 5.3b and 5.3c in DSSC 171

8.3.2.1.2 Solar cell assembled with functionalized carbon nanotubes 180
8.3.3 Organic solar cells 184
8.4 Conclusions 187
8.5 References 188
Chapter 9.... 192
9.1 Conclusions and future work 192
9.1.1 Conclusions 192
9.1.2 Future work and recommendations 194
9.1.2.1 Functionalization of carbonaceous materials 194
9.1.2.2 Photovoltaic Device applications 195
9.2 Reference 197

List of Figures

Page

1. Figure **2.1** Diagrams of (a) metallic (5,5) SWNT, (b) pyramidalization angle (θ_P), and (c) the π-orbital misalignment angles (ϕ) along the C1-C4 in the (5,5) SWNT and its capping fullerene, C_{60}. ……..……..…...13
2. Figure **2.2** Polymers involving the C_{60} moiety. (Ia), Pendant on-chain (Ib) pendant on-surface, (II) in-chain, (III)dendritic, (IV) cross-link and (**V**) end-chain …….……...20
3. Figure **2.3** Photoinduced generation of reactive nitrenes in the presence of nanotubes…….…...……24
4. Figure **2.4** 1,3-dipolar cycloaddition of azomethine ylides n the surface of CNTs. ……..25
5. Figure **2.5** Reaction pathway for obtaining water-soluble ammonium-modified nanotubes…….…. …….…...…25
6. Figure **2.6** 1,3-Dipolar cycloaddition of nitrile imines to nanotubes. …….……..26
7. Figure **2.7** Derivatization reactions of acid-cut nanotubes through the defect sites of the graphitic surface. ...…….……...…27
8. Figure **2.8** Direct thermal mixing of nanotubes and long chain amines. …….……27
9. Figure **2.9** Operation principle of a dye sensitized solar cell. …….……..…32
10. Figure **2.10** Current-voltage (I-V) curves of a solar cell……..……..33
11. Figure **2.11** Schematic representation of interfacial electron transfer following light absorption for *cis*-[Ru(dcbH$_2$)$_2$LL'] with some ancillary igands…….……..34
12. Figure **2.12** Representation of a donor–acceptor heterojunction. ……..…36
13. Figure **2.13** Theoretical principle of a donor–acceptor heterojunction…….……37
14. Figure **2.14** Molecular structures of some semiconducting conjugated polymers used in fullerene-based solar cells. ……..……..38
15. Figure **2.15** Schematic representation of a bulk-heterojunction solar cell with the ITO/PEDOT-SS/P3HT:[60]PCBM/LiF/Al device. ……..…..…….…….....…39
16. Figure **3.1** FT-IR spectra of the samples in KBr pellet form. (A) Polynorbornene **3.4**, Co-polymers **3.6B-E**: (**B**) mole ratio 50:1, (**C**) mole ratio 100:1, (**D**) mole ratio 500:1, (**E**) mole ratio 1000:1, (**F**) C_{60}-cyclopentadiene cycloadduct **3.3**, (**G**) C_{60} **3.1…**……..…63
17. Figure **3.2** UV-visible spectra in toluene of co-polymers **3.6B-E** and polynorbornene **3.6A**: (**A**) Polynorbornene, Copolymers **3.6B-E**: (**B**) 50:1 mole ratio, (**C**) 100:1 mole ratio, (**D**)

500:1 mole ratio, (**E**) 1000:1 mole ratio, (**F**) C_{60} **3.1**, (**G**) C_{60}-Cyclopentadiene cycloadduct **3.3**……...65

18. Figure **3.3** Differential Scanning Calorimetry Tg analyses (scan rate 5^{o}C/min): Co-polymers **3.3A-E:** (**A**) Polynorbornene, (**B**) 50:1 mole ratio, (**C**) 100:1 mole ratio, (**D**) 500:1 mole ratio, (**E**) 1000:1 mole ratio……..……..…….....67
19. Figure **3.4** TGA curves of the polymers (rate 10^{o}C/ min) under a nitrogen atmosphere: (**A**) Polynorbornene, Co-polymers **3.6B-E:** (**B**) 50:1 mole ratio, (**C**) 100:1 mole ratio, (**D**) 500:1 mole ratio, (**E**) 1000:1 mole ratio…….……..……...….69
20. Figure **4.1** FT-IR spectra of the samples in KBr pellet form (mole ratio **4.4**:**4.7**): **4.9A** (1:0), **4.9B** (1000:1), **4.9C** (700:1), **4.9D** (500:1), **4.9E** (300:1), **4.9F** (100:1), **4.9G** (50:1), **4.9H** C_{60}-cyclopentadiene cycloadduct **4.7**, **4.9I** C_{60} **4.5**..…….…….…78
21. Figure **4.2** UV-visible spectra of co-polymers **4.9A-I** (in toluene, mole ratio **4.4**:**4.7**): **4.9A** (1:0), **4.9B** (1000:1), **4.9C** (700:1), **4.9D** (500:1), **4.9E** (300:1), **4.9F** (100:1), **4.9G** (50:1), **4.9H** C_{60}-cyclopentadiene cycloadduct **4.7**, **4.9I** C_{60} **4.5**…….…….....79
22. Figure **4.3** Differential scanning calorimetry T_g analyses (scan rate 5 ^{o}C/min) under nitrogen atmosphere: Co-polymers **4.9A-G** (mole ratio **4.4**:**4.7**): **4.9A** (1:0), **4.9B** (1000:1), **4.9C** (700:1), **4.9D** (500:1), **4.9E** (300:1), **4.9F** (100:1), **4.9G** (50:1)……..…….....…..…82
23. Figure **4.4** TGA curves of the polymers (rate 10 ^{o}C/ min) under a nitrogen atmosphere (mole ratio **4.4**:**4.7**): **4.9A** (1:0), **4.9B** (1000:1), **4.9C** (700:1), **4.9D** (500:1), **4.9E** (300:1), **4.9F** (100:1), **4.9G** (50:1)……...……...…..84
24. Figure **5.1** Different types of traid regioisomers of poly(3-hexylthiophene).....95
25. Figure **5.2** ^{1}H NMR spectra of the monomer, polymer and copolymers of the synthesised polymers ($CDCl_3$, r.t). 97
26. Figure **5.3a**. FT-IR spectra of the polythiophene derivatives in KBr pellet. ……..…...98
27. Figure **5.3b**. FT-IR spectra of the polyhexyl derivatives in KBr pellet. …….....……...99
28. Figure **5.4** UV-visible absorption spectrum of poly(3-hexylthiophene) **5.5**, compounds **5.2** and **5.3,** and copolymers **5.8a, 5.8b, 5.8c** and **5.9** in THF 104
29. Figure **5.5a**. TGA thermograms of copolymers **5.6**, **5.7** and polythiophene (**5.4**).....…….105
30. Figure **5.5b.** TGA thermogram of copolymers **5.8a**, **5.8b**, **5.8c** and poly(3-hexylthiophene) (**5.5**)……...106
31. Figure **6.1** Raman spectra of A) unfunctionalized N-CNTs **6.3**; B) functionalized N-CNTs **6.4**; C) unfunctionalized CNTs **6.1**; D) functionalized CNTs **6.2**.....122
32. Figure **6.2** TEM image of (1) undoped CNT **6.1**; (3) N-CNTs **6.3**…...……..…123

33. Figure **6.3** TEM images of A) polymer attached CNTs **6.5**; and B) polymer attached N-CNTs **6.6**…..…….……..……..….124
34. Figure **6.4** Schematic diagram of the *cis* and *trans* olefinic and allylic protons.....125
35. Figure **6.5** ^{1}H NMR spectra (in $CDCl_3$) of the monomer norbornene; polynorbornene; copolymer from undoped CNT-polynorbornene **6.5** and copolymer from N-doped-polynorbornene copolymers **6.6**……..….……..…….126
36. Figure **6.6a** FT-IR of Pristine undoped CNTs **6.1**; functionalized undoped CNTs **6.2**; pristine N-CNTs **6.3**; functionalized N-CNTs **6.4**…….…….….…….128
37. Figure **6.6b** FT-IR of polynorbornene-attached CNT **6.5**; polynorbornene-attached N-CNT **6.6**; polynorbornene and norbornene monomer.....129
38. Figure **6.7a** TGA scan of **1**) pristine CNT **6.1**; **2**) pristine N-CNT **6.2**; **3**) functionalized CNT **6.3**; **4**) functionalized N-CNT **6.4**.....130
39. Figure **6.7b** TGA scan of polynorbornene-attached CNT **6.5**; polynorbornene-attached N-CNT **6.6**; and polynorbornene.....131
40. Figure **6.8** DSC scan of polynorbornene-attached CNT **6.5**; polynorbornene-attached N-CNT **6.6**; and polynorbornene run under N_2 at 5 ^{o}C/min heating rate.....132
41. Figure **7.1** A) Poly(3-hexylthiophene) **7.9**; B) undoped CNT-poly(3-hexylthiophene) **7.5**; C) N-doped CNT-poly(3-hexylthiophene) **7.6**.....144
42. Figure **7.2** Raman spectra of **A**) unfunctionalized CNTs **7.1**; B) functionalized CNTs **7.2**; **C**) unfunctionalized N-CNTs **7.3**; **D**) functionalized N-CNTs **7.4**.....145
43. Figure **7.3** TEM images of A) CNTs **7.1** and B) N-CNTs **7.3**..……..……..……146
44. Figure **7.4** TEM images of functionalized N-CNTs **7.4 …...**……..……...147
45. Figure **7.5a** TEM images of **A** and **B** are for poly(3-hexylthiophene) attached undoped CNTs **7.5 ; C** and **D** for poly(3-hexylthiophene) attached N-CNTs **7.6**..……....148
46. Figure **7.5 b** TEM images of **A** and **B,** and **C** polythiophene attached N-CNTs **7.7** and undoped CNTs **7.8**, respectively…….....149
47. Figure **7.5c** TEM images for unfunctionalized CNT and polythiophene mixed **7.11**.....150
48. Figure **7.6** ^{1}H NMR spectra of the monomer and copolymers ($CDCl_3$), Poly(3-hexylthiophene) **7.9**; undoped CNT poly(3-hexylthiophene) **7.5**; N-doped poly(3-hexylthiophene) **7.6**……..……..…151
49. Figure **7.7** FT-IR of unfunctionalized undoped CNTs **7.1**; functionalized undoped CNTs **7.2**; unfunctionalized N-CNTs **7.3**; functionalized N-CNTs **7.4**……..…..……..…153

50. Figure **7.8a** FT-IR of poly(3-hexylthiophene) **7.9**; poly(3-hexylthiophene) attached undoped CNTs **7.6**; poly(3-hexylthiophene) attached N-CNTs **7.5** and 3-hexylthiophene ……154
51. Figure **7.8b** FT-IR of polythiophene attached N-CNT **7.7**; polythiophene attached undoped CNT **7.8** and polythiophene **7.9**.....155
52. Figure **7.9** UV-vis absorption spectra in THF of A) poly(3-hexylthiophene) **7.9** ; B) polymer attached undoped CNTs **7.5**; C) polymer attached N-doped CNTs **7.6** ....……..156
53. Figure **7.10** Photoluminescence at 500 nm excitation wavelength in THF of A) poly(3-hexylthiophene) **7.9**; B) polymer attached undoped CNTs **7.5**; C) polymer attached N-CNT **7.6**……..……..……157
54. Figure **7.11** TGA profile of functionalized CNTs **7.2** and **7.4**……...……158
55. Figure **7.12a** TGA profile of A) poly(3-hexylthiophene) **7.9**; B) polymer attached undoped CNTs **7.5**; C) polymer attached N-doped CNTs **7.6**; D) unfunctionalized undoped CNTs **7.1**; E) unfunctionalized N-doped CNTs **7.3**…….……..……..……...……159
56. Figure **7.12 b** TGA profile of F) polymer attached N-CNTs **7.7**; G) polymer attached undoped CNTs **7.8**; H) polythiophene **7.10**…….……..……..……159
57. Figure **7.13** DSC scan of the synthesized of A) poly(3-hexylthiophene) **7.9**; B) polymer attached undoped CNTs **7.5**; C) polymer attached N-CNTs **7.6**..……..……..……161
58. Figure **8.1**. Schematic representation of: (a) a DSSC with the FTO/TiO_2/C_{60}-containing copolymer +TiO_2/ electrolyte/Pt; (b) microscopic representation of the TiO_2 and C_{60}-copolymer interaction on FTO glass. (Note: the schematic representations are not drawn to scale.)……..……..……173
59. Figure **8.2** DSSC current-voltage curves (100 mW cm^{-2} incident light) for the TiO_2/C_{60}-copolymer + TiO_2/electrolyte/Pt system: A) **5.3a**; B) **5.3b**; C) **5.3c**. Power-voltage curves: D) **5.3a**; E) **5.3b**; F) **5.3c**..……...174
60. Figure **8.3** DSSC current density vs voltage (vs Pt counter electrode) curves obtained under dark conditions for the cells assembled with A) 10:1 mole ratio (**5.3a**); B) 500:1 mole ratio (**5.3b**) and C) 1000:1 mole ratio (**5.3c**) C_{60}:hexylthiophene copolymer……175
61. Figure **8.4**. Schematic representation of a DSSC with: a) the glass-FTO/TiO_2/dye/**5.3a** copolymer/electrolyte/Pt; b) the glass-FTO/TiO_2/dye/**5.3a** copolymer + TiO_2/electrolyte/Pt; c) microscopic representation of the TiO_2+dye and **5.3a** copolymer + TiO_2 interaction on FTO glass. (Note: the schematic representations are not drawn to scale.)……...176

62. Figure **8.5**. DSSC current-voltage curves (100 mW cm^{-2} incident light): A) **5.3a** copolymer without TiO_2; B) **5.3a** copolymer with TiO_2; C) only with N719 dye……..…..…...177
63. Figure **8.6** Current density - voltage (I-V) curves obtained under dark conditions with DSSCs based on **5.3a** copolymer: A) mixed with TiO_2; B) without TiO_2……..……178
64. Figure **8.7**. DSSC current-voltage curves (100 mW cm^{-2} incident light) for the TiO_2/dye/C_{60}-copolymer + TiO_2/electrolyte/Pt system: A) **5.3a**; B) **5.3b**; C) **5.3c**. Power-voltage curves are also shown: D) **5.3a**; E) **5.3b**; F) **5.3c**. ……..……..…..…..….179
65. Figure **8.8.** DSSC current-voltage curves under dark conditions for the cells made from TiO_2/dye/C_{60} copolymer + TiO_2/electrolyte/Pt system: (A) 10:1 mole ratio (**5.3a**); (B) 500:1 mole ratio (**5.3b**); (C) 1000:1 mole ratio (**5.3c**)……..……..…..…...180
66. Figure **8.9.** Schematic representation of the DSSC solar cell with the glass-FTO/TiO_2/CNT-copolymer + TiO_2 / electrolyte/ Pt. (Note: the schematic representation is not drawn to scale)…….……...….181
67. Figure **8.10**. DSSC current-voltage curves (100 mW cm^{-2} incident light) for the TiO_2/CNT-copolymer + TiO_2/ electrolyte/ Pt system: A) N-CNT copolymer **7.6**; B) CNT copolymer **7.5**. Power-voltage curves are also shown: C) N-CNT copolymer **7.6**; D) CNT-copolymer **7.5**…….…….……...182
68. Figure **8.11** Current-voltage curves under condition dark for A) N-CNT copolymer **7.6**; B) CNT copolymer **7.5**……..……...….182
69. Figure **8.12** Schematic representation of the DSSC made from glass-FTO/TiO_2/dye/CNT copolymer / electrolyte/ Pt. (the schematic representation is not to scale)……...…...183
70. Figure **8.13**. DSSC current-voltage curves (100 mW cm^{-2} incident light) of the glass-FTO / TiO_2 / dye/CNT + TiO_2/electrolyte/Pt system: A) CNT copolymer **7.5**; B) N-CNT copolymer **7.6**. Power-voltage curves are also shown: C) CNT copolymer **7.5**; E) N-CNT copolymer **7.6**…….…….…....184
71. Figure **8.14** Schematic representation of the organic solar cell with the ITO/PEDOT-PSS/P3HT:C_{60}-copolymer/Al device. (Note: the schematic representation is not drawn to scale)……...…….……..186
72. Figure **8.15** Current-voltage curves of organic solar cells based on: a) glass-ITO/PEDOT-PSS/P3HT: **5.3a** (10:1 mole ratio C_{60}-copolymer)/Al; b) glass-ITO/PEDOT-PSS/**5.3b** (500:1mole ratio C_{60}-copolymer) /Al (both under dark conditions and 60 mW cm^{-2} irradiation)…….……..…….....187

List of Tables

1. Table **3.1** UV-visible λmax of the co-polymers **3.6B-E** and polynorbornene 3.**6A**…...…..66
2. Table **3.2** T_g of C_{60}-containing polymers **3.6B-E** and **3.6A**. ……68
3. Table **4.1** Details of the synthesized polymer **4.9A** and the co-polymers **4.9B-I**..…….....78
4. Table **4.2** UV-visible λmax of the polymer **4.9A** and the co-polymers **4.9B-I** ….....……81
5. Table **4.3** T_g and thermal decomposition temperature of C_{60}-containing polymers **4.9B-E** and **4.9A**. ……..……..……83
6. Table **5.1** Summary of FTIR of the copolymers, polymers and C_{60} derivatives (values in cm^{-1}) 102
7. Table **5.2** UV visible spectra of poly(3-hexylthiophene) (**5.5**), **5.2**, **5.3**, copolymers **5.8a-c** and **5.9**.....103
8. Table **5.3** summary of thermal decomposition temperature vs mass losses of copolymers and pure polymers.....107
9. Table **6.1** Summary of *cis* and *trans* ratios of the polymer and functionalized copolymers……127
10. Table **7.1** intensity ratios of the D and G Raman bands ….……...…....146
11. Table **7.2** Summary of FT-IR of the monomer, poly(3-hexylthiophene) and CNT attached polymers (values in cm^{-1}) ……...……153
12. Table **7.3** Summary of the Photoluminescence and UV-visible spectra maximum in THF ……..157
13. Table **8.1** Photovoltaic performance of the DSSCs based on TiO_2/C_{60}-copolymer + TiO_2 /electrolyte/Pt……175
14. Table **8.2** Photovoltaic performance of the DSSCs based on glass-FTO/TiO_2/dye/C_{60}-copolymer + TiO_2 /electrolyte/Pt ……180
15. Table **8.3** Photovoltaic performance of the DSSCs made from glass-FTO/TiO_2/CNT copolymer + TiO_2 /electrolyte/Pt ..……..…..183

16. Table **8.4**. Photovoltaic performance of the DSSCs based on glass-FTO/TiO_2/dye/CNT-copolymer + TiO_2 /electrolyte/Pt ……184
17. Table **8.5** Photovoltaic performance of organic solar cell based on glass-ITO/PEDOT-PSS/C_{60}-copolymer /Al……..……..……..……187

List of Abbreviations

a. u.	Arbitrary units
CNT(s)	Carbon nanotubes(s)
CVD	Chemical vapor deposition
ROMP	Ring opening metathesis polymerization
FAB	Fast atom bombardment
FT-IR	Fourier transform infrared
TGA	Thermal gravimetric analysis
DSC	Differential scanning calorimetry
TEM	Transmission electron microscope
I_D/I_G ratio	The intensity ratio of D to G band
I_h symmetry	Icosahedral symmetry
LUMO	Lowest unoccupied molecular orbital
HOMO	Highest occupied molecular orbital
MS	Mass spectrosopy
m/z	Mass-to-charge ratio
r.t	rom temprature
NMR	Nuclear magnetic resonance
Tg	Glass transition temperature
PEDOT	poly(3,4-ethylenedioxythiophene)
PSS	poly(styrenesulfonate)
ITO	indium tin oxide
FTO	Floride tin oxide
MEH-PPV	poly[2-methoxy-5-(2'-ethyl-hexyloxy)-1,4-phenylene vinylene]
[60]PCBM	[6,6]-Phenyl C61 butyric acid methyl ester

P3HT	Poly(3-hexylthiophene)
DMF	*N*,*N*-Dimethylformamide
THF	Tetrahydrofuran
TMS	Tetramethylsilane
UV-VIS	Ultra-violet visible
IR	Infrared
DSSC	Dye sensitized solar cells
Voc	open circuit voltage
Isc	short circuit current
FF	fill factor
min	minute
h	hour
mA	milliamperes
V	Volt
AM1.5G	Air mass 1.5 global (Part of the standard test conditions for PV cells. The intensity of insolation equivalent to the Sun shining through the atmosphere to sea level, with oxygen and nitrogen absorption, at an oblique angle 48.2deg from the zenith.)

Introduction

1.1 Background and rationale

Among the renewable energy sources, solar energy is of great importance. It is clean and environmentally friendly. Sunlight can be transformed into electricity using solar cells. Solar cells have applications in many different fields such as in calculators, solar lamps and can be used on spacecraft and satellites.

Bulk heterojunction structures based on carbon materials have attracted a great deal of interest for both fundamental scientific reasons and for potential applications in various new optoelectronic devices, e.g. photovoltaic solar cells. Thus far, although many materials have been reported for making a heterojunction-based solar cell, only silicon has found commercial use [1, 2]. Conventional solar cells hve been built from inorganic materials such as silicon and the efficiency of such solar cells has reached 24 % [3]. However, the cost of these solar cells is too high to to allow their extensive use in daily life since the materials are expensive and they require energy intensive processing techniques to produce them. Moreover, silicon has also a drawback that under illumination it degrades, which limits its lifetime and stability. Therefore, it is crucial to find a new kind of clean and cheap material for solar cells. In the search for alternative materials, carbon is highly attractive because it is expected to have similar properties to silicon and would be highly stable. Carbon is a remarkable element existing in a variety of stable forms ranging from insulator/semiconducting diamond (or diamond-like amorphous film [4]) to metallic/semi-metallic graphite (or graphene [5, 6]), conducting/semiconducting fullerenes (e.g. C_{60}) [7] and carbon nanotubes (CNTs) [8, 9], all of which show many interesting optoelectronic, physical and chemical properties. The various forms of carbon have attracted a

great deal of interest in recent years because of their unique structures, properties and potential applications in energy storage and conversion [10-12].

A lot of effort is being put into the development of new fabrication techniques using organic, [13], hybrid [14] and photoelectrochemical (dye sensitized) solar cells [15] which could act as alternatives to conventional silicon solar cells. Organic solar cells mainly consist of two organic materials; an electron-donating material and an electron-accepting material that make a percolating structure with interpenetrating networks [16]. A hybrid solar cell on the other hand, is a combination of both organic and inorganic materials and therefore combines the unique properties of inorganic semiconductors with the film forming properties of conjugated polymers [17]. Organic materials are generally inexpensive, easily processable and their functionality can be tailored by molecular design and chemical synthesis. On the other hand, inorganic semiconductors can be manufactured as nanoparticles. Inorganic semiconductor nanoparticles offer the advantage of having high absorption coefficients and size tunability. By varying the size of the nanoparticles the bandgap can be tuned and therefore the absorption range can be tailored [18].

Since the first demonstration by O'Reagan and Gratzel in 1991 [19], dye sensitised or photoelectrochemical solar cells (DSSCs or PECs) have attracted significant and sustained interest [20-22] and moreover, these cells have been regarded as promising cells for next generation photovoltaic devices due to their attractive features of high power conversion efficiency (>10%) and low production cost [23-28]. DSSCs have been studied extensively using wide band gap nano-crystalline TiO_2 sensitized with ruthenium polypyridine complexes [29] or with metal free organic dyes [30] as photo-electrodes.

Carbon nanotubes offer a wide range of band gaps [31-33] to match the solar spectrum, enhanced optical absorption [34, 35] and reduced carrier scattering for hot carrier transport [36, 37]. The latter may even result in a near-ballistic transport in nanotubes with submicron-meter lengths [38]. Castrucci *et al.* [39] have demonstrated that MWNTs can generate a photocurrent in the visible and ultraviolet spectral range. Recently, Cheong *et al.* [40] have investigated the photoresponsive conductance switching of MWNTs-SPO (SPO = spironaphthoxazines) under a 365 nm UV irradiation. In their study, they reported that during the cyclic irradiation of MWNTs-SPO by UV light the composites showed a reversible response, in which the change of HOMO–LUMO band gap in SPO strongly affects the conductivity of the MWNTs.

Among donor–acceptor type organic solar cells, the most promising material combination is poly(3-octylthiophene) (P3OT), poly(3-hexylthiophene) (P3HT) and the fullerene derivative (6,6)- phenyl-C_{61}-butyricacidmethylester (PCBM) [41]. These are reagents although expensive though PCBM can form film-like structures with high electron mobility. Investigation of carbon-based organic solar cells has been conducted towards developing alternative low-cost, light weight, flexible devices. Two typical carbon materials, fullerenes (C_{60}) and CNTs, are always involved, particularly when combined with p-conjugated polymers and several have been found to be photo-active materials. It is well known that C_{60} is a good electron acceptor and is efficient in charge separation [42]. Semiconducting CNTs can be a suitable replacement for C_{60} by forming ideal hetero-junctions. The work function (F) of CNTs is in the range of 4.5–5.1eV, which is close to the valence band of P3OT/P3HT. Therefore, CNTs can help to improve exciton dissociation at the CNT/polymer interface and provide efficient hole or electron transport.

Functionalization of carbonaceous material is a crucial step in making their solar cell devices. In this regard, a [3+2] cycloaddtion method has been employed by research groups for the functionalization of carbonaceous materials [43-45]. During the reaction a reactive intermediate, azomethine ylide, is generated *in situ* by the decarboxylation of immonium salts derived from the thermal condensation of amino acids and aldehydes (or ketones), or the thermal ring opening of aziridines. It has been shown that this approach is one of the most flexible methods for the functionalization of fullerenes and CNTs, and has been widely used [43-45]. The application of azomethine ylides for the functionalization of CNTs was first reported by Georgakilas *et al.* [45]. The 1,3-dipolar cycloaddition of azomethine ylides with alkene or alkyne is a very effective method for the construction of pyrrolidine- and pyrrole-rings in the synthesis of pyrrolidine- and pyrrole-containing molecules. Different fragments with important electronic properties have been covalently attached to the fullerene system using azomethine ylides and molecules such as porphyrins [46], subphthalocyanines [47], dendrimers [48] and conjugated oligomers [49].

1.2 Objectives

i. To synthesize both nitrogen doped and undoped MWCNTs using well developed methods.
ii. To functionalize C_{60} and both nitrogen doped and un-doped MWCNTs using azomethine ylides (the Prato reaction) and subsequently to bind the C_{60} and MWCNT derivatives covalently either to a polymer polythiophene or polynorbornene system.
iii. To study the photovoltaic behavior of the newly synthesized materials in DSSC and organic solar cells.
iv. To characterise the synthesised materials using transmission electron microscopy (TEM), thermogravimetric analysis (TGA), as well as NMR, Raman, FT-IR, UV visible and photoluminescence spectroscopy.

1.3 Thesis outline

Chapter 1: gives a motivation of the work presented in the subsequent chapters. Although each chapter briefly introduces itself, the information contained in this chapter is of a general nature and gives a justification to the problems presented and briefly what measures were undertaken to address them and how this was achieved.

Chapter 2: is a general literature review. The chapter gives a detailed description of the chemistry of carbonaceous materials. Common methods of CNT/C_{60} functionalization, polymer composite synthesis and their application in photovoltaic devices are also described.

Chapter 3: presents a report on the synthesis of a C_{60}-cyclopentadiene cycloadduct and polymerization of a co-monomer with norbornene, using the Grubbs second generation catalyst, in order to obtain a new range of samples containing different amounts of C_{60}.

Chapter 4: this chapter presents the investigation of the synthesis and properties of a series of novel C_{60}-containing polymeric materials based on the ROMP of a *N*-(cycloheptyl)-*endo*-norbornene-5,6-dicarboximide monomer with a C_{60}-cyclopentadiene cycloadduct. This reagent was chosen in the hope that it would enhance the solubility of the fullerene containing polymers.

Chapter 5: this chapter describes the functionalization of C_{60} using azomethine ylides (the Prato reaction) and its subsequent reaction to incorporate the C_{60} derivatives covalently to a polymer polythiophene system. The electronic and thermal properties of the synthesized copolymers were investigated.

Chapter 6: in this chapter a new approach to the functionalization of the N-doped and non-doped CNTs based on ring opening metathesis (ROMP) using Grubbs' catalyst, after sidewall functionalization of both N-doped and non-doped CNTs were studied is given. The thermal and electronic properties of these new co-polymers were investigated.

Chapter 7: a new approach for the functionalization of N-doped and undoped CNTs using a 1,3-dipolar cycloaddition of azomethine ylides and their subsequent *in situ* polymerization with thiophene is discussed. The resulting polymers were characterized and their thermal and electronic properties studied.

Chapter 8: in this chapter the photovoltaic behaviour of the synthesized materials were studied. The use of polymer attached C_{60} and MWCNTs were investigated both in DSSC and organic solar cells.

Chapter 9: presents a general summary and gives conclusions to the work presented in this thesis. The chapter highlights the successes of the project and the usefulness of the outcomes. Future studies described from the conclutions are given.

1.4 References

1 A. G. Aberle, Prog. *Photovoltaics:Res. Appl*., **2000**, 8, 473.

2 M. A. Green, *Physica E,* **2002**, 14, 65.

3 M. Green, *Progress in Photovoltaics*, **2001**, 9, 123.

4 J. Robertson, *Mater. Sci .Eng*., **2002**, R37, 129.

5 K. S. Novoselov, A. K. Geim, S. V. Morozov, D. Jiang, Y. Zhang, S. V. Dubonos, I. V. Grigorieva, A. A. Firsov, *Science*, **2004**, 306, 666.

6 A. K. Geim, K. S. Novoselov, *Nat. Mater*., **2007**, 6, 183.

7 H. W. Kroto, J. R. Heath, S. C. O'Brien, R. F. Curl, R. E. Smalley, *Nature*, **1985**, 318,162.

8 S. Iijima, *Nature*, **1991**, 354, 56.

9 R. H. Baughman, A. A. Zakhidov, W. A. de Heer, *Science*, **2002**, 297, 787.

10 G. L. Che, B. B. Lakshmi, E. R. Fisher, C. R. Martin, *Nature*, **1998**, 393, 346.

11 C. Wang, M. Waje, X. Wang, J. M. Tang, R. C. Haddon,Y. S. Yan, *NanoLett.*, **2004**, 4, 345.

12 D. A. Stewart, F. Lonard, *NanoLett.,* **2005**, 5, 219.

13 S. E. Shaheen, C. Brabec, N. S. Sariciftci, F. Padinger, T. Fromherz, J. C. Hummelen, *App. Phys. Lett.*, **2001**, 78, 841.

14 (a) E. Arici, D. Meissner, N. S. Sariciftci, in *Encyc. Nanoscience and Nanotech.,* edited by H. S. Nalwa, **2004**, 1. (b) W. Huynh, X. Peng, A. P. Alivisatos, *Adv. Mat.*, **1999**, 11, 11.

15 M. Gratzel, *J. Photochem. Photobiol. A*, **2004**, 164, 3.

16 G. Yu, J. Gao, J. C. Hummelen, F. Wudl, A. J. Heeger, *Science*, **1995**, 270, 1789.

17 E. Arici, N. S. Sariciftci, D. Meissner, *Adv. Func. Mat.*, **2003**, 2, 13.

18 H. Weller, *Angew. Chemie., Int. Eng. Ed.*, **1993**, 32, 4.

19 F. B. O'Regan, M. Gratzel, *Nature*, **1991**, 353, 737.

20 P. Xie, F. Guo, *Curr. Org. Chem*., **2007**, 11, 1272.

21 W. R. Duncan, O. V. Prezhdo, *Annu. Rev. Phys. Chem*., **2007**, 58, 143.

22 M. Grätzel, *Nature*, **2001**, 414, 338.

23 M. K. Nazeerudin, F. De Angetis, S. Fantacci, A. Selloni, G. Viscardi, P. Liska, S. Ito, T. Bessho, M. Gratzel, *J. Am. Chem. Soc.,* **2005**, 127, 16835.

24 M. Gratzel, *Chem. Lett.,* **2005**, 34, 8.

25 Y. Chiba, A. Islam, Y. Watanabe, R. Kamiya, N. Komiya, N. Koide, L. Han, *Jpn. J. Appl. Phys. Part 2*, **2006**, 45, 24.

26 M. Wang, X. R. Xiano, X.W. Zhou, X. P. Li, Y. Lin, *Sol. Energy Mater. Sol. Cells*, **2007**, 91, 785.

27 D. B. Kuang, C. Klen, H. J. Snaith, J. E. Moser, R. Humphry-Baker, P. Campte, S. M. Zakeeruddin, M. Gratzel, *Nano Lett.*, **2006**, 6, 769.

28 M. K. Nazeerudin, A. Kay, I. Rodicio, R. Humphry-Baker, E. Muller, P. Liska, N. Viachopoulos, M. Gratzel, *J. Am. Chem. Soc.*, **1993**,115, 6382.

29 (a) Z. S.Wang, C. H. Huang, B. W. Zhang, Y. J. Hou, P. H. Xie, H. J. Qian, K. Ibrahim, *New J. Chem.*, **2000**, 24, 567 (b) S. H. Kang, S. H. Choi, M. S. Kang, J. Y. Kim, H. S. Kim, T. Hyeen, Y. E. Sung, *Adv. Mater.*, **2008**, 20, 54. (c) N. G. Park, K. Kim, *Phys. Stat. Sol.*, **2008**, 1, 1. (d) C. Bauer, G. Boschloo, E. Mukhlar, A. Hagfeldt, *J. Phys. Chem. B*, **2002**, 106, 12693. (e) C. Klein, M. K. Nazeeruddin, P. Liska, D. Di Censo, N. Hitrata, E. Palomares, J. R. Durrant, M. Gratzel, *Inorg. Chem.*, **2005**, 44, 178. (f) X. Yin, H. Zhao, L. Chen, W. Tab, J. Zhang, Y. Wang, Z. Shuai, X. Xiao, X. Zhou, X. Li, Y. Lin, *Surf. Interface Anal*., **2007**, 39, 809. (g) M. Wei, Y. Konishi, H. Zhou, M. Yanagida, H. Sugihara, H. Arahawa, *J. Mater. Chem*., **2006**, 16, 1287.

30 (a) Z. S. Wang, K. Sayama, H. Sugihara, *J. Phys. Chem. B*, **2005**, 109, 22449. (b) S. L. Li, K. J. Jiang, H. F. Shao, L. M. Yang, *Chem. Commun*., **2006**, 2792. (c) T. Horiuchi, H. Miura, K. Sumioka, S. Uchida, *J. Am. Chem. Soc*., **2004**, 126, 12218. (d) T. Kitamura, M. Ikeda, K. Shigaki, T. Inoue, N. A. Anderson, X. Ai, T. Q. Lian, S. Yanagida, *Chem. Mater*., **2004**, 16, 1806.

31 M. S. Dresselhaus, G. Dresselhaus, R. Saito, *Carbon*, **1995**, 33, 883.

32 N. Hamada, S. Sawada, A. Oshiyama, *Phys. Rev. Lett.*, **1992**, 68, 1579.

33 R. Saito, M. Fujita, M. S. Dresselhaus, G. Dresselhaus, *Phys. Rev. B*, **1992**, 46, 1804.

34 J. W. G. Wildoer, L. C. Venema, A. G. Rinzler, R. E. Smally, *Nature*, **1998**, 391, 59.

35 T. W. Odom, J.-L. Huang, P. Kim, C. M. Lieber, *Nature*, **1998**, 391, 62.

36 M. Freitag, Y. Martin, J. A. Misewich, R. Martel, P. Avouris, *Nano Lett*., **2003**, 3, 1067.

37 J. Guo, C. Yang, Z. M. Li, M. Bai, H. J. Liu, G. D. Li, E. G. Wang, C. T. Chan, Z. K. Tang, W. K. Ge, X. Xiao, *Phys. Rev. Lett.*, **2004**, 93, 017402.

38 A. Javey, J. Guo, Q. Wang, H. Dai, *Nature*, **2003**, 424, 654.

39 P. Castrucci, F. Tombolini, M. Scarselli, E. Speiser, S. Del Gobbo, W. Richter, M. De Crescenzi, M. Diociaiuti, E. Gatto, M. Venanzi, *Appl. Phys. Lett.*, **2006**, 89, 253107.

40 I. W. Cheong, S. Wang, H. S. Ki, S.-H. Kim, *Curr. Appl. Phys.*, **2009**, 9, 1269.

41 R. A. J. Janssen, J. C. Hummelen, N. S. Sariciftci, , *MRS Bull*, **2005**, 30, 33.

42 H. Hoppe, C. Winder, J. Kraut, R. Heisgen, A. Hinsch, D. Meissner, N. S. Sariciftci, *Adv. Funct. Mater*., **2004**, 14, 1005. (b) C. Waldauf, P. Schilinsky, J. Hauch, C. J. Brabec, *Thin Solid Films*, **2004**, 451,105. (c) M. Al-Ibrahim, H. K. Roth, M. Schroedner, A. Konkin, U. Zhokhavets, G. Gobsch, P. Scharff, S. Sensfuss, *Org. Electron.*, **2005**, 6, 65. (d) H. Hoppe, N. S. Sariciftci, *J. Mater. Chem*., **2006**, 16, 45.

43 M. Maggini, G. Scorrano, M. Prato, *J. Am. Chem. Soc.*, **1993**, 115, 9798.

44 M. Prato, M. Maggini, *Acc. Chem. Res.*, **1998**, 31, 519.

45 V. Georgakilas, K. Kordatos, M. Prato, D. M. Guldi, M. Holzinger, A. Hirsch, *J. Am. Chem. Soc.*, **2002**, 124, 760.

46 (a) R. Fong, D. I. Schuster, S. R. Wilson, *Org. Lett.*, **1999**, 1, 729. (b) H. Imahori, H. Yamada, Y. Nishimura, I. Yamazaki, Y. Sakata, *J. Phys. Chem. B*, **2000**, 104, 2099. (c) H. Imahori, H. Yamada, S. Ozawa, Y. Sakata, K. Ushida, *Chem. Commun*., **1999**, 1165. (d) H. Imahori, H. Norteda, H. Yamada, Y. Nishimura, I. Yamazaki, Y. Sakata, S. Fukuzumi, *J. Am. Chem. Soc.*, **2001**, 123, 100. (e) C. Luo, D. M. Guldi, H. Imahori, K. Tamaki, Y. Sakata, *J. Am. Chem. Soc.*, **2000**, 122, 6535. (f) A. S. D. Sandanayaka, K.-I. Ikeshita, Y. Araki, N. Kihara, Y. Furusho, T. Takata, O. Ito, *J. Mater. Chem*., **2005**, 15, 2276.

47 D. Gonzalez-Rodrıiguez, T. Torres, D. M. Guldi, J. Rivera, M. A. Herranz, L. Echegoyen, *J. Am. Chem. Soc.*, **2004**, 126, 6301.

48 (a) T. Chuard, R. Deschenaux, *J. Mater. Chem*., **2002**, 12, 1944. (b) Y. Rio, J.-F. Nicoud, J. L. Rehspringer, J.-F. Nierengarten, *Tetrahedron Lett.*, **2000**, 41, 10207. (c) S. Campidelli, E. Vazquez, D. Milic, M. Prato, J. Barbera, D. M. Guldi, M. Marcaccio, D. Paolucci, F. Paolucci, R. Deschenaux, *J. Mater. Chem*., **2004**, 14, 1266. (d) S. Campidelli, J. Lenoble, J. Barbera, F. Paolucci, M. Marcaccio, D. Paolucci, R. Deschenaux, *Macromolecules*, **2005**, 38, 7915.

49 (a) T. Gu, J.-F. Nierergarten, *Tetrahedron Lett*., **2001**, 42, 3175. (b) J.-F. Eckert, J.-F. Nicoud, J.-F. Nierengarten, S.-G. Liu, L. Echegoyen, F. Barigelletti, N. Armaroli, L. Ouali, V. Krasnikov, G. Hadziioannou, *J. Am. Chem. Soc.*, **2000**, 122, 7467. (c) C. Martineau, P. Blanchard, D. Rondeau, J. Delaunay, J. Roncali, *Adv. Mater*., **2002**, 14, 283.

Literature review

2.0 General

2.1 Carbon nanotubes, fullerene (C_{60}) and other carbonaceous materials

Carbon-based materials, clusters, and molecules are unique in many ways. One distinction relates to the many possible configurations of the electronic states of a carbon atom, which is known as the hybridization of atomic orbitals and relates to the bonding of a carbon atom to its nearest neighbours. Carbon is the sixth element of the periodic table and has the lowest atomic number of any element in column 14 of the periodic table. Each carbon atom has six electrons which occupy the $1s^2$, $2s^2$, and $2p^2$ atomic orbitals. The $1s^2$ orbital contains two strongly bound core electrons. Four more weakly bound electrons occupy the $2s^2 2p^2$ valence orbitals. In the crystalline phase, the valence electrons give rise to 2*s*, 2*px*, 2*py*, and 2*pz* orbitals which are important in forming covalent bonds in carbon materials.

The various bonding states are connected with certain structural arrangements, so that *sp* bonding gives rise to chain structures, sp^2 bonding to planar structures and sp^3 bonding to tetrahedral structures. The sp^2 bonded graphite is the ground state phase of carbon under ambient conditions while at higher temperatures and pressures, sp^3 bonded cubic diamond is more stable. Other forms of stable carbons such as hexagonal diamond, hexagonal carbenes [1-3], and liquid carbon [4] have been reported. It is believed that a variety of novel π-electron carbon bulk phases remain to be discovered and explored.

Recently, much attention has been focused on small carbon clusters [5], since the discovery of fullerenes in 1985 by Kroto *et al.* [6] and of carbon nanotubes in 1991 by Iijima [7]. A carbon nanotube is often considered as a rolled sheet of graphene cylinder [8]. Nanotubes can be rolled from a graphene sheet in many ways [5,8]. There are many possible orientations of the hexagons on the nanotubes, even though the basic shape of the carbon nanotube wall is a cylinder. The electronic bonding in carbon nanotubes is sp^2 which is characteristic of graphite and plays a significant role in the properties of carbon nanotubes. The curvature of the nanotubes contains a

small amount of sp^3 bonding so that the force constants (bonding) in the circumferential direction are slightly weaker than along the nanotube axis.

Nanotubes can be broken down into two broad categories. The first, called the multiwalled carbon nanotubes (MWNT), were the first to be discovered. These are similar to hollow graphite fibers [9], except that these have a much higher degree of structural perfection. They are made of concentric cylinders placed around a common central hollow, with a spacing between the layers close to that of the interlayer distance in graphite (0.34 nm). This interlayer spacing in MWNTs is slightly larger than the single-crystal graphite value (0.335 nm) since in the nanotubes there is a severe geometrical constraint when forming perfect cylinders while maintaining the graphite spacing between them. The three-dimension structural correlation that prevails in single crystal graphite (ABAB stacking) is lost in the nanotubes, and the layers are rotationally disordered with respect to each other. The second variety is close to an ideal fullerene fiber; in size they are close to fullerenes and have single-layer cylinders extending from end to end [10, 11]. These tubes are called the single-walled nanotubes (SWNTs) and possess good uniformity in diameter (1-2 nm).

When SWNTs are produced in the vapor phase, they self-assemble into larger bundles (ropes) that consist of several tens of nanotubes [12-14]. These tubes then assemble into a one-dimensional triangular lattice structure with a lattice constant of 1.7 nm and a tube-tube separation of 0.315 nm [14]. This organization of the nanotube units into a crystal structure was theoretically predicted prior to their observation [15]. Both varieties of nanotubes can be regarded as aggregates of nanotube units (cylinders), the MWNTs consisting of a concentric assembly and the SWNTs made up of ropes of close packed nanotube units.

2.2 Chemistry of fullerene (C_{60})

2.2.1 General introduction to fullerenes (C_{60})

The existence of fullerenes in sooting flames was first revealed by mass spectrometry studies [16] and then macroscopic quantities of fullerenes were first generated by resistive heating of graphite [17]. This method was based on the technique for the production of amorphous carbon films in a vacuum evaporator [18]. Since then, different methods have been used to maximize the production of fullerenes [19-21]. For instance, fullerenes can also be obtained by the pyrolysis

of hydrocarbons, preferably aromatics. The first example of this methodology was the pyrolysis of naphthalene at 1000 °C in an Ar stream [22].

Each fullerene contains 2(10 + *M*) carbon atoms, corresponding to exactly 12 pentagons and *M* hexagons. This building principle is a simple consequence of Euler's theorem. Starting at C_{20}, any even-membered carbon cluster, except C_{22}, can form at least one fullerene structure. With increasing *M* the number of possible fullerene isomers rises dramatically, from only 1 for M = 0 to over 20 000 for *M* = 29 [23, 24]. The C_{60} isomer [60-I_h] fullerene is the smallest stable fullerene. The structure of [60-I_h] fullerene was determined theoretically [25-28] and also experimentally [29-32]. These investigations confirm the icosahedral structure of [60-I_h] fullerene. The two features of this C_{60} structure are that all twelve pentagons are isolated by hexagons and that the bonds at the junctions of two hexagons ([6,6] bonds) are shorter than the bonds at the junctions of a hexagon and a pentagon ([5,6] bonds). The pentagons within fullerenes are needed to introduce curvature, since a network consisting of hexagons only, is planar.

Electronically, C_{60} is described as having a closed-shell configuration consisting of 30 bonding molecular orbitals with 60 *p* electrons [33], which gives rise to a completely full fivefold degenerate h_u highest occupied molecular orbital (HOMO) that is energetically located approximately 1.5 to 2.0 eV lower than the corresponding anti-bonding lowest unoccupied molecular orbital (LUMO) [34, 35]. The first electron, on reduction of C_{60}, is added to a triply degenerate t_{1u} unoccupied molecular orbital that is highly delocalized [36]. This threefold-degeneracy, together with the low-energy possession of the LUMO, makes C_{60} a fairly good electron acceptor with the ability of reversibly gaining up to six electrons upon reduction [37, 38]. This high degree of symmetry in the arrangement of the molecular orbitals of C_{60} provides the foundation for physicochemical, electronic, and magnetic properties. Although the semiconducting [39], magnetic [40, 41], and superconducting [42] properties of unmodified C_{60} have been intensively investigated, the functionalized fullerenes have as yet not been fully explored.

The fullerenes are more reactive than CNTs. This is due to the fact that enormous strain is engendered by their spherical geometry as reflected in the pyramidalization angles of the carbon atoms [42a]. For an sp^2-hybridized (trigonal) carbon atom with pyramidalization angle of θ_P = 0°, planarity is strongly preferred, whereas an sp^3-hybridized (tetrahedral) carbon atom requires θ_P = 19.5° (Figure 1.1b). All of the carbon atoms in C_{60} have θ_P = 11.6°, and hence their geometry is more appropriate for tetrahedral than trigonal hybridization. Thus the chemical conversion of any trivalent carbon atom in C_{60} to a tetravalent carbon atom relieves the strain at the point of attachment and eases the strain at the 59 remaining carbon atoms [42a]. Hence, stability is accelerated by strain relief, and this strongly favours fullerene addition chemistry [42a-44]. Just as in the case of a fullerene, a perfect SWNT without functional groups is chemically inert. However, curvature-induced pyramidalization and misalignment of the π-orbitals [42a, 45-52] of the carbon atoms induces a local strain (Figure **2.1**), and carbon nanotubes are therefore expected to be more reactive than a flat graphene sheet.

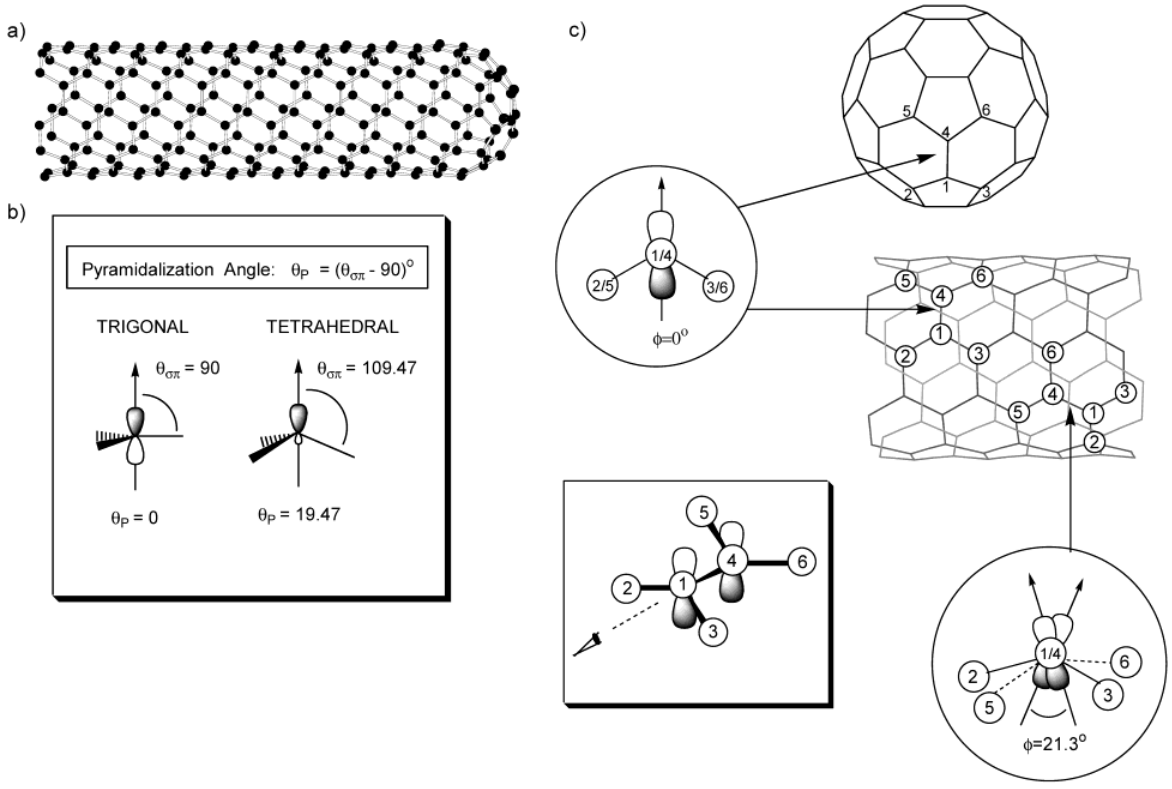

Figure **2.1** Diagrams of (a) metallic (5,5) SWNT, (b) pyramidalization angle (θ_P), and (c) the π-orbital misalignment angles (ϕ) along the C1-C4 in the (5,5) SWNT and its capping fullerene, C_{60} [42a].

2.2.2 Reactions of fullerene (C_{60})

Chemical functionalization allows for the preparation of soluble C_{60} derivatives that maintain the electronic properties of fullerenes. The chemistry of [60]fullerene is characteristic of electron-deficient alkenes and, as a consequence, it reacts with nucleophiles and its [6,6] bonds are good dienophiles. Cycloaddition reactions, such as [2+2], [3+2], and [4+2], play an important role in the preparation of C_{60} derivatives and a wide variety of cycloadducts have been prepared [53]. In the next sections representative examples of these types of cycloadditions will be described.

2.2.3 [2+2] Cycloadditions

Four-membered rings fused to 6,6-ring junctions are formed upon [2+2] cycloadditions. Hoke *et al.* [54] and Tsuda *et al.* [55] were the first to report the [2+2] thermal addition of benzyne to C_{60}. In addition, Schuster and coworkers [56-59] reported photochemical [2+2] cycloadditions of cyclic enones and 1,3-diones. Recently, the interest in the synthesis of fullerene dimers has increased [60], as they can be used as building blocks for nanotechnological applications. The first report was by Komatsu and coworkers [61, 62]; when the researchers reacted C_{60} (Scheme **2.1**) in a high-speed vibration mill (HSVM), in the presence of potassium cyanide, it produced a dimer, but when the reaction was conducted in solution only C_{60}-cyanated derivatives were obtained [63]. Similarly, using the same technique, Murata *et al.* [64], Forman *et al.* [65] and Tagmatarchis *et al.* [66] have reported reactions between C_{60} and pentanocene, the dimerization of C_{70}, as well as the synthesis of C_{60}–C_{70}, respectively.

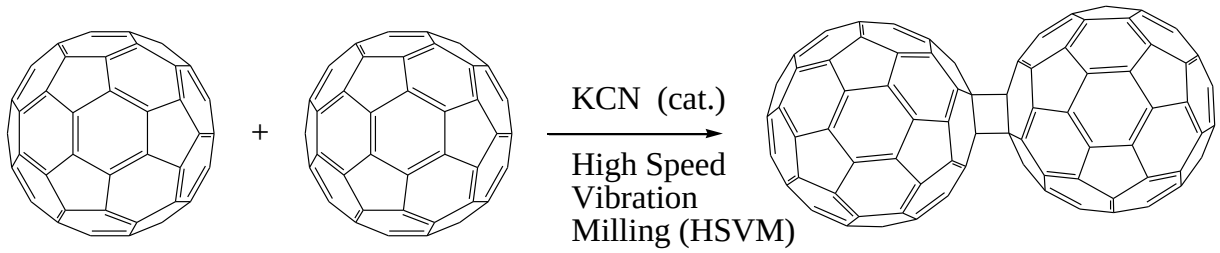

Scheme 2.1 Synthesis of C_{120} by reaction with KCN under the 'high-speed vibration milling' conditions.

2.2.4 [3+2] Cycloadditions

In [3+2] cycloadditions, five-membered rings fused to 6,6-junctions can be formed. Azomethine ylides are reactive intermediates that can be generated *in situ* by the decarboxylation of immonium salts derived from the thermal condensation of amino acids and aldehydes (or ketones) (Scheme **2.2**), or the thermal ring opening of aziridines. It has been shown that this approach is one of the most flexible methods for the functionalization of fullerenes and has been widely used [67, 68]. For example, the 1,3-dipolar addition of azomethine ylides to C_{60} yields fulleropyrrolidines that are formed across the 6,6-junction. The most important features of this type of reaction are that the utilization of functionalized aldehydes leads to the formation of 2-substituted fulleropyrrolidines, whereas utilization of *N*-substituted glycines affords *N*-substituted fulleropyrrolidines (Scheme **2.2**). Moreover, mono-fulleropyrrolidines are formed by controlling the stoichiometry of the reagents and the reaction conditions. Therefore, through this methodology, different fullerene derivatives can be obtained, either by using properly functionalized azomethine ylides or by modifying a fulleropyrrolidine intermediate.

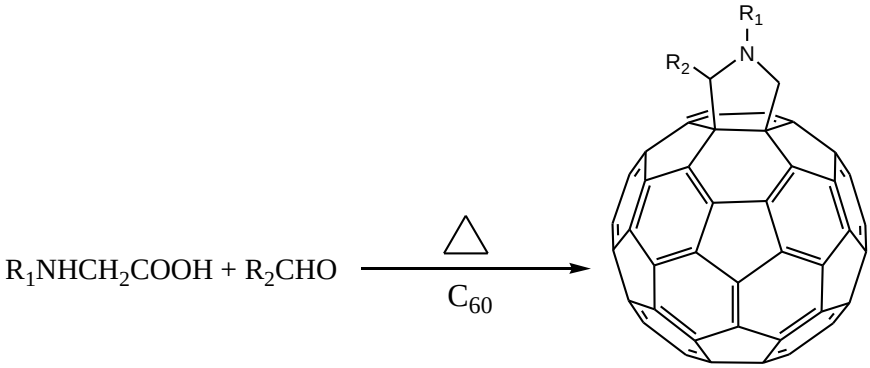

Scheme **2.2** [3+2] Cycloaddition using azomethine ylides.

Functionalized fullerene skeletons combined with further substituents or reactions can lead to the making of fullerene-based materials with unique properties. For instance, amphiphilic fulleropyrrolidines bearing suitable hydrophilic addends have been found to form true monolayers that transfer onto solid substrates, while the formation of Langmuir–Blodgett (LB) films could not be formed from their corresponding hydrophobic analogs [69-75]. The

functionalization of fullerene with polar side-chains [76] and with positively charged groups [77] has been reported and the enhancement of the solubility of these adducts allowed sufficiently high concentrations to be produced to allow study of the biological activity of the fulleropyrrolidines [78]. In addition, the solubilization of fullerenes in water allows the possibility to explore their properties in different fields such as medicinal chemistry and biotechnology.

In further examples, Kang *et al*. [79] reported a fulleropyrrolidine–mercaptophenyl hybrid material that was synthesized and self-assembled in two-dimensional arrays. In their report they indicated that the material showed reversible electrochemistry and electronic properties suitable for making well-ordered nanostructural morphologies and thin film functional materials.

Finally, using the 1,3-dipolar additions method, Holmes *et al*. [80]prepared large unnatural amino acids containing the natural α-amino acid proline condensed to a [6,6] ring junction of C_{60} [81]. Alternatively, fulleroprolines could be obtained via the thermal ring opening of aziridines [82]. In addition, di- and tri-peptides can also be prepared by incorporating fulleroproline at their *N*- or *C*-terminal [83-85].

2.2.5 [4+2] Cycloadditions

The [6,6] double bonds of [60]fullerene are excellent dienophiles (comparable to maleic anhydride). Thus, C_{60} can react with different dienes by a Diels–Alder cycloaddition reaction. Depending on the reactivity of the diene, heating the reaction under reflux in a high boiling solvent may be required. In some instances the use of microwave energy afforded better results [86].

The first example of a [4+2] cycloaddition reaction of C_{60} was carried out using cyclopentadiene [59] as the 1,4-diene system (Scheme **2.3**). Cyclopentadiene derivatives, such as methylcyclopentadiene and cyclopentadienone, afforded the corresponding monoadducts [87, 88]. The dienophilic behaviour of C_{60} in [4+2] cycloaddition reactions was also demonstrated in the reaction of C_{60} with anthracene (Scheme **2.3**) and other anthracene derivatives [89].

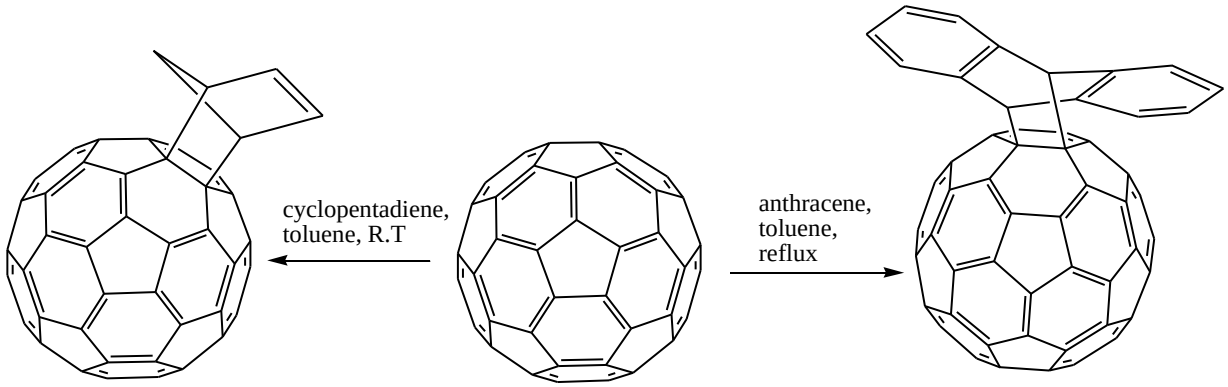

Scheme **2.3** [4+2] cycloaddition reactions of C_{60}.

2.2.6 Other types of reactions on Fullerenes (C_{60})

2.2.6.1 Electrochemical reactions

The possibility of electrochemical production of C_{60} anions in a defined oxidation state was reported by applying a proper potential to synthesize fulleride salts [90-96]. The resulting fulleride anions could also be used to synthesize covalent organofullerene derivatives by quenching the anions with electrophiles. This was well demonstrated in the synthesis of dimethyldihydro[60] fullerene [97]. Other methods that have used C_{60} anions as precursors for the synthesis of fullerene derivatives usually involve chemical formation of the anion. Alkylation of C_{60} has also been accomplished, for example, by reduction with propanethiol and potassium carbonate in DMF [98, 99], sodium methanethiolate in acetonitrile [100], the naphthalene radical anion in benzonitrile [101], potassium naphthalide [102] or simply with zinc [103].

2.2.6.2 Reduction with metals

Fullerenes can easily be chemically reduced by reaction with electropositive metals such as alkali and alkaline earth metals [104]. The anions C_{60}^{n-} (n = 1–5) can be generated in solution by titrating a suspension of C_{60} in liquid ammonia with a solution of rubidium in liquid ammonia [105]. Similarly alkaline earth metals can also be intercalated with C_{60} [104, 106, 107]. The preparation of Ca_5C_{60}, Ba_6C_{60} [108], Ba_xC_{60} (with x = 3–6) or Ba_4C_{60} and Sr_4C_{60} [108] have been achieved by the direct reaction of C_{60} with the corresponding alkaline earth metal vapor. A bulk

reduction of C_{60} in solution was reported with less electropositive metals such as mercury, leading to C_{60}^{-} or C_{60}^{2-} [109].

2.2.6.3 Addition of carbon nucleophiles

C_{60} readily reacts with alkyl, phenyl or alkynyl organolithium and Grignard compounds to form the anions RC_{60}^{-} as primary intermediates [110]. Other Li acetylides, Li-C≡C-R with R = hexyl [111] or benzylether dendrons [112, 113], have been attached to C_{60}. Besides protonation, alkyl-, benzyl-, cycloheptatrienyl-, benzoyl- or vinylether-derivatives, formaldehyde and dichloroacetylene have also been used as electrophiles [110f, 114].

2.2.6.4 Addition of amines

Owing to their high nucleophilicity, primary and secondary aliphatic amines undergo nucleophilic additions with electron-deficient C_{60} [110, 115]. Seshadri *et. al.* [115b] have reported that a reaction of C_{60} with excess methylamine in toluene solution at r.t. was nearly instantaneous and gave a yellow product containing a mixture of adducts. Characterization of the products using a mass spectroscopy further indicated that up to 14 amine units add to C_{60}. Furthermore, the addition of a secondary amine such as dimethylamine to C_{60} under similar conditions also gives a yellow product mainly containing adducts corresponding to the addition of 1, 2 and 6 amines units. Kampe *et. al*. [116] have revealed that diamines such as N,N'-dimethylethylenediamine, piperazine, or homopiperazine in toluene between 0 and 100 ^{o}C, (both reactants in low concentrations) togather with C_{60} gave mono- and bisadducts as the predominant products.

2.2.6.5 Addition of phosphorus nucleophiles

Compared with the wide range of existing carbon or nitrogen nucleophiles that react with C_{60} there are few examples of reactions with phosphorus nucleophiles. Neutral trialkylphosphines are less reactive with C_{60} even at elevated temperatures [117]. Lithiated phosphines and phosphites however readily, add to the [6,6] double bond of C_{60} [117, 118].

2.2.7 Application in polymers

Polymers involving C_{60} [119] are of considerable interest since: (a) the fullerene properties can be combined with those of specific polymers, (b) suitable fullerene polymers should be spin coatable, solvent-castable or melt-extrudable, and (c) fullerene-containing polymers as well as surface-bound C_{60} layers are expected to have remarkable electronic, magnetic, mechanical, optical or catalytic properties [120]. Several prototypes of polymers or solids containing the covalently bound C_{60} moiety are possible (Figure **2.2**) [119b, 121]. They include: fullerene pendant systems **Ia** with C_{60} on the side chain of a polymer (on-chain type or "charm bracelet") [122] or on the surface of a solid **Ib** [123], in-chain polymers **II** with the fullerene as a part of the main chain ("pearl necklace") [122], dendritic systems **III**, starburst or cross-link type **IV** or end-chain type polymers **V** that are terminated by a fullerene unit. For **III** and **IV**, one-, two- and three-dimensional variants can be considered. In addition, combinations of all of these types of polymers are possible.

The addition of living polystyrene to C_{60} leads to the formation of star-shaped polymers with C_{60} in the center (Figure **2.2**, **III**) [124]. These polymers are highly soluble and melt processable [124]. Different "living" anionic polymers such as polystyrene, the block copolymer polystyrene-*b*poly(phenylvinylsulfoxide) [125] (as a precursor for polyacetylene) or polyisoprene [126] have been grafted onto C_{60}. Star-shaped polymers with up to six branches are also possible by using reactive carbanions such as styryl or isoprenyl [119b].
A similar approach was used in the grafting of C_{60} onto a pregenerated lithiated polyethylene surface [123]. A polyethylene film with terminal diphenylmethyl groups was deprotonated with BuLi to yield an anionic polyethylene surface that was treated with C_{60} and quenched with methanol. This reaction also worked for polyisopropene, polybutadiene [123], poly(vinylbenzyl chloride) or poly(*N*-vinylcarbazole) (PVK) [120] with BuLi or NaH as a base.

The facile addition of primary and secondary amines to C_{60} has also been used to synthesize polymer-bound C_{60} [127-134]. Solutions of precursor polymers containing primary amino groups in the side chain or secondary amino groups in the main chain [133] were allowed to react with C_{60} in a "buckyball" fishing process. Fullerene end capped polymers (type **V**) were accessible by

reaction of amino terminated polystyrene [129], poly(ethylene glycol) or poly(propylene glycol) with C_{60} [130].

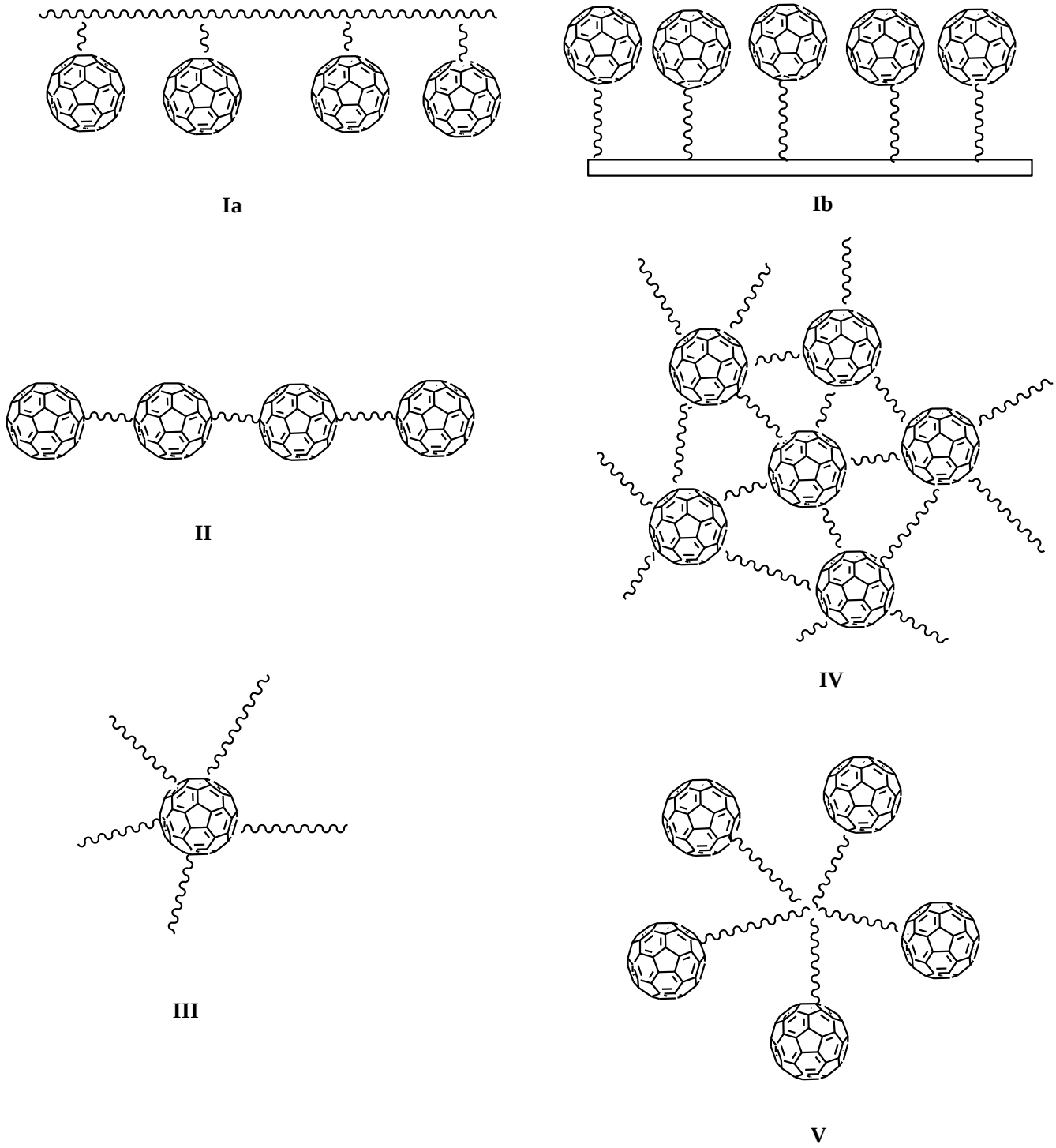

Figure **2.2** Polymers involving the C_{60} moiety. (**Ia**), pendant on-chain (**Ib**) pendant on-surface, (**II**) in-chain, (**III**) dendritic, (**IV**) cross-link and (**V**) end-chain [121-124].

2.3 Chemistry of carbon nanotubes (CNTs)

2.3.1 General introduction

The insolubility of CNTs, practically in all solvents, makes then difficult to manipulate. Although dispersion of CNTs in some solvents is possible by sonication, precipitation immediately occurs when this process is interrupted. On the other hand, it has been demonstrated that CNTs can interact with different classes of compounds to form composites [135-140].

The curvature-induced pyramidalization of π-orbitals of carbon atoms also induces misalignment of the π-orbitals of carbon atoms in SWNTs [135]. As a result, the sidewall of a SWNT should be more reactive than a flat graphene sheet; a SWNT of smaller diameter having larger π-orbital pyramidalization and misalignment angles suffers more severe curvature-induced weakening of π-conjugation and, hence, is more reactive. However, due to the different bending patterns, nanotubes have less curvature compared with fullerenes with comparable diameters (see Figure **2.1**); accordingly nanotubes are generally less reactive than fullerenes, and harsher experimental conditions are required to functionalize carbon nanotubes.

By utilization of the misalignment of the π-orbitals of carbon atoms that is induced by the curvature of the side wall CNTs, CNTs can undergo chemical modifications that make them more soluble for integration into inorganic, organic, and biological systems [141]. The main approaches for modification can be grouped into three categories: (1) the covalent attachment of chemical groups through reactions with the π-conjugated skeleton of CNT; (2) the noncovalent adsorption or wrapping of various functional molecules around the CNTs; and (3) the endohedral filling of the inner empty cavity of the CNTs.

2.3.2 Covalent functionalization of carbon nanotubes

2.3.3 Sidewall halogenation of CNTs

The side wall fluorination of CNTs has been achieved using elemental fluorine in the range between room temprature and 600 °C [142-146]. Nakajima *et al*. [142] studied the fluorination of CNTs under a wide range of temperatures and found that covalently fluorinated CNTs could be made between 250 °C and 400 °C. On other hand, Mickelson *et al.* [144] indicated that the

best results for fluorination reactions on the sidewall of CNTs was between 150 and 400 °C as at higher temperatures the graphitic network decomposes. The highest degree of functionalization was estimated to be about C_2F by elemental analysis. However, when fluorination was applied to small diameter single-walled CNTs, the nanotubes were cut to an average length of less than 50 nm [145].

Theoretical studies on the thermodynamics of side wall fluorination have been reported [146-148]. In addition, the structures of fluorinated CNTs have been compared both experimentally and theoretically. However there is controversy regarding the favorable pattern of F addition onto the sidewalls of CNTs. Based on scanning tunneling microscopy (STM) images and semiempirical calculations, Kelly *et al*. [149] proposed that two possible sidewall addition reactions, 1,2-addition or 1,4-addition, were possible. From their studies they concluded that the latter addition reaction gives a more stable product. However, using DFT calculations on a fluorinated carbon nanotube it was predicted that a 1,2-addition pattern is energetically more favorable than the 1,4-addition by about 16 kJ/mol [146e].

The fluorination reaction is a very useful reaction since further modification reactions can be accomplished after F addition [150-152]. For example, alkyl groups could replace the fluorine atoms, using Grignard [151b] or organolithium [152] reagents. As a result, the alkylated CNTs can be well dispersed in common organic solvents such as THF. In addition, several diamines [151a] or diols [153] were reported to react with fluoronanotubes via nucleophilic substitution reactions.

Mickelson *et al.* [154] reported that a moderate degree of solvation was achieved after sonicating fluorinated nanotubes in a variety of alcoholic solvents and further reactions were reported on those CNTs by reacting them with hydrazine. On the other hand, recovery of pristine CNTs was possible after fluorination by heating under an inert atmosphere [155, 156] the majority of the fluorine atoms could be detached after suspension of CNTs in 2-propanol hydrazine solution [147c, 157].

2.3.4 Hydrogenation

Hydrogenation of CNTs has been reported by Pekker *et al*. [158] by reducing pristine CNTs with Li metal and methanol dissolved in liquid ammonia (Birch reduction). The hydrogenated material was found to be stable up to 400 °C. Moreover, CNTs have been functionalized with atomic hydrogen using a glow discharge [159-161] or by proton bombardment [162]. The hydrogen storage capacity of CNTs (hydrogen to carbon atom ratio of 0.52) was reported by Liu *et al*. [163] at r.t. under a modestly high pressure (about 10 mega Pascal) for a SWNT. Recently, Yang *et al*. [164] have reported that the hydrogen storage capacity increased from 1.2 wt % to 1.52 wt % at 77 K and 1 bar and from 0.3 wt % to 0.61 wt % at 298 K and 95 bar using a hybrid composite of acid-treated multiwalled carbon nanotubes (MWNTs) and MOF-5 [MOF-5 = $Zn_4O(bdc)_3$; bdc = 1,4-benzenedicarbocylate].

2.3.5 Cycloadditions

Cycloadditions are reactions in which two or more unsaturated molecules (or parts of the same molecule) combine with the formation of a cyclic adduct in which there is a net reduction of the bond multiplicity.

The Haddon group was the first to apply carbene [2+1] cycloadditions to pristine CNTs [165-169]. During the reaction, carbene was generated *in situ* using a chloroform/sodium hydroxide mixture or a phenyl(bromodichloromethyl) mercury reagent. The [2+1] cycloadditions reactions then took place on the side wall of the CNTs.

Hirsch *et al*. [170, 171] performed studies that showed that the nucleophilic addition of carbenes to CNTs preferably produced zwitterionic 1:1 adducts rather than cyclopropane systems. Another possible [2+1] cycloaddition reaction was the thermal functionalization of CNTs by nitrenes. During this reaction, the first step was initiated by thermal decomposition of an azide which produces alkoxycarbonylnitrene via nitrogen elimination, followed by the [2+1] cycloaddition of the nitrene to the sidewalls of the CNTs affording alkoxycarbonylaziridino-CNT [170-174].

Different types of organic functional groups, such as alkyl chains and crown ethers, were successfully attached onto CNTs using this method. A subsequent reaction on the modified CNTs containing chelating donor groups in the addends allowed complexation of metal ions, such as Cu and Cd [172].

Another example involved the irradiation of a photoactive azidothymidine in the presence of CNTs, which resulted in the formation of very reactive nitrene groups in the proximity of the carbon lattice. In a cycloaddition reaction, these nitrene groups coupled to the CNTs and formed aziridine adducts (Figure **1.3**). Theoretical studies have supported the possibility of the reactions of CNT with carbenes (or nitrenes) from a thermodynamic point of view [175, 176].

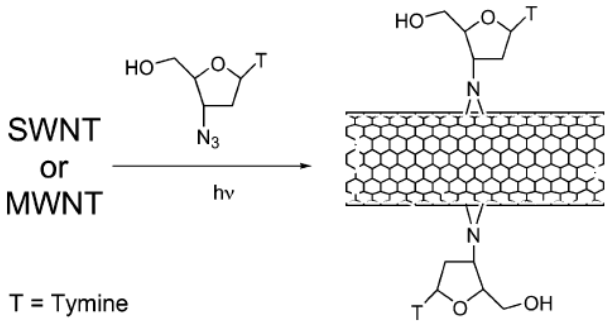

Figure **2.3** Photoinduced generations of reactive nitrenes in the presence of nanotubes.

The application of azomethine ylides was first reported by Georgakilas *et al.* [177] for the functionalization of CNTs. The azomethine ylides were formed thermally *in situ* by condensation of an R-amino acid and an aldehyde, and was successfully added to the graphitic surface via a 1,3-dipolar cycloaddition reaction, forming pyrrolidine fused rings [177, 178] (Figure **2.4**). The 1,3-dipolar cycloaddition reactions of azomethine ylides involves planar molecules composed of one nitrogen atom and two terminal sp^2 carbons, and they have four π electrons spread over the three-atom C-N-C unit. The 1,3-dipolar cycloaddition of azomethine ylides with alkene or alkyne is a very effective method for the construction of pyrrolidine- and pyrrole-rings in the synthesis of pyrrolidine- and pyrrole-containing molecules. These molecules are very important pharmaceuticals, natural alkaloids, organic catalysts, and building blocks in organic synthesis [17].

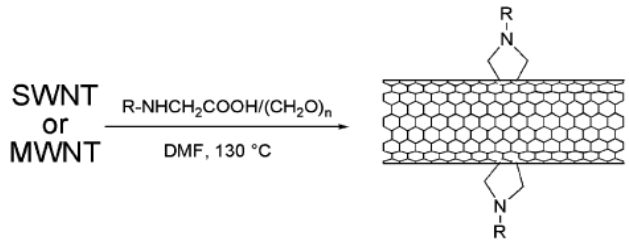

Figure **2.4** 1,3-dipolar cycloaddition of azomethine ylides n the surface of CNTs.

The amino functionalized CNTs were particularly suitable for the covalent immobilization of molecules or for the formation of complexes based on positive/negative charge interaction [179]. Various biomolecules have also been attached onto amino-CNTs, such as amino acids, peptides, and nucleic acids (Figure **2.5**) [179-184].

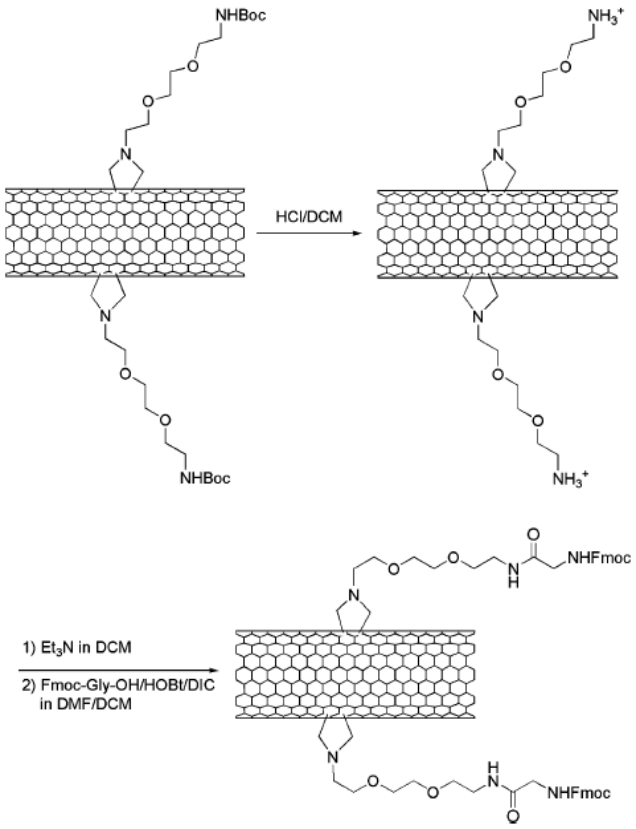

Figure **2.5** Reaction pathway for obtaining water-soluble ammonium- modified nanotubes.

Alvaro *et al.* [185] studied modified CNTs obtained by the thermal 1,3-dipolar cycloaddition of nitrile imines. Similarly the reaction under microwave conditions afforded the functionalized

material in 15 min (Figure **2.6**) [185a]. Photochemical studies showed that, by photoexcitation of the modified tubes, electron transfer took place from the substituents to the graphitic walls [185a].

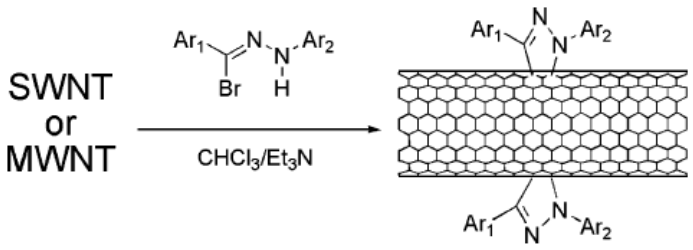

Figure **2.6** 1,3-Dipolar cycloaddition of nitrile imines to nanotubes.

Hayden *et.al*. [186] have investigated the interactions between MWNTs and diaminotetrazine. In their report they claim that a series of interactions occurred between tetrazines and carbon nanotubes including π–π interactions, cycloaddition (Diels–Alder) and cross-linking reactions. Finally, Delgado *et al.* [187] studied the reaction of a dienophile with the sidewalls of CNTs under microwave irradiation.

2.3.6 Amidation/Esterification Reactions

A carboxylation reaction is an oxidation reaction by an oxidizing acid, or a combination of acids such as a mixture of concentrated nitric and sulfuric acids [188]. This method is widely used for the purification of the raw CNTs [189]. This is achieved by inducing the opening of the tube caps as well as the formation of holes in the sidewalls. Liu *et al*. [190] demonstrated that carboxylate groups generated by the acid-cut nanotubes could be derivatized chemically by thiolalkylamines through an amidation reaction. In addition, Chen *et al*. [167] were the first to treat oxidized nanotubes with long chain alkylamines via acylation with the result that the functionalized material was soluble in organic solvents (Figure **2.7**). Direct thermal mixing of oxidized CNTs and alkylamines to produce functionalized material through the formation of zwitterions has also been reported [191].

Esterification reactions can produce soluble functionalized nanotubes (Figure **2.7**) [190]. Sano *et al.* reported that the condensation reaction of a carboxylate and other oxygenated functional groups produced perfect rings at the ends of the oxidized SWNT [192]. Using similar methodology Sun and coworkers [193-196] were able to attached lipophilic and hydrophilic dendrimers to oxidized CNTs via amidation or esterification reactions (Figure **2.8**). More recently, Shi *et al*. [197] have studied multifunctional dendrimer modified MWNTs for in vitro cancer cell targeting.

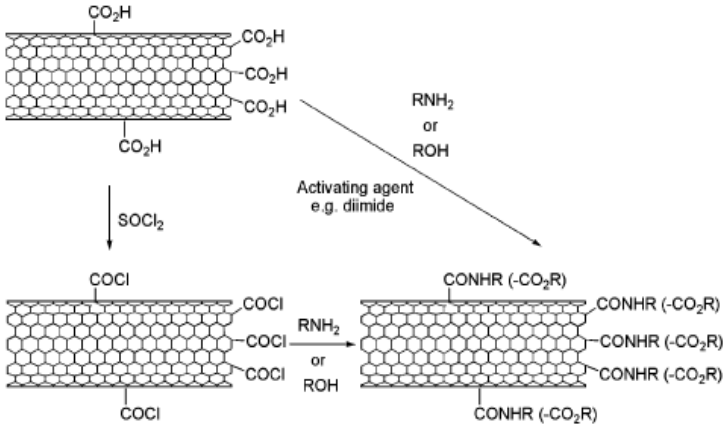

Figure **2.7** Derivatization reactions of acid-cut nanotubes through the defect sites of the graphitic surface.

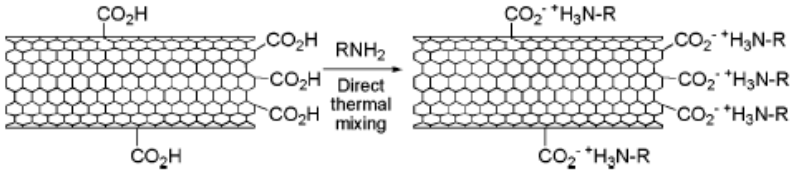

Figure **2.8** Direct thermal mixing of nanotubes and long chain amines.

2.3.7 Grafting of Polymers

The covalent reaction of CNTs with polymers is an important reaction since long polymer chains could help to dissolve the tubes in a wide range of solvents, even with a low degree of functionalization. There are two main methodologies for the covalent attachment of polymeric substances to the surface of nanotubes, namely "grafting to" and "grafting from" methods.

"Grafted to" is the synthesis of a polymer with a specific molecular weight, followed by end group transformation. Subsequently, this polymer chain is attached to the graphitic surface of CNTs. The "grafting from" method is based on the covalent immobilization of the polymer precursors on the surface of the CNTs and subsequent propagation of the polymer in the presence of monomeric species. In the next section a number of representative examples will be described.

Chemical reaction of CNTs and poly(methyl methacrylate) (PMMA) using the ultrasonication method of "grafting to" was reported by Koshio *et al*. [198] Similarly Wu *et al*. [199] have studied the nucleophilic reaction of polymeric carbanions with CNTs. In their studies organometallic reagents, such as sodium hydride or n-butyllithium, were mixed with poly(vinylcarbazole) or poly-(butadiene), and the resulting polymeric anions were grafted to the surface of CNTs. An alternative approach was reported by Blau *et al.* [200] using MWNTs functionalized with *n*-butyllithium and subsequently coupled with halogenated polymers. Finally, Qin *et al*. [201] reported a grafting of functionalized polystyrene to CNT via a cycloaddition reaction.

Jia *et al.* [202] have reported the "grafting from" of CNT-polymer composites by an *in situ* radical polymerization process. They further claimed that the double bonds of the nanotube surface were opened by initiator molecules and that the CNT surface played the role of grafting agent. Qin *et al.* [203a] have studied the grafting of polystyrenesulfonate (PSS) by *in situ* radical polymerization. In their study they reported that due to the negative charges of the polymer chain the resulting material dispersed in aqueous media. In a subsequent study [203b] they have reported polyvinyl pyridine (PVP)-grafted polymers from SWNTs by *in situ* polymerization. MWNTs grafted with poly(methyl methacrylate) have been prepared by emulsion polymerization of the monomer in the presence of a radical initiator [204a], or a cross-linking agent [204b]. Petrov *et al.* [205] have studied the modification of MWNTs with polyacrylonitrile chains by applying electrochemical polymerization of the monomer. More recently, Che *et al.* [206] reported the "grafting-from" approach to the synthesis of dendritic poly(amidoamine) (PAMAM) on SWNTs and they demonstrated the good dispersion and high reinforcement efficiency of these functionalized CNTs in an epoxy matrix. Finally, Yan *et. al*. [207] have

recently reported a novel approach to graft polyamide 6 (PA6) onto the surface of MWNTs. MWNTs were initially covalently functionalized with copoly(styrene-maleic anhydride) (SMA) via free radical polymerization followed by a ring-opening polymerization of ε-caprolactam to graft PA6 onto the surface of MWNTs. The resulting product had good dispensability in many organic solvents such as formic acid and melted ε-caprolactam.

2.3.8 Other reactions

Radical addition is another form of covalent sidewall functionalization of CNTs. This type of reaction has been intensively studied [170, 171, 208-211]. The formation of aryl radicals is triggered by an electron transfer between CNTs and the aryl diazonium salts in a self-catalyzed reaction [212-219]. A similar reaction was later described, utilizing water-soluble diazonium salts, which have been shown to react selectively with metallic CNTs [215].

Electrophilic [220] and inorganic compound [221-226] additions has also been extensively studied. Reaction of CNTs with *trans*-$IrCl(CO)(PPh_3)_2$ gave nanotube-metal complexes [227]. It was found that coordination mainly occurred at defect sites [227b, c]. The development of this chemistry was crucial for applications of SWNTs as a reusable catalyst support. Carbon nanotubes-metal interconnections were obtained by covalent attachment of CNTs to an inorganic metal complex treated in a ammonia atmosphere with [ruthenium-(4,4′-dicarboxy-2,2′-bipyridine)(2,2′-bipyridyl)$_2$]$(PF_6)_2$ [228].

Studies have also shown that ozonolysis reactions of single-walled CNTs can occur at r.t. [229] and at -78 °C [230]. On the other hand, pristine CNTs have been subjected to cleavage by chemical treatment with hydrogen peroxide or sodium borohydride [230a], yielding a high proportion of carboxylic acid/ester, ketone/aldhyde, and alcohol groups on the CNT surface. This substantially broadens the chemical reactivity of the carbon nanostructures. Furthermore, Cai *et al.* [231] have demonstrated the attachment of ozonized CNTs to gold surfaces by using conjugated oligo(phenylene ethynylenes).

Nucleophilic addition to CNTs has been studied by Basiuk *et al*. [232]. Their approach involved the use of a solvent-free amination of the closed caps of MWNTs with octadecylamine. It was

suggested that the addition took place only on the five membered rings of the graphitic network of the nanotubes and that the benzene rings were inert to direct amination. Lastly, to covalently modify CNTs with both alkyl and carboxylic groups, Chen *et al*. [232b] treated pristine material with *sec*-BuLi and subsequently with carbon dioxide.

An alternative approach to the chemical modification of CNTs, involving radiofrequency glow-discharge plasma activation, has been developed by Chen *et al*. [233]. In this study they treated CNTs with aldehyde plasma, and subsequently amino dextran chains were immobilized through the formation of Schiff-base linkages. The resulting material possessed a highly hydrophilic surface due to the presence of the polysaccharide-type moieties.

2.3.9 Mechanochemical functionalization

The ball-milling of MWNTs in reactive atmospheres has also been shown to produce short tubes containing different chemical functional groups such as amines, amides, thiols and mercaptans [234]. In an analogous strategy, SWNTs have been reacted with potassium hydroxide through a simple solid-phase milling technique [235]. Using the same approach, Li *et al*. [236] have studied the attachment of C_{60} fullerene to the graphitic network of CNTs.

2.4 The application of fullerene (C_{60}) and carbon nanotubes in solar cells

2.4.1 General introduction

Among the renewable energy sources, solar energy is of great importance. The Sun has always been the most powerful energy source for earth and it provides energy that is clean and environmentally friendly. Sunlight can be transformed into electricity using solar cells. Solar cells have applications in many different fields such as in calculators, solar lamps and can be used even on spacecraft and satellites. Historically, conventional solar cells were built from inorganic materials such as silicon. The efficiency of such conventional solar cells made from inorganic materials, for instance silicon crystals in solar cells, has reached 24% [237]. However, solar cells made from inorganic materials are generally expensive and require energy intensive processing techniques. For example, purification of silicon is difficult and much silicon is wasted

during purification. In addition, since the performance of silicon cells degrades as the temperature increases, the long lasting, concentrated operation of silicon cells requires a cooling system.

A lot of effort is being put into the development of new fabrication techniques using organic, [238], hybrid [239] and photoelectrochemical (dye sensitized) solar cells [240] which could act as alternatives to conventional silicon solar cells.

Organic solar cells mainly consist of two organic materials, an electron-donating material and an electron-accepting material that make a percolating structure with interpenetrating networks [241]. The realization that photoinduced charge transfer can occur from a conjugated polymer to fullerene derivatives has led the development of "bulk heterojunction" organic solar cells [242].

A hybrid solar cell is a combination of both organic and inorganic materials and therefore combines the unique properties of inorganic semiconductors with the film forming properties of the conjugated polymers [243]. Organic materials are generally inexpensive, easily processable and their functionality can be tailored by molecular design and chemical synthesis. On the other hand, inorganic semiconductors can be manufactured as nanoparticles. Inorganic semiconductor nanoparticles offer the advantage of having high absorption coefficients and size tunability. By varying the size of the nanoparticles the bandgap can be tuned and therefore the absorption range can be tailored [244].

In dye-sensitized solar cells (DSSC), combinations of several different materials, such as two transparent conducting oxide (TCO) substrates, and fluorine doped tin oxide (FTO) on glass or polymeric substrates, has been used [245, 246]. One TCO is a photo anode, composed of a sensitizer adsorbed onto the surface of the nanocrystalline semiconductor electrode (typically nanostructured TiO_2), and the other a photo inert counter electrode with a thin layer of a catalyst (for instance, platinum) sandwiching an electrolyte/relay medium (usually a solution containing the I_3^-/I^- pair). *n*-TiO_2 is the most employed semiconductor material in dye-sensitized photoelectrochemical solar cells due to its favorable energetics, stability, low price and easy process ability [247, 248]. Semiconductor colloids are typically obtained via a sol–gel process from titanium isopropoxide or directly from commercial TiO_2. The preparation of colloids from Degussa TiO_2 is easier and faster than from the isopropoxide hydrolysis method and results in

transparent to translucent semiconductor films [249]. A schematic presentation of the operational principles of a DSSC is given in Figure **2.9**.

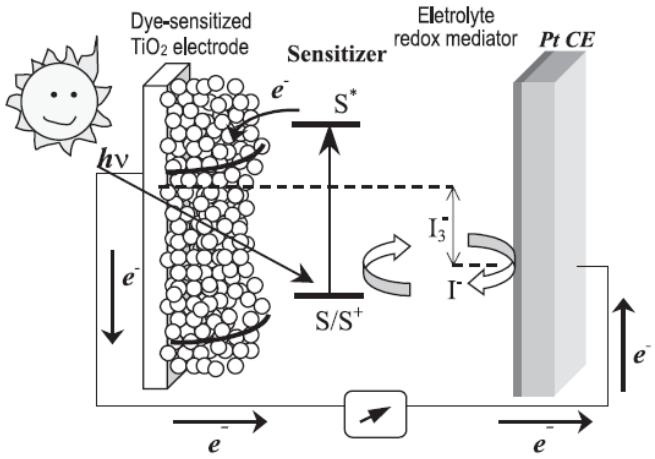

Figure **2.9** Operational principles of a dye sensitized solar cell [249b].

In the first step, the photoexcited sensitizer injects electrons into the conduction band of the semiconductor. The oxidized sensitizer (S+) is then quickly reduced back to S by the redox mediator couple, I_3^-/I^-, present in the electrolyte, it is regenerated at the counter electrode, concluding the redox cycle. The reduction of I_3^- is catalyzed *in situ* by Pt deposited on the surface of the counter electrode [249].

The photovoltaic characteristics of a solar cell can be evaluated from an *I–V* curve. The *I-V* curve is shifted down compared to the curve obtained in the dark (Figure **2.10**). In the dark, there is almost no current flowing, until the contacts start to inject heavily at a forward bias for voltages larger than the open circuit voltage. Under illumination, the current flows in the opposite direction compared to the injected current. At (a) in Figure **2.10** the maximum generated photocurrent flows under a short circuit current, while at (b) in Figure **2.10** the photo generated current is balanced at zero (flat band condition). Between (a) and (b), the device generates power. At a certain point, denoted as the maximum power point (MPP), the product between current and voltage, and hence the power output, is largest i.e. I_{mpp} X V_{mpp}= P_{max} [249].

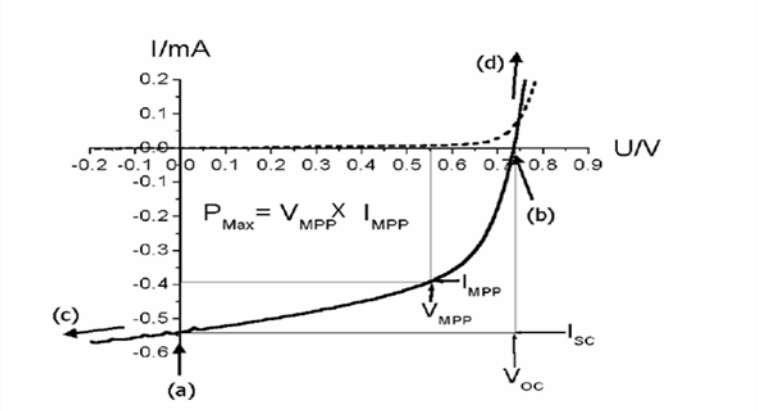

Figure **2.10** Current-voltage (*I-V*) curves of a solar cell (dark: dashed; illuminated: full line). The characteristic intersections with the abscissa and the ordinate are the open circuit voltage (V_{oc}) and the short circuit current (I_{sc}), respectively. The largest power output (P_{max}) is determined by the point where the product of voltage and current maximized. Division of P_{max} by the product of I_{sc} and V_{oc} yields the fill factor (FF) [249].

To determine the efficiency of a solar cell, this power needs to be compared with the incident light intensity. Typically, the fill factor is calculated as:

$$FF = \frac{Vmpp \times Impp}{Voc \times Isc}$$

Where V_{mpp} = voltage at maximum power point

I_{mpp} = current at maximum power point

to denote the part of the product of Voc and Isc, that can be used. Using this equation, the power conversion efficiency can be written as:

$$\eta = \frac{Pout}{Pin} = \frac{Impp \times Vmpp}{Pin} = \frac{FF \times Isc \times Voc}{Pin}$$

Where P_{out} = power output

P_{in} = power input

The most efficient photosensitizers have an intense absorption in the visible region, strong adsorption onto the semiconductor surface and efficient electron injection into the conduction band of the semiconductor. Moreover, the photosensitizers must be rapidly regenerated by the mediator layer in order to avoid electron recombination processes and be fairly stable, both in the ground and excited states. Many different compounds have been investigated for semiconductor sensitization, such as porphyrins [250, 251], phthalocyanines [252], coumarin 343 [253, 254], and carboxylated derivatives of anthracene [254, 255]. Among the photosensitizers investigated, transition metal complexes have been the best so far [256, 257].

Metal complex sensitizers usually have anchoring ligands and ancillary ligands. Anchoring ligands are responsible for the complex adsorption onto the semiconductor surface and are also often chromophoric groups (Figure **2.11**).

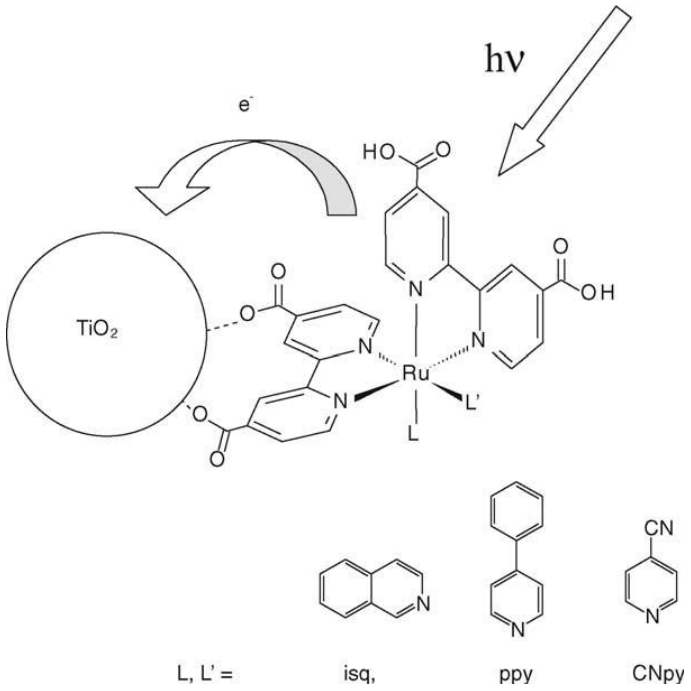

Figure **2.11** Schematic representation of interfacial electron transfer following light absorption for *cis*-[Ru(dcbH$_2$)$_2$LL'] with some ancillary ligands [258].

Polypyridinic complexes of d^6 metal ions show intense metal to ligand charge transfer (MLCT) bands in the visible region with potential interest for promoting charge injection processes to the conduction band of wide band gap semiconductors, such as TiO_2, SnO_2 and ZnO. The energies

of the MLCT states can be altered systematically by modifying the anchoring ligands as well as by changing the ancillary ligands or its substituents. The wide possibilities to tune the MLCT energy have led to the preparation of many different compounds that have been investigated for semiconductor sensitization. Among them, the best light-to-electricity conversion efficiency has been achieved by using ruthenium(II) polypyridyl complexes as TiO_2 sensitizers in dye-sensitized solar cells. Ruthenium polypyridinic complexes have been intensively employed as sensitizers due to their appropriate redox, spectroscopic, and excited-state properties [259]. In particular, ruthenium(II) complexes with carboxylic pyridine derivatives are able to react readily with oxide surfaces to form the corresponding esters [257], presenting efficient adsorption onto the semiconductor surface and improved light harvesting efficiency, leading to good results.

2.4.2 C_{60} fullerene in photo cells

Since the discovery of C_{60} fullerene [260] and its subsequent large scale production at the beginning of the 1990s [261], this molecule has drawn the attention of researchers for its utilization in materials science. The interaction of C_{60} with light has attracted considerable interest in the exploration of applications related to photophysical, photochemical and photoinduced charge transfer properties of [60]fullerene derivatives. Its unique electrochemical properties, with six reversible single-electron reduction waves [262], and its photophysical properties [263] make C_{60} an interesting molecule to study photo-driven redox phenomena. Photoinduced electron and energy transfer processes are of great significance since they govern natural photosynthesis, and considerable effort has been devoted to the construction of C_{60}-based molecular structures as artificial photosynthetic systems [264]. Moreover, Sariciftci *et al.* [265] demonstrated that a *n*-conjugated polymer was able to efficiently transfer electrons to the C_{60} core giving rise to long-lived charge separated states. Since then, intensive research programs have been focused on the utilization of fullerene derivatives acting as electron acceptors in organic solar cells.

Organic solar cells are based on the photosynthesis process in plants, in which the absorption of sunlight by the chlorophyll "dye" creates a charge separation, thus converting carbon dioxide, water in the presence of minerals into organic compounds and oxygen. Typically, solid-state heterojunctions are fabricated using p-type donor (D) and n-type acceptor (A) semiconductors. Organic [60]fullerene-based solar cells are fabricated by inserting the p-type and n-type materials between two different electrodes. One of the electrodes must be (semi-) transparent, often indium

tin oxide (ITO), but a thin metal layer can also be used. The other electrode is very often aluminium although calcium, magnesium, gold are also used (Figure **2.12**).

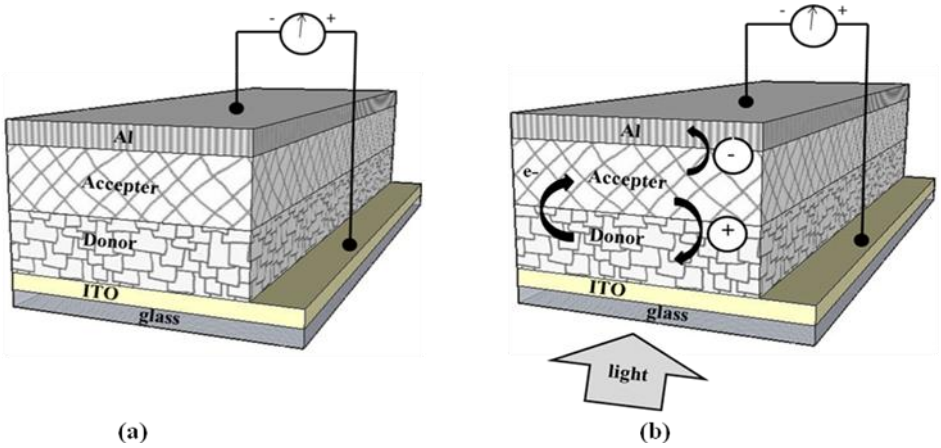

Figure **2.12** Representation of a donor–acceptor heterojunction: (a) structure of the solar cell; (b) under illumination, electron transfer from the donor to the acceptor and generation of excitons followed by charge separation and transport of carriers to the electrodes inducing a photocurrent.

The principal feature of a p-n heterojunction is built-in potential at the interface between both materials presenting a difference of electronegativities [266]. The promotion of an electron from the highest occupied molecular orbital (HOMO) [or the valence band (VB)] of the donor to the lowest unoccupied molecular orbital (LUMO) [or the conducting band (CB)] of the acceptor induced by the absorption of light generates an exciton at the interface of the junction [267]. The charge separation occurs at donor/accepter interfaces and free charge carriers are transported through semiconducting materials with the electron reaching the cathode (Al) and the hole reaching the anode (ITO) (Figure **2.13**).

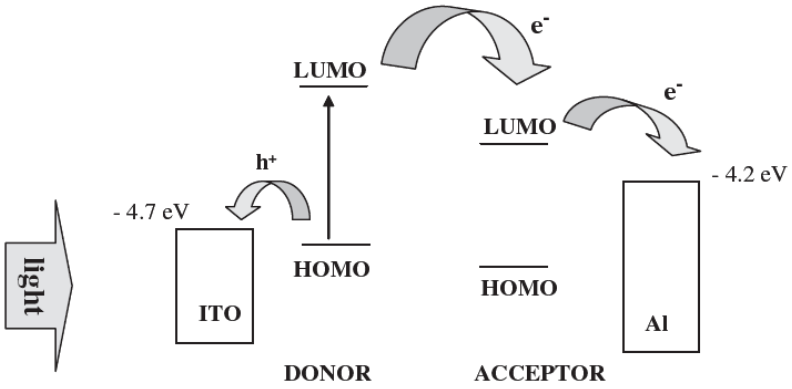

Figure **2.13** Theoretical principle of a donor–acceptor heterojunction. It is usually assumed that for a semiconductor the HOMO corresponds to the VB and the LUMO corresponds to the CB [267].

Miller *et al.* [268] indicated that solvent-cast films of [60]fullerene showed a photovoltaic response typical of n-type semiconductors. Similarly, Brabec *et al.* [269] reported in their studies that, after photo-excitation an ultra-fast photoinduced electron transfer from a conjugated polymer to C_{60} occurred in approximately 45 fs. This implies a large exchange integral of the excited state orbitals of donor and accepter molecules. Sariciftci *et al.* [270] and Morita *et al.* [271] independently reported the photophysical properties of blends composed of pristine C_{60} and MEH-PPV or poly(alkylthiophene) (PAT), respectively (Figure **2.14**).

The first hetero junction with a conjugated polymer and C_{60} was reported by Sariciftci *et al*. [270]. In their work under monochromatic illumination, a relatively high fill factor (FF) of 0.48 and a energy conversion efficiency of 0.04 % was reported. Moreover, it was demonstrated that the photocurrent increased by a factor of twenty when a bilayer photo-diode polymer/C_{60} was used instead of a single polymer layer device, indicating that [60]fullerene strongly assists the charge separation. Significant improvement was reported by Roman *et al.* [272] with a photodiode in which the aluminum electrode was used as electron collector and a PEDOT-PSS/ITO [(poly(3,4-ethylenedioxythiophene)-poly(styrenesulfonate)/indium tin oxide] electrode was used as hole collector.

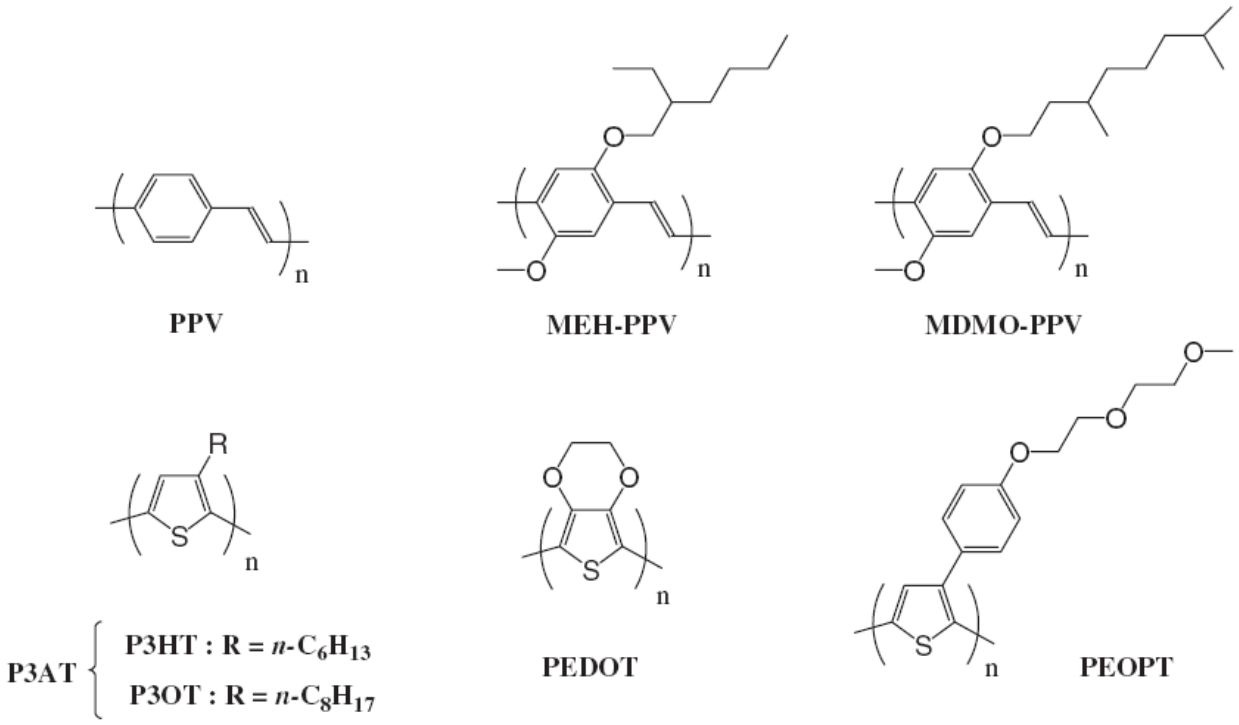

Figure **2.14** Molecular structures of some semiconducting conjugated polymers used in fullerene-based solar cells.

The "bulk-heterojunction" concept, first realized by Yu *et al*. [273], was a crucial and major breakthrough towards efficient-organic devices. It involved an interpenetrating network of a (p-type) donor conjugated polymer and C_{60} or another fullerene derivative as (n-type) acceptor material. The photoactive layers of those types of solar cells consist of blends of a conjugated polymer and a fullerene derivative (Figure **2.12**). The effective interaction between the donor and the acceptor compounds within bulk-heterojunction solar cells can take place in the entire device volume. Hence, the separated charge carriers are transported to the electrodes *via* an interpenetrating network. However, this kind of device is associated with the tendency, especially for pristine C_{60}, to phase separate and then to crystallize. This aggregation phenomenon imposes important consequences on the solubility of C_{60} within a conjugated polymer matrix.

The first example of this type of cell used a blend between MEH-PPV (poly[2-methoxy-5-(2'-ethyl-hexyloxy)-1,4-phenylene vinylene]) and [60]PCBM and it exhibited a PCE of 2.9 % under monochromatic low intensity light [273, 274]. However, there were concerns about a major difference of relative-acceptor strength between C_{60} and [60]PCBM. Pristine C_{60} appears to be a

poorer electron acceptor. The LUMO of C_{60} (-3.83 eV) is lower in energy than that of PCBM (-3.75 eV) [275, 315].

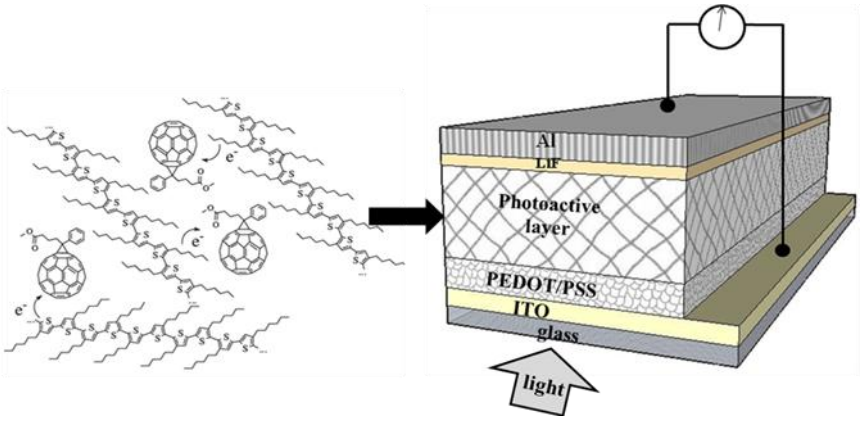

Figure **2.15** Schematic representation of a bulk-heterojunction solar cell with the ITO/PEDOT-SS/P3HT:[60]PCBM/LiF/Al device. The use of a LiF/Al electrode is now commonly adopted providing an ohmic contact between the metal and the organic layer [276].

In order to increase the efficiency of organic photovoltaic devices an alternative approach was reported by Baffreau *et al.* [277] and Gomez *et al.* [278]. In both studies the researchers reported C_{60}-antenna dyads that could absorb strongly in the visible light range. In this case, the dye could act as an antenna by absorption of sunlight with the aim of inducing an intramolecular energy transfer to the fullerene. Dendrimer based light-harvesting structures have also attracted attention, the peripheral chromophores being able to transfer the collected energy to the central core of the dendrimer. A fullerene core and peripheral oligophenylenevinylene (OPV) subunits appear as potentially interesting systems with light-harvesting properties [279].

Very recently, a visible light-absorbing nano-array integrating four C_{60} moieties and a single π-conjugated oligomer was synthesized [280]. It was demonstrated that pure oligomer-tetrafullerene gave no significant photovoltaic effect. However, when P3HT was incorporated in the device a photovoltic effect was noted; this phenomenon was explained by an energy transfer occurring between C_{60} units and the *n*-conjugated oligomer.

On the other hand, double-cable molecular systems, fullerene-based substituents that are grafted onto the conjugated polymer chain, were also explored in order to overcome some problems

associated with bulk-heterojunction systems. Limitations, such as limited miscibility of both donor and acceptor materials, especially because clusters of fullerenes can be formed within the photoactive film [281], so that the transport of electrons is located in separated domains, are avoided. In order to prevent such undesirable effects, a second molecular strategy was proposed by simply chemically linking the hole-conducting moiety to the electron-conducting fullerene subunit. This direct covalent bonding of different n-electron donors [282] and π-conjugated oligomeric systems [283] has emerged as a very active field of research to develop new organic photovoltaic devices. This has given rise to the synthesis of a huge number of dyads or triads involving donor groups covalently attached onto C_{60}.

In such systems, the effective donor-acceptor interfacial contact is maximized and the phase separation and clustering phenomena prevented as well. Basically, the realization of effective double-cable polymers brought the p-n heterojunction to the molecular level [281]. Double-cable materials could be consequently seen at the frontier with the molecular heterojunction. [284] They can exhibit characteristic electronic and excited-state properties, which make them promising candidates for the investigation of photoinduced electron transfer processes and long-lived charge-separated states.

2.4.3 Carbon nanotubes in solar cells

Carbon nanotubes offer a wide range of band gaps [285-287] to match the solar spectrum, enhanced optical absorption [288, 289] and reduced carrier scattering for hot carrier transport [290, 291]. The latter may even result in a near-ballistic transport in nanotubes with submicron-meter lengths [292]. Castrucci *et al.* [293] have demonstrated that MWNTs can generate photocurrent in the visible and ultraviolet spectral range. Recently, Cheong *et al.* [294] have investigated the photoresponsive conductance switching of MWNTs-SPO (SPO= spironaphthoxazines) under a 365 nm UV irradiation. In their study, they reported that during the cyclic irradiation of MWNTs-SPO by UV light the composites showed a reversible response, in which the change of HOMO–LUMO band gap in SPO strongly affects the conductivity of the MWNTs.

Khaziji *et al*. [295] have investigated the photo-electrochemical properties of single wall carbon nanotubes (SWNTs) and the photon-to-photocurrent efficiency (IPCE). However, the efficiency has remained low (about 0.15 %) due to rapid exciton annihilation [296]. On other hand, covalently linking of the desired molecular assemblies on the SWNTs walls was found to enhanc the photoconversion efficiency [297]. Results were also obtained from the dispersion of semiconducting quantum dots [298] and metallic nanoparticles [299] on SWNTs and MWNTs sidewalls.

Blending CNTs with conjugated polymers may not only yield electron acceptors but also allow the transferred electrons to be efficiently transported along their length, thus providing percolation paths [300]. Indeed, the extremely high surface area, ~1600 m^2/g, reported for purified SWNT [301] offers a tremendous opportunity for exciton dissociation. Since SWNTs have diameters of ~1 nm and lengths of ~1–10 μm, these materials exhibit very large aspect ratios ($>10^3$). Thus, percolation pathways could be established at low doping levels, providing the means for high electron mobility. Electrical conductivity data has validated that SWNT-doped polymer composites demonstrate extremely low percolation thresholds. For SWNT-epoxy composites, for example, the electrical conductivity has been claimed to rise by nearly 10^5 when SWNT concentrations of only 0.1–0.2 % are used [302]. Electrical and photoelectrical properties of CNT/conjugated polymer composites and interfaces have been investigated since the mid 90s [303-308]. A bulk heterojunction solar cells based on conjugated polymers, blended with multiwalled carbon nanotubes (MWNT) [309] and SWNTs [310-312] have been reported. For 1 % SWNT/poly-3-octyl-thiophene (P3OT) bulk heterojunction solar cells, high values of V_{oc} = 0.75 V were achieved and reasonably explained in terms of HOMO–LUMO electronic structures of P3OT and SWNTs [311]. However, the efficiency of the best SWNT/P3OT devices is well below 1 % due to a low photocurrent, mostly limited by incomplete phase separation and the lack of light absorption. Improvement of the light absorption was achieved by a dye (naphthalocyanine, NaPc) coating of CNTs that were blended with P3OT in a bulk heterojunction configuration [313]. For the same purpose, Jin and Dai suggested that instead of randomly mixing CNTs with polymers, a cell could contain a network of vertically aligned CNTs separated by vertical polymer layers [314].

2.5 References

1 A. G. Whittaker, E. J. Watts, R. S. Lewis, E. Anders, *Science*, **1980,** 209, 1512.

2 A. G. Whittaker, P. L. Kintner, *Carbon*, **1985**, 23, 255.

3 V. I. Kasatochkin, V. V. Korshak, Y. P. Kudryavtsev, A. M. Sladkov, I. E. Sterenberg, *Carbon*, **1973**, 11, 70.

4 M. S. Dresselhaus, J. Steinbeck, *Journal of the Japanese Carbon Society, Tanso,* **1988,** 132, 44.

5 M. S. Dresselhaus, G. Dresselhaus, P. C. Eklund, *Science of Fullerenes and Carbon Nanotubes* (Academic, New York **1996**).

6 H. W. Kroto, J. R. Heath, S. C. O'Brien, R. F. Curl, R. E. Smalley, *Nature,* **1985**, 18, 162.

7 S. Iijima, *Nature,* **1991**, 354, 56.

8 R. Saito, G. Dresselhaus, M. S. Dresselhaus, *Physical Properties of Carbon Nanotubes,* (Imperial College Press, London **1998**).

9 M. S. Dresselhaus, G. Dresselhaus, K. Sugihara, I. L. Spain, H. A. Goldberg, *Graphite Fibers and Filaments*, (Springer-Verlag: New York, **1988**).

10 S. Iijima, T. Ichihashi, *Nature,* **1993**, 363, 603.

11 D. S. Bethune, C. H. Kiang, M. S. de Vries, G. Gorman, R. Savoy, J. Vazquez, R. Beyers, *Nature,* **1993**, 363, 605.

12 C. H. Kiang, W. A. Goddard, R. Beyers, D. S. Bethune, *Carbon,* **1995**, 33, 903.

13 A. Thess, R. Lee, P. Nikolaev, H. Dai, P. Petit, J. Robert, C. Xu, Y. H. Lee, S. G. Kim, A. G. Rinzler, D. T. Colbert, G. E. Scuseria, D. Tomanek, J. E. Fischer, R. E. Smalley, *Science,* **1996**, 273, 483.

14 C. Journet, W. K. Maser, P. Bernier, A. Loiseau, M. Lamy de laChappelle, S. Lefrant, P. Deniard, R. Lee, J. E. Fischer, *Nature,* **1997**, 388, 756.

15 J.-C. Charlier, X. Gonze, J.-P. Michenaud, *Europhys. Lett.*, **1995**, 29, 43.

16 P. Gerhardt, S. Löffler, K. H. Homann, *Chem. Phys. Lett.*, **1987**, 137, 306.

17 W. Kratschmer, L. D. Lamb, K. Fostiropoulos, D. R. Huffman, *Nature,* **1990**, 347, 354.

18 D. E. Bradley, *Brit. J. Appl. Phys.*, **1954**, 5, 96.

19 W. A. Scrivens, J. M. Tour, *J. Org. Chem.*, **1992**, 57, 6932.

20 K. Kikuchi, N. Nakahara, M. Honda, S. Suzuki, K. Saito, H. Shiromaru, K. Yamauchi, I. Ikemoto, T. Kuramochi, *Chem. Lett.*, **1991**, 1607.

21 Z. M. Markovic, T. L. Jokic, B. M. Todorovic-Markovic, J. L. Blanusa, T. M. Nenadovic, *Fullerene Sci. Technol.*, **1997**, 5, 903.

22 R. Taylor, G. J. Langley, H. W. Kroto, D. R. M. Walton, *Nature*, **1993**, 366, 728.

23 D. E. Manolopoulos, J. C. May, S. E. Down, *Chem. Phys. Lett.*, **1991**, 181, 105.

24 P. W. Fowler, R. C. Batten, D. E. Manolopoulos, *J. Chem. Soc.*, *Faraday Trans.*, **1991**, 87, 3103.

25 J. M. Schulman, R. L. Disch, M. A. Miller, R. C. Peck, *Chem. Phys. Lett.*, **1987**, 141, 45.

26 H. P. Lüthi, J. Almlof, *Chem. Phys. Lett.*, **1987**, 135, 357.

27 G. E. Scuseria, *Chem. Phys. Lett.*, **1991**, 176, 423.

28 M. Haser, J. Almlof, G. E. Scuseria, *Chem. Phys. Lett.*, **1991**, 181, 497.

29 C. S. Yannoni, P. P. Bernier, D. S. Bethune, G. Meijer, J. R. Salem, *J. Am. Chem. Soc.*, **1991**, 113, 3190.

30 W. I. F. David, R. M. Ibberson, J. C. Matthewman, K. Prassides, T. J. S. Dennis, J. P. Hare, H. W. Kroto, R. Taylor, D. R. M. Walton, *Nature,* **1991**, 353, 147.

31 K. Hedberg, L. Hedberg, D. S. Bethune, C. A. Brown, H. C. Dorn, R. D. Johnson, M. De Vries, *Science,* **1991**, 254, 410.

32 S. Liu, Y.- J. Lu, M. M. Kappes, J. A. Ibers, *Science,* **1991**, 254, 408.

33 R. C. Haddon, L. E. Brus, K. Raghavachari, *Chem. Phys. Lett.*, **1986**, 125, 459.

34 R. C. Haddon, L. E. Brus, K. Raghavachari, *Chem. Phys. Lett.*, **1986**, 131, 165.

35 S. H. Yang, C. L. Pettiette, J. Conceicao, O. Cheshnovsky, R. E. Smalley, *Chem. Phys. Lett.*, **1987**, 139, 233.

36 L. Echegoyen, F. Diederich, L. E. Echegoyen, Electrochemistry of Fullerenes, in Fullerenes*: Chemistry, Physics, and Technology*, (Kadish, K. M., Ruoff, R. S., *Ed.*,Wiley, New York, **2000**, p. 1).

37 L. Echegoyen, L. E. Echegoyen, *Acc. Chem. Res.*, **1998**, 31, 593.

38 F. Arias, L. Echegoyen, S. R. Wilson, Q. Lu, Q. Y. Lu, *J. Am. Chem. Soc.*, **1995**, 117,1422.

39 R. C. Haddon, A. S. Perel, R. C. Morris, A. F. Hebard, *Appl. Phys. Lett.*, **1995**, 67, 121.

40 B. Narymbetov, A. Omerzu, V. V. Kabanov, M. Tokumoto, H. Kobayashi, D. Mihailovic, *Nature,* **2000**, 407, 883.

41 K. Mizoguchi, M. Machino, H. Sakamoto, T. Kawamoto, Tokumoto, *Phys. Rev. B,* **2001**, 6314.

42 (a) R. C. Haddon, *Science,* **1993**, 261, 1545. (b) P. Grant, *Nature*, **2001**, 413, 264. (c) E. Dagotto, *Science*, **2001**, 93, 2410.

43 R. Taylor, D. M. R. Walton, *Nature,* **1993**, 363, 685.

44 R. C. Haddon, S. Fang, A. M. Rao, P. C. Eklund, W. H. Lee, E. C. Dickey, E. A. Grulke, J. C. Pendergrass, A. Chavan, B. E. Haley, R. E. Smalley, *J. Mater. Res.,* **1998**, 13, 2423.

45 M. A. Hamon, M. E. Itkis, S. Niyogi, T. Alvaraez, C. Kuper, M. Menon, R. C. Haddon, *J. Am. Chem. Soc.*, **2001**, 123, 11292.

46 R. C. Haddon, *J. Am. Chem. Soc*., **1990**, 112, 3385.

47 P. W. Rabideau, A. Sygula, *Acc. Chem. Res*., **1996**, 29, 235.

48 L. T. Scott, M. S. Bratcher, S. Hagen, *J. Am. Chem. Soc.*, **1996**, 118, 8743.

49 R. C. Haddon, K. Raghavachari, *Tetrahedron,* **1996**, 52, 5207.

50 B. R. Weedon, R. C. Haddon, H. P. Spielmann, M. S. Meier, *J. Am. Chem. Soc*., **1999**, 121, 335.

51 G. J. Bodwell, J. N. Bridson, T. J. Houghton, J. W. J. Kennedy, M. R. Mannion, *Chem. Eur. J*., **1999**, 5, 1823.

52 D. Srivastava, D. W. Brenner, J. D. Schall, K. D. Ausman, M. Yu, R. S. Ruoff, *J. Phys. Chem. B*, **1999**, 103, 4330.

53 M. A. Yurovskaya, I. V. Trushkov, *Russ. Chem. Bull., Int. Ed*., **2002**, 51, 367.

54 S. H. Hoke II, J. Molstad, D. Dilettato, M. J. Jay, D. Carlson, B. Kahr, R. G. Cooks, *J. Org. Chem.*, **1992**, 57, 5069.

55 M. Tsuda, T. Ishida, T. Nogami, S. Kurono, M. Ohashi, *Chem. Lett.*, **1992**, 2333.

56 S. R. Wilson, N. Kaprinidis, Y. Wu, D. I. Schuster., *J. Am. Chem. Soc.*, **1993**, 115, 8495.

57 S. R. Wilson, Y. Wu, N. A. Kaprinidis, D. I. Schuster, C. J. Welch, *J. Org. Chem.*, **1993**, 58, 6548.

58 D. I. Schuster, J. Cao, N. Kaprinidis, Y. Wu, A. W. Jensen, Q. Lu, H. Wang, S. R. Wilson, *J. Am. Chem. Soc.*, **1996**, 118, 5639.

59 A. W. Jensen, A. Khong, M. Saunders, S. R. Wilson, D. I. Schuster, *J. Am. Chem. Soc.*, **1997**, 119, 7303.

60 J. L. Segura, N. Martin, *Chem. Soc. Rev.*, **2000**, 29, 13.

61 G.-W. Wang, K. Komatsu, Y. Murata, M. Shiro, *Nature*, **1997**, 387, 583.

62 K. Komatsu, G.-W. Wang, Y. Murata, T. Tanaka, K. Fujiwara, *J. Org. Chem.*, **1998**, 63, 9358.

63 M.-K. Keshavarz, B. Knight, G. Srdanov, F. Wudl, *J. Am. Chem. Soc.*, **1995**, 117, 11371.

64 Y. Murata, N. Kato, K. Fujiwara, K. Komatsu**,** *J. Org. Chem.*, **1999**, 64, 3483.

65 G. S. Forman, N. Tagmatarchis, H. Shinohara, *J. Am. Chem. Soc.*, **2002,** 124, 178.

66 N. Tagmatarchis, G. S. Forman, A. Taninaka, H. Shinohara, *Synlett.*, **2002**, 235.

67 M. Maggini, G. Scorrano, M. Prato, *J. Am. Chem. Soc.*, **1993**, 115, 9798.

68 M. Prato, M. Maggini, *Acc. Chem. Res.*, **1998**, 31, 519.

69 P. Wang, R. M. Metzger, B. Chen, *Thin Solid Films*, **1998**, 327, 96.

70 Z. Guo, Y. Li, J. Xu, Z. Mao, Y. Wu, D. Zhu, *Synth. Commun.*, **1998**, 28, 1957.

71 H. Murakami, M. Shirakusa, T. Sagara, N. Nakashima, *Chem. Lett.*, **1999,** 815.

72 Z. X. Ge, Y. L. Li, Z. X. Guo, Z. Q. Shi, D. B. Zhu, *Tetrahedron Lett.*, **1999**, 40, 5759.

73 Z. Guo, J. Yan, Y. Li, Z. Ge, D. Zhu, *Synth. Met.*, **1999**, 102**,** 1567.

74 L. Leo, G. Mele, G. Rosso, L. Valli, G. Vasapollo, D. M. Guldi, G. Mascolo, *Langmuir*, **2000**, 16, 4599.

75 S. Zhang, L. Gan, C. Huang, *Chem. Phys. Lett.*, **2000**, 331, 143.

76 V. Tomberli, T. Da Ros, S. Bosi, M. Prato, *Carbon*, **2000**, 38, 1551.

77 S. Bosi, T. Da Ros, S. Castellano, E. Banfi, M. Prato, *Bioorg. Med. Chem. Lett.*, **2000**, 10, 1043.

78 K. Kordatos, T. Da Ros, S. Bosi, E. Vàzquez, M. Bergamin, C. Cusan, F. Pellarini, V. Tomberli, B. Baiti, D. Pantarotto, *J. Org. Chem.*, **2001**, 66, 4915.

79 S. H. Kang, H. Ma, M. S. Kang, K. S. Kim, A. K. Y. Jen, M. H. Zareie, M. Sarikaya, *Angew. Chem., Int. Ed. Engl*., **2004**, 43, 1512.

80 A. B. Holmes, G. R. Stephenson, *Chem. Ind.*, **1994**, 303.

81 M. Maggini, G. Scorrano, A. Bianco, C. Toniolo, R. P. Sijbesma, F. Wudl, M. Prato. *J. Chem. Soc., Chem. Commun*., **1994**, 305.

82 A. Bianco, F. Gasparrini, M. Maggini, D. Misiti, A. Polese, M. Prato, G. Scorrano, C. Toniolo, C. Villani, *J. Am. Chem. Soc*., **1997**, 119, 7550.

83 A. Bianco, M. Maggini, G. Scorrano, C. Toniolo, G. Marconi, F. Gasperini, D. Misiti, M. Prato. *J. Am. Chem. Soc.*, **1996**, 118, 4072.

84 A. Bianco, T. Bertolini, M. Crisma, G. Valle, C. Toniolo, M. Maggini, G. Scorrano, M. Prato, *J. Pept. Res.*, **1997**, 50, 159.

85 A. Bianco, V. Lucchini, M. Maggini, M. Prato, G. Scorrano, C. Toniolo, *J. Pept. Sci.*, **1998**, 4, 364.

86 F. Langa, P. de la Cruz, A. de la Hoz, A. Diaz-Ortiz , E. Diez-Barra, *Contemp. Org. Synth*., **1997**, 373.

87 (a) V. M. Rotello, J. B. Howard, T. Yadav, M. M. Conn, E. Viani, L. M. Giovane, A. L. Lafleur, *Tetrahedron Lett*., **1993**, 34, 1561; (b) M. Tsuda, T. Ishida, T. Nogami, S. Kurono M. Ohashi, *J. Chem. Soc., Chem., Commun*., **1993**, 1296.

88 (a) M. F. Meidine, A. G. Avent, A. D. Darwish, H. W. Kroto, O. Ohashi, R. Taylor, D. R. M. Walton, *J. Chem. Soc., Perkin Trans.*, **1994**, 1189, (b) H. Takeshita, J.-F. Liu, N. Kato, A. Mori, R. Isobe, *Chem. Lett*., **1995**, 24, 377, (c) S. R. Wilson, M. E. Yurchenko, D. I. Schuster, A. Khong, M. Saunders, *J. Org. Chem*., **2000**, 65, 2619.

89 (a) J. A. Schluter, J. M. Seaman, S. Taha, H. Cohen, K. R. Lykke, H. H. Wang, J. M. Williams, *J. Chem. Soc., Chem. Commun*., **1993**, 972; (b) K. Komatsu, Y. Murata, N. Sugita, K. Takeuchi, T. S. M. Wan, *Tetrahedron Lett*., **1993**, 34, 8473.

90 P. M. Allemand, G. Srdanov, A. Koch, K. Khemani, F. Wudl, Y. Rubin, F. Diederich, M. M. Alvarez, S. J. Anz, R. L. Whetten, *J. Am. Chem. Soc.*, **1991**, 113, 2780.

91 U. Becker, G. Denninger, V. Dyakonov, B. Gotschy, H. Klos, G. Rösler, A. Hirsch, H. inter, *Europhys. Lett.*, **1993**, 21, 267.

92 V. Dyakonov, G. Rosler, H. Klos, B. Gotschy, G. Denninger, A. Hirsch, *Synth. Methods*, **1993**, 56, 3214.

93 H. Moriyama, H. Kobayashi, A. Kobayashi, T. Watanabe, *J. Am. Chem. Soc.*, **1993**, 115, 1185.

94 A. Penicaud, A. Perez-Benitez, R. Gleason, V. E. Munoz, P. R. Escudero, *J. Am. Chem. Soc.*, **1993**, 115, 10392.

95 C. A. Foss, D. L. Feldheim, D. R. Lawson, P. K. Dorhout, C. M. Elliott, C. R. Martin, B. A. Parkinson, *J. Electrochem. Soc.*, **1993**, 140, L84.

96 B. Miller, J. M. Rosamilia, *J. Chem. Soc., Faraday Trans.*, **1993**, 89, 273.

97 C. Caron, R. Subramanian, F. D'Souza, J. Kim, W. Kutner, M. T. Jones, K. M. Kadish, *J. Am. Chem. Soc.*, **1993**, 115, 8505.

98 E. Allard, L. Riviere, J. Delaunay, D. Rondeau, D. Dubois, J. Cousseau, *Proc. Electrochem. Soc.*, **2000**, 2000, 88.

99 E. Allard, J. Delaunay, F. Cheng, J. Cousseau, J. Orduna, J. Garin, *Org. Lett.*, **2001**, 3, 3503.

100 E. Allard, J. Delaunay, J. Cousseau, *Org. Lett.,* **2003**, 5, 2239.
101 S. Fukuzumi, T. Suenobu, T. Hirasaka, R. Arakawa, K. M. Kadish, *J. Am. Chem. Soc.,* **1998**, 120, 9220.
102 Y. Ederle, C. Mathis, *Macromolecules,* **1997**, 30, 4262.
103 Z. Wang, M. S. Meier, *J. Org. Chem.,* **2003**, 68, 3043.
104 (a) C. A. Reed, R. D. Bolskar, *Chem. Rev.,* **2000**, 100, 1075. (b) T. Yildirim, O. Zhou, J. E. Fischer, *Phys. Chem. Mater.,* **2000**, 23, 23. (c) T. Yildirim, O. Zhou, J. E. Fischer, *Phys. Chem. Mater.,* **2000**, 23, 67. (d) T. Yildirim, O. Zhou, J. E. Fischer, *Phys. Chem. Mater.,* **2000**, 23, 249.
105 W. K. Fullagar, I. R. Gentle, G. A. Heath, J. W. White, *J. Chem. Soc., Chem. Commun.,* **1993**, 525.
106 (a) S. Margadonna, K. Prassides, *J. Solid State Chem.,* **2002**, 168, 639. (b) O. Gunnarsson, *Rev. Mod. Phys.,* **1997**, 69, 575. (c) Y. Iwasa, T. Takenobu, *J. Phys. Cond. Mater.,* **2003**, 15, 495. (d) Y. Chen, F. Stepniak, J. H. Weaver, L. P. F. Chibante, R. E. Smalley, *Phys. Rev. B,* **1992**, 45, 8845. (e) A. R. Kortan, N. Kopylov, S. Glarum, E. M. Gyorgy, A. P. Ramirez, R. M. Fleming, F. A. Thiel, R. C. Haddon, *Nature*, **1992**, 355, 529. (f) A. R. Kortan, N. Kopylov, E. Ozdas, A. P. Ramirez, R. M. Fleming, R. C. Haddon, *Chem. Phys. Lett.,* **1994**, 223, 501. (g) A. R. Kortan, N. Kopylov, S. Glarum, E. M. Gyorgy, A. P. Ramirez, R. M. Fleming, O. Zhou, F. A. Thiel, P. L. Trevor, R. C. Haddon, *Nature,* **1992**, 360, 566. (h) M. Bänitz, M. Heinze, K. Lüders, H. Werner, R. Schlögl, M. Weiden, G. Sparn, F. Steglich, *Solid State Commun.,* **1995**, 96, 539. (i) C. M. Brown, S. Taga, B. Gogia, K. Kordatos, S. Margadonna, K. Prassides, Y. Iwasa, K. Tanigaki, A. N. Fitch, P. Pattison, *Phys. Rev. Lett.,* **1999**, 83, 2258. (j) Y. Iwasa, H. Hayashi, T. Furudate, T. Mitani, *Phys. Rev. B,* **1996**, 54, 14960.
107 Y. Iwasa, M. Kawaguchi, H. Iwasaki, T. Mitani, N. Wada, T. Hasegawa, *Phys. Rev. B,* **1998**, 57, 13395.
108 G. K. Wertheim, D. N. E. Buchanan, J. E. Rowe, *Chem. Phys. Lett.,* **1993**, 206, 193.
109 P. Boulas, R. Subramanian, W. Kutner, M. T. Jones, K. M. Kadish, *J. Electrochem. Soc.,* **1993**, 140, L130.
110 (a) P. J. Fagan, P. J. Krusic, D. H. Evans, S. A. Lerke, E. Johnston, *J. Am. Chem. Soc.,* **1992**, 114, 9697. (b) M. Keshavarz-K, B. Knight, G. Srdanov, F. Wudl, *J. Am. Chem. Soc.,* **1995**, 117, 11371. (c) Y. Murata, K. Komatsu, T. S. M. Wan, *Tetrahedron Lett.,* **1996**, 37, 7061. (d) H. Nagashima, H. Terasaki, E. Kimura, K. Nakajima, K. Itoh, *J. Org. Chem.,* **1994**, 59, 1246. (e) H. Nagashima, H. Terasaki, Y. Saito, K. Jinno, K. Itoh, *J. Org. Chem.,* **1995**, 60, 4966. (f) Y. Murata, K. Motoyama, K. Komatsu, T. S. M. Wan, *Tetrahedron,* **1996**, 52, 5077.
111 H. Okamura, Y. Murata, M. Minoda, K. Komatsu, T. Miyamoto, T. S. M. Wan, *J. Org. Chem.* **1996**, 61, 8500.
112 R. Kunieda, M. Fujitsuka, O. Ito, M. Ito, Y. Murata, K. Komatsu, *J. Phys. Chem. B,* **2002**, 106, 7193.

113 Y. Murata, M. Ito, K. Komatsu, *J. Mater. Chem.*, **2002**, 12, 2009.
114 P. Timmerman, H. L. Anderson, R. Faust, J.-F. Nierengarten, T. Habicher, P. Seiler, F. Diederich, *Tetrahedron*, **1996**, 52, 4925.
115 (a**)** A. Hirsch, Q. Li, F. Wudl, *Angew. Chem., Int. Ed. Engl*., **1991**, 103, 1339. (b) R. Seshadri, A. Govindaraj, R. Nagarajan, T. Pradeep, C. N. R. Rao, *Tetrahedron Lett.*, **1992**, 33, 2069. (c) A. L. Balch, B. Cullison, W. R. Fawcett, A. S. Ginwalla, M. M. Olmstead, K. Winkler, *J. Chem. Soc., Chem. Commun.*, **1995**, 2287. (d) G. Schick, K.-D. Kampe, A. Hirsch, *J. Chem. Soc., Chem. Commun.*, **1995**, 2023. (e) A. Skiebe, A. Hirsch, H. Klos, B. Gotschy, *Chem. Phys. Lett.*, **1994**, 220, 138.
116 K.-D. Kampe, N. Egger, M. Vogel, *Angew. Chem. Inr. Ed. Engl.*, **1993**, 32, 1174.
117 S. Yamago, M. Yanagawa, H. Mukai, E. Nakamura, *Tetrahedron*, **1996**, 52, 5091.
118 S. Yamago, M. Yanagawa, E. Nakamura, *J. Chem. Soc., Chem. Commun.*, **1994**, 2093.
119 (a) K. E. Geckeler, S. Samal, *Polym. Int.*, **1999**, 48, 743. (b) M. Prato, *Top. Curr. Chem.*, **1999**, 199, 173 (c) M. S. Meier, *Springer Ser. Mater. Sci.*, **2000**, 38, 369.
120 K. E. Geckeler, S. Samal, *Polym. Int.*, **1999**, 48, 743.
121 A. Hirsch, *Adv. Mater.*, **1993**, 5, 859.
122 T. Suzuki, Q. Li, K. C. Khemani, F. Wudl, O. Almarsson, *J. Am. Chem. Soc.*, **1992**, 114, 7300.
123 D. E. Bergbreiter, H. N. Gray, *J. Chem. Soc., Chem. Commun.*, **1993**, 645.
124 E. T. Samulski, J. M. DeSimone, M. O. Hunt, Jr., Y. Z. Menceloglu, R. C. Jarnagin, G. A. York, K. B. Labat, H. Wang, *Chem. Mater.*, **1992**, 4, 1153.
125 Y. Ederle, C. Mathis, *Macromolecules*, **1997**, 30, 2546.
126 Y. Ederle, D. Reibel, C. Mathis, *Synth. Methods*, **1996**, 77, 139.
127 A. O. Patil, G. W. Schriver, B. Carstensen, R. D. Lundberg, *Polym. Bull.*, **1993**, 30, 187.
128 K. E. Geckeler, A. Hirsch, *J. Am. Chem. Soc.*, **1993**, 115, 3850.
129 C. Weis, C. Friedrich, R. Mülhaupt, H. Frey, *Macromolecules*, **1995**, 28, 403.
130 N. Manolova, I. Rashkov, F. Beguin, H. van Damme, *J. Chem. Soc., Chem. Commun.*, **1993**, 1725.
131 Y.-P. Sun, B. Liu, D. K. Moton, *Chem. Commun.*, **1996**, 2699.
132 Z. Li, J. Qin, *J. Appl. Polym. Sci.*, **2003**, 89, 2068.
133 Y.-P. Sun, C. E. Bunker, B. Liu, *Chem. Phys. Lett.*, **1997**, 272, 25.
134 S. Samal, B. -J. Choi, K. E. Geckeler, *Chem. Commun.*, **2000**, 1373.
135 (a) J. L. Bahr, J. M. Tour, *J. Mater. Chem.*, **2002**, 12, 1952. (b) C. A. Dyke, J. M. Tour, *Chem. Eur. J.*, **2004**, 10, 812. (c) C. A. Dyke, J. M. Tour, *J. Phys. Chem. A*, **2004**, 108, 11151.
136 S. B. Sinnott, *J. Nanosci. Nanotechnol.*, **2002**, 2, 113.
137 (a) Y.-P. Sun, K. Fu, Y. Lin, W. Huang, *Acc. Chem. Res.*, **2002**, 35, 1096. (b) K. Fu, Y.-P. Sun, *J. Nanosci. Nanotechnol.*, **2003**, 3, 351.
138 S. Niyogi, M. A. Hamon, H. Hu, B. Zhao, P. Bhowmik, R. Sen, M. E. Itkis, R. C. Haddon, *Acc. Chem. Res*., **2002**, 35, 1105.

139 J. J. Davis, K. S. Coleman, B. R. Azamian, C. B. Bagshaw, M. L. H. Green, *Chem. Eur. J.*, **2003**, 9, 3732.

140 R. Andrews, D. Jacques, D. Qian, T. Rantell, *Acc. Chem. Res.*, **2002**, 35, 1008.

141 L. Meng, C. Fu, Q. Lu, *Pro. Nat. Sci*., **2009**, 19, 801.

142 T. Nakajima, S. Kasamatsu, Y. Matsuo, *Eur. J. Solid State Inorg. Chem.*, **1996**, 33.

143 A. Hamwi, H. Alvergnat, S. Bonnamy, F. Beguin, *Carbon*, **1997**, 35, 723.

144 E. T. Mickelson, C. B. Huffman, A. G. Rinzler, R. E. Smalley, R. H. Hauge, J. L. Margrave, *Chem. Phys. Lett.*, **1998**, 296, 188.

145 (a) H. Touhara, F. Okino, *Carbon*, **2000**, 38, 241. (b) Z. Gu, H. Peng, R. H. Hauge, R. E. Malley, J. L. Margrave, *Nano Lett.*, **2002**, 2, 1009.

146 (a) N. F. Yudanov, A. V. Okotrub, Y. V. Shubin, L. I. Yudanova, L. G. Bulusheva, A. L. Chuvilin, J. M. Bonard, *Chem. Mater.*, **2002**, 14, 1472. (b) H. F. Bettinger, K. N. Kudin, G. E. Scuseria, *J. Am. Chem. Soc.*, **2001**, 123, 12849. (c) K. N. Kudin, H. F. Bettinger, G. E. Scuseria, *Phys. Rev. B,* **2001**, 63, 045413.

147 (a) H. F. Bettinger, *Org. Lett.*, **2004**, 6, 731. (b) G. Van Lier, C. P. Ewels, F. Zuliani, A. De Vita, , J.-C. Charlier. *J. Phys. Chem. B,* **2005**, 109, 6153. (c) M. J. Root, *Nano Lett.*, **2002**, 2, 541.

148 (a) R. L. Jaffe, *J. Phys. Chem. B,* **2003**, 107, 10378. (b) N. G. Lebedev, I. V. Zaporotskova, L. A. Chernozatonskii, *Microelec. Engin.*, **2003**, 69, 511.

149 K. F. Kelly, I. W. Chiang, E. T. Mickelson, R. H. Hauge, J. L. Margrave, X. Wang, G. E. Scuseria, C. Radloff, N. J. Halas, *Chem.Phys. Lett.*, **1999**, 313, 445.

150 (a) U. Dettlaff-Weglikowska, V. Skakalova, J. Meyer, J. Cech, B. G. Mueller , S. Roth, *Curr. Appl. Phys.*, **2007**, 7, 42. (b) L. Valentini, D. Puglia, F. Carniato, E. Boccaleri, L. Marchese, J. M. Kenny, *Comp. Sci. Tech.*, **2008**, 68, 1008. (c)V. N. Khabashesku, W. E. Billups, J. L. Margrave, *Acc. Chem.Res.*, **2002**, 35, 1087.

151 (a) J. L. Stevens, A. Y. Huang, H. Peng, I. W. Chiang, V. N. Khabashesku, J. L.Margrave, *Nano Lett.*, **2003**, 3, 331. (b) E. Unger, A. Graham, F. Kreupl, M. Liebau, W. Hoenlein, *Curr. Appl. Phys.*, **2002**, 2, 107. (c) P. J. Boul, J. Liu, E. T. Mickelson, C. B. Huffman, L. M. Ericson, I. W. Chiang, K. A. Smith, D. T. Colbert, R. H. Hauge, J. L. Margrave, R. E. Smalley, *Chem. Phys. Lett.*, **1999**, 310, 367.

152 R. K. Saini, I. W. Chiang, H. Peng, R. E. Smalley, W. E. Billups, R. H. Hauge, J. L. Margrave, *J. Am. Chem. Soc.*, **2003**, 125, 3617.

153 L. Zhang, V. U. Kiny, H. Peng, J. Zhu, R. F. M. Lobo, J. L. Margrave, V. N. Khabashesku, *Chem. Mater.*, **2004**, 16, 2055.

154 E. T. Mickelson, I. W. Chiang, J. L. Zimmerman, P. Boul, J. Lozano, J. Liu, R. E. Smalley, R. H. Hauge, J. L. Margrave, *J. Phys. Chem. B,* **1999**, 103, 4318.

155 W. Zhao, C. Song, B. Zheng, J. Liu, T. Viswanathan, *J. Phys. Chem. B,* **2002**, 106, 293.

156 P. E. Pehrsson, W. Zhao, J. W. Baldwin, C. Song, J. Liu, S. Kooi, B. Zheng, *J. Phys. Chem. B,* **2003**, 107, 5690.

157 P. R. Marcoux, J. Schreiber, P. Batail, S. Lefrant, J. Renouard, G. Jacob, D. Albertini, J.-Y. Mevellec, *Phys. Chem. Chem. Phys.*, **2002**, 4, 2278.

158 S. Pekker, J.-P. Salvetat, E. Jakab, J.-M. Bonard, L. Forro, *J. Phys.Chem. B*, **2001**, 105, 7938.

159 B. N. Khare, M. Meyyappan, A. M. Cassell, C. V. Nguyen, J. Han, *Nano Lett.*, **2002**, 2, 73.

160 B. N. Khare, M. Meyyappan, J. Kralj, P. Wilhite, M. Sisay, H. Imanaka, J. Koehne, C. W. Baushchlicher, *Appl. Phys. Lett.*, **2002**, 81, 5237.

161 K. S. Kim, D. J. Bae, J. R. Kim, K. A. Park, S. C. Lim, J.-J. Kim, W. B. Choi, C. Y. Park, Y. H. Lee, *Adv. Mater.*, **2002**, 14, 1818.

162 B. Khare, M. Meyyappan, M. H. Moore, P. Wilhite, H. Imanaka, B. Chen, *Nano Lett.*, **2003**, 3, 643.

163 C. Liu, Y. Y. Fan, M. Liu, H. T. Cong, H. M. Cheng, M. S. Dresselhaus, *Science*, **1999**, 286, 1127.

164 S. J. Yang, J. Y. Choi, H. K. Chae, J. H. Cho, K. S. Nahm, C. R. Park, *Chem. Mater.*, **2009**, 21, 1893.

165 Y. Chen, R. C. Haddon, S. Fang, A. M. Rao, P. C. Eklund, W. H. Lee, E. C. Dickey, E. A. Grulke, J. C. Pendergrass, A. Havan, B. E. Haley, R. E. Smalley, *J. Mater. Res.*, **1998**, 13, 2423.

166 J. Chen, M. A. Hamon, H. Hu, Y. Chen, A. M. Rao, P. C. Eklund, R. C. Haddon, *Science*, **1998**, 282, 95.

167 W. H. Lee, S. J. Kim, W. J. Lee, J. G. Lee, R. C. Haddon, P. J. Reucroft, *Appl. Surf. Sci.*, **2001**, 181, 121

168 K. Kamaras, M. E. Itkis, H. Hu, B. Zhao, R. C. Haddon, *Science*, **2003**, 301, 1501.

169 H. Hu, B. Zhao, M. A. Hamon, K. Kamaras, M. E. Itkis, R. C. Haddon, *J. Am. Chem. Soc.*, **2003**, 125, 14893.

170 (a) A. Hirsch, *Angew. Chem., Int. Ed.*, **2002**, *41*, 1853. (b) A. Hirsch, O. Vostrowsky, *Top. Curr. Chem.*, **2005**, 245, 193.

171 M. Holzinger, O. Vostrovsky, A. Hirsch, F. Hennrich, M. Kappes, R. Weiss, F. Jellen, *Angew., Chem. Int. Ed.*, **2001**, 40, 4002.

172 M. Holzinger, J. Abraham, P. Whelan, R. Graupner, L. Ley, F. Hennrich, M. Kappes, A. Hirsch, *J. Am. Chem. Soc.*, **2003**, 125, 8566.

173 M. Holzinger, J. Steinmetz, D. Samaille, M. Glerup, M. Paillet, P. Bernier, L. Ley, R. Graupner, *Carbon*, **2004**, 42, 941.

174 (a) M. J. Moghaddam, S. Taylor, M. Gao, S. Huang, L. Dai, M. J. McCall, *Nano Lett.*, **2004**, 4, 89.

175 (a) X. Lu, F. Tian, Q. Zhang, *J. Phys. Chem. B*, **2003**, *107*, 8388. (b) Y.-Y. Chu, M. -D. Su, *Chem. Phys. Lett.*, **2004**, 394, 231.

176 H. S. Kang, *J. Chem. Phys.*, **2004**, 121, 6967.

177 V. Georgakilas, K. Kordatos, M. Prato, D. M. Guldi, M. Holzinger, A. Hirsch, *J. Am. Chem. Soc.*, **2002**, 124, 760.

178 N. Tagmatarchis, M. Prato, *J. Mater. Chem.*, **2004**, 14, 437.

179 (a) A. Bianco, M. Prato, *Adv. Mater.*, **2003**, 15, 1765. (b) A. Bianco, *Exp. Opin. Drug Deliv.*, **2004**, 1, 57. (c) A. Bianco, K. Kostarelos, C. D. Partidos, M. Prato, *Chem. Commun.*, **2005**, 571. (d) K. Kostarelos, L. Lacerda, C. D. Partidos, M. Prato, A. Bianco, *J. Drug Deliv. Sci. Technol.*, **2005**, 15, 41.

180 V. Georgakilas, N. Tagmatarchis, D. Pantarotto, A. Bianco, J.-P. Briand, M. Prato, *Chem. Commun.*, **2002**, 3050.

181 D. Pantarotto, C. D. Partidos, R. Graff, J. Hoebeke, J.-P. Briand, M. Prato, A. Bianco, *J. Am. Chem. Soc.*, **2003**, 125, 6160.

182 D. Pantarotto, C. D. Partidos, J. Hoebeke, F. Brown, E. Kramer, J.-P. Briand, S. Muller, M. Prato, A. Bianco, *Chem. Biol.*, **2003**, 10, 961.

183 D. Pantarotto, J.-P. Briand, M. Prato, A. Bianco, *Chem. Commun.*, **2004**, 16.

184 (a) D. Pantarotto, R. Singh, D. McCarthy, M. Erhardt, J.-P. Briand, M. Prato, K. Kostarelos, A. Bianco, *Angew. Chem., Int. Ed.*, **2004**, 43, 5242. (b) A. Bianco, J. Hoebeke, S. Godefroy, O. Chaloin, D. Pantarotto, J.-P. Briand, S. Muller, M. Prato, C. D. Partidos, *J. Am. Chem. Soc.*, **2005**, 127, 58. (c) R. Singh, D. Pantarotto, D. McCarthy, O. Chaloin, J. Hoebeke, C. D. Partidos, J.-P. Briand, M. Prato, A. Bianco, K. Kostarelos, *J. Am. Chem. Soc.*, **2005**, 127, 4388.

185 (a) M. Alvaro, P. Atienzar, P. de la Cruz, J. L. Delgado, H. Garcia, F. Langa, *J. Phys. Chem. B*, **2004**, 108, 12691. (b) Y. Wang, Z. Iqbal, S. Mitra, *Carbon*, **2005**, 43, 1015.

186 H. Hayden, Y. K. Gun'ko, T. S. Perova, *Chem. Phys. Lett*., **2007**, 435, 84.

187 (a) J. L. Delgado, P. de la Cruz, F. Langa, A. Urbina, J. Casado, J. T. L. Navarrete, *Chem. Commun.*, **2004**, 1734. (b) X. Lu, F. Tian, N. Wang, Q. Zhang, *Org. Lett.*, **2002**, 4, 4313.

188 (a) B. X. Yang, J. H. Shi, K. P. Pramoda, S. H. Goh, *Nanotechnology*, **2007**, 18, 125606. (b) H.W. Goh, S. H. Goh, G. Q. Xu, K. P. Pramoda, W.D. Zhang, *Chem. Phys. Lett.*, **2003,** 373, 277. (c) T. Ramanathan, F. T. Fisher, R. S. Ruoff, L. C. Brinson, *Chem. Mater.*, **2005**,17, 1290.

189 (a) J. A. Mapkar, G. Iyer, M. R. Coleman, *Appl. Surf. Sci*., **2009**, 255, 4806. (b) Z. Wang, Q. Liu, H. Zhu, H. Liu, Y. Chen, M. Yang, *Carbon*, **2007**, 45, 285. (c) V. Ivanov, A. Fonseca, J. B. Nagy, A. Lucas, P. Lambin, D. Bernaerts, X. B. Zhang, *Carbon*, **1995**, 33, 1727. (c) J. Liu, A. G. Rinzler, H. J. Dai, J. H. Hafner, R. K. Bradley, P. J. Boul, A. Lu, T. Iverson, K. Shelimov, C. B. Huffman, F. Rodriguez-Macias, Y. S. Shon, T. R. Lee, D. T. Colbert, R. E. Smalley, *Science*, **1998**, 280, 1253.

190 M. A. Hamon, H. Hui, P. Bhowmik, H. M. E. Itkis, R. C. Haddon, *Appl. Phys. A*, **2002**, 74, 333.

191 J. Chen, A. M. Rao, S. Lyuksyutov, M. E. Itkis, M. A. Hamon, H. Hu, R. W. Cohn, P. C. Eklund, D. T. Colbert, R. E. Smalley, R. C. Haddon, *J. Phys. Chem. B*, **2001**, 105, 2525.

192 M. Sano, A. Kamino, J. Okamura, S. Shinkai, *Science*, **2001**, 293, 1299.

193 (a) Y.-P. Sun, W. Huang, Y. Lin, K. Fu, A. Kitaygorodskiy, L. A. Riddle, Y. J. Yu, D. L. Carroll, *Chem. Mater.*, **2001**, 13, 2864. (b) Y.-P. Sun, B. Zhou, K. Henbest, K. F. Fu, W. J. Huang, Y. Lin, S. Taylor, D. L. Carroll, *Chem. Phys. Lett.*, **2002**, 351, 349. (c) Y. Lin, S. Taylor, W. Huang, Y.-P. Sun, *J. Phys. Chem. B*, **2003**, 107, 914.

194 (a) K. Fu, A. Kitaygorodskiy, A. M. Rao, Y.-P. Sun, *Nano Lett.*, **2002**, 2, 1165. (b) K. Fu, H. Li, B. Zhou, A. Kitaygorodskiy, L. F. Allard, Y.-P. Sun, *J. Am. Chem. Soc.*, **2004**, 126, 4669.

195 (a) L. W. Qu, R. B. Martin, W. J. Huang, K. F. Fu, D. Zweifel, Y. Lin, Y.-P. Sun, C. E. Bunker, B. A. Harruff, J. R. Gord, L. F. Allard, *J. Chem. Phys.*, **2002**, 117, 8089. (b) R. B. Martin, L. Qu, Y. Lin, B. A. Harruff, C. E. Bunker, J. R. Gord, L. F. Allard, Y.-P. Sun, *J. Phys. Chem. B*, **2004**, 108, 11447.

196 K. Fu, W. Huang, Y. Lin, L. A. Riddle, D. L. Carroll, Y.-P. Sun, *Nano Lett.*, **2001**, 1, 439.

197 X. Shi, S. H. Wang, M. Shen, M. E. Antwerp, X. Chen, C. Li, E. J. Petersen, Q. Huang, W. J. Jr Weber, J. R. Jr Baker, *Biomacromolecules*, **2009**, 10, 1744.

198 (a) A. Koshio, M. Yudasaka, M. Zhang, S. Iijima, *Nano Lett.*, **2001**, 1, 361. (b) M. Yudasaka, M. Zhang, C. Jabs, S. Iijima, *Appl. Phys. A*, **2001**, 71, 449.

199 W. Wu, S. Zhang, Y. Li, J. Li, L. Liu, Y. Qin, Z.-X. Guo, L. Dai, C. Ye, D. Zhu, *Macromolecules*, **2003**, 36, 6286.

200 (a) R. Blake, Y. K. Gunko, J. Coleman, M. Cadek, A. Fonseca, J. B. Nagy, W. J. Blau, *J. Am. Chem. Soc.*, **2004**, 126, 10226. (b) J. N. Coleman, M. Cadek, R. Blake, V. Nicolosi, K. P. Ryan, C. Belton, A. Fonseca, J. B. Nagy, Y. K. Gun'ko, W. J. Blau, *Adv. Funct. Mater.*, **2004**, 14, 791.

201 S. Qin, D. Qin, W. T. Ford, D. E. Resasco, J. E. Herrera, *Macromolecules*, **2004**, 37, 752.

202 Z. J. Jia, Z. Y. Wang, C. Xu, J. Liang, B. Q. Wei, D. H. Wu, S. W. Zhu, *Mater. Sci. Eng.*, **1999**, A271, 395.

203 (a) S. Qin, D. Qin, W. T. Ford, J. T. Herrera, D. E. Resasco, S. M. Bachilo, R. B. Weisman, *Macromolecules*, **2004**, 37, 3965. (b) S. Qin, D. Qin, W. T. Ford, J. T. Herrera, D. E. Resasco, *Macromolecules*, **2004**, 37, 9963.

204 (a) G. L. Hwang, Y.-T. Shieh, K. C. Hwang, *Adv. Funct. Mater.*, **2004**, 14, 487. (c) Y. Liu, J. Tang, J. H. Xin, *Chem. Commun.*, **2004**, 2828.

205 P. Petrov, X. Lou, C. Pagnoulle, C. Jerome, C. Calberg, R. Jerome, *Macromol. Rapid Commun.*, **2004**, 25, 987.

206 J. Che, W. Yuan, G. Jiang, J. Dai, S. Y. Lim, M. B. Chan-Park, *Chem. Mater.*, **2009**, 21, 1471.

207 D. Yan, G. Yang, *Mater. Lett.*, **2009**, 63, 298.

208 K. Min-Lee, L. Li, L. Dai, *J. Am. Chem. Soc.*, **2005**, 127, 4122.

209 (a) T. Nakamura, M. Ishihara, T. Ohana, A. Tanaka, Y. Koga, *Chem. Commun.*, **2004**, 1336. (b) T. Nakamura, M. Ishihara, T. Ohana, A. Tanaka, Y. Koga, *Diamond Relat. Mater.*, **2004**, 13, 1971.

210 B. N. Khare, P. Wilhite, R. C. Quinn, B. Chen, R. H. Schingler, B. Tran, H. Imanaka, C. R. So, C. W. Bauschlicher, M. Meyyappan, *J. Phys. Chem. B*, **2004**, 108, 8166.

211 M. G. Ruther, F. Frehill, J. E. O'Brien, A. I. Minett, W. J. Blau, J. G. Vos, M. Panhuis, *J. Phys. Chem. B,* **2004**, 108, 9665.
212 J. L. Bahr, J. Yang, D. V. Kosynkin, M. J. Bronikowski, R. E. Smalley, J. M. Tour, *J. Am. Chem. Soc.*, **2001**, 123, 6536.
213 C. A. Dyke, M. P. Stewart, F. Maya, J. M. Tour, *Synlett.*, **2004**, 155.
214 P. R. Marcoux P. Hapiot, P. Batail, J. Pinson, *New J. Chem.*, **2004**, 28, 302.
215 (a) M. S. Strano, C. A. Dyke, M. L. Usrey, P. W. Barone, M. J. Allen, H. Shan, C. Kittrell, R. H. Hauge, J. M. Tour, R. E. Smalley, *Science,* **2003**, 301, 1519. (b) M. S. Strano, *J. Am. Chem. Soc.*, **2003**, 125, 16148. (c) C. A. Dyke, J. M. Tour, *Nano Lett.*, **2003**, 3, 1215. (d) H. C. Leventis, G. G. Wildgoose, I. G. Davies, L. Jiang, T. G. J. Jones, R. G. Compton, *Chem. Phys. Chem.*, **2005**, 6, 590.
216 J. L. Bahr, J. M. Tour, *Chem. Mater*., **2001**, 13, 3823.
217 (a) C. A. Mitchell, J. L. Bahr, S. Arepalli, J. M. Tour, R. Krishnamoorti, *Macromolecules,* **2002**, 35, 8825. (b) J. Q. Pham, C. A. Mitchell, J. L. Bahr, J. M. Tour, R. Krishnamoorti, P. F. Green, *J. Polym. Sci., Part B,* **2003**, 41, 3339. (c) V. G. Hadjiev, C. A. Mitchell, S. Arepalli, J. L. Bahr, J. M. Tour, R. Krishnamoorti, *J. Chem. Phys.*, **2005**, 122, 124708.
218 J. L. Hudson, M. J. Casavant, J. M. Tour, *J. Am. Chem. Soc.*, **2004**, 126, 11158.
219 C. A. Dyke, J. M. Tour, *J. Am. Chem. Soc.*, **2003**, 125, 1156.
220 N. Tagmatarchis, V. Georgakilas, M. Prato, H. Shinohara, *Chem. Commun.*, **2002**, 2010.
221 H. C. Kolb, M. S. VanNieuwenhze, K. B. Sharpless, *Chem. Rev.*, **1994**, 94, 2483.
222 X. Lu, F. Tian, Y. Feng, X. Xu, N. Wang, Q. Zhang, *Nano Lett.*, **2002**, 2, 1325.
223 (a) J. Cui, M. Burghard, K. Kern, *Nano Lett.*, **2003**, 3, 613. (b) K. C. Hwang, *Chem. Commun.*, **1995**, 173. (c) S. Banerjee, S. S. Wong, *J. Am. Chem. Soc.*, **2004**, 126, 2073.
224 F. Nunzi, F. Mercuri, A. Sgamellotti, N. Re, *J. Phys. Chem. B,* **2002**, 106, 10622.
225 F. Nunzi, F. Mercuri, F. De Angelis, A. Sgamellotti, N. Re, P. Giannozzi, *J. Phys. Chem. B,* **2004**, 108, 5243.
226 R. Dagani, *Chem. Eng. News,* **1999**, 77, 31.
227 (a) S. Banerjee, S. S. Wong, *NanoLett.*, **2002**, 2, 49. (b) S. Banerjee, S. S. Wong, *J. Am. Chem. Soc.*, **2002**, 124, 8940. (c) T. Hemraj-Benny, S. Banerjee, S. S. Wong, *Chem. Mater.*, **2004**, 16, 1855.
228 F. Frehill, J. G. Vos, S. Benrezzak, A. A. Koos, Z. Konya, M. G. Ruther, W. J. Blau, A. Fonseca, J. B. Nagy, L. P. Biro, A. I. Minett, M. Panhuis, *J. Am. Chem. Soc.*, **2002**, 124, 13694.
229 D. B. Mawhinney, V. Naumenko, A. Kuznetsova, J. T., Jr. Yates, J. Liu, R. E. Smalley, *J. Am. Chem. Soc.*, **2000**, 122, 2383.
230 (a) S. Banerjee, S. S. Wong, *J. Phys. Chem. B,* **2002**, 106, 12144. (b) S. Banerjee, T. Hemraj-Benny, M. Balasubramanian, D. A. Fischer, J. A. Misewich, S. S. Wong, *Chem. Commun.*, **2004**, 772. (c) S. Banerjee, S. S. Wong, *Nano Lett.*, **2004**, 4, 1445.
231 L. Cai, J. L. Bahr, Y. Yao, J. M. Tour, *Chem. Mater.*, **2002**, 14, 4235.

232 (a) E. V. Basiuk, M. Monroy-Pelaez, I. Puente-Lee, V. A. Basiuk, *Nano Lett.*, **2004**, 4, 863. (b) S. Chen, W. Shen, G. Wu, D. Chen, M. Jiang, *Chem. Phys. Lett.*, **2005**, 402, 312.

233 (a) Q. Chen, L. Dai, M. Gao, S. Huang, A. Mau, *J. Phys. Chem. B*, **2001**, 105, 618. (b) S. Chen, W. Shen, G. Wu, D. Chen, M. Jiang, *Chem. Phys. Lett.*, **2005**, 402, 312.

234 (a) Z. Konya, I. Vesselenyi, K. Niesz, A. Kukovecz, A. Demortier, A. Fonseca, J. Delhalle, Z. Mekhalif, J. B. Nagy, A. A. Koos, Z. Osvath, A. Kocsonya, L. P. Biro, I. Kiricsi, *Chem. Phys. Lett.*, **2002**, 360, 429. (b) R. Barthos, D. Mehn, A. Demortier, N. Pierard, Y. Morciaux, G. Demortier, A. Fonseca, J. B. Nagy, *Carbon*, **2005**, 43, 321.

235 H. L. Pan, L. Q. Liu, Z. X. Guo, L. M. Dai, F. S. Zhang, D. B. Zhu, R. Czerw, D. L. Carroll, *Nano Lett.*, **2003**, 3, 29.

236 X. Li, L. Liu, Y. Qin, W. Wu, Z.-X. Guo, L. Dai, D. Zhu, *Chem.Phys. Lett.*, **2003**, 377, 32.

237 M. Green, *Progress in Photovoltaics*, **2001**, 9, 123.

238 S. E. Shaheen, C. Brabec, N. S. Sariciftci, F. Padinger, T. Fromherz, J. C. Hummelen, *App. Phys. Lett.*, **2001**, 78, 841.

239 (a) E. Arici, D. Meissner, N. S. Sariciftci, in *Encyc. Nanoscience and Nanotech.*, edited by H. S. Nalwa, **2004**, 1. (b) W. Huynh, X. Peng, A. P. Alivisatos, *Adv. Mat.*, **1999**, 11, 11.

240 M. Grätzel, *J. Photochem. Photobiol. A*, **2004**, 164, 3.

241 G. Yu, J. Gao, J. C. Hummelen, F. Wudl, A. J. Heeger, *Science*, **1995**, 270, 1789.

242 N. S. Sariciftci, L. Smilowitz, A. J. Heeger, F. Wudl, *Science*, **1992**, 258, 1474.

243 E. Arici, N. S. Sariciftci, D. Meissner, *Adv. Func. Mat.*, **2003**, 2, 13.

244 H. Weller, *Angew. Chemie., Int. Eng. Ed.*, **1993**, 32, 4.

245 M. Grätzel, *Prog. Photovolt. Res. Appl*., **2000**, 8,171.

246 A. Hagfeldt, M. Grätzel, *Chem. Rev.*, **1995**, 95, 49.

247 H. O. Finklea (Ed.), *Semiconductor Electrodes*, Elsevier, Amsterdam, **1988**.

248 A. Mills, S. L. Hunte, *J. Photochem. Photobiol. A: Chem*., **1997**, 108, 1.

249 (a) C. G. Garcia, N. Y. Murakami, *Int. J. Photoenergy*, **2001**, 3, 137. (b) C. Longo, M.-A. De Paoli, *J. Braz. Chem. Soc.*, **2003**, 14, 889.

250 K. Kalyanasundaram, N. Vlachopoulos, V. Krishnan, A. Monnier, M. Grätzel, *J. Phys. Chem.*, **1987**, 91, 2342.

251 H. H. Mao, H. Deng, Y. Li, Z. Shen, H. Lu, J. Xu, *Photochem. Photobiol. A: Chem*., **1998**, 114, 209.

252 (a) J. Fang, J. Wu, X. Lu, Y. Shen, Z. Lu, *Chem. Phys. Lett*., **1997**, 270, 145. (b) M. K. Nazeeruddin, R. Humphry-Baker, M. Grätzel, B. A. Murrer, *Chem Commun*., **1998**, 719. (c) J. J. He, A. Hagfeldt, S. E. Lindquist, H. Grennberg, F. Korodi, L. C. Sun, B. Akermark, *Langmuir*, **2001**, 17, 2743. (d) V. Aranyos, J. Hjelm, A. Hagfeldt, H. Grennberg, *J. Chem. Soc., Dalton Trans*., **2003**, 1280.

253 O. Enea, J. Moser, M. Grätzel, *J. Eletroanal. Chem*., **1989**, 259, 59.

254 (a) J. M. Rehm, G. L. McLendon, Y. Nagasawa, K. Yoshihara, J. Moser, M. Grätzel, *J. Phys. Chem*., **1996**, 100, 9577. (b) P. V. Kamat, W. E. Ford, *Chem. Phys. Lett*., **1987**, 135 421.

255 P. V. Kamat, *J. Phys. Chem*., **1989**, 93, 859.
256 N. Y. M. Iha, C.G. Garcia, C. A. Bignozzi, in: H.S. Nalwa (Ed.), *Handbook of Photochemistry and Photobiology*, (vol 1, American Scientific Publishers, Los Angeles, **2003**, p. 49).
257 K. Kalyanasundaram, M. Grätzel, *Coord. Chem. Rev*., **1998**, 177, 347.
258 C. G. Garcia, N. Y. M. Iha, R. Argazzi, C. A. Bignozzi, *J. Braz. Chem. Soc*., **1998**, 9, 13.
259 (a) H. Sugihara, L. P. Singh, K. Sayama, H. Arakawa, M. K. Nazeeruddin, M. Grätzel, *Chem. Lett*., **1998**, 1005. (b) M. Yanagida, L. P. Singh, K. Sayama, K. Hara, R. Katoh, A. Islam, H. Sugihara, H. Arakawa, M. K. Nazeeruddin, M. Grätzel, *J. Chem. Soc., Dalton Trans*., **2000,** 2817. (c) K. Hara, H. Sugihara, L. P. Singh, A. Islam, R. Katoh, M. Yanagida, K. Sayama, S. Murata, H. Arakawa, *J. Photochem. Photobiol. A: Chem.,* **2001**, 145, 117. (d) K. Hara, H. Sugihara, Y. Tachibana, A. Islam, M. Yanagida, K. Sayama, H. Arakawa, G. Fujihashi, T. Horiguchi, T. Kinoshita, *Langmuir*, **2001**, 17 5992. (e) A. Islam, H. Sugihara, K. Hara, L. P. Singh, R. Katoh, M. Yanagida, Y. Takahashi, S. Murata, H. Arakawa, *J. Photochem. Photobiol. A: Chem*., **2001**, 145, 135. (f) M. K. Nazeeruddin, E. Muller, R. Humphry-Baker, N. Vlachopoulos. M. Grätzel, *J. Chem. Soc., Dalton Trans*., **1997**, 4571. (g) M. Yanagida, A. Islam, Y. Tachibana, G. Fujihashi, R. Katoh, H. Sugihara, H. Arakawa, *New J. Chem*., **2002**, 8, 963.
260 H. W. Kroto, J. R. Heath, S. C. O'Brien, R. F. Curl, R. E. Smalley, *Nature*, **1985**, 318, 162.
261 (a) W. Kratschmer, L. Lamb, K. Fostiropoulos, D. R. Huffman, *Nature*, **1990**, 357, 354. (b) W. Kratschmer, K. Fostiropoulos, D. R. Huffman, *Chem. Phys. Lett*., **1990**, 170, 167. (c) H. W. Kroto, A. W. Allaf, S. P. Balm, *Chem. Rev*., **1991**, 91, 1213.
262 Q. Xie, E. Perez-Cordero, L. Echegoyen, *J. Am. Chem. Soc*., **1992**, 114, 3978.
263 (a) C. S. Foote, in *Topics in Current Chemistry; Photophysical and Photochemical Properties of Fullerenes*, J.Matty, (Ed.), (Springer Berlin, **1994**, 169, 347). (b) Y.-P. Sun, in *Molecular and Supermolecular Photochemistry; Photophysics and Photochemistry of Fullerene Materials*, V. Ramamurthy, K. S. Schanze (Ed.), (Marcel Dekker, New York, **1997**, 1, 325), (c) D. M. Guldi, P. V. Kamat, in *Fullerenes, Chemistry, Physics, and Technology*, K. M. Kadish, R. S. Ruoff (Ed.) (Wiley, New York, **2000**, 5, 225).
264 (a) H. Imahori, Y. Sakata, *Adv. Mater.*, **1997**, 9, 537. (b) H. Imahori, *Org. Biomol. Chem*., **2004**, 2, 1425.
265 N. S. Sariciftci, L. Smilowitz, A. J. Heeger, F. Wudl, *Science*, **1992**, 258, 1474.
266 N. S. Sariciftci, A. J. Heeger, *U.S. Patent 005331183A*, **1994**.
267 H. Spanggaard, F. C. Krebs, *Solar Energy Mater. Solar Cells*, **2004**, 83, 125.
268 B. Miller, J. M. Rosamilia, G. Dabbagh, R. Tycko, R. C. Haddon, A. J. Muller, W. Wilson, D. W. Murphy, A. F. Hebard, *J. Am. Chem. Soc*., **1991**, 113, 6291.
269 C. J. Brabec, G. Zerza, G. Cerullo, S. De Silvestri, S. Luzzati, J. C. Hummelen, N. S. Sariciftci, *Chem. Phys. Lett*., **2001**, 340, 232.

270 (a) N. S. Sariciftci, D. Braun, C. Zhang, V. I. Srdanov, A. J. Heeger, G. Stucky, F. Wudl, *Appl. Phys. Lett.*, **1993**, 62, 585. (b) S. Morita, A. A. Zakhidov, K. Yoshino, *Solid State Commun.*, **1992**, 82, 249.

271 S. Morita, A. A. Zakhidov, K. Yoshino, *Solid State Commun*., **1992**, 82, 249.

272 L. S. Roman, W. Mammo, L. A. A. Pettersson, M. R. Andersson, O. Inganas, *Adv. Mater.*, **1998**, 10, 774.

273 G. Yu, J. Gao, J. C. Hummelen, F. Wudl, A. J. Heeger, *Science*, **1995**, 270, 1789.

274 C. J. Brabec, N. S. Sariciftci, J. C. Hummelen, *Adv. Funct.Mater*., **2001**, 11, 15315.

275 S. Sensfuss, M. Al-Ibrahim, *in Organic Photovoltaics*, S. Sun, N.S. Sariciftci (eds), **2004**, 23, 529.

276 (a) G. E. Jabbour, B. Kippelen, N. R. Armstrong, N. Peyghambarian, *Appl. Phys. Lett*., **1998**, 73, 1185; (b) L. S. Hung, C. W. Tang, M. G. Mason, *Appl. Phys. Lett*., **1997**, 70, 152.

277 J. Baffreau, L. Perrin, S. Leroy-Lhez, P. Hudhomme, *Tetrahedron Lett*., **2005**, 46, 4599.

278 R. Gomez, J. L. Segura, N. Martin, *Org. Lett*., **2005**, 7, 717.

279 G. Accorsi, N. Armaroli, J.-F. Eckert, J.-F. Nierengarten, *Tetrahedron Lett*., **2002**, 43, 65.

280 C. M. Atienza, J. Fernandez, L. Sanchez, N. Martin, I. Sa-Dantas, M. M. Wienk, R. A. J. Janssen, G. M. A. Rahman, D. M. Guldi, *Chem. Commun.*, **2006**, 5, 514.

281 A. Cravino, S. Sariciftci, *J. Mater. Chem*., **2002**, 12, 1931.

282 N. Martin, L. Sanchez, B. Illescas, I. Perez, *Chem. Rev*., **1998**, 98, 2527.

283 (a) J.-F. Nierengarten, *Solar Energy Mater. Solar Cells*, **2004**, 83, 187; (b) J. L. Segura, N. Martin, D. M. Guldi, *Chem. Soc. Rev.*, **2005**, 34, 31; (c) J. Roncali, *Chem. Soc. Rev*., **2005**, 34, 483.

284 A. Cravino, S. Sariciftci, *Nature Mater*., **2003**, 2, 360.

285 M. S. Dresselhaus, G. Dresselhaus, R. Saito, *Carbon*, **1995**, 33, 883.

286 N. Hamada, S. Sawada, A. Oshiyama, *Phys. Rev. Lett.*, **1992**, 68, 1579.

287 R. Saito, M. Fujita, M. S. Dresselhaus, G. Dresselhaus, *Phys. Rev. B*, **1992**, 46, 1804.

288 J. W. G. Wildoer, L. C. Venema, A. G. Rinzler, R. E. Smally, *Nature*, **1998**, 391, 59.

289 T. W. Odom, J.-L. Huang, P. Kim, C. M. Lieber, *Nature*, **1998**, 391, 62.

290 M. Freitag, Y. Martin, J. A. Misewich, R. Martel, P. Avouris, *Nano Lett*., **2003**, 3, 1067.

291 J. Guo, C. Yang, Z. M. Li, M. Bai, H. J. Liu, G. D. Li, E. G. Wang, C. T. Chan, Z. K. Tang, W. K. Ge, X. Xiao, *Phys. Rev. Lett.*, **2004**, 93, 017402.

292 A. Javey, J. Guo, Q. Wang, H. Dai, *Nature*, **2003**, 424, 654.

293 P. Castrucci, F. Tombolini, M. Scarselli, E. Speiser, S. Del Gobbo, W. Richter, M. De Crescenzi, M. Diociaiuti, E. Gatto, M. Venanzi, *Appl. Phys. Lett.*, **2006**, 89, 253107.

294 I. W. Cheong, S. Wang, H. S. Ki, S.-H. Kim, *Curr. Appl. Phys.*, **2009**, 9, 1269.

295 A. C. Khazraji, S. Hotchandani, S. Das, P. V. Kamat, *J. Phys. Chem. B*, **1999**, 103, 4693.

296 S. Barazzouk, S. Hotchandani, K. Vinodgopal, P.V. Kamat, *J. Phys. Chem. B*, **2004**, 108, 17015.

297 (a) D. M. Guldi, G. M. A. Rahman, M. Prato, N. J. Jux, S. Qin, W. Ford, *Angew. Chem., Int. Ed. Engl.,* **2005**, 44, 2015. (b) T. Hasobe, S. Fukuzumi, P. Kamat, *J. Phys. Chem. B*, **2006**, 110, 25477.

298 (a) P.V. Kamat, *Nano Today*, **2006**, 1, 20. (b) A. Kongkanand, R. M. Dominguez, P. V. Kamat, *Nano Lett.*, **2007**, 7, 676. (c) I. Robel, B. Bunker, P. V. Kamat, *Adv. Mater*., **2005**, 17, 2458. (d) F. Vietmeyer, B. Seger, P. V. Kamat, *Adv. Mater.,* **2007**, 19, 2935. (e) B. Xue, P. Chen, Q. Hong, J. Lin, K. L. Tan, *J. Mater. Chem.*, **2001**, 11, 2378.

299 (a) C. Bittencourt, A. Felten, J. Ghijsen, J. J. Pireaux, W. Drube, R. Enri, G. Van Tendeloo, *Chem. Phys. Lett.*, **2007**, 436, 368. (b) Y. Cho, C. Kim, H. Moon, Y. Choi, S. Park, C. K. Lee, S. Han, *Nano Lett.*, **2007**, 8, 81. (c) A. N. Androitis, M. Menon, G. E. Froudakis, *Appl. Phys. Lett.,* **2000**, 76, 3890.

300 (a) J. K. W. Sandler, J. E. Kirk, I. A. Kinloch, M. S. P. Shaffer, A. H. Windle, *Polymer*, **2003**, 44, 5893. (b) A. Allaoui, S. Bai, H. M. Cheng, J. B. Bai, *Compos. Sci. Technol.*, **2002**, 62, 1993. (c) J. B. Bai, A. Allaoui, *Compos. Appl. Sci. Manuf*., **2003**, 34, 689.

301 M. Cinke, J. Li, B. Chen, A. Cassell, L. Delzeit, J. Han, M. Meyyappan, *Chem. Phys. Lett.*, **2002**, 365, 69.

302 M. J. Biercuk, M. C. Llaguno, M. Radosavljevic, J. K. Hyun, A. T. Johnson, J. E. Fischer, *Appl. Phys. Lett.*, **2002**, 80, 2767.

303 D. B. Romero, M. Carrard, W. de Heer, L. Zuppiroli, *Adv. Mater*., **1996**, 8, 899.

304 K. Yoshino, H. Kajii, H. Araki, T. Sonoda, H. Take, S. Lee, *Full. Sci. Tech*., **1999**, 695,

305 H. Ago, M. S. P. Shaffer, D. S. Ginger, A. H. Windle, R. H. Friend, *Phys. Rev. B*, **2000**, 61 2286.

306 S. B. Lee, T. Katayama, H. Kajii, H. Araki, K. Yoshino, *Synth. Met*., **2001**, 121, 1591.

307 H. S. Woo, R. Czerw, S. Webster, D. L. Carroll, J. W. Park, J. H. Lee, *Synth. Met.*, **2001**, 116 369.

308 L. M. Dai, A. W. H. Mau, *Adv. Mater*., **2001**, 13, 899.

309 H. Ago, K. Pettrish, M. S. P. Shaffer, A. H. Windle, R. H. Friend, *Adv. Mater.*, **1999**, 11 1281.

310 E. Kumakis, G. A. J. Amaratunga, *Appl. Phys. Lett*., **2002**, 80, 112.

311 E. Kumakis, I. Alexandrou, G. A. J. Amaratunga, *J. Appl. Phys*., **2003**, 93, 1764.

312 B. J. Landi, R. P. Raffaelle, S. L. Castro, S. G. Bailey, *Prog. Photovolt: Res. Appl.*, **2005**, 13, 165.

313 E. Kumakis, G. A. J. Amaratunga, *Sol. Energ. Mater. Sol. Cells*, **2003**, 80 465.

314 M. H.-C. Jin, L. Dai, in "*Organic Photovoltaics: Mechanisms, Materials and Devices*" (S.-S. Sun and N.S. Sariciftci, Ed.), pp. 579–598, Taylor & Francis, Boca Raton, London, **2005**.

Chapter 3

Ring-opening co-polymerization of a C_{60}-cyclopentadiene cycloadduct and norbornene with the Grubbs second generation catalyst*

3.1 Introduction

Since methods for the mass production of fullerenes have been developed, there has been much interest in the synthesis of fullerene-containing polymers [1]. The physical and chemical properties of C_{60}-attached polymer chains change significantly when compared to the properties of the parent polymer [1]. The polymer properties affected include increased filming properties [2], improved optical limiting properties [3], enhanced thermal stabilities [4] and photoconductivities [5]. In addition to this, fullerene-containing polymers can potentially acquire many of the properties associated with the fullerene [6]. It has also been noted that the incorporation of covalently-bound fullerene into polymers significantly affects the mechanical behaviour, including the tensile strength and fracture toughness, of the polymers [7]. Within the field of biological applications, the neuroprotective, enzymatic, antiapoptotic, antibacterial, DNA photocleavage, nitric oxide synthase inhibition, and chemotactic activities of fullerenes and their derivatives have been studied [8-10].

Due to their unique electronic and chemical properties, fullerenes have a tremendous potential as building blocks for molecular engineering, new molecular materials and supramolecular chemistry [11]. In this regard, heterogeneous mixing of fullerenes and fullerene derivatives with π-conjugated polymers has been used to produce excellent materials for photovoltaic devices [12]. Upon irradiation of fullerene/polymer blends, charge transfer from the polymer to C_{60} occurs, resulting in efficient photo conductivities.

On other hand, physical and thermal properties of fullerene containing natural rubber have been studied by Jurkowska *et al* [13]. In the study, the addition of fullerene was shown to lead to increased elastic modulus at different elongations, Schob elasticity, and hardness of cured rubber to a degree that depends on fullerene content. Moreover it significantly reduced the effect of accelerated aging of

*Published: M. A. Mamo, N. J. Coville, W. A. L. van Otterlo, *Fullerenes, Nanotubes, and Carbon Nanostructures*, **2007,** 15, 341.

rubber and no visible influence of fullerene concentrations on Tg, tan δ, and *G*-modulus within a temperature range -150 to -50°C when rubber is rigid was noted.

The synthesis of modified C_{60} scaffolds has seen tremendous activity over the last decade. Due to C_{60}'s electron-deficient "poly-alkene" characteristics, fullerene addition reactions have therefore been one of the main chemical transformation types investigated [14]. In particular, it has been observed that C_{60} reacts as an electron deficient dienophile with a number of electron-rich dienes and cycloaddition reactions have thus become a very useful method for the functionalization of C_{60} [14]. It has been through this controlled modification of C_{60} that it has been possible to obtain different types of C_{60}-containing polymers such as side chain polymers, main chain polymers, star-shaped polymers, etc, and this field has been extensively reviewed [1]. Amongst many approaches, the application of ring opening metathesis polymerization (ROMP) to synthesise C_{60}-containing polymers was first reported in 1995 [15]. In this communication, by Prato and co-workers, the fullerene monomer was initially prepared by the cycloaddition of quadricyclane to C_{60}, and the C_{60}-containing polymer was prepared from the monomer by a Schrock catalyst-mediated ROMP reaction with norbornene [15]. While the study and exploitation of ROMP reactions have carried on unabated in the polymer literature, little extension of this methodology to building carbon materials (C_{60}, carbon nanotubes, carbon spheres, etc.) into polymers by way of this approach, have since been reported [16].

We have now commenced a systematic study to exploit the ROMP methodology and to apply this approach to the manufacture of carbon-containing materials incorporating fullerenes, carbon nanotubes and carbon spheres. This should lead to the generation of novel materials based on covalent linkages between polymers and carbon materials. To this end we have synthesized a C_{60}-cyclopentadiene cycloadduct and have polymerised this co-monomer with norbornene, using the Grubbs second generation catalyst, in order to obtain a new range of samples containing different amounts of C_{60}. This work describes our investigation into the synthesis and properties of these new C_{60}-containing polymeric materials.

3.2 Experimental

3.2.1 General procedure

Infrared spectra of the polymers were recorded using a Varian 800 FT-IR spectrometer using KBr pellets. Transmittance values are reported on the wave number (cm^{-1}) scale in the range of 400-3200 cm^{-1}. Ultraviolet and visible spectra were recorded using a Varian 50 CONC UV-Visible spectrophotometer. Mass spectra were collected using a VG70-SEQ instrument in a positive ion mode using FAB ionization.

Differential scanning calorimetry (DSC) data was obtained on a DSC822e calorimeter from Mettler-Toledo. Each pan was run in the temperature range 30-75 ^{o}C under a nitrogen atmosphere at a rate of 5 ^{o}C/min Thermal gravimetric analysis (TGA) was performed at a heating rate of 10 ^{o}C/min under nitrogen with a Perkin Elmer, Pyris 1 TGA instrument.

3.2.2 Synthesis of the C_{60}-cyclopentadiene cycloadduct **3.3**

The synthesis of C_{60}-cyclopentadiene cycloadduct **3.3** was performed according to a literature procedure [12] in which cyclopentadiene **2** (0.060 g, 0.83 mmol), dissolved in toluene (15 mL), was added drop-wise to C_{60} **1** (0.50 g, 0.69 mmol) in toluene (15 mL) over 15 min at r.t. During this time the initial purple color of the solution slowly changed to a brown color. After the reaction mixture had been left to stir for a further 30 min, the solvent was removed under reduced pressure to afford a brown solid. This solid was purified using column chromatography (SiO_2, 5 % CS_2: toluene) to afford the desired cycloadduct (0.26 g, 52 % based on C_{60}).

3.2.3 Polymerization of Polynorbornene **3.4**

Norbornene (bicyclo[2.2.1]-2-heptene) (1.0 g, 10.6 mmol) **4** was dissolved in xylene (~35 mL) and stirred for 15 min under dry N_2, at r.t. Grubbs II catalyst **5** (10 mg, 11.8 mmol) was then added to the solution, after which the reaction mixture was left stirring for a further 45 min The polymerization process was then terminated by the addition of ethyl vinyl ether (~2–3 drops). The reaction mixture was then poured into an excess of MeOH (100 mL) containing a few drops of 1 M HCl to precipitate the crude polymer. This material was obtained after filtration and then purified by solubilization in $CHCl_3$. Subsequent precipitation by the addition of excess MeOH (~100 mL), followed by filtration

then afforded the purified polymer **3.6A**. This polymer was then dried in a vacuum oven at 358 ^{o}C to a constant weight (0.88 g, yield: 88 % based on norbornene **3.4**).

3.2.4 Co-polymerization of **3.3** and norbornene **3.4**

All co-polymerization reactions were carried out under a dry N_2 atmosphere in xylene (~35 mL) at r.t. In all cases, a catalytic amount of metathesis co-polymerization of C_{60}-cyclopentadiene Grubb's (II) catalyst (10 mg, 11.8 mmol) was added to the solution to initiate polymerization. The molar ratios of norbornene **4** to C_{60}-cyclopentadiene adduct **3** was varied in order to obtain 50:1, 100:1, 500:1 and 1000:1 molar ratios. The solutions containing the co-monomers were stirred for 15 min before the catalyst was added, under N_2, after which the reaction mixtures were left to stir for a further 45 min The polymerization reactions were then inhibited by the addition of ethyl vinyl ether (a few drops). The solutions were then poured into an excess of MeOH (~100 mL) containing a few drops of 1 M HCl. The co-polymers were purified by solubilization in $CHCl_3$ and then precipitated by the addition of MeOH (~100 mL). The obtained co-polymers **3.6B–E** were dried in a vacuum oven at 358 ^{o}C to constant weight and were found to be dark to light brown in color depending on the amount of C60-cyclopentadiene cycloadduct **3** used as co-monomer (polymer mass returns: **3.6B** 93 %, **3.6C** 84 %, **3.6D** 86 %, **3.6E** 87 %).

3.3 Results and Discussion

3.3.1 Synthesis of copolymers

The C_{60}-cyclopentadiene cycloadduct **3.3** was readily synthesized, by way of a Diels-Alder reaction between C_{60} **3.1** and freshly cracked cyclopentadiene **3.2**, as previously described in the literature (Scheme 1) [17,18]. The functionalized C_{60} **3.3** and norbornene **3.4** were then pre-mixed in varying molar ratios (**3.4**:**3.3**: **3.6A** 1:0, **3.6B** 50:1, **3.6C** 100:1, **2.6D** 500: 1, **3.6E** 1000:1) and co-polymerized using a ROMP approach with catalytic amounts of Grubbs second generation catalyst **3.5** (Scheme **3.1**). After 30 min of stirring the reaction mixtures became highly viscous. For the pure polynorbornene reaction **3.6A** a clear-coloured reaction solution was observed, but for the C_{60}-cycloadduct-norbornene co-polymers **3.6B**-**E** the solution colours varied from a dark brown to light brown colour with the colour proportional to the concentration of the C_{60}-cyclopentadiene cycloadduct

3.3. After a further 15 min of stirring the polymerization reactions were terminated and the rubbery, purified C_{60}-containing polymers **3.6B**-**E** were obtained by precipitation. The yields obtained for the dried polymers **3.6B**-**E** were all good (84-93 %). From the polymeric material in hand it was evident that the color of the polymers was indicative of C_{60} incorporation as the polymer color lightened in the order **3.6B**→**3.6C**→**3.6D**→**3.6E**. The solubility of the co-polymerized polymers **3.6B**-**E** was good in organic solvents such as toluene and CH_2Cl_2 but decreased noticeably as the content of C_{60} increased [19]. Similar observations concerning the relationship between C_{60}-content of the polymers and solubility have also been reported in the literature [20].

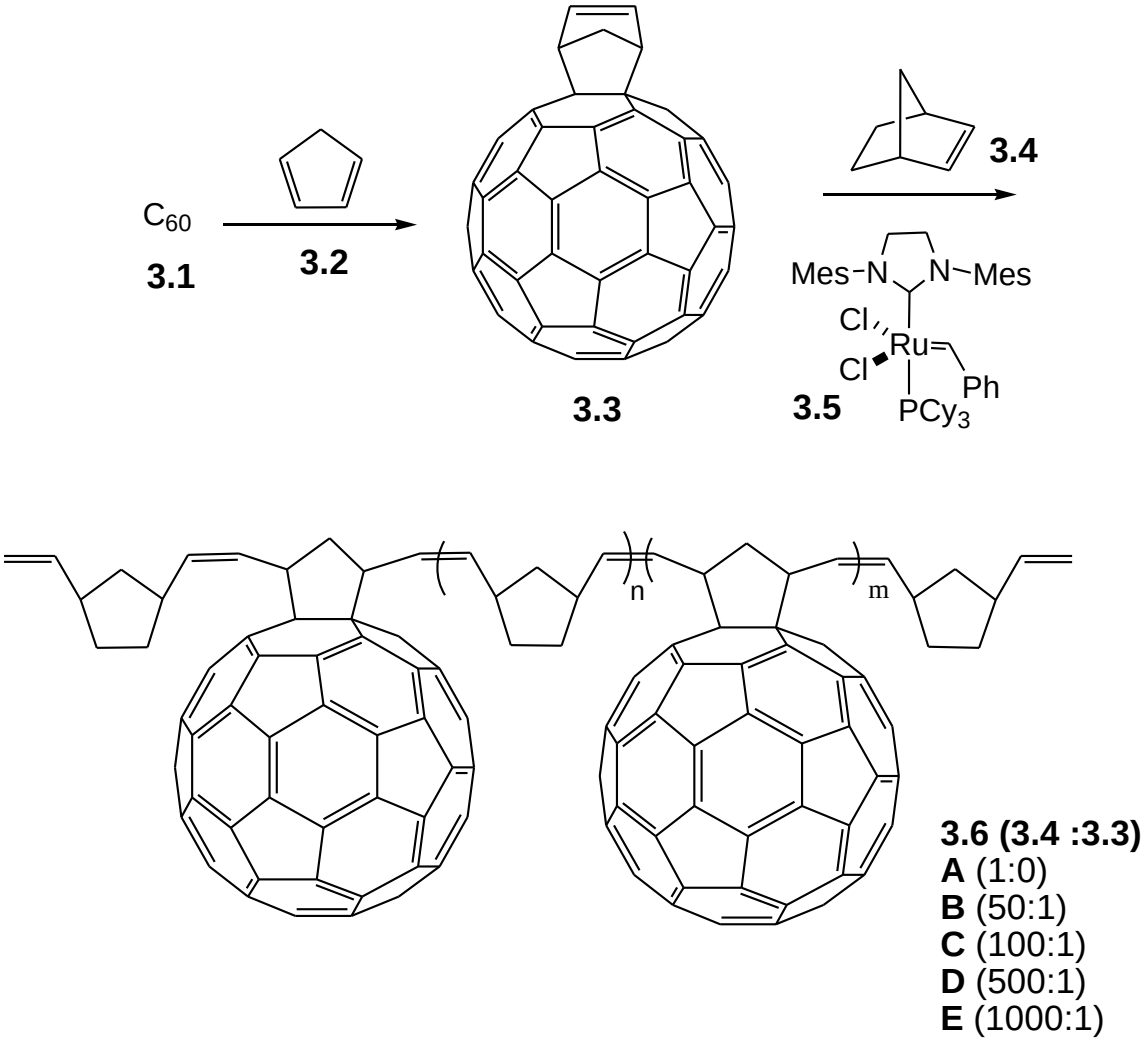

Scheme **3.1** Synthesis of C_{60}-cyclopentadiene adduct-norbornene polymers **3.6B**-**E** by ROMP

3.3.2 Spectroscopic Studies of synthesized materials.

3.3.2.1 FTIR studies of synthesized materials

FTIR spectra were recorded for all the samples of the C_{60}-containing polymers **3.6B-E** and the data confirmed both the presence of C_{60} and polynorbornene (Figure **3.1**) in the polymers. The characteristic peak for C_{60}, ~528 cm^{-1} (see inset Fig **3.1**), was only observed in samples with relatively low norbornene content, *viz*. **3.6B** and **3.6C** [21]. Medium and broad bands that appeared in the region of 3013-2828 cm^{-1} were assigned to the C-H stretching mode. The intense, broad line centered at 1727 cm^{-1} was assigned to the -C=C- stretching mode of an alkene chain and the medium band at around 1455 cm^{-1} was assigned to the $-CH_2-$ bending frequency [15]. The strong band at 964 cm^{-1} was assigned to a *trans* $^{-}HC=CH^{-}$ linkage [14].

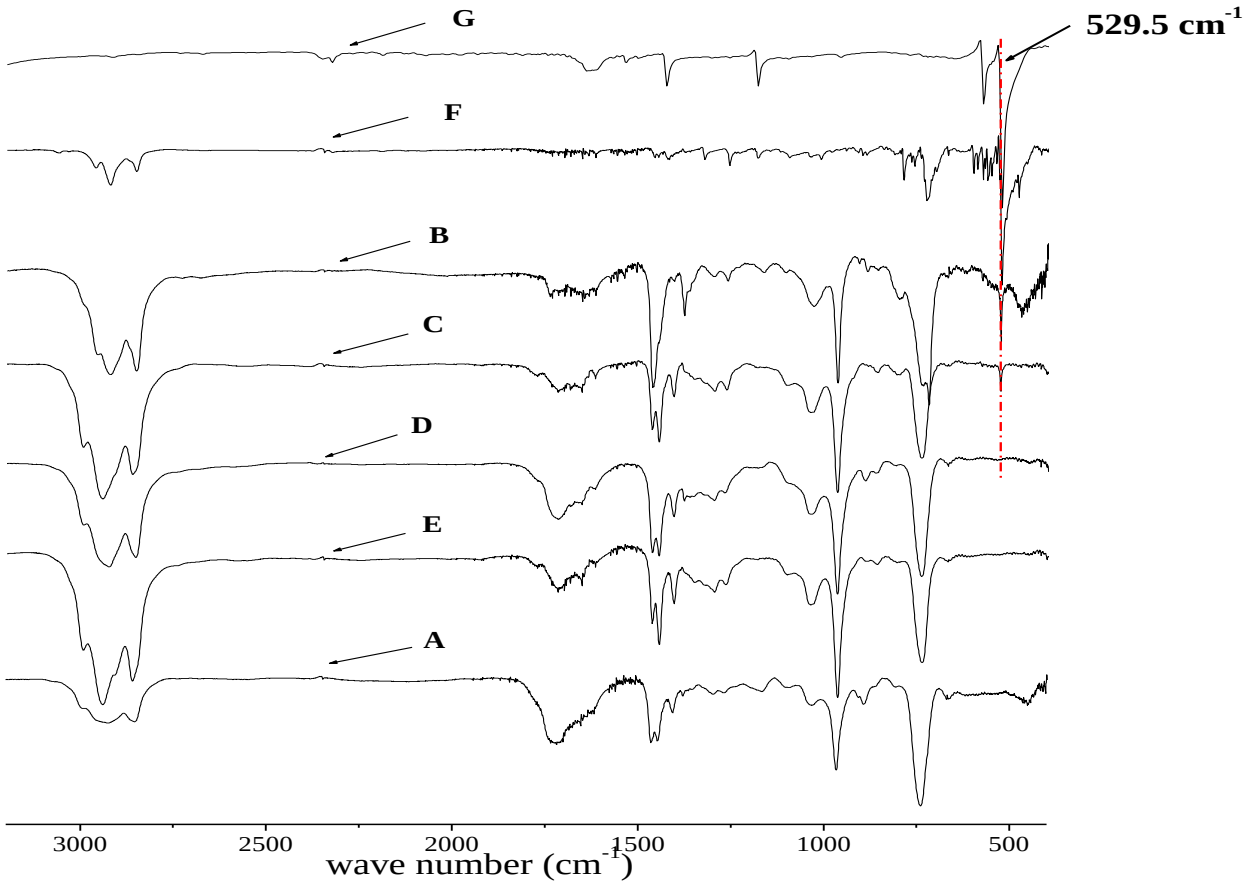

Figure **3.1** FT-IR spectra of the samples in KBr pellet form. (A) Polynorbornene **3.4**, Co-polymers **3.6B-E**: (**B**) mole ratio 50:1, (**C**) mole ratio 100:1, (**D**) mole ratio 500:1, (**E**) mole ratio 1000:1, (**F**) C_{60}-cyclopentadiene cycloadduct **3.3**, (**G**) C_{60} **3.1**.

3.3.2.2 UV-visible absorption spectroscopic studies of synthesized materials

Electronic absorption UV-visible spectra of the fullerene co-polymerized polymers **3.6B-E** were also informative (summarized in Table **3.1**). The spectrum of the C_{60}-containing polynorbornene **3.6C** and **3.6D** displayed two new absorption peaks at 256 and 326.5 nm which are due to the presence of C_{60} [2b, 21a,22] and were absent in polynorbornene **3.6A** (Figure **3.2**). In contrast the UV-visible spectrum of C_{60} **3.1** (**G**) showed a peak at 364.8 nm and for the C_{60}-cyclopentadiene cycloadduct **3.3** (**F**) at 358.3 nm, respectively, shifting to shorter wavelengths relative to the 326.5 nm peak for the C_{60}-

containing polymers (see inset Fig **2.2**). This indicates that the electronic structure of C_{60} has been modified by incorporation into the norbornene polymer by the ROMP reactions [2, 3b].

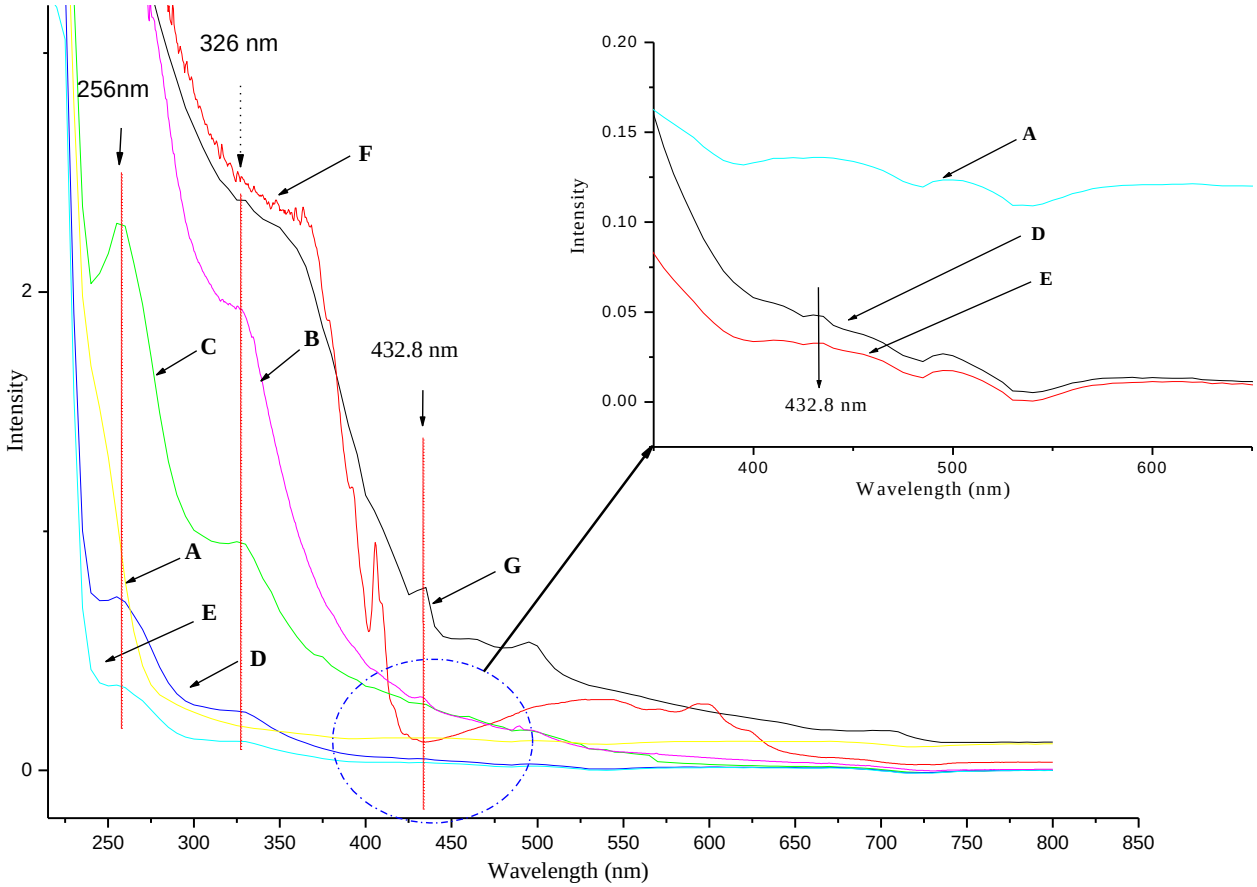

Figure **3.2** UV-visible spectra in toluene of co-polymers **3.6B-E** and polynorbornene **3.6A**: (**A**) Polynorbornene, (**B**) 50:1 mole ratio, (**C**) 100:1 mole ratio, (**D**) 500:1 mole ratio, (**E**) 1000:1 mole ratio, (**F**) C_{60} **3.1**, (**G**) C_{60}-Cyclopentadiene cycloadduct **3.3**.

Table **3.1** UV-visible λmax of the co-polymers **3.6B-E** and polynorbornene **3.6A**

Polymer	λmax (nm)
3.6A	No λmax
3.6B	326.5, 432.8, 489.5
3.6C	256.0, 326.5, 432.8, 494.0,
3.6D	256.0, 326.5, 432.8
3.6E	256.0, 326.5, 432.8
3.1 F	364.8, 406.0, broad peak 460 – 650
3.3 G	326.5, 434.3, 358.3, 496.3

The presence of a band centered at 326.5 and 432.8 (weak) nm for all co-polymers is regarded as characteristic of a 6-6 ring fusion. In recent studies the bands at these wavelengths have been considered indicative of a 'closed' 6-6 ring bridged methanofullerene derivatives [23]. A band appeared at 434.3 nm for the case of C_{60}-cyclopentadiene cycloadduct **3.3.** This band is slightly blue shifted to 432.8 nm for the fullerene-containing polymers and it is very weak in the case of the products formed in the 1000:1 (**3.6E**) and 500:1 (**3.6D**) mole ratio polymerization reactions (inserted in Figure **3.2**).

3.3.3 Thermal Degradation Studies of synthesized materials

3.3.3.1 Differential scanning calorimetry (DSC)

The glass transition (T_g) temperatures for each of the polymers **3.6A-E** synthesized were determined using a heating rate of 5 ^oC/min under N_2. It is clear from the results that the T_g of the C_{60}-containing

co-polymers was directly proportional to the C_{60} content (Figure **3.3**). A similar trend has been observed for the relationship between the C_{60} content and T_g in other C_{60}-containing polymers [3b,21c,24]. The T_g change with C_{60} content can be explained in terms of the modification of the plasticizing and reinforcing abilities of the fullerene in the polymer [3c]. It has been postulated that when the C_{60} content of the polymers is increased, many polymer chains or several part of a polymer chain may be linked by the C_{60} molecules, thus increasing the T_g of the polymer (Table **3.2**) [3].

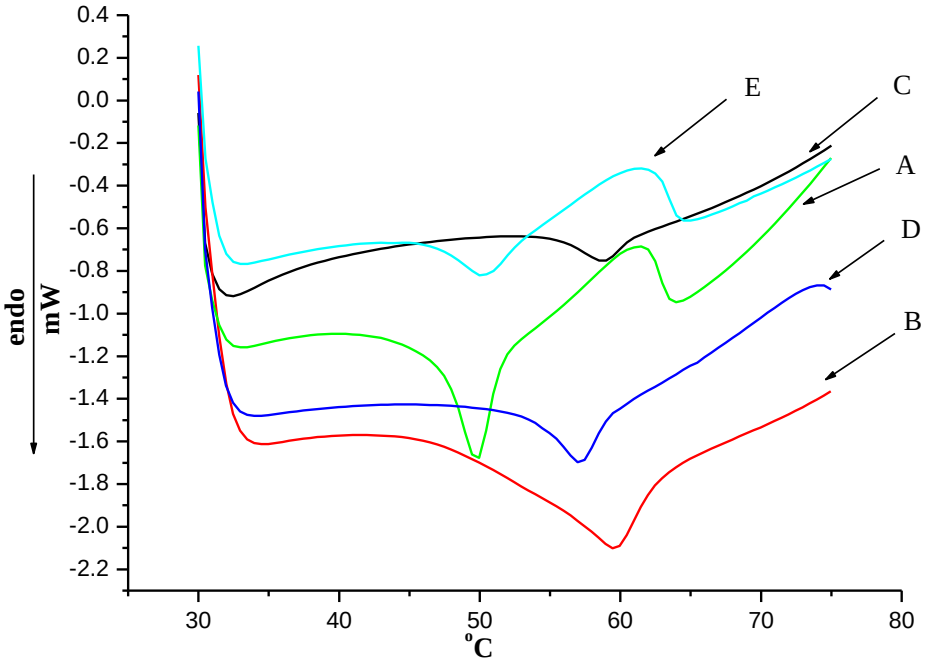

Figure **3.3** Differential Scanning Calorimetry Tg analyses (scan rate 5°C/min): Co-polymers **3.6A-E:** (**A**) Polynorbornene, (**B**) 50:1 mole ratio, (**C**) 100:1 mole ratio, (**D**) 500:1 mole ratio, (**E**) 1000:1 mole ratio.

Table **3.2** T_g of C_{60}-containing polymers **3.6B-E** and **3.6A**.

Polymer	Mole ratio **3.4** : **3.3**	C_{60} content (mole %)	Yield %	T_g (^oC)	Decomposition Temp. (^oC)	C.P[a] decomposition Temp. (^oC)
3.6B	50:1	2	93	59.6	377	327
3.6C	100:1	1	84	58.8	359	418
3.6D	500:1	0.2	86	57.1	373	395
3.6E	1000:1	0.1	87	50.3	385	359
3.6A	Polynorbornene	0	88	49.9	346	283

a C.P= Cross polymerized

3.3.3.2 Thermogravimetric analysis (TGA)

Thermogravimetric analysis (TGA) results provides a measure of the C_{60} content in the polymers. The TGA data clearly reveal that as the C_{60} content of the norbornene-C_{60} co-polymers **3.6B-E** increases, the thermal stability of the materials increases relative to polynorbornene **3.6A** (see Figure. **3.4** and Table **3.2**). It is also to be noted that the residual material after reaction at $T^o > 600^oC$ provides a qualitative measure of both the ruthenium and C_{60} content. The polymers which contain C_{60} appeared to be thermally more stable than polynorbornene. This finding is contrary to an earlier report where the thermogravimetric analysis showed that the polymer degraded at 470 ^oC, indicating that the C_{60}-containing polymer is a robust material, but of lower thermal stability than polynorbornene [15].

Significant mass losses were observed after ~350 ^oC for polynorbornene **3.6A** and for the C_{60}-containing co-polymers **3.6B-E** the mass loss occurred at about 360 ^oC in all cases. Interestingly the residue after thermolysis increases with C_{60} content in the polymers, A = ~0%, B = 23%, C = 15%, D = 11%, E = 7%. Similar observations, regarding the C_{60} content of a polymer and the residues after thermolysis have also been reported [21c].

The synthesized co-polymers were also subjected to cross-polymerization [15] by heating at 80 ^oC for 72 h and their thermal stability compared with the parent polymer **3.6A** (Table **3.2**). Of interest was

that the results were found not to be linearly related. In some cases the cross polymerized compound was found to be more thermally stable than the parent polymer **3.6A**, for instance, the polymers containing 100:1 and 500:1 mole ratios, **3.6C** and **3.6D** respectively. However for the other C_{60}-containing polymers this was not the case.

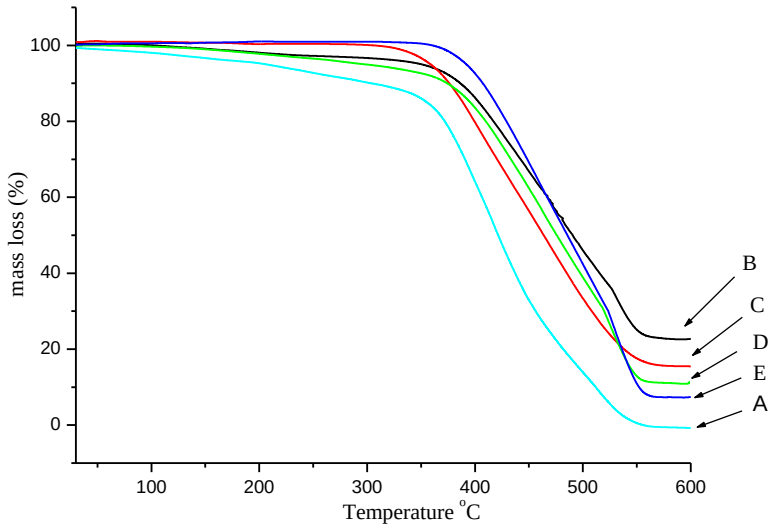

Figure **3.4** TGA curves of the polymers (rate 10°C/ min) under a nitrogen atmosphere: (**A**) Polynorbornene, Co-polymers **3.6B-E:** (**B**) 50:1 mole ratio, (**C**) 100:1 mole ratio, (**D**) 500:1 mole ratio, (**E**) 1000:1 mole ratio.

3.4 Conclusion

We have successfully synthesized a set of C_{60}-cyclopentadiene cycloadduct/ norbornene polymers using ROMP with the Grubbs second-generation catalyst. By spectroscopic evaluation we were able to show that incorporation of the fullerene into the polymers had occurred and that the relative amount of C_{60} affected the polymers thermal properties by increasing both the decomposition and the glass transition temperatures, relative to polynorbornene.

3.5 References

1 (a) C. Wang, Z.-X. Guo, T. Yadav, S. Fu, W. Wu, D. Zhu, *Prog. Polym. Sci.* **2004**, 29, 1079. (b) M. Prato, *J. Mater. Chem.*, **1997**, 7, 1097.

2 See for example: A. Kraus, K. Mullen, *Macromolecules*, **1999**, 32, 4214.

3 See for example: (a) R. Tong, H. Wu, B. Li, R. Zhu, G. You, S. Qian, Y. Lin, R. Cai, *Physica B*, **2005**, 366, 192. (b) B. Z. Tang, S. M. Leung. H. Peng, N. T. Yu, K. C. Su, *Macromolecules*, **1997**, 30, 2848. and references cited therein.

4 See, for example, (a) C. Mathis, B. Schmaltz, M. Brinkmann, *C. R. Chimie*, 2006, 9, 1075. (b) O. F. Pozdnyakov, A. O. Pozdnyakov, B. Schmaltz, C. Mathis, *Polymer, 2006*, 47, 1028.

5 For recent reviews see: (a) H. Spanggaard, F. C. Krebs, *Sol. Energy Mater. Sol. Cells*, **2004**, 83, 125. (b) J.-F. Nierengarten, *Sol. Energy Mater. Sol. Cells*, **2004**, 83, 187. (c) C. J. Brabec, *Sol. Energy Mater. Sol. Cells*, **2004**, 83, 273.

6 S. Shi, K. C. Khemani, Q. C. Li, F. Wudi, *J. Am. Chem. Soc.*, **1992**, 114, 10656

7 See for examples: (a) T. Song, S. H. Goh, S. Y. Lee, *Polymer*, **2003**, 44, 2563. (b) C.-C. M. Ma, S.-C. Sung, F.-Y. Wang, L. Y. Chiang, L. Y. Wang, C.-L. Chiang, *J. Polym. Sci., Part B: Polym. Phys.*, **2001**, 39, 2436 and references cited therein.

8 T. Da Ros, M. Prato, *Chem. Commun.*, **1999**, 663.

9 A. W. Jensen, S. R. Wilson, D. I. Schuster, *Bioorg. Med. Chem.*, **1996**, 4, 767.

10 S. R. Wilson, Biological aspects of fullerenes. In *Fullerenes*: *Chemistry, Physics, and Technology*, (Kadish K, Ruoff R (Ed). Wiley: New York, **2000**, 437).

11 (a) F. Diederich, M. Gomez-Lopez, *Chem. Soc. Rev.*, **1999**, 28, 263. (b) F. Diederich, M. Gomez-Lopez, *Chimia*, **1998**, 52, 551.

12 A. Cravino, N. S. Sariciftci, *J. Mater.Chem.*, **2002**, 12, 1931.

13 B. Jurkowski, P. Kamrowski, S. S. Pesetskii, V. N. Koval, L. S. Pinchuk, Y. A. Olkhov, *J. Appl. Poly. Sci.*, **2006**, 100, 390.

14 (a) M. A. Yurovskaya, I. V. Trushkov, *Russ. Chem. Bull. Int Ed.*, **2002**, 51, 367. (b) P. Hudhomme, C. R. *Chimie*, **2006**, 9, 881. (c) R. Taylor, C. R. *Chimie*, **2006**, 9, 982. (d) J. Yli-Kauhaluoma, *Tetrahedron*, **2001**, 57, 7053.

15 N. Zhang, S. R. Schricker, F. Wudl, M. Prato, M. Maggini, G. Scorrano, *Chem. Mater.*, **1995**, 7, 441.

16 (a) Z. T. Ball, K. Sivula, J. M. J. Fréchet, *Macromolecules*, **2006**, 39, 70. (b) K. Sivula, Z. T. Ball, N. Watanabe, J. M. J. Fréchet, *Adv. Mater.*, **2006**, 18, 206.

17 V. M. Rotello, J. B. Howard, T. Yadav, M. M. Conn, E. Viani, L. M. Giovane, A. L. Lafleur, *Tetrahedron Lett.* **1993**, 34, 1561.

18 For other examples, involving the reaction of substituted or unsubstituted cyclopentadienes to C60 by way of a Diels-Alder reaction, see: (a) S. R. Wilson, M. E. Yurchenko, D. I. Shuster, A. Khong, M. Saunders, *J. Org. Chem*., **2000**, 65, 2619. (b) R. Schwenniger, T. Muller, B. Krautler, *J. Am. Chem. Soc*., **1997**, 119, 9317. (c) B. Nie, V. M. Rotillo, *J. Org. Chem*., **1996**, 61, 1870. (d) M. F. Meidine, A. G. Avent, A. D. Darwish, H. W. Kroto, O. Ohashi, R. Taylor, D. R. M. Walton, *J. Chem. Soc. Perkin Trans. 2*, **1994**, 1189. (e) K. I. Guhr, M. D. Greaves, V. M. Rotello, *J. Am. Chem. Soc.*, **1994**, 116, 5997.

19 On formation the polymers **6B-E** were generally very soluble. However after precipitation and drying of the polymers, addition of organic solvents caused gel formation rather than facile solubilization.

20 H. W. Goh, S. H. Goh, G. Q. Xu, *J. Polym. Sci., Polym. Chem.*, **2002**, 40, 1157.

21 (a) K. E. Geckeler, A. Hirsch, *J. Am .Chem. Soc.*, **1993**, 115, 3850. (b) T. Suzuki, Q. Li, K. C. Khemani, F. Wudi, *J. Am. Chem. Soc.* **1992**, 114, 7301. (c) X. Zhang, A. B. Sieval, J. C. Hummelen, B. Hessen, *Chem. Commun.*, **2005**, 1616.

22 W. J. Li, W. J. Liang, *Spectrochim. Acta Part A: Mol. Biomol. Spectrosc,* **2007**, 67, 1346.

23 (a) C.-C. Chu, T.-I. Ho, L. Wang, *Macromolecules*, **2006**, 39, 5657. (b) S. Xiao, Y. Li, Y. Li, H. Liu, H. Li, J. Zhuang, Y. Liu, F. Lu, D. Zhang, D. Zhu, *Tetrahedron Lett.*, **2004**, 45, 3975. (c) S. Xiao, Y. Li, H. Fang, H. Li, H. Liu, Z. Shi, L. Jiang, D. Zhu, *Org. Lett.*, **2002**, 4, 3063. (d) F. Giacalone, J. L. Segura, N. Martín, *J. Org. Chem.*, **2002**, 67, 3529. (e) M. W. J. Beulen, J. A. Rivera, M. A. Herranz, B. Illescas, N. Martín, L. Echegoyen, *J. Org. Chem.*, **2001**, 66, 4393.

24 See for example: (a) A. G. Camp, A. Lary, W. T. Ford, *Macromolecules*, **1995**, 28, 7959. (b) L. Y. Chiang, L. Y. Wang, C. –S. Kuo, *Macromolecules*, **1995**, 28, 7574. (c) L. Dai, A. W. H. Mau, H. J. Griesser, T. H. Spurling, *J. Phys. Chem.*, **1995**, 99, 17302. (d) C. J. Hawker, *Macromolecules*, **1994**, 27, 4836.

Chapter 4

Ring-opening metathesis co-polymerization of a C_{60}-cyclopentadiene cycloadduct and *N*-(cycloheptyl)-endo-norbornene-5,6-dicarboximide

4.1 Introduction

The discovery and consequent characterisation of fullerenes has generated particular interest in the field of materials science. The incorporation of fullerenes into existing materials such as polymers, electronic devices, thin films and liquid crystals have all been attempted, and in so doing so, scientists have produced unique carbonaceous materials. In particular, the development of new synthetic polymers incorporating fullerenes has seen keen interest [1]. It has also been convincingly demonstrated that the physical and chemical properties of C_{60}-attached polymer chains change significantly when compared to the properties of the parent polymer and that the fullerene-containing polymers can potentially acquire many of the properties usually associated with the fullerene [1,2]. Examples of the properties affected by the incorporation of fullerene include the polymeric tensile strength and fracture toughness [3].

Ring-opening metathesis polymerization (ROMP) is seeing increasing usage in the synthesis of C_{60}-containing polymers. This approach was first reported in 1995 by Prato and co-workers using the molybdenum-based Schrock's catalyst [4].While the study and exploitation of ROMP reactions have carried on unabated in the polymer literature, the Prato approach to fullerene-containing polymers is still under-utilized. Relatively few examples of this methodology, to incorporate carbon materials (C_{60}, carbon nanotubes, carbon spheres, etc.) into polymers, have been reported [5]. Of interest is that the utilization of olefin metathesis on nanostructures has been the focal point of a recent review [6], and two examples of the use of ROMP on derivative nanotubes were discussed [7,8].

In the previous Chapter the copolymerization of a C_{60}-cyclopentadiene cycloadduct with norbornene [9] was described using the Grubbs second generation catalyst [10]. In the work described in this Chapter we reported our investigation into the synthesis and properties of a series of novel C_{60}-containing polymeric materials based on the ROMP of a *N*-(cycloheptyl)-

endo-norbornene-5,6-dicarboximide monomer with a C_{60}-cyclopentadiene cycloadduct. This reagent was chosen in its hope that it would enhance the solubility of the fullerene containing polymers. Indeed the polymers thus synthesisied show better solubility in most common polar organic solvents than the products described in Chapter 2.

4.2 Experimental

4.2.1 General procedures

Infrared spectra of the polymers were recorded with a Varian 800 FT-IR spectrometer using KBr pellets. Transmittance values are reported on the wave number (cm^{-1}) scale in the range of 400–3200 cm^{-1}. Ultraviolet and visible spectra were recorded with a Varian 50 CONC UV-Visible spectrophotometer and mass spectra were collected with a VG70-SEQ instrument in a positive ion mode using FAB ionization. Differential scanning calorimetry (DSC) data was obtained on a DSC822e calorimeter from Mettler-Toledo; each pan was run in the temperature range 30-75 ^oC under a N_2 atmosphere at a rate of 5 ^oC/min Finally, thermal gravimetric analysis (TGA) was performed at a heating rate of 10 ^oC/min, under N_2, with a Perkin Elmer Pyris 1 TGA instrument.

4.2.2 Synthesis of C_{60}-cyclopentadiene cycloadduct 4.7

The synthesis of C_{60}-cyclopentadiene cycloadduct **4.7** was performed according to a literature procedure [13] and as described by us previously [9].

4.2.3 Synthesis of *N*-(cycloheptyl)-endo-norbornene-5,6-dicarboximide 4.4

Cis-norbornene-*endo*-2,3-dicarboxylic anhydride **4.1** (5.0 g, 30 mmol) and cycloheptylamine **4.2** (3.8 mL, 30 mmol) were dissolved in distilled toluene (35 mL), and stirred at 90 °C for 24 h. The resulting mixture was then cooled to r.t. Ac_2O (26.5 mL, 278 mmol) and NaOAc (2.42 g, 17.8 mmol) were added to the foregoing mixture, which was then stirred at 90 °C for a further 24 h. Upon cooling, a white crystalline matrix formed throughout the solution. The toluene solvent was removed under reduced pressure and the resultant solid was repeatedly extracted with a mixture of hexane and distilled H_2O (3:1 ratio, ~250 mL total volume). The hexane layer was subsequently collected and evaporated, resulting in a crystalline product **4.4**. This material was

dried under reduced pressure to a constant mass (5.5 g, 83 %). The structure of product **4.4** was confirmed from its spectral data. ^{1}H NMR: 6.09 (2H, br s, 2 × C=CH), 3.97–3.90 (1H, m, NCH), 3.37 (2H, br s, 2 × CH), 3.17–3.16 (2H, m, 2 × CH), 2.11–2.01 (2H, m, CH_2), 1.76–1.69 (4H, m, 2 × CH_2), 1.61–1.36 (8H, m, 4 × CH_2); ^{13}C NMR: 177.6 (2 × C=O), 134.2 (C=C), 53.1 (NCH),[a] 52.1 (CH_2),[a] 45.2 (2 × CH), 45.0 (2 × CH), 31.7 (2 × CH_2), 27.4 (2 × CH_2), 25.5 (2 × CH_2); FT-IR: 2931, 2861, 1685, 1399, 1370, 1335, 1210, 1166, 843, 723; *m/z* (FAB): 260 (M^{+1}, 100%), 194 (60), 164 (20).

4.2.4 Polymerization of *N*-(cycloheptyl)-endo-norbornene-5,6-dicarboximide 4.4 to afford 4.9A

Norbornene derivative **4.4** (0.500 g, 1.83 mmol) was dissolved in toluene (25 mL) and stirred for 30 min, under Ar at r.t. Grubbs' 2nd generation catalyst **4.8** (6 mg, 7.08 μmol) was then added to the solution, after which the reaction mixture was left stirring for a further 5 days. The polymerization process was then terminated by the addition of ethyl vinyl ether (~2-3 drops). The solvent was then removed under vacuum and the resultant material washed with hexane (100 mL). After filtration, the solid polymer was dissolved in $CHCl_3$ (20 mL) and then poured into an excess of MeOH (100 mL), containing a few drops of 1 M HCl to precipitate the crude polymer. This was followed by filtration of the solid which afforded the purified polymer **4.9A**. This polymer was then dried in a vacuum oven at 35 ^{o}C to a constant weight (0.480 g, yield: 96 % based on norbornene derivative **4.4**).

4.2.5 Co-polymerization of C_{60}-cyclopentadiene 4.7 and *N*-(cycloheptyl)-endo-norbornene-5,6-dicarboximide 4.4

All co-polymerization reactions were carried out under Ar in toluene (25 mL) at r.t. In all cases a catalytic amount of Grubbs 2nd generation catalyst **4.8** (6 mg, 7.08 μmol) was then added to the solution to initiate polymerization. The molar ratios of *N*-(cycloheptyl)-*endo*-norbornene-5,6-dicarboximide **4.4** to C_{60}-cyclopentadiene adduct **4.7** was varied in order to obtain 1000:1 **4.9B**, 700:1 **4.9C**, 500:1 **4.9D**, 300:1 **4.9E**, 100:1 **4.9F** and 50:1 **4.9G** molar ratios. The solutions containing the co-monomers were stirred for 30 min before the catalyst was added, after which the reaction mixtures were left to stir for a further 5 days under Ar. The polymerization reactions were then inhibited by the addition of ethyl vinyl ether (a few drops). The solvent was then

removed under vacuum and the resultant solid then washed with hexane (100 mL). After filtration the solid polymer was dissolved in $CHCl_3$ (20 mL), and then poured into an excess of MeOH (100 mL), containing a few drops of 1 M HCl, to precipitate the crude polymer. After filtration, the obtained co-polymers **4.9B-E** were dried under vacuum and were found to be dark to light brown in color, depending on the amount of C_{60}-cyclopentadiene cycloadduct **4.7** used as co-monomer (polymer mass returns: **4.9B** 80 %, **4.9C** 84 %, **4.9D** 79 %, **4.9E** 92 %, **4.9F** 80 % and **4.9G** 96 %).

4.3 Results and Discussion

4.3.1 Synthesis of 4.4 and copolymers

The work started with the synthesis of *N*-(cycloheptyl)-*endo*-norbornene-5,6-dicarboximide **4.4** using commercially available norbornene-*endo*-5,6-dicarboxylic anhydride **4.1** as a precursor, and used methodology developed by Riande (Scheme **4.1**) [11]. We found that the condensation reaction of compound **4.1** and heptyl amine **4.2** readily afforded the novel *N*-(cycloheptyl)-*endo*-norbornene-5,6-dicarboximide **4.4** in 83 % yield, presumably by way of intermediate **4.3**.

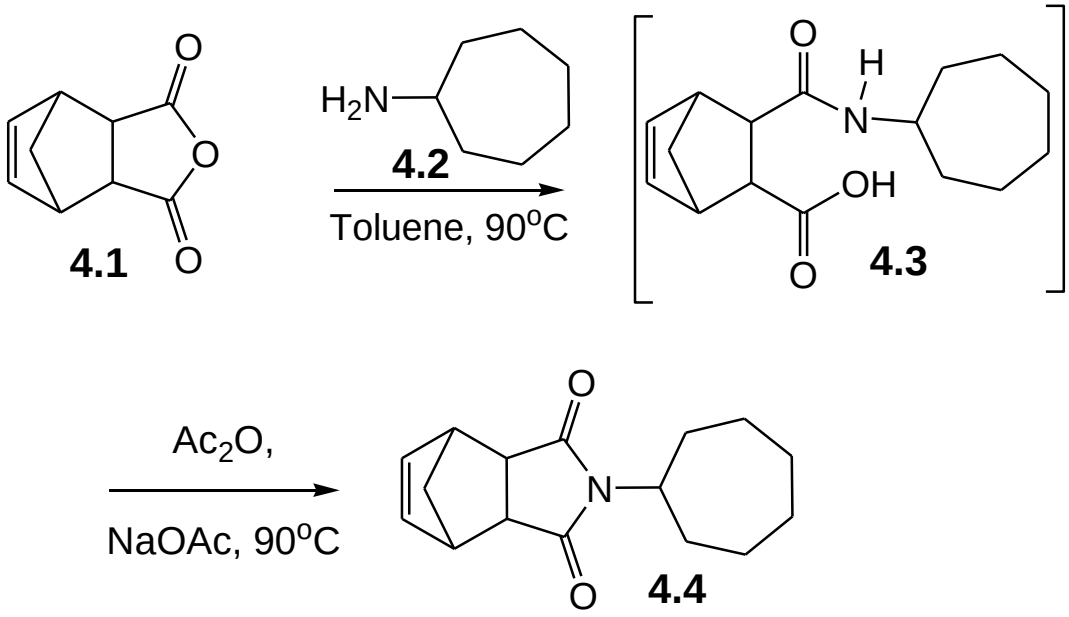

Scheme **4.1** Synthesis of *N*-(cycloheptyl)-*endo*-norbornene-5,6-dicarboximide **4.4**

The C_{60}-cyclopentadiene cycloadduct **4.7** was also readily synthesized, by way of a Diels-Alder reaction between C_{60} **4.5** and freshly cracked cyclopentadiene **4.6**, as previously described in the literature [13-15] and our previous paper (Scheme **4.2**) [9]. C_{60}-cyclopentadiene cycloadduct **4.7** and *N*-(cycloheptyl)-*endo*-norbornene-5,6-dicarboximide **3.4** were then pre-mixed in varying molar ratios (**4.4**:**4.7**: **4.9A** 1:0, **4.9B** 1000:1, **4.9C** 700:1, **4.9D** 500: 1, **4.9E** 300:1, **4.9F** 100: 1, **4.9G** 50:1) and co-polymerized using a ROMP approach with catalytic amounts of Grubbs' second generation catalyst **4.8** (Scheme **4.2**). After 30 min of stirring the reaction solutions became viscous to afford reaction mixtures with colours that varied from a dark brown to a light brown colour, with the colour proportional to the concentration of the C_{60}-cyclopentadiene cycloadduct **4.7**. It was found that allowing the ROMP to proceed for 5 days gave the best polymer returns, as less reaction time resulted in poor polymer yields. Thus after 5 days of stirring, the polymerization reactions were terminated and the powdery C_{60}-containing polymers **4.9B-H** were obtained by precipitation (see experimental Section for details). In addition a polymer containing no fullerene was also generated by the ROMP of monomer **4.4**, which resulted in polymer **4.9A**. Use of the approach afforded products for which the yields obtained for the dried polymers **4.9A-H** were all good (84-96 %); the colours of the obtained polymers (light to dark brown) was indicative of the amounts of C_{60} incorporated into them. The results of the ROMP syntheses are summarized in Table **4.1**. Of interest was that the solubilities of the co-polymerized polymers **4.9B-H** were very good in organic solvents such as toluene, dichloromethane and chloroform but noticeably decreased as the content of C_{60} increased, as was the case in our earlier investigation [9,16,17]. A comparative solubility test was conducted on each of **4.9D** and **3.6D** (60 mg of copolymer in 15 mL toluene in each case) and after 24h stirring at r.t. copolymers **4.9D** showed better solubility than copolymers **3.6D**.

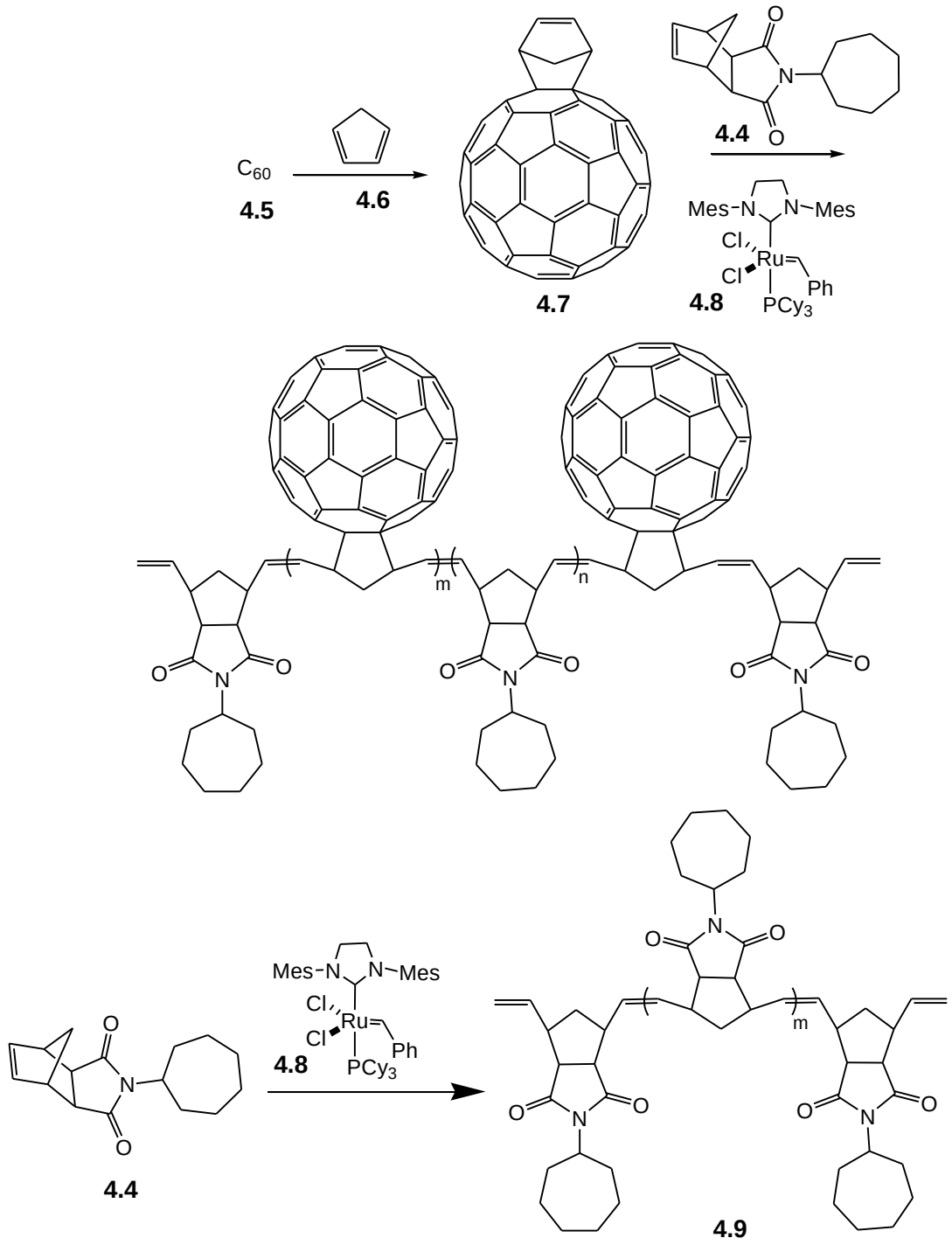

Scheme 4.2 Synthesis of C_{60}-cyclopendadiene adduct–*N*-(cycloheptyl)-*endo*-norbornene-5,6-dicarboximide polymers **4.9B-E** by ROMP (mole ratio **4.4**:**4.7**): **4.9A** (1:0), **4.9B** (1000:1), **4.9C** (700:1), **4.9D** (500:1), **4.9E** (300:1), **4.9F** (100:1), **4.9G** (50:1).

Table **4.1** Details of the synthesized polymer **4.9A** and the co-polymers **4.9B-G**.

Polymer	Mole ratio **4.4**:**4.7**	C_{60} content (mole %)	Yield %
4.9A	1:0	0	96
4.9B	1000:1	0.092	80
4.9C	700:1	0.128	84
4.9D	500:1	0.183	79
4.9E	300:1	0.303	92
4.9F	100:1	0.916	80
4.9G	50:1	1.832	96

4.3.2 Spectroscopic Studies of the synthesized materials

4.3.2.1 FTIR studies of synthesized materials

FTIR spectra were recorded for all the synthesized samples. In the C_{60}-containing polymers **4.9B-G** the presence of C_{60} in some of the synthesized polymers (Figure **4.1**) was confirmed by a characteristic peak at ~526 cm^{-1} [18]. This peak was only observed in samples with relatively high C_{60} content, *viz*. **4.9G** and **4.9F**. This effect was also seen in our previously published work [9]. In addition, strong peaks at ~1761 $cm^{-1}$and ~1694 cm^{-1} were evident for all the synthesized polymers and these bands were assigned to the C=O stretches [11b]. The the C=O stretches peak is absent in **4.9H** and **I** since those are pure C_{60} and the functionalized C_{60} respectively with out further copolymerization.

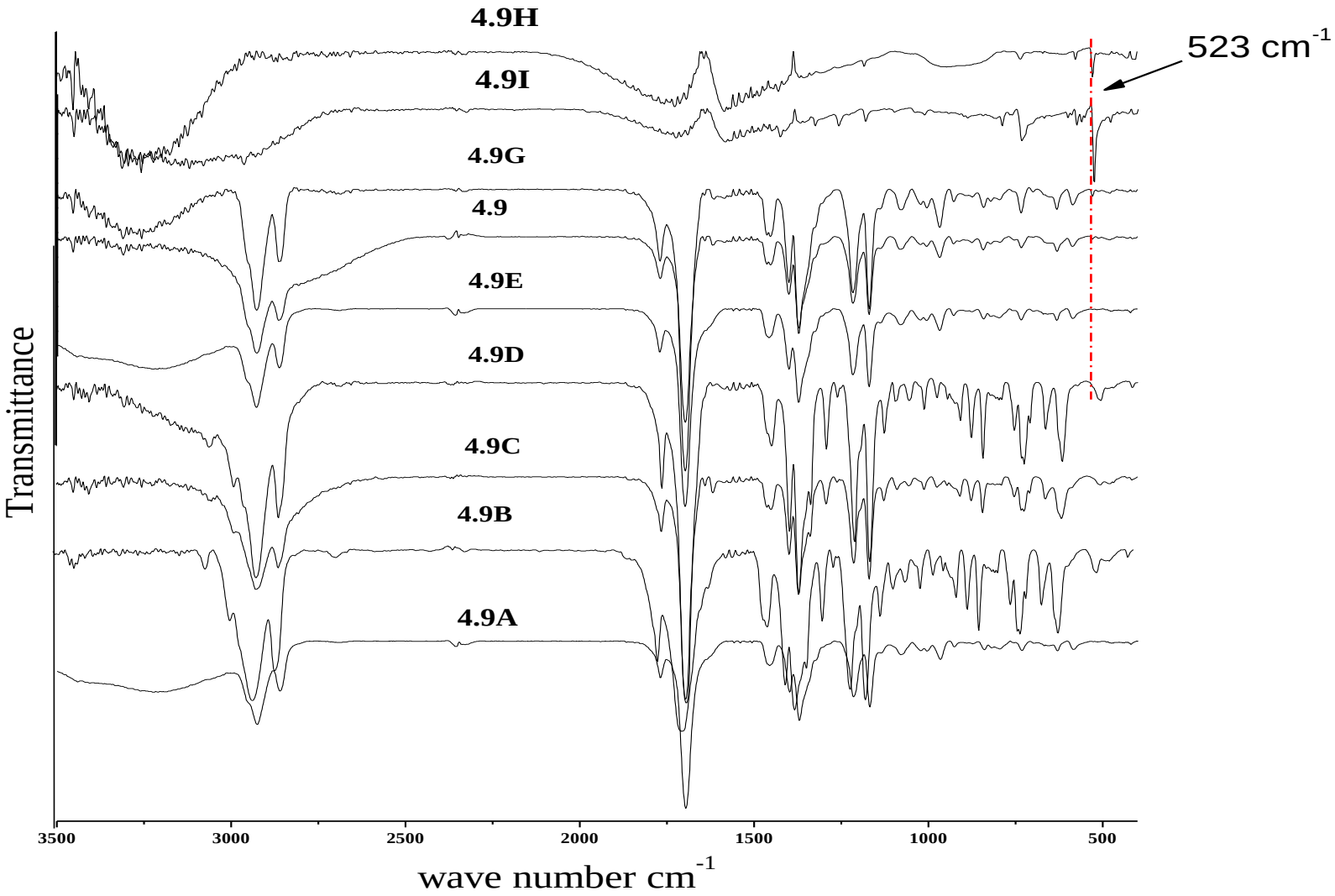

Figure **4.1** FT-IR spectra of the samples in KBr pellet form (mole ratio **4.4:4.7**): **4.9A** (1:0), **4.9B** (1000:1), **4.9C** (700:1), **4.9D** (500:1), **4.9E** (300:1), **4.9F** (100:1), **4.9G** (50:1), **4.9H** C_{60}-cyclopentadiene cycloadduct **4.7**, **4.9I** C_{60} **4.5**.

4.3.2.2 UV-visible absorption spectroscopic studies of synthesized materials

Electronic absorption UV-visible spectra of the fullerene co-polymerized polymers **4.9B-H** were also indicative of the presence of C_{60} in the polymers (Figure **4.2**, data summarized in Table **4.2**). The spectrum of the C_{60}-containing poly[*N*-(cycloheptyl)-*endo*-norbornene-5,6-dicarboximide] **4.9B-G** complexes displayed a new absorption peak at 329 nm which is presumably due to the presence of C_{60} [18a,19]. However, an absorption band was recorded at 380 nm for both C_{60} **4.5**

(**4.9I**) and C_{60}-cyclopentadiene cycloadduct **4.7** (**3.9H**), but was absent in poly[*N*-(cycloheptyl)-*endo*-norbornene-5,6-dicarboximide] **4.9A** (Figure **4.2**). The relative shift in the absorption band indicates that the electronic structure of C_{60} has been modified by its incorporation into the norbornene polymer by the ROMP reaction [20].

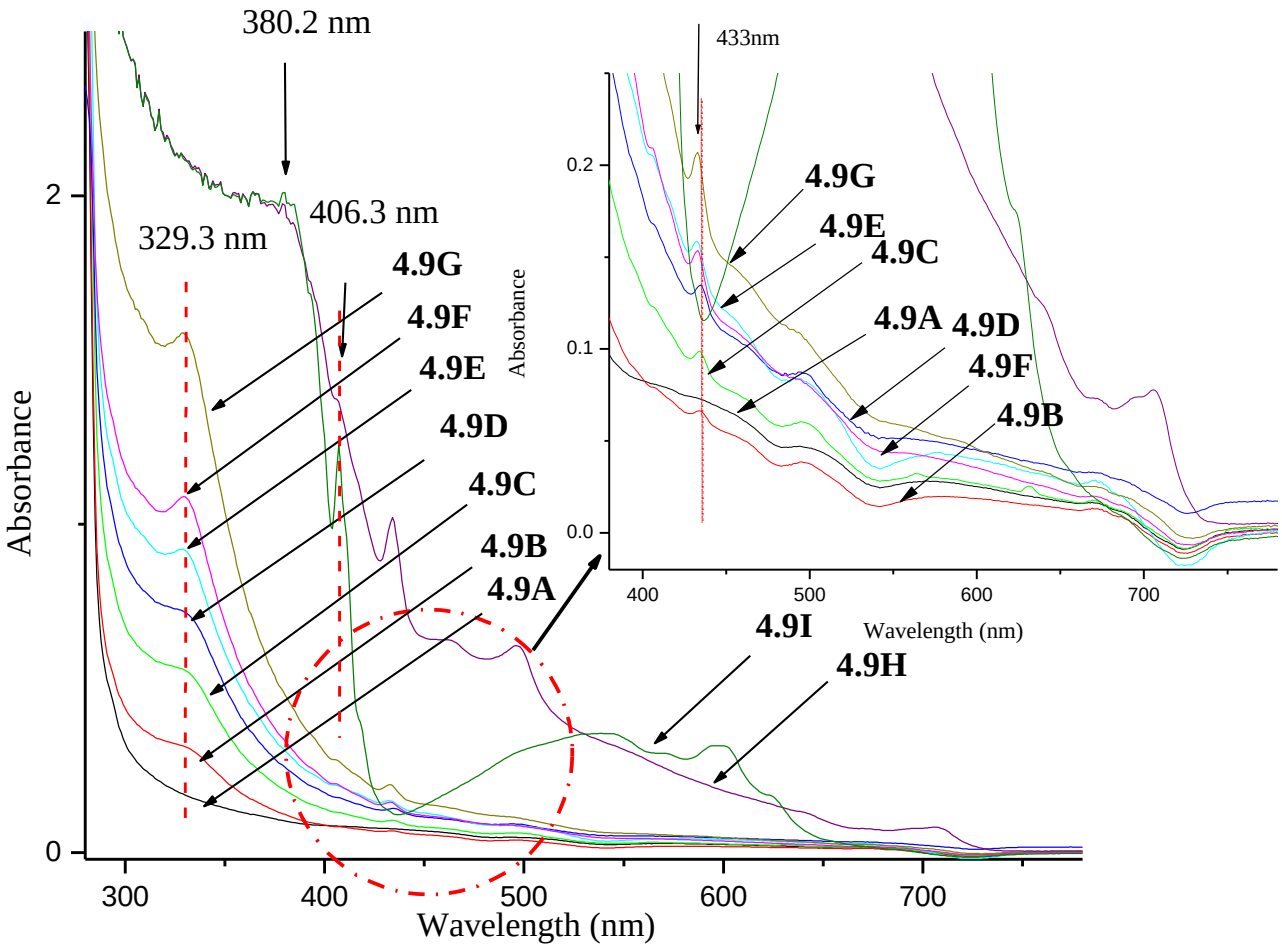

Figure **4.2** UV-visible spectra of co-polymers **4.9A-I** (in toluene, mole ratio **4.4:4.7**): **4.9A** (1:0 mole ratio), **4.9B** (1000:1 mole ratio), **4.9C** (700:1 mole ratio), **4.9D** (500:1 mole ratio), **4.9E** (300:1 mole ratio), **4.9F** (100:1 mole ratio), **4.9G** (50:1 mole ratio), **4.9H** C_{60}-cyclopentadiene cycloadduct **4.7**, **4.9I** C_{60} **4.5**.

Table **4.2** UV-visible λmax of the polymer **4.9A** and the co-polymers **4.9B-I**

Polymer	mole ratio **4.4:4.7**	λmax (nm)
4.9A	1:0	No λmax
4.9B	1000:1	329, 406, 433
4.9C	700:1	329,406, 433
4.9D	500:1	329, 406, 433
4.9E	300:1	329, 406, 433
4.9F	100:1	329, 406, 433
4.6G	50:1	329, 406, 433
3.9H	0:1	380, 434, 496, 709
3.9I	**4.5** only	380, 406, broad peak 460–650

In other published studies, the UV-visible absorption band of methanofullerene derivatives [21] and C_{60} monoaddducts [22] were recorded at ~432 nm; this band being attributed to the 6-6 ring fusion present in the compounds. Similarly, in this work, a band centered at 433 nm for all co-polymers (weak, inset Figure **4.2**) and the C_{60}-cyclopentadiene cycloadduct **4.7** was considered as characteristic of a 6-6 ring fusion.

4.3.3 Thermal Degradation Studies

4.3.3.1 Differential scanning calorimetry (DSC)

The glass transition temperatures for the synthesized polymer and copolymers were also determined under a nitrogen atmosphere. According to the results, there is no clear correlation

between the concentration of C_{60} in the polymers and the glass transition temperatures, unlike that observed in our early work [9]. However, for **4.9D-G** there is an observable trend in that as the concentration of C_{60} increases in the polymers, the T_g decreases (see Figure **4.3**). For pure polymer **4.9A** and the co-polymer **4.9G,** two T_g values were observed at 77 ^oC and 80 ^oC and 72 ^oC and 62 ^oC respectively (see Figure **4.3**). For the other polymers only a single T_g temperature was observed. (See Table **4.3** for a summary of these results).

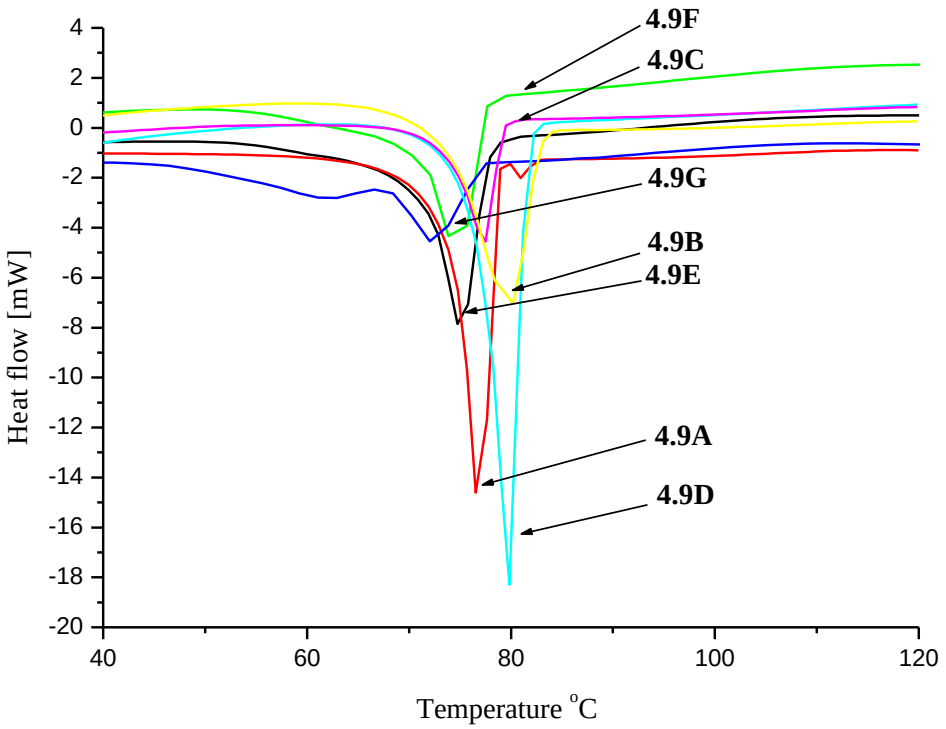

Figure **4.3** Differential Scanning Calorimetry T_g analyses (scan rate 5 ^oC/min) under nitrogen atmosphere: Co-polymers **4.9A-G** (mole ratio **4.4**:**4.7**): **4.9A** (1:0), **4.9B** (1000:1), **4.9C** (700:1), **4.9D** (500:1), **4.9E** (300:1), **4.9F** (100:1), **4.9G** (50:1).

Table **4.3** T_g and thermal decomposition temperature of C_{60}-containing polymers **4.9B-E** and **4.9A**.

Polymer	Mole ratio **4.4**:**4.7**	T_g (^oC)	Decomposition Temp.[a]
4.9A	1:0	77, 80	192, 436
4.9B	1000:1	80	190, 430
4.9C	700:1	77	252, 433
4.9D	500:1	80	242, 428
4.9E	300:1	75	443
4.9F	100:1	74	193,440
4.9G	50:1	72, 62	432

a Measured by derivative method

4.3.3.2 Thermogravimetric analysis (TGA)

The thermogravimetric analysis (TGA) results revealed that incorporation of C_{60} in the polymer did not significantly increase the thermal stability of the synthesised polymers. Two stages of decompositions were observed for **4.9A** and for the C_{60}-containing co-polymers **4.9B-H** at approximately 200 and 440 ^oC; however significant mass losses were observed after ~430 ^oC (Figure **4.4**). During the first stage decomposition of co-polymers **4.9C** and **4.9D** mass losses were 29 and 36 %, respectively, while for the others it ranged from 5 to 10 %. After thermal decomposition of the polymers (700 ^oC) the mass of the residues obtained were proportional to the content of C_{60} in the polymers, i.e. polymers which contained lesser amounts of fullerene retained smaller amounts of residue [23].

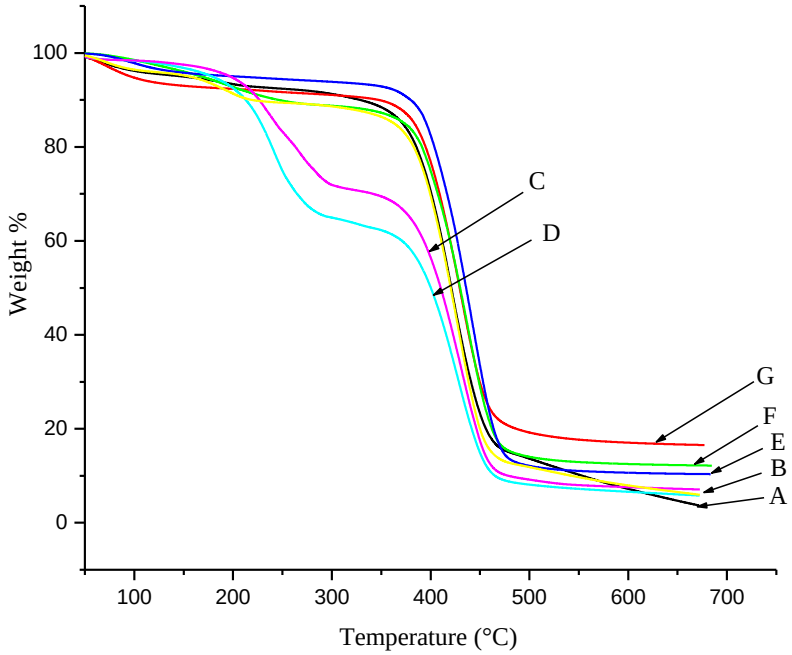

Figure **4.4** TGA curves of the polymers (rate 10 ^{o}C/ min) under a nitrogen atmosphere (mole ratio **4.4:4.7**): **4.9A** (1:0), **4.9B** (1000:1), **4.9C** (700:1), **4.9D** (500:1), **4.9E** (300:1), **4.9F** (100:1), **4.9G** (50:1).

4.4 Conclusion

In this work we successfully synthesized a series of C_{60}-containing polymers by the co-polymerization of a C_{60}-cyclopentadiene cycloadduct **4.7** and *N*-(cycloheptyl)-*endo*-norbornene-5,6-dicarboximide **4.4** in varying ratios. This work demonstrated that the methodology we developed for the production of covalently-linked, fullerene-containing polymers has been amenable to the use of a different co-monomer (in place of norbornene). The polymerization was readily facilitated by a catalytic amount of Grubbs' second generation catalyst **4.8**. The co-polymers thus formed were investigated by spectroscopic and thermal techniques and the results of these studies confirmed that the relative amounts of C_{60} in the polymers affected the polymer's physical properties.

4.5 References

1 (a) F. Giacalone, N. Martín, *Chem. Rev.,* **2006**, 106, 5136. (b) C. Wang, Z.-X. Guo, S. Fu, W. Wu, D. Zhu, *Prog. Polym. Sci.,* **2004**, 29, 1079. (c) K. E. Geckeler, S. Samal, *Polym. Int.* **1999**, 48, 743. (d) M. Prato, *J. Mater. Chem.,* **1997**, 7, 1097.

2 See for example: S. Shi, K. C. Khemani, Q. C. Li, F. Wudl, *J. Am. Chem. Soc.,* **1992**, 114, 10656.

3 See for examples: (a) T. Song, S. H. Goh, S. Y. Lee, *Polymer*, **2003**, 44, 2563. (b) C.-C. M. Ma, S.-C. Sung, F.-Y. Wang, L. Y. Chiang, L. Y. Wang, C.-L. Chiang, *J. Polym. Sci., Part B: Polym. Phys.,* **2001**, 39, 2436 and references cited therein.

4 N. Zhang, S. R. Schricker, F. Wudl, M. Prato, M. Maggini, G. Scorrano, *Chem. Mater.,* **1995**, 7, 441.

5 See for example: (a) Z. T. Ball, K. Sivula, J. M. J. Fréchet, *Macromolecules***, 2006**, 39, 70. (b) K. Sivula, Z. T. Ball, N. Watanabe, J. M. J. Fréchet, *Adv. Mater*., **2006**, 18, 206. (c) A. de la Escosura, M. V. Martínez-Díaz, T. Torres, R. H. Grubbs, D. M. Guldi, H. Neugebauer, C. Winder, M. Drees, N. S. Sariciftci, *Chem. Asian J.*, **2006**, 1-2, 148.

6 X. Liu, A. Basu, *J. Organomet. Chem.***, 2006**, 691, 5148.

7 F. J. Gómez, R. J. Chen, D. Wang, R. M. Waymouth, H. Dai, *Chem. Commun*., **2003**, 190.

8 Y. Liu, A. Andronov, *Macromolecules*, **2004**, 37, 4755.

9 M. A. Mamo, N. J. Coville, W. A. L. van Otterlo, *Fullerenes, Nanotubes and Carbon Nanostructures*, **2007**, 15, 341.

10 For a paper describing the development of this catalyst see: (a) T. M. Trnka, R. H. Grubbs, *Acc. Chem. Res.,* **2001,** 34, 18. For recent applications of this catalyst to our work, see the following recent references and citations therein: (b) R. Pathak, J.-L. Panayides, T. D. Jeftic, C. B. de Koning, W. A. L.van Otterlo, *S. Afr. J. Chem.* **2007**, 60, 1. (c) E. M Coyanis, J.-L. Panayides, M. A. Fernandes, C. B. de Koning, W. A. L. van Otterlo, *J. Organomet. Chem.,* **2006**, 691, 5222.

11 (a) A. P. Contreras, M. A. Tlenkopatchev, M. del Mar López-González, E. Riande, *Macromolecules*, **2002**, 35, 4677. (b) B. Liu, X. Wanga, Y. Wang, W. Yan, H. Li, I. Kim, *Reactive & Functional Polymers*, 2009, 69, 606.

12 For related work concerning *N*-alkylated norbornene dicarboximides and their application in ROMP see the following representative publications: (a) J. Vargas, A. A. Santiago, R. Gaviño, A. M. Cerda, M. A. Tlenkopatchev, *Express Polym. Lett.*, **2007**, 1, 274. (b) A. A. Santiago, J. Vargas, R. Gaviño, A. M. Cerda, M. A. Tlenkopatchev, *Macromol. Chem. Phys.*, **2007**, 208, 1085. (c) S. Hilf, A. F. M. Kilbinger, *Macromol. Rapid Commun.*, **2007**, 28, 1225. (d) C. C. Thomas, K. Ezat, R. H. Lian, *Macromolecules*, **2006**, 39, 5639. (e) T. C. Castle, E. Khosravi, L. R. Hutchings, *Macromolecules*, **2006**, 39, 5639. (f) R. Madan, R. C. Anand, I. K. Varma, *J. Polym. Sci.: Part A: Polym. Chem.*, **1997**, 35, 2917.

13 V. M. Rotello, J. B. Howard, T. Yadav, M. M. Conn, E. Viani, L. M. Giovane, A. L. Lafleur, *Tetrahedron Lett.*, **1993**, 34, 1561.

14 For other examples, involving the reaction of substituted or unsubstituted cyclopentadienes to C_{60} by way of a Diels-Alder reaction, see the following papers and references cited therein: (a) S. R. Wilson, M. E. Yurchenko, D. I. Schuster, A. Khong, M. Saunders, *J. Org. Chem.*, **2000**, 65, 2619. (b) R. Schwenninger, T. Müller, B. Kräutler, *J. Am. Chem. Soc.*, **1997**, 119, 9317. (c) B. Nie, V. M. Rotello, *J. Org. Chem.*, **1996**, 61, 1870.

15 For reviews on cycloadditions to C_{60} see: (a) M. A. Yurovskaya, I. V. Trushkov, *Russ. Chem. Bull. Int. Ed.*, **2002**, 51, 367. (b) P. Hudhomme, *C.R. Chimie*, **2006**, 9, 881. (c) R. Taylor, *C.R. Chimie*, **2006**, 9, 982. (d) J. Yli-Kauhaluoma, *Tetrahedron*, **2001**, 57, 7053.

16 H. W. Goh, S. H. Goh, G. Q. Xu, *J. Polym. Sci. Part A: Polym. Chem.*, **2002**, 40, 1157.

17 On formation, the polymers **3.9A-G** were generally very soluble. However after precipitation and drying of the polymers, addition of organic solvents often caused gel formation rather than facile solubilization.

18 See for example: (a) K. E. Geckeler, A. Hirsch, *J. Am. Chem. Soc.*, **1993**, 115, 3850. (b) T. Suzuki, Q. Li, K. C. Khemani, F. Wudl, *J. Am. Chem. Soc.*, **1992**, 114, 7301. (c) X. Zhang, A. B. Sieval, J. C. Hummelen, B. Hessen, *Chem. Commun.*, **2005**, 1616.

19 W. J. Li, W. J. Liang, *Spectrochim. Acta Part A*, **2007**, 67, 1346.

20 B. Z. Tang, S. M. Leung, H. Peng, N.-T. Yu, K. C. Su, *Macromolecules*, **1997**, 30, 2848.

21 See examples in the following papers and references cited therein: (a) C. -C. Chu, T.-I. Ho, L. Wang, *Macromolecules*, **2006**, 39, 5657. (b) S. Xiao, Y. Li, Y. Li, H. Li, J.

Zhuang, Y. Liu, F. Lu, D. Zhang, D. Zhu, *Tetrahedron Lett.*, **2004**, 45, 3975. (c) S. Xiao, Y. Li, H. Fang, H. Li, H. Liu, Z. Shi, L. Jiang, D. Zhu, *Org. Lett.*, **2002**, 4, 3063.

22 A. Kraus, K. Mullen, *Macromolecules*, **1999**, *32*, 4214.

23 See for example: (a) A. G. Camp, A. Lary, W. T. Ford, *Macromolecules*, **1995**, 28, 7959. (b) L. Y. Chiang, L. Y. Wang, C.-S. Kuo, *Macromolecules*, **1995**, 28, 7574. (c) L. Dai, A. W. H. Mau, H. J. Griesser, T. H. Spurling, J. *Phys. Chem.*, **1995**, 99, 17302. (d) C. J. Hawker, *Macromolecules*, **1994**, 27, 4836.

Chapter 5

Polymerization of a C_{60} derivative with thiophene in the presence of $FeCl_3$

5.1 Introduction

Since the discovery of C_{60} (fullerene) [1], its subsequent large scale production has attracted the attention of researchers in terms of chemistry [2] and applications [3]. A large number of studies have indicated that fullerenes possess interesting electrochemical [4], photophysical [5], optical [6], semiconducting [7] and magnetic [8] properties. As result novel properties associated with functionalized fullerenes have been reported by various researchers include superconductivity, ferromagnetism, and optical nonlinearity [9].

The design of molecules bearing covalently linked electron donors to C_{60} has received increasing attention in the past few years as these systems can be used in artificial photosynthesis and for photoelectronic applications [10]. Compounds that combine C_{60} with π-conjugated oligomers are of particular interest in photoelectronics [11-14]. On one hand, they provide entry into photoinduced intramolecular processes such as energy and electron transfer [12]. On the other hand, such hybrid compounds can be used for the preparation of solar cells allowing a detailed structure–activity exploration for a better understanding of the photovoltaic system [13].

It is well know that 1,3-dipolar addition of azomethine ylides to C_{60} yields fulleropyrrolidines that form across the 6,6-junction [15]. The azomethine ylides are reactive intermediates that are generated *in situ* by decarboxylation of immonium salts derived from thermal condensation of either amino acids and aldehydes (or ketones), or the thermal ring opening of aziridines. It has been shown to be one of the most flexible methods for the functionalization of fullerenes and has been widely used [16]. Different functional groups with important electronic properties have been attached to the fullerene system using azomethine ylides such as porphyrins [17], subphthalocyanines [18], dendrimers [19] and conjugated oligomers [20].

In donor-acceptor-linked fullerene molecule systems the donors have been constructed from a variety of dyad molecules including aniline [21], carotenoid [22], porphyrin [23,24], pyrazine [25], and tetrathiophene [26] moieties, making use of synthetic strategies which include the Prato reaction. These systems have been designed to achieve efficient intramolecular energy transfer [11f]. In addition, the particular problem of phase segregation caused by bi-component composite (mixture) materials in these devices, is thought to be minimized [27, 28]. However, it is important to note that in many triad and dyad systems using the Prato reaction, the π-conjugated repeating units are limited to below ten [11f, g].

The use of electron-accepting fullerenes in combination with π-conjugated systems, as electron donors, offers several attractive features. In particular, fullerene, due to its low reorganization energy [12b] in electron-transfer reactions, accelerates charge separation and decelerates charge recombination, compared to two dimensional, planar electron acceptors [27]. This is beneficial for stabilizing the charge-separated state in C_{60}-based materials as required in artificial electron transfer systems [28]. The design of electron donors covalently linked to C_{60} has thus received increasing attention in the past few years as these systems can be used in artificial photosynthesis and for photoelectronic applications [24]. Compounds that combine C_{60} with π-conjugated oligomers are of particular interest in photoelectronics [11].

In solar cells, conductive organic polymers such as poly(3-alkylthiophenes) (P3ATs) [29] play a crucial role as an electron donor and in charge transport [30]. They have also attracted much attention in organic electronics, because of their chemically tunable electronic properties and their processability from a variety of solvents [31].

Covalent bonding of polymers with C_{60} [32-34] is of considerable interest since the fullerene properties can be combined with those of specific polymers. Suitable fullerene polymers should be spin coatable, solvent-castable or melt-extrudable and the fullerene-containing polymers as well as surface-bound C_{60} layers are expected to have remarkable electronic, magnetic, mechanical, optical or catalytic properties [32]. Fullerenes can also be incorporated to and on the side chain of a polymer (on-chain type or “charm bracelet”) [35] or on the surface of a solid [36], in chain polymers with the fullerene as a part of the main chain (“pearl necklace”) [35], dendritic

systems, starburst or cross-link type material. End-chain type polymers that are terminated by a fullerene unit have also been reported.

In this work we report the functionalization of C_{60} using azomethine ylides (the Prato reaction [15]) and on subsequent reactions that incorporate the C_{60} derivatives covalently to a polymer polythiophene system. The electronic and thermal properties of the synthesized copolymers were then investigated and the results will be discussed in this Chapter.

5.2 Experimental

5.2.1 General procedures

The synthesised polymers, copolymers and C_{60} derivatives were characterised by thermo-gravimetric analysis (TGA), differential scanning calorimetry (DSC), mass spectrometry, UV-visible, FT-IR and NMR spectroscopy. The infrared spectra were recorded using a Varian 800 FT-IR spectrometer (KBr pellets) and transmittance values are reported in the wave number (cm^{-1}) scale in the range of 400–4000 cm^{-1}. Ultraviolet and visible spectra were recorded with a Varian 50 CONC UV-visible spectrophotometer and mass spectra were collected with a VG70-SEQ instrument in a positive ion mode using FAB ionization. The NMR spectra (chemical shift data in ppm) were recorded in $CDCl_3$ at ambient probe temperature using a Bruker Avance 300 (^1H, 300.13 MHz) spectrometer. Finally, TGA analyses were performed at a heating rate of 10 ^oC/min, under air using a Perkin Elmer Pyris 1 TGA instrument.

5.2.2 Functionalization of C_{60}

5.2.2.1 Synthesis of 5.2 [15]

C_{60} **5.1** (0.3 g, 0.42 mmol) was added to predried toluene (~50 mL) and the mixture was heated to 115 ^oC to dissolve all the C_{60}. After the solution was cooled to r.t., 2-thiophenecarboxaldehyde (0.048 g, 0.42 mmol) was added to the toluene solution. *N*-methylglycine (0.08 g, 0.9 mmol) was added to the above reaction mixture in small portions over 5 days (about 0.016 g per 24 h). The reaction mixture was then stirred at reflux for a further five days during which the purple color of the solution slowly changed to brown. The reaction mixture was then left to cool to r.t. and the solvent was removed under reduced pressure to afford a brown solid. The brown product was then purified using column chromatography (SiO_2, toluene, then 1 % DMF in toluene). After

removing the solvent under reduced pressure the product was dried under vacuum for 48 h to afford the desired product **5.2** (0.306 g, 85 % based on C_{60}).

5.2.2.2 Synthesis of 5.3 [15]

C_{60} **5.1** (0.5 g, 0.69 mmol) was added to pre-dried toluene (~75 mL) and the mixture was heated to 115 ^{o}C to dissolve all the C_{60}. After the solution was cooled to r.t., 3-thiophenecarboxaldehyde (0.077 g, 0.69 mmol) was added to the toluene solution. *N*-methylglycine (0.13 g, 1.426 mmol) was then added to the reaction mixture in small portions over 5 days (about 25 mg per 24 h). The reaction mixture was then left to heat at reflux under continuous stirring for a further five days during this time the purple color of the solution slowly changed to brown. The reaction mixture was then left to cool to r.t. and the solvent was removed under reduced pressure to afford a brown solid. The brown product was then purified using column chromatography (SiO_2, toluene, then 1 % DMF in toluene). After solvent removal under reduced pressure the product was dried under vacuum for 48 h to afford **5.3** (495 mg, 83 % based on C_{60}).

5.2.3 Polymerization reactions

5.2.3.1 Polymerization reactions to synthesize polythiophene 5.4 and poly(3-hexylthiophene) 5.5 [37]

$FeCl_3$ (3.90 g, 23.6 mmol) was added to dry chloroform (~25 mL) in each of two round bottom flasks and the mixtures were stirred for 10 min. Either thiophene (0.05 mg, 5.95 mmol) or 3-hexylthiophene (1.0 g, 5.9 mmol), in dry chloroform (~25 mL), was then added drop-wise over 10 min to the flask that contained the $FeCl_3$ mixtures and the reaction mixtures were stirred overnight under Ar. The polymerization reactions were terminated by pouring the reaction mixtures into an excess of MeOH (~50 mL) to precipitate the crude polymers. The synthesised polymers were subsequently filtered using a membrane filter paper (1 µm). The products were then washed with ethanol (100 mL), several times with a 1:1 distilled water and acetone mixture (500 mL) and finally several times with acetone (500 mL). The dark brown solid products were dried under vacuum for 48 h and 0.326 g (65 % based on thiophene monomer) of a brick red powder of pholythiophene and 0.855 g (86 % based on hexylthiophene monomer) of a dark brown spongy solid of poly(3-hexylthiophene) was obtained, respectively.

5.2.3.2 Copolymerization reactions

5.2.3.3 Copolymerization reactions to form polymers 5.6 and 5.7

$FeCl_3$ (0.35 g, 2.15 mmol) was added to dry dichloromethane (~25 mL) in each of two round bottom flasks and the mixtures were stirred under Ar for about 15 min. Thiophene (each 0.039 g, 0.46 mmol) and either **5.2** or **5.3** (each 0.040 g, ~0.046 mmol) were dissolved in dry dichloromethane (~10 mL) and the mixture was then added drop-wise over 30 min to a flask that contained the $FeCl_3$. The reaction mixtures were then left to stir for 24 h. The polymerization reactions were terminated by pouring the reaction mixture into an excess of MeOH (~50 mL) to precipitate the crude products. The precipitates that formed from the two reactions were filtered using a membrane filter (1 µm). The filtrates were each washed with a 1:1 mixture of distilled water and acetone (5x, total volume of 500 mL). The products were then dried under reduced pressure for 48 h to afford 0.069 g (87 % yield) and 0.073 g (92 % yield) of the dark brown products of **5.6** and **5.7**, respectively.

5.2.3.4 Copolymerization reactions to form polymers 5.8a, 5.8b and 5.8c

$FeCl_3$ (0.35 g, 2.15 mmol for **5.8a**; 7.0 g, 40 mmol for **5.8b** and 13.0 g, 80 mmol for **5.8c**) was added to dry dichloromethane (~25 mL) in each of three round bottom flasks and the mixtures were stirred under argon for about 15 min A mixture of 3-hexylthiophene (0.078 g, 0.463 mmol for **5.8a**; 1.66 g, 9.85 mmol for **5.8b** and 3.32 g, 19.7 mmol for **5.8c**) and **5.3** (0.040 g, 0.046 mmol for **5.8a**; 0.016 g, 0.0184 mmol for **5.8b** and **5.8c**) in different mole ratio (1000:1 for **5.8c**, 500:1 for **5.8b**, 10:1 for **5.8a**) were dissolved in dry dichloromethane (~10 mL) and added to the $FeCl_3$ mixture, drop-wise over 25 min The reaction mixtures were then left to stir for 24 h. Methanol (~50 mL) was added to the mixtures and the precipitates that formed were filtered using a membrane filter (1 µm). The filtrates were washed with a 1:1 mixture of distilled water and acetone (5x, total volume of 500 mL). The products were then dried under reduced pressure for 48 h to afford 0.103 g (87 % yield), 1.59 g (96 % yield) and 3.22 g (97 % yield) of dark brown products of polymers **5.8a**, **5.8b** and **5.8c**, respectively.

5.2.3.5 Copolymerization reaction to form polymer 5.9

$FeCl_3$ (0.350 g, 2.15 mmol) was added to dry dichloromethane (~ 25 mL) and the mixture was then stirred under argon for 15 min A mixture of **5.2** (0.040 g, 0.046 mmol) and 3-hexylthiophene (0.078 g, 0.463 mmol) was dissolved in dry dichloromethane (~10 mL) and was then added to the $FeCl_3$ mixture drop-wise over 25 min The reaction mixture then was left to stir for 24 h. MeOH (50 mL) was then added to the mixture and the precipitate that formed was filtered using a membrane filter (1 µm). The filtrate was washed with a 1:1 mixture of distilled water and acetone (5x, total volume of 500 mL). The product was then dried under reduced pressure for 48 h to afford 0.105 g (89 % yield) of a dark brown product.

5.3 Results and discussion

5.3.1 Synthesis of 5.2, 5.3 and copolymers

Prato *et al.* [15] have developed a powerful procedure for the functionalization of C_{60}. The Prato reagent is made by adding an aldehyde and a glycine. The reagents form azomethine ylides at high temperature that react via a 1,3-dipolar cycloaddtion with C_{60} to give functionalized fullerenes. This procedure permits the synthesis of a wide range of substituted fullerenes by variation of the aldehyde and glycine functional groups. In this study the use of 2 and 3-thiophene aldehyde and *N*-methylglycine was utilized for the synthesis of the C_{60} complexes. The products were isolated and then purified using column chromatography (SiO_2, toluene, 1% DMF in toluene) in good yields (> 83 %.). In an earlier report [11c], using 3-thiophene aldehyde, the overall isolated yield of this type of reaction was 10-40 % after heating the reaction mixture at reflux for 5-24 h. In our case, by heating the reaction mixture at reflux for longer times (five days) the overall yield was much improved. Mass spectroscopic (*m/z* = 860 [M+1] with 2.6%) and UV-visible results confirmed that indeed the reaction had offered the expected addition products **5.2** and **5.3** (Scheme **5.1**).

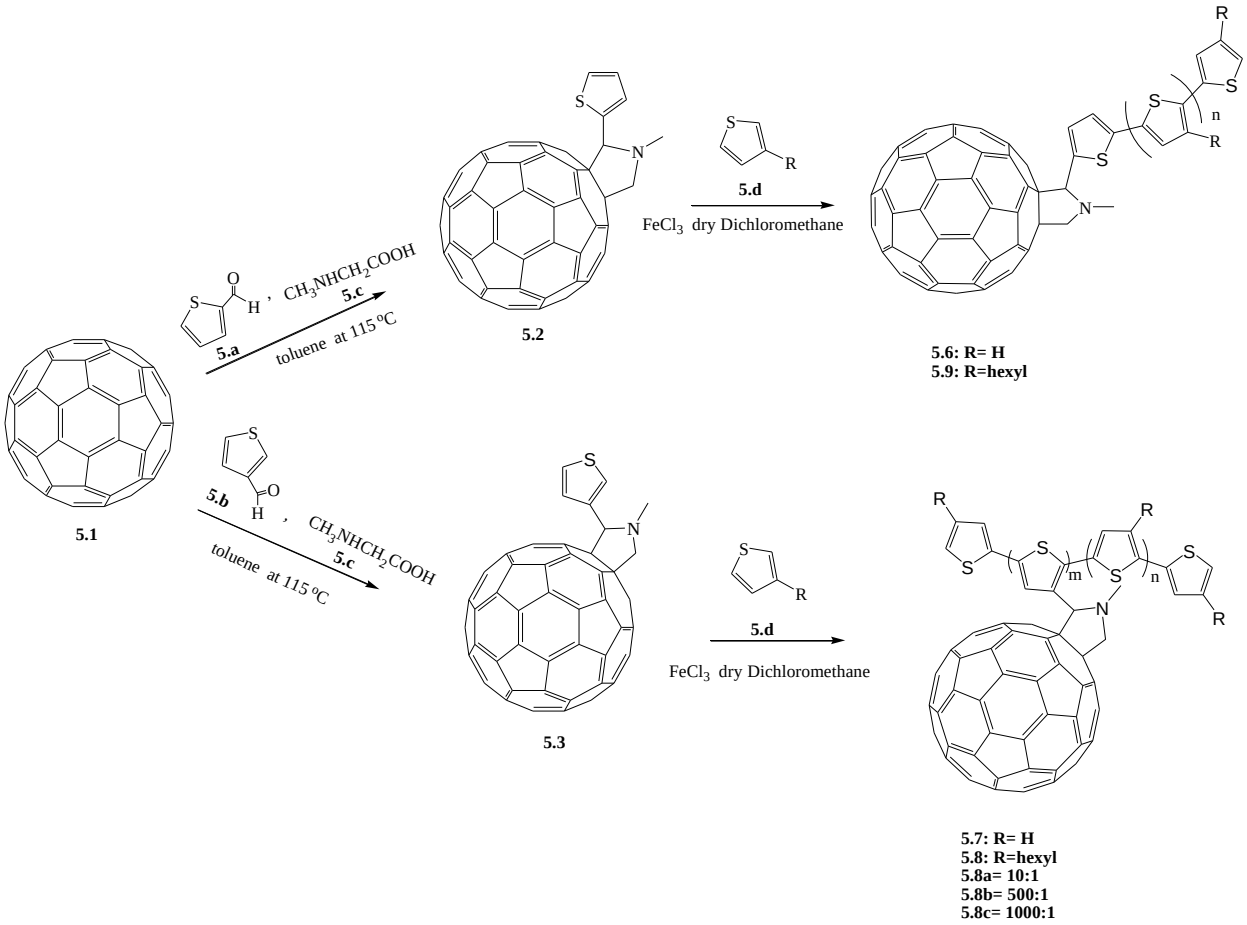

Scheme 5.1 Synthetic route to new copolymers using the Prato reaction to functionalization C_{60} followed by oxidative polymerization of thiophene.

The two C_{60} derivatives (**5.2** and **5.3**) have similar chemical formulae but different reactiveties in the polymerisation reactions with the thiophene used. Thiophene derivative **5.3** will generate pearl type polymers since it has two reactive sites at which propagation can occur. However, Thiophene derivative **5.2** can only result in end-cup polymers since only a single site is available for a polymerization reaction (see scheme **5.1**).

5.3.2 Polymerization reactions of the synthesised materials

3-Alkylthiophenes have been previously polymerized to the corresponding polyalkylthiophenes, either by electrochemical [38] or chemical polymerization [39] methods. However, studies have indicated that electrochemical polymerization reactions have several drawbacks when compared

to chemical polymerisation reactions. These include lower yields and generally a higher degree of regio-irregularities which results in decreased π-electron delocalization that limits the solubility of the polymer, as compared to polymers obtained by chemical methods [40]. Jen *et al.* [39] and Österhom *et al.* [39b] have used Grignard coupling reactions to chemically prepare polyalkylthiophenes. An earlier study by Sugimoto *et al.* [37] indicated that a direct one step oxidation of 3-alkythiophene with excess $FeCl_3$ (4 times stoichiometric proportion to the monomer) in chloroform, at r.t., gave the polymerized product in high yield.

It is to be noted that during polymerization the 3-alkyl substituent in a thiophene ring can be incorporated into a polymer chain with two different regioregularites, namely head-to-tail (HT) and head-to-head (HH). This results in four traid regioisomers in the polymer chain: the HT-HT, HT-HH, TT-HT and TT-HH traids (see Figure **5.1**).

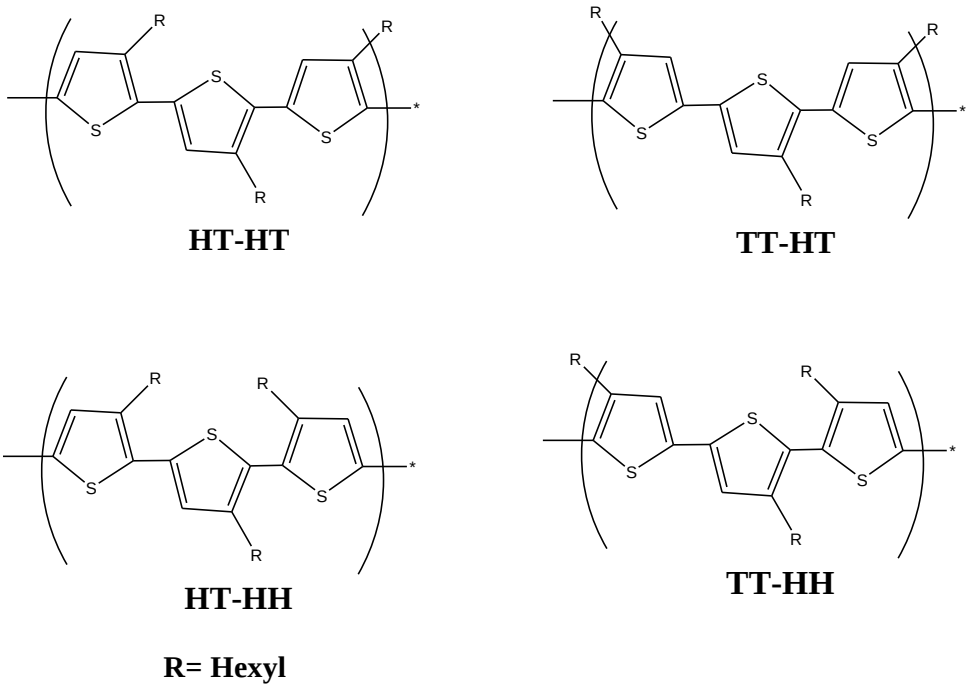

Figure **5.1** Different types of traid regioisomers of poly(3-hexylthiophene) [41].

The synthesised pure polymers **5.4** and **5.5** (Scheme **5.2**), were obtained using the latter approach as brick red powders and a spongy, dark brown coloured material in good yields of 66 % and 86 % for **5.4** and **5.5**, respectively. However, polymer **5.4** was not soluble in any organic solvents,

while polymer **5.5** was soluble in THF and 1,2-dichlorobenzene and sparingly soluble in dichloromethane, chloroform and hexane.

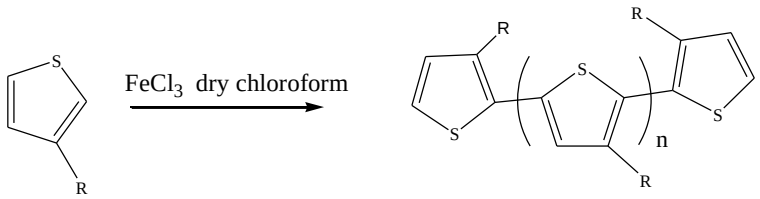

5.4: R= H
5.5: R=hexyl

Scheme **5.2** Synthetic route to the thiophene polymers.

The copolymers (**5.6**, **5.7**, **5.8a**, **5.8b**, **5.8c**, and **5.9**) were subsequently obtained in good yields (> 87 %) as brown powder or spongy, dark brown colour materials from the reaction of **5.2** and **5.3** with thiophene and 3-hexylthiophene, respectively (Scheme **5.1**). The unsubstituted polythiophene copolymers (**5.6** and **5.7**) found to be totally insoluble in all solvents. The hexyl substituted copolymers (**5.8a, 5.8b**, **5.8c** and **5.9**) found to have similar solubilities to the pure poly(3-hexylthiophene) (**5.5**); however the solubility decreased as the C_{60} concentration increase in the series **5.8c** < **5.8b** < **5.8a** .

5.3.3 Characterization of the synthesized copolymer

5.3.3.1 ^{1}H NMR spectroscopy of the synthesized copolymers

Solution NMR studies could not be performed on the insoluble, unsubstituted polythiophene polymers and co-polymers. The copolymers that were soluble were analyzed by using NMR spectroscopy in $CDCl_3$. The ^{1}H NMR spectra provided important information on the substitution pattern in the polymer backbone [42]. The substitution patterns have been shown to play an important role in the π-electron delocalization and solubility of the resulting polymers [46].

The NMR spectrum of 3-hexythiophene (Figures **5.2)** contained a narrow peak at δ = 0.9 assigned to the methyl protons **f**. Peaks at δ = 1.3 and 1.6 were assigned to the **e** and **d** methylene protons of the monomer, respectively. Similarly a triplet peak at δ = 2.6 was assigned to the methylene protons **c**. The aromatic hydrogen atoms of the thiophene rings were assigned at δ =

6.9 and 7.2 to the **a**/**a'**, and **b** protons respectively [41]. This spectrum provides the references for the analysis of the hexylthiophene polymers and co-polymers.

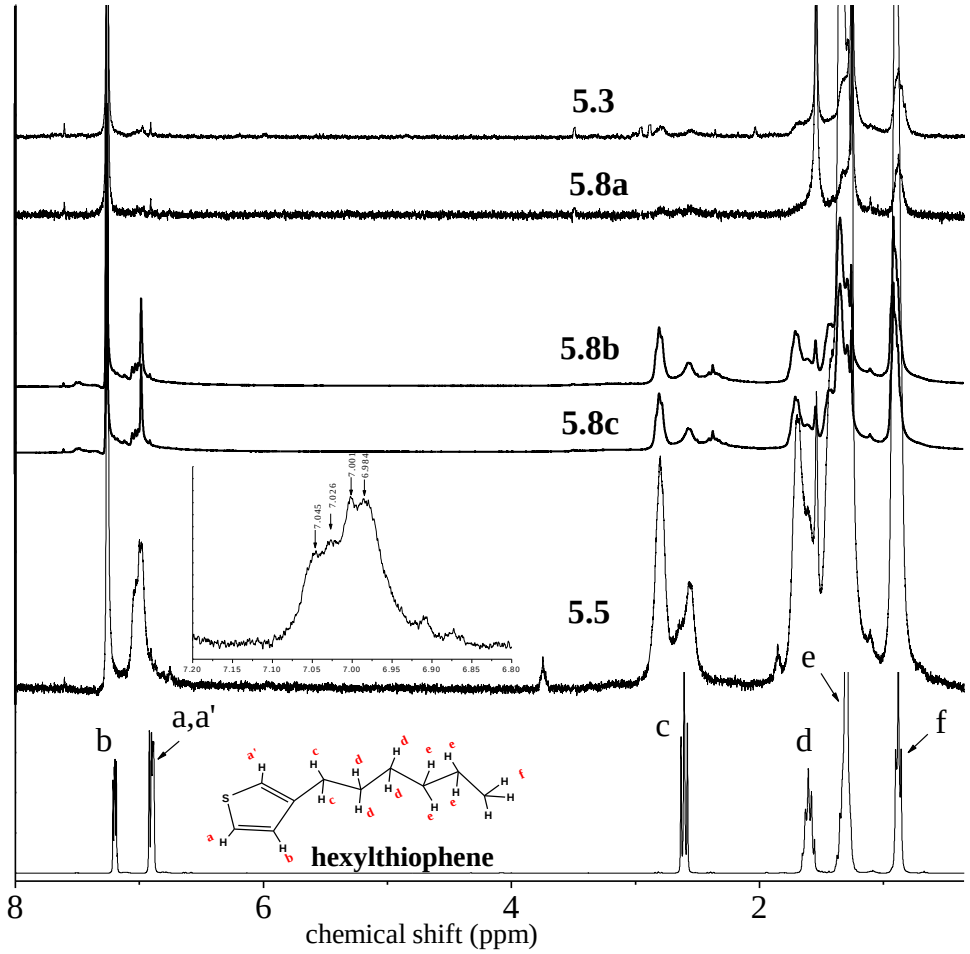

Figure **5.2.** ^{1}H NMR spectra of the monomer, polymer and copolymers for the synthesised polymers (in $CDCl_3$, 40 mg samples were used in each case, r.t., 300.13 MHz).

As expected, the resonance peaks found in the spectrum of poly(3-hexylthiophene) (**5.5**) and the copolymers attached to C_{60} have similar chemical shifts to those observed for the monomer. A broad peak at δ = 0.9 in both polymer and copolymers was assigned to the methyl protons **f**. Similarly broad peaks between δ = 1.3-1.6 was assigned to the methylene protons **e** and **d**. A triplet peak at δ = 2.6, was proposed to be due to the methylene proton **c** in the monomers, that splits into two broad peaks at δ = 2.6 and 2.8 after polymerization. This is due to the existence of HT and HH regioisomers, respectively [41]. The HT:HH ratio of the poly(3-hexylthiophene) was

deduced from the ^{1}H NMR spectrum by integration of the peaks at δ = 2.6 and 2.8 and was estimated to be 60:40. Disappearance of the thiophene aromatic hydrogen atoms of **a**/**a'** at δ = 6.9 after polymerization is evidence that polymerization indeed has taken places. The proton in the **b** position of the thiophene ring can occur in four different chemical environments in a mixture of the four possible traid regioismers (see Figure **5.1**). These four chemical shifts give distinct protons that are uniquely distinguished in the ^{1}H NMR spectra of poly(3-hexylthiophene) (**5.5**) (see inseted Figure **5.2**). The observed spectra were consistent with a new totally random mixture of the four traid structures depicted (HT-HT at δ = 6.98, TT-HT at δ = 7.00, HT-HH at δ = 7.03, TT-HH at δ = 7.05) [41].

Similarly, the HT:HH ratio of the copolymers **5.8b** and **5.8c** were deduced from the ^{1}H NMR spectrum by integration and found to be 70:30 and 65:35, respectively. Those incorporation of the C_{60} thiophene derivative into the thiophene backbone appeared to slightly favor the HT isomers. Due to poor resolution of ^{1}H NMR for **5.8a** it was not possible to deduce the HT:HH ratio for this particular copolymer.

5.3.3.2 FTIR spectroscopy of the synthesized copolymers

The FTIR spectra of the polymers are shown in Figure **5.3a** and **5.3b** for the polythiophene and poly(3-hexylthiophene) derivatives respectively. A summary of the FTIR band positions, and their assignments for the polymers, is given in Table **5.1**

A distinct peak for the fullerene derivatives (**5.2** and **5.3**) and copolymers in the range of 520-530 cm^{-1} is expected for a substituted C_{60} complexes [43]. This strong and distinctive peak in the spectra progressively disappeared as the concentration of C_{60} derivative was reduced in the copolymers (see Fig **5.3a**).

In the thiophene monomer, a strong band at 702 cm^{-1} was attributed to the =C-H out of plane vibration. Unlike in the polymer and copolymers, bands at 1510 and 1457 cm^{-1} were absent in the monomer. These bands are associated with 2,5-disubstituted thiophene in the polymers [44,45]. Finally, the aromatic C-H stretching band, at 3108 cm^{-1} appeared to be very weak for all the samples investigated.

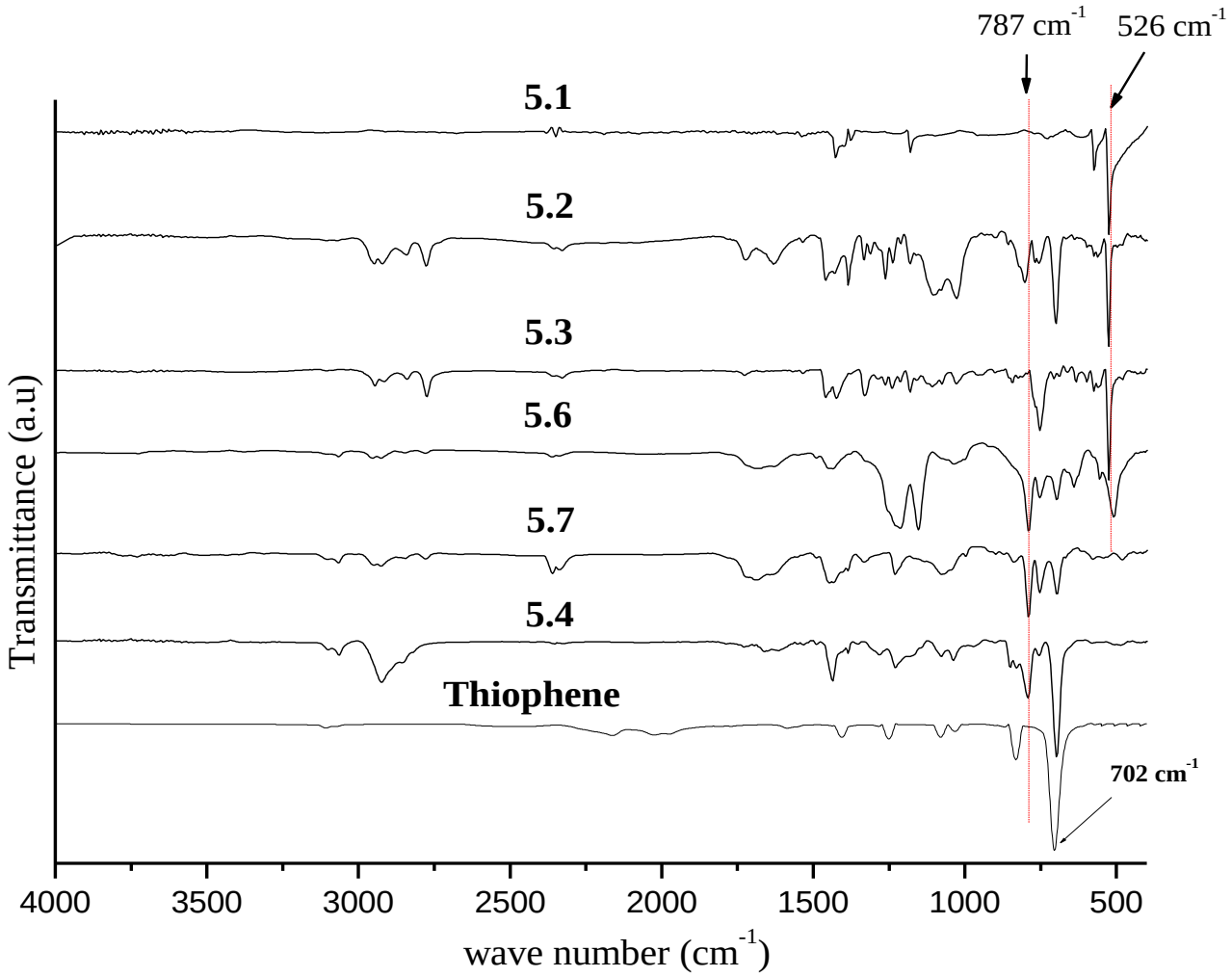

Figure **5.3a**. FT-IR spectra of the monomer and polythiophene derivatives KBr pellets.

The IR spectra for 3-hexylthiophene materials are shown in figure **5.3b**. A strong and characteristic band at 660 cm^{-1} was attributed to the =C-H out of plane vibration for the 3-hexylthiophene monomer and a band at ~720 cm^{-1} was assigned to the C-S-C out of plane deformation [46]. The aromatic C=C stretching vibration of the thiophene ring was recorded at 1654 cm^{-1}. Furthermore, the aliphatic C-H stretching bands were recorded between 2823-2714 cm^{-1}, and the aromatic C-H stretching appeared to be very weak at 3095 cm^{-1}.

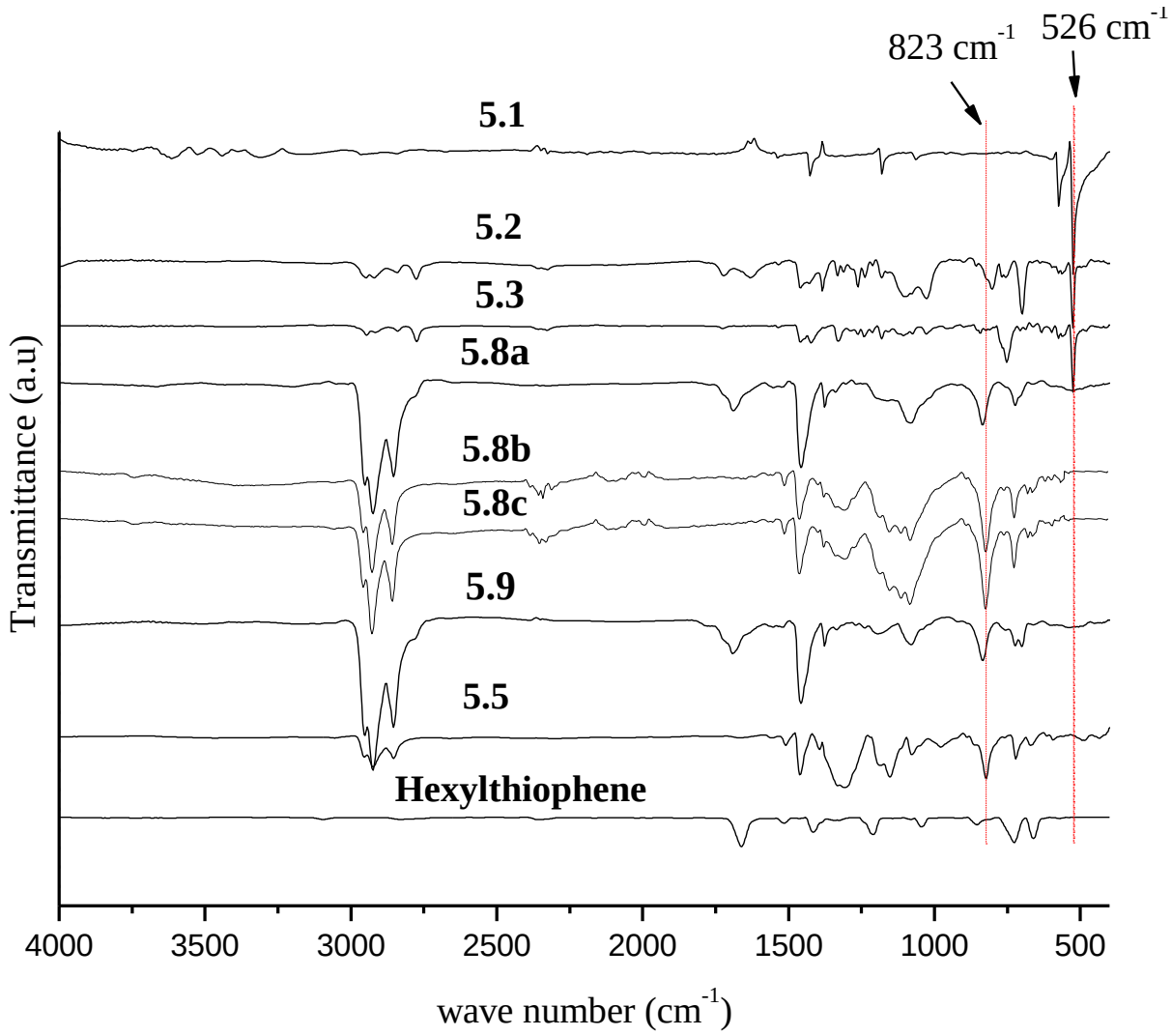

Figure **5.3b**. FT-IR spectra of the poly(3-hexylthiophene) derivatives KBr pellets.

Unlike in the monomers, some new and characteristic bands were recorded for both polymers and copolymers after polymerization. A band at around 787 cm^{-1} and 823 cm^{-1} were assigned to the =C-H out of plane vibration for the 2,5-disubstituted thiophene chains [44,45], in copolymers **5.6**, **5.7** and polythiophene (**5.4**) and, **5.8b** and **5.8c** and poly(3-hexylthiophene) polymers, respectively. However, in the case of **5.8a** and **5.9** this particular band shifted to lower energy at 835 cm^{-1}. Chen *et al*. [41] reported that regioregular HT poly(3-hexylthiophene) gave an absorbtion band at 820-822 cm^{-1}. On the other hand, regiorandom poly(3-hexylthiophene) gave bands at 827-829 cm^{-1}. Accordingly, our synthesized copolymers **5.8a** and **5.9** are considered to be regiorandom (due to the presence of the high concentration of C_{60}), while the **5.8b** and **5.8c**

and poly(3-hexylthiophene) (**4.5**) were more regioregular. A band at 666 cm^{-1}, that probably arises from 2-monosubstitution [44,45] at the end of the polymer chains, was noted in the two C_{60} derivatives (**5.2** and **5.3**), and copolymers **5.8a-c**, **5.9** and poly(3-hexylthiophene) (**5.5**). However, in the case of **5.6**, **5.7** and polythiophene (**5.4**) it was recorded at lower energy (< 690 cm^{-1}). In the case of functionalized C_{60} derivatives **5.2** and **5.3** this stretching band was probably due to the thiophene attachment that was associated with the Prato reagents. In all cases this band was very weak. The stretching vibration bands of the 2,5-disubstituted thiophene rings were recorded at around 1490 cm^{-1} and 1442 cm^{-1} for **5.6**, **5.7** and polythiophene (**5.4**) and 1510 cm^{-1} and ~1457 cm^{-1} for polymers **5.8a-c**, **5.9** and poly(3-hexylthiophene) (**5.5**) [44,45,47,48]. The aliphatic C-H stretching band was recorded at more or less similar wave numbers from 2955-2850 cm^{-1} and 2992-2720 cm^{-1} for all the copolymers [49] and C_{60} derivatives, respectively. As before, the aromatic C-H stretching vibration at 3065 cm^{-1} also appeared to be weak.

Table **5.1** Summary of FTIR of the copolymers, polymers and C_{60} derivatives (values in cm^{-1})[a]

Sample	Ar C-H str.	Alipha C-H str.	Ring str.		Ar C-H out of plane		C_{60} band
5.1							526 (s)
5.2		2992-2720 (br. s)				696 (vw)	526 (s)
5.3		2992-2720 (br. s)				696 (vw)	526 (s)
5.4	3065 (w)		1490 (vw)	1442 (m)	787 (m)	690 (s)	
5.5	3065(w)	2955-2850 (br. s)	1510 (vw)	1457 (s)	823 (s)	666(m)	
5.6	3065 (vw)	2955-2850 (w)	1490 (vw)	1442 (m)	787 (m)	690 (m)	520 (vw)
5.7	3065 (vw)	2955-2850 (br. s)	1510 (vw)	1457 (s)	823 (s)	666 (vw)	527 (vw)
5.8a	3065 (vw)	2955-2850 (w)	1490 (vw)	1442 (m)	787 (m)	690 (m)	520 (vw)
5.8b	3065(w)	2955-2850 (br. s)	1510 (vw)	1457 (s)	823 (s)	666(m)	
5.8c	3065(w)	2955-2850 (br. s)	1510 (vw)	1457 (s)	823 (s)	666(m)	
4.9	3065 (vw)	2955-2850 (br. s)	1510 (vw)	1457 (s)	829 (s)	666 (vw)	527 (vw)
thiophene	3108 (vw)					702 (s)	
3-hexylthiophene	3095 (vw)	2823-2714 (br. m)				660 (s)	

Ar = Aromatic; [a] vw = very weak, w = weak, m = medium, s = strong, br. s = broad and strong

5.3.3.3 UV-visible spectroscopy of the synthesized copolymers

The UV-visible absorbance spectra of C_{60} derivatives (**5.2** and **5.3**) and the **5.8a-c**, **5.9** copolymers were recorded in THF (see Table **5.2** and Figure **5.4**). A characteristic peak at 431 nm was observed for both C_{60} derivatives (**5.2** and **5.3**) and copolymers **5.8a-c** (see inset **Fig. 5.4**). In the case of copolymer **5.9**, however, the peak shifted into the blue region, a region largely dominated by the absorption band from poly(3-hexylthiophene). This absorption peak is proposed to be due to 6-6 fusion following monoaddition of the ylide to C_{60} [11c].

Table **5.2** UV visible spectra of poly(3-hexylthiophene) (**5.5**), **5.2**, **5.3**, copolymers **5.8a-c** and **5.9**

Sample	λ_{max} centre in nm
5.2	298, 432
5.3	298, 432
5.5	276, 426
5.8a	278, 432,
5.8b	276, 429
5.8c	276, 429
5.9	278, 432

The absorption peak at 276 nm is associated with poly(3-hexylthiophene) (**5.5**). A strong absorbance peak at 426 nm, due to poly(3-hexylthiophene), corresponds to the π-π* transition of its conjugated segments [50]. In case of **5.8b** and **5.8c,** this absorption peak was found to be shifted to the red region (429 nm), relative to the pure poly(3-hexylthiophene) (**5.5**).

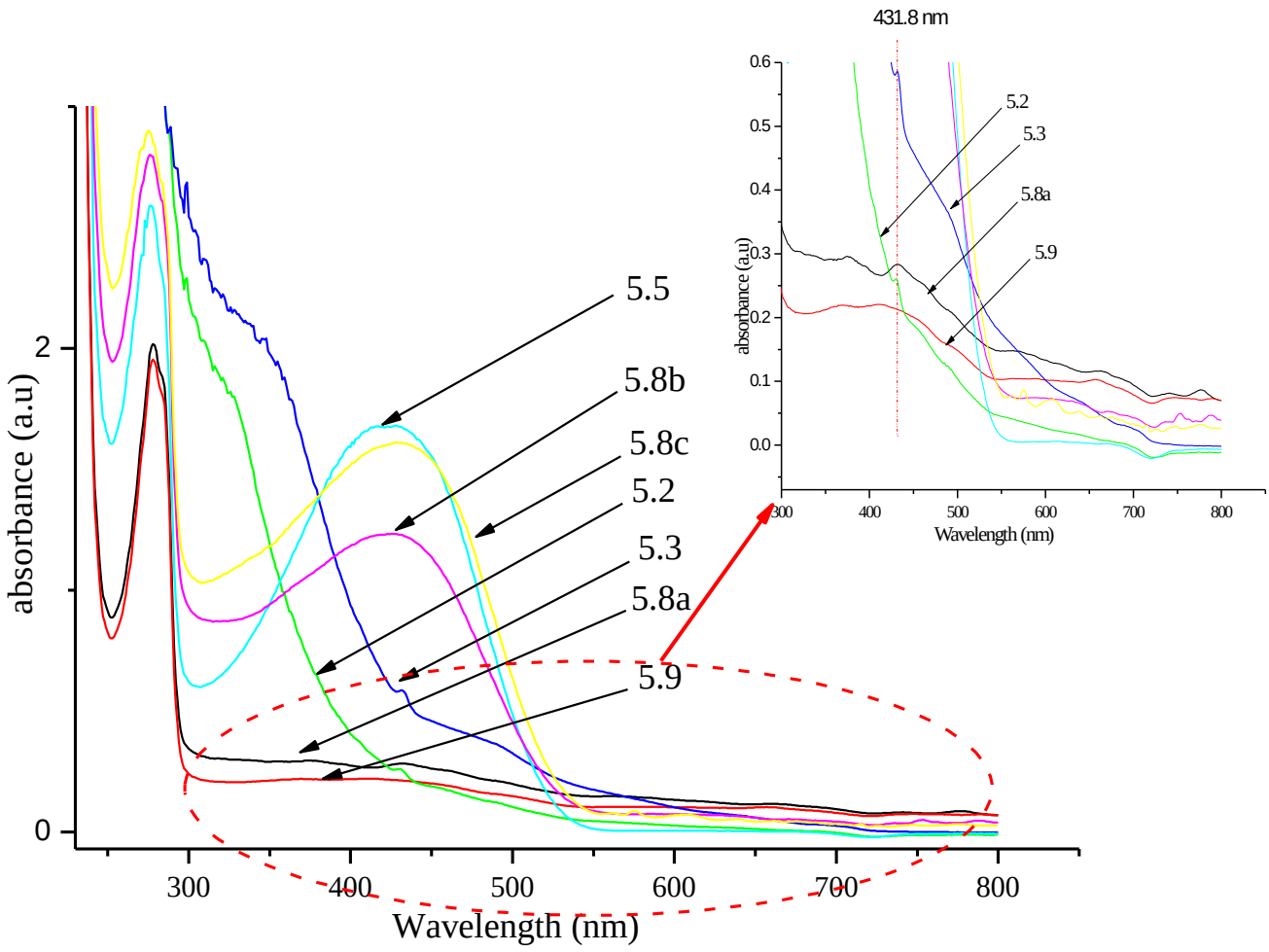

Figure **5.4** UV-visible absorption spectrum of poly(3-hexylthiophene) (**5.5**), compounds **5.2** and **5.3,** and copolymers **5.8a, 5.8b, 5.8c** and **5.9** in THF.

5.3.3.4 Thermogravimetric analysis (TGA)

The thermal stability of the synthesized polymers were examined by TGA [51] under air, by heating to 600 ^{o}C at a 10 ^{o}C/min heating rate (see Figure **5.5**). The summary of the decomposition stages and mass losses are given in Table **5.3**.

Copolymer **5.7** shows two decomposition reactions. The first decomposition occurs at 279 ^{o}C, and the second one occurs at 425 ^{o}C after 80 % mass loss. In contrast, copolymer **5.6** had three

decomposition reactions stages, while polythiophene (**5.4**) underwent only a single stage of decomposition at 214 ^{o}C (Figure **5.5a**.). The first decomposition temperature of copolymer **5.6** was much higher at 260 ^{o}C, followed by the second decomposition at 371 ^{o}C. The second stage of the decomposition reactions were accompanied by a 37 % mass loss for the copolymer **5.6**. This multiple decomposition reaction for copolymer **5.6** could be the end cuped polymer de-attached from the fullerene. The final decomposition reaction was at about 472 ^{o}C. From the TGA results copolymers **5.6** and **5.7** were more thermally stable than polythiophene **5.4**. Moreover, copolymer **5.6** was found to be thermally less stable than copolymer **5.7**.

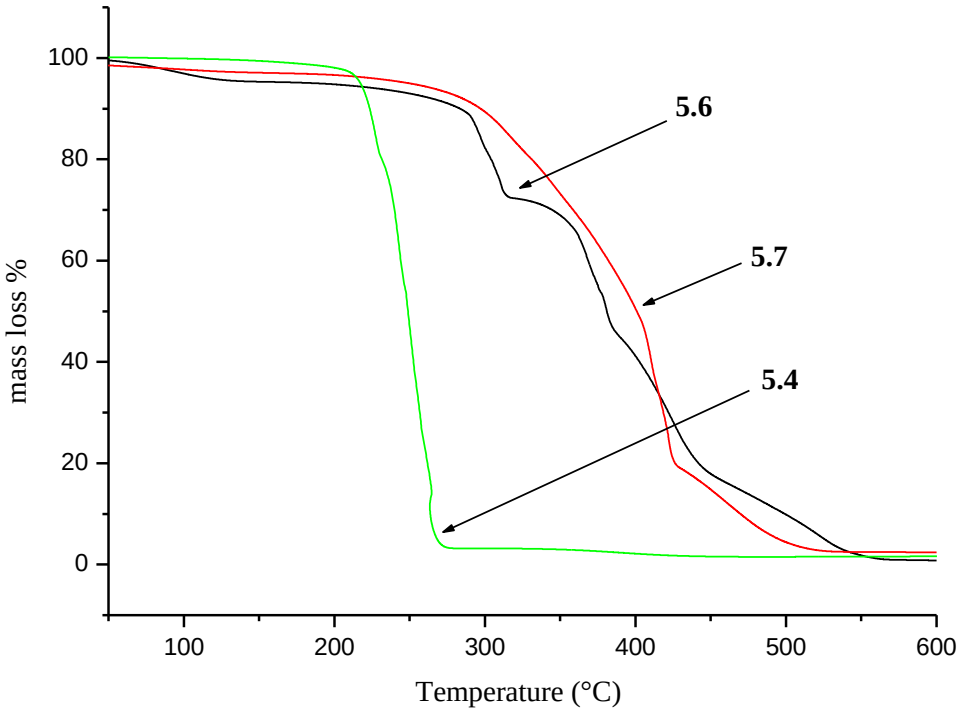

Figure **5.5a**. TGA thermograms of copolymers **5.6**, **5.7** and polythiophene (**5.4**)

The copolymers **5.8a, 5.8b, 5.8c** and poly(3-hexylthiophene) **5.5** all underwent one stage of decomposition at 300 ^{o}C (Figure **5.5b**). During this stage about > 99 % mass losses were recorded for copolymers **5.8a**, **5.8b**, **5.8c** and poly(3-hexylthiophene) (**5.5**). From the TGA results, incorporation of C_{60} into the polymers did not seem to improve the thermal properties of

the copolymers unlike that observed for the unsubstituted polythiophene derivatives of copolymers.

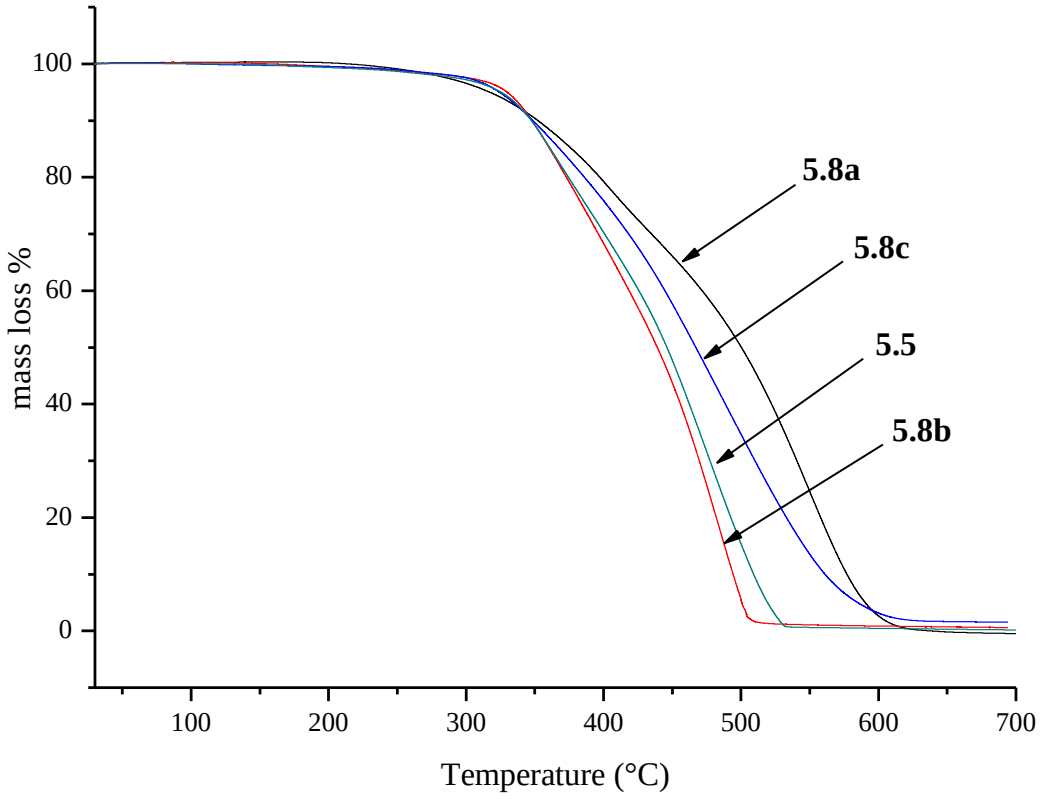

Figure **5.5b.** TGA thermogram of copolymers **5.8a**, **5.8b**, **5.8c** and poly(3-hexylthiophene) (**5.5**).

Table **5.3** summary of thermal decomposition temperature vs mass losses of copolymers and pure polymers.

Sample	1st decomposition		2nd decomposition	
	Temp. (°C)	Mass loss (%)	Temp. (°C)	Mass loss (%)
5.4	~214	>97		
5.5	~300	>99		
5.6	279	80	425	>98
5.7	260	55	371	87
5.8a	~300	>99		
5.8b	~300	>99		
4.8c	~300	>99		

5.4 Conclusion

A successful covalent functionalization of the C_{60} with thiophene was achieved by using a Prato approach. The synthesis of the two C_{60} derivatives (**5.2** and **5.3**) were confirmed by mass spectroscopic (*m/z* = 860 [M+1] with 2.6 %) and UV-visible techniques. Furthermore, covalent attachment of a poly(3-hexylthiophene) backbone were accomplished by $FeCl_3$ oxidative polymerization. According to the FT-IR results copolymers **5.8a** and **5.9** were found to be regiorandom (due to the presence of the high concentration of C_{60}), while the copolymers **5.8b** and **5.8c**, and poly(3-hexylthiophene) (**5.5**) were more regioregular. From the TGA results copolymers **5.6** and **5.7** are more thermally stable than polythiophene (**5.4**). Moreover, end-capped, copolymer **5.6**, was found to be less stable than the pearl copolymer **5.7**. However, in case of copolymers **5.8a**, **5.8b, 5.8c,** and **5.9**, incorporation of C_{60} derivatives into the thiophenes backbone did not improve the thermal stability of the polymer.

5.5 References

1 H. W. Kroto, J. R. Heath, S. C. O'Brien, R. F. Curl, R. E. Smalley, *Nature* **1985**, 318, 162.

2 (a) R. Taylor, D. R. M. Walton, *Nature*, **1993**, 363, 6431. (b) E. Champeil, C. Crean, C. Larraya, G. Pescitelli, G. Proni, L. Ghosez, *Tetrahedron*, **2008**, 64, 10319.

3 See for example: (a) D. Bonifazi, O. Enger, F. Diederich, *Chem. Soc. Rev.*, **2007**, 36, 390. (b) C. Wang, Z.-X. Guo, T. Yadav, S. Fu, W. Wu, D. Zhu, *Prog. Polym. Sci.* **2004**, 29, 1079.

4 (a) L. Echegoyen, L. E. Echegoyen, *Acc. Chem. Res.*, **1998**, 31, 593. (b) C. Bruno, I. Doubitski, M. Marcaccio, F. Paolucci, D. Paolucci, A. Zaopo, *J. Am. Chem. Soc.*, **2003**, 125, 15738.

5 D. M. Guldi, M. Prato, *Acc. Chem. Res.*, **2000**, 33, 695.

6 L. W. Tutt, A. Kost, *Nature*, **1992**, 356, 225.

7 R. C. Haddon, A. S. Perel, R. C. Morris, T. T. M. Palstra, A. F. Hebard, R. M. Fleming, *Appl. Phys. Lett.*, **1995**, 67, 121.

8 B. Narymbetov, A. Omerzu, V. V. Kabanov, M. Tokumoto, H. Kobayashi, D. Mihailovic, *Nature*, **2000**, 407, 883.

9 (a) A. F. Hebard, M. J. Rosesernsky, R. C. Haddon, D. W. Murphy, S. H. Glarum, T. T. M. Palstra, A. P. Ramirez, A. R. Kortan, *Nature*, **1991**, 350, 600.

10 (a) N. Martin, L. Sanchez, B. Illescas, I. Perez, *Chem. Rev.*, **1998**, 98, 2527. (b) H. Imahori, Y. Sakata, *Eur. J. Org. Chem.*, **1999**, 2445 (c) D. Gust, T. A. Moore, A. L. Moore, *Acc. Chem. Res.*, **2001**, 34, 40.

11 (a) F. Effenberger, G. Grube, *Synthesis*, **1998**, 1372. (b) Y. Obara, K. Takimiya, Y. Aso, T. Otsubo, *Tetrahedron Lett.*, **2001**, 42, 6877. (c) S.-H. Liu, L. Shu, J. Rivera, H. Liu, J.-M. Raimundo, J. Roncali, A. Gorgues, L. Echegoyen, *J. Org. Chem.*, **1999**, 64, 4884. (d) S. Campidelli, R. Deschenaux, J.-F. Eckert, D. Guillon, J.-F. Nierengarten, *Chem. Commun.*, **2002**, 656. (e) T. Gu, J.-F. Nierengarten, *Tetrahedron Lett.*, **2001**, 42, 3175. (f) J.-F. Eckert, J.-F. Nicoud, J.-F. Nierengarten, S.-G. Liu, L. Echegoyen, F. Barigelletti, N. Armaroli, L. Ouali, V. Krasnikov, G. Hadziioannou, *J. Am. Chem. Soc.*, 2000, **122**, 7467-7479. (g) E. Peeters, P. A. van Hal, J. Knol, C. J. Brabec, N. S. Sariciftci, J. C. Hummelen, R. A. J. Janssen, *J. Phys. Chem. B*, 2000, **104**, 10174-10190.

12 (a) N. Armaroli, F. Barigelletti, P. Ceroni, J.-F. Eckert, J.-F. Nicoud, J.-F. Nierengarten, *Chem. Commun*., **2000**, 599. (b) M. Fujitsuka, O. Ito, T. Yamashiro, Y. Aso, T. Otsubo, *J. Phys. Chem., A,* **2000**, 104, 4876. (c) T. Yamasshiro, Y. Aso, T. Otsubo, H. Tang, Y. Harima, K. Yamashita, *Chem. Lett*., **1999**, 443. (d) J. L. Segura, R. Gomez, N. Martin, D. M. Guldi, *Chem. Commun*., **2000**, 701. (e) J. J. Apperloo, C. Martineau, P. A. van Hal, J. Roncali, R. A. J. Janssen, *J. Phys. Chem. A,* **2002**, 106, 21.

13 (a) J.-F. Nierengarten, J.-F. Eckert, J.-F. Nicoud, L. Ouali, V. Krasnikov, G. Hadziioannou, *Chem. Commun*., **1999**, 617. (b) J.-F. Eckert, J.-F. Nicoud, J.-F. Nierengarten, S.-G. Liu, L. Echegoyen, F. Barigelletti, N. Armaroli, L. Ouali, V. Krasnikov, G. Hadziioannou, *J. Am. Chem. Soc*., **2000**, 122, 7467. (c) E. Peeters, P. A. van Hal, J. Knol, C. J. Brabec, N. S. Sariciftci, J. C. Hummelen, R. A. J. Janssen, *J. Phys. Chem. B,* **2000**, 104, 10174. (d) D. M. Guldi, C. Luo, A. Swartz, R. Gomez, J. L. Segura, N Martin, C. Brabec, N. S. Sariciftci, *J. Org. Chem*., **2002**, 67, 1141. (e) T. Gu, D. Tsamouras, C. Melzer, V. Krasnikov, J.-P. Gisselbrecht, M. Gross, G. Hadziioannou, J.-F. Nierengarten, *Chem. Phys. Chem.,* **2002**, 124. (f) N. Armaroli, G. Accorsi, J.-P. Gisselbrecht, M. Gross, V. Krasnikov, D. Tsamouras, G. Hadziioannou, M. J. Gomez-Escalonilla, F. Langa, J.-F. Eckert, J.-F. Nierengarten, *J. Mater. Chem*., **2002**, 12, 2077.

14 (a) J. J. Apperloo, , B. M. W. J. Langeveld-VossKnol, J. C. Hummelen, R. A. J. Janssen, *Adv. Mater*., **2000**, 12, 908. (b) J. L. Segura, N. Martin, *Tetrahedron Lett*., **1999**, 40, 3239. (c) C. Martineau, P. Blanchard, D. Rondeau, J. Delaunay, J. Roncali, *Adv. Mater*., **2002**, 14, 283.

15 (a) M. Maggini, G. Scorrano, M. Prato, *J. Am. Chem. Soc*., **1993**, 115, 9798. (b) M. Prato, M. Maggini, *Acc. Chem. Res.*, **1998**, 31, 519.

16 See the following representative examples: (a) F. Effenberger, G. Grube, *Synthesis,* **1998**, 1372. (b) Y. Obara, K. Takimiya, Y. Aso, T. Otsubo, *Tetrahedron Lett*., **2001**, 42, 6877. (c) S. Campidelli, R. Deschenaux, J.-F. Eckert, D. Guillon, J.-F. Nierengarten, *Chem. Commun*., **2002**, 656. (d) T. Gu, J.-F. Nierengarten, *Tetrahedron Lett*., **2001**, 42, 3175. (e) N. Armaroli, F. Barigelletti, P. Ceroni, J.-F. Eckert, J.-F. Nicoud, J.-F. Nierengarten, *Chem. Commun*., **2000**, 599. (f) T. Yamasshiro, Y. Aso, T. Otsubo, H. Tang, Y. Harima, K. Yamashita, *Chem. Lett*., **1999**, 443. (g) J. L. Segura, R. Gómez, N. Martín, D. M. Guldi,

Chem. Commun., **2000**, 701. (h) J. J. Apperloo, C. Martineau, P. A. van Hal, J. Roncali, R. A. J. Janssen, *J. Phys. Chem. A,* **2002**, 106, 21. (i) J.-F. Nierengarten, J.-F. Eckert, J.-F. Nicoud, L. Ouali, V. Krasnikov, G. Hadziioannou, *Chem. Commun*., **1999**, 617. (j) J.-F. Eckert, J.-F. Nicoud, J.-F. Nierengarten, S.-G. Liu, L. Echegoyen, F. Barigelletti, N. Armaroli, L. Ouali, V. Krasnikov, G. Hadziioannou, *J. Am. Chem. Soc*., **2000**, 122, 7467. (k) E. Peeters, P. A. van Hal, J. Knol, C. J. Brabec, N. S. Sariciftci, J. C. Hummelen, R. A. J. Janssen, *J. Phys. Chem. B,* **2000**, 104, 10174. (l) D. M. Guldi, C. Luo, A. Swartz, R. Gómez, J. L. Segura, N. Martín, C. Brabec, N. S. Sariciftci, *J. Org. Chem*., **2002**, 67, 1141. (m) J. J. Apperloo, , B. M. W. Langeveld-Voss, J. Knol, J. C. Hummelen, R. A. J. Janssen, *Adv. Mater*., **2000**, 12, 908. (n) C. Martineau, P. Blanchard, D. Rondeau, J. Delaunay, J. Roncali, *Adv. Mater*., **2002**, 14, 283.

17 (a) R. Fong II, D. I. Schuster, S. R. Wilson, *Org. Lett.,* **1999**, 1, 729. (b) H. Imahori, H. Yamada, Y. Nishimura, I. Yamazaki, Y. Sakata, *J. Phys. Chem. B,* **2000**, 104, 2099. (c) H. Imahori, H. Norieda, H. Yamada, Y. Nishimura, I. Yamazaki, Y. Sakata, S. Fukuzumi, *J. Am. Chem. Soc*., **2001**, 123, 100. (d) C. Luo, D. M. Guldi, H. Imahori, K. Tamaki, Y. Sakata, *J. Am. Chem. Soc.*, **2000**, 122, 6535.

18 D. González-Rodriguez, T. Torres, D. M. Guldi, J. Rivera, M. A. Herranz, L. Echegoyen, *J. Am. Chem. Soc.,* **2004**, 126, 6301.

19 (a) Y. Rio, J.-F. Nicoud, J.-L. Rehspringer, J.-F. Nierengarten, *Tetrahedron Lett.,* **2000**, 41, 10207. (b) S. Campidelli, E. Vázquez, D. Milic, M. Prato, J. Barberá, D. M. Guldi, M. Marcaccio, D. Paolucci, F. Paolucci, R. Deschenaux, *J. Mater. Chem*., **2004**, 14, 1266. (c) S. Campidelli, J. Lenoble, J. Barberá, F. Paolucci, M. Marcaccio, D. Paolucci, R. Deschenaux, *Macromolecules*, **2005**, 38, 7915.

20 (a) T. Gu, J.-F. Nierengarten, *Tetrahedron Lett*., **2001**, 42, 3175. (b) T. Gu, D. Tsamouras, C. Melzer, V. Krasnikov, J.-P. Gisselbrecht, M. Gross, G. Hadziioannou, J.-F. Nierengarten, *Chem.Phys.Chem.,* **2002**, 124.

21 R. M. Williams, J. M. Zwier, J. W. Verhoeven, *J. Am. Chem. Soc.,* **1995**, 117, 4093.

22 (a) H. Imahori, S. Cardoso, D. Tatman, S. Lin, L. Noss, G. R. Seely, L. Sereno, C. Silber, T. A. Moore, A. L. Moore, D. Gust, *Photochem. Photobiol.,* **1995**, 62, 1009. (b) D. Gust, T. A. Moore, A. L. Moore, *Res. Chem. Intermed.,* **1997**, 23, 621.

23 D. Kuciauskas, S. Lin, G. R. Seely, A. L. Moore, T. A. Moore, D. Gust, T. Drovetskaya, C. A. Reed, P. D. W. Boyd, *J. Phys. Chem.*, **1996**, 100, 15926.

24 (a) H. Imahori, K. Hagiwara, M. Aoki, T. Akiyama, S. Taniguchi, T. Okada, M. Shirakawa, Y. Sakata, *J. Am. Chem. Soc.*, **1996**, 118, 11771. (b) H. Imahori, K. Hagiwara, T. Akiyama, M. Aoki, S. Taniguchi, T. Okada, M. Shirakawa, Y. Sakata, *Chem. Phys. Lett.*, **1996**, 263, 545.

25 D. M. Guldi, G. Torres-Garscia, J. Mattay, *J. Phys. Chem. A*, **1998**, 102, 9679.

26 M. Fujitsuka, O. Ito, T. Yamashiro, Y. Aso, T. Otsubo, *J. Phys. Chem. A*, **2000,** 104, 4876.

27 G. Yu, Y. Gao, J. C. Hummelen, F. Wudl, A. J. Heeger, *Science*, **1995**, 270, 1789.

28 N. S. Sariciftci, L. Smilowitz, A. J. Heeger, F. Wudl, *Science*, **1992**, 258, 1474.

29 R. D. McCullough, *Adv. Mater.*, **1998**, 10, 93.

30 (a) M. Reyes-Reyes, K. Kim, D. L. Carroll, *Appl. Phys. Lett.*, **2005**, *87*, 083506. (b) G. Li, V. Shrotriya, J. Huang, Y. Yao, T. Moriarty, K. Emery, Y. Yang, *Nat. Mater.*, **2005**, *4*, 864. (c) J. Y. Kim, K. Lee, N. E. Coates, D. Moses, T. Nguyen, M. Dante, A. J. Heeger, *Science*, **2007**, *317*, 222.

31 (a) T. Skotheim, J. Reynolds, R. Elsembauer, *Handbook of Conducting Polymers*, Marcel Dekker: New York, **1998**., (b) H. S. Nalwa, *Handbook of Organic Conductive Molecules and Polymers*, J. Wiley & Sons: New York, **1996**.

32 K. E. Geckeler, S. Samal, *Polym. Int.*, **1999**, 48, 743.

33 M. Prato, *Top. Curr. Chem.*, **1999**, 199, 173.

34 M. S. Meier, *Springer Ser. Mater. Sci.*, **2000**, 38, 369.

35 T. Suzuki, Q. Li, K. C. Khemani, F. Wudl, O. Almarsson, *J. Am. Chem. Soc.*, **1992**, 114, 7300.

36 D. E. Bergbreiter, H. N. Gray, *J. Chem. Soc., Chem. Commun.*, **1993**, 645.

37 R. Sugimoto, S. Takeda, H. B. Gu, K. Yoshino, *Chem. Express*, **1986**, 1, 635.

38 M. Sato, S. Tanaka, K. Kaeriyama, *J. Chem. Soc., Chem. Commun.*, **1986**, 873.

39 J.-E. Österholm, J. Laakso, P. Nyholm, H. Isotalo, H. Stubb, O. Inganäs, W.R. Salaneck, *Synth. Met.*,**1989**, 28, 435

40 M. Leclerc, F. M. Diaz, G. Wegner, *Makromol. Chem.*, **1989**, 190, 3105.

41 T. Chen, X. Wu. R.D. Rieke, *J. Am. Chem. Soc.*, **1995**, 117, 233.

42 (a) R. M. S. Maior, K. Hinkelmann, H. Eckert, F. Wudl, *Macromolecules,* **1990**, 23, 1268. (b) M.-A. Sato, H. Morii, *Macromolecules*, **1991**, 24, 1196. (c) M.-A. Sato, H. Morii, *Polym. Commun.*, **1991**, 32, 42. (d) G. Barbarella, A. Bongini, M. Zambianchi, *Macromolecules,* **1994**, 27, 3039.

43 F. Andreania, E. Salatellia, M. Lanzia, F. Bertinellib, A. M. Ficherac, M. Gazzanoc, *Polymer*, **2000**, 41, 3147.

44 M. Akimoto, Y. Furukawa, H. Takeuchi, I. Harada, Y. Soma, M. Soma, *Synth. Met.*, **1986**, 15, 353.

45 Y. Furukawa, M. Akimato, I. Harada, *Synth. Met.*, **1987**, 18, 151

46 (a) F. Mohammad, *J. Phys. D: Appl. Phys*., **1998**, 31, 951. (b) Y. Yagci, F. Yilmaz, S. Kiralp, L. Toppare, *Macromol. Chem. Phys*., **2005**, 206, 1178. (c) B. Sari, M. Talu, F. Yildirim, E. K. Balci, *Appl. Surf. Sci*., **2003**, 205, 27. (d) M. G. Han, S. H. Foulger, *Adv. Mater*., **2004**, 16, 231. (e) Y. A. Udum, K. Pekmez, A. Yildiz, *Eur. Polym., J.* **2005**, 41, 1136.

47 S. Hotta, S. D. D. V. Rughooputh, A. J. Heeger, F. Wudl, *Macromolecules*, **1987**, 20, 212.

48 S. Hotta, W. Shimotsuma, M. Taketani, S. Kohiki, *Synth. Met.*, **1985**, 11,139.

49 B. K. Kuila, S. Malik, S. K. Batabyal, A. K. Nandi, *Macromolecule*, **2007**, 40, 278.

50 B. K. Kuila, S. Malik, S. K. Batabyal, A. K. Nandi, *Macromolecules,* **1987**, 20, 212.

51 M.-H. Yang, *Polym. Testing*, **1998**, 17, 191.

Chapter 6
Functionalization of nitrogen doped and undoped carbon nanotubes using ring opening metathesis polymerization with norbornene

6.1 Introduction

Since the discovery of CNTs in 1991 [1], the interest in their utilization has been steadily increasing. The prospect of developing novel carbon-based nanomaterials from those materials has been explored because of their unique structure-dependent electronic and mechanical properties [2-4]. For example, carbon-based nanoscale diodes or transistors have become one of the main topics in CNT-based nanoelectronics [5].

Furthermore, doping of heteroatoms into CNTs may lead to the formation of electron-excess *n*-type (e.g., N-CNTs) or electron-deficient *p*-type (e.g., B-CNTs) semiconducting nanotubes [6]. Doping with different elements, such as nitrogen, is thus a promising method to tailor the electronic properties of CNTs [7] as the additional electrons contributed by the nitrogen atoms provide electron carriers for the conduction band [8]. N-doped nanotubes have been found to be either metallic or narrow energy gap semiconductors [9,10], thus offering the possibility of greater electrical conductivity as compared to pure carbon nanotubes.

Different kinds of precursors, including carbon and nitrogen containing molecules such as C_5H_5N [11], CH_3CN [12d], and $HOCN(CH_3)_2$ [13f] or mixtures of carbon/nitrogen containing gaseous species such as CH_4/N_2 [14a-c] and C_2H_2/NH_3 [14c,e,f], have been used for the synthesis of N-CNTs. In most cases the growth temperature of N-CNTs is in the range of 700-1100 °C, and the average nitrogen content is between 1-10 % [11,13].

The mechanical properties of CNTs are thought to have important potential for future developments in the areas of science and technology. In studies [15,16] the Young's modulus and tensile strength were found to be up to 1 TPa and 60 GPa respectively. However, to access these extraordinary properties, the polymer-nanotube interfacial stress transfer must be

maximized in order to achieve the best possible reinforcement. Cadek *et al.* [17] showed a significant increased in Young's modulus by up to a factor of two to 1.4 TPa.

In nanotube-based nanocomposites, solvent casting and melt mixing are two of the most common methods to make composites. Qian *et al.* [18] studied a MWNT/polystyrene (PS)/toluene nanocomposite and the data revealed a product with enhanced elastic modulus and break stress. Benoit *et al*. [19] have obtained electrically conductive nanocomposites by dispersing SWNTs and poly(methyl methacrylate) (PMMA) in toluene, followed by drop casting of the mixture on substrates. Generally nanocomposites with a range of thermoplastic matrices have been fabricated by solvent casting [20], but nanotubes tend to agglomerate during solvent evaporation, which leads to inhomogeneous nanotube distribution in the polymer matrix. To solve this problem, Haggenmueller *et al.* [21] used combined methods of solvent casting and melt mixing with sonication, to make SWNT/PMMA composites. With this procedure they found a considerable improvement in nanotube dispersion.

In addition to the solvent casting, melt mixing, and coagulation methods, which combine nanotubes with high molecular weight polymers, *in situ* polymerization methods have also been used to make nanotube-based nanocomposites starting with nanotubes and monomers. The most common *in situ* polymerization methods involve epoxy in which the resins (monomers) and hardeners are combined with SWNTs or MWNTs prior to curing (polymerization) [22,23].

Many of the methods described above require nanotubes to be well dispersed in solvents. The nanotube dispersion in the polymer matrix largely depends on the state of nanotube dispersion in a solvent. However, the chemical structure of CNTs makes dissolving long CNTs in common solvents to form true solutions, virtually impossible.

Large fractions of individual nanotubes have thus only been achieved, either by functionalizing the nanotubes or by surrounding the nanotubes with dispersing agents, such as surfactants and polymers. The improved nanotube suspensions resulting from functionalization or dispersing agents can be employed in many of the methods described above to make nanotube nanocomposites with improved nanotube dispersion. Furthermore, functionalized CNTs might also allow covalent bonds to form between the nanotubes and the polymer matrix, thereby influencing the nanotube-polymer interaction.

Recently, chemically modified and solubilised carbon nanotubes have emerged as an area of research on nanotube-based materials and successful covalent functionalisation of both single-walled (SWNTs) and multi-walled (MWNTs) carbon nanotubes have been reported [24-28]. Covalent functionalisation could be possible thorough two main reactions: the first category involves direct attachment of functional groups to the CNT side wall [28,29]. The second category can arise from intrinsic or induced carbon defects. The latter generally refers to the creation of functionalized terminal carbons by the acidification of CNTs during oxidation [30,31]. Although it is widely accepted that chemical functionalisation disrupts the extended π-conjugation of nanotubes and thereby reduces the electrical conductivity of isolated nanotubes, recent reports show that covalent functionalisation can indeed improve the electrical properties of the composites [32-34].

Georgakilas *et al.* [35] have observed the functionalisation of CNT sidewalls using a 1,3-dipolar cycloaddition of azomethine ylides, generated by the condensation of an amino acid and an aldehyde (the Prato reaction) . The main advantage of this type of reaction is the easy attachment of substituted pyrrolidine rings to the sidewalls of nanotubes. After this, subsequent reactions to afford products with customized properties could be achieved. This method of reaction has previously resulted in functionalized CNTs that form stable solutions in organic solvents [36], or have been used in polymer composites [36b], medical application [36c], drug delivery [37], or energy conservation [38] studies.

In this work, we have investigated a new approach to the functionalization of N-doped and non-doped CNTs based on ring opening metathesis (ROMP) using Grubbs' catalyst, after sidewall functionalization of both N-doped and non-doped CNTs. The thermal and electronic properties of these new co-polymers were then investigated.

6.2 Experimental

6.2.1 General procedures

The synthesised CNTs were characterised by elemental analysis, thermogravimetric analysis (TGA) transmission electron microscopy (TEM), as well as Raman, NMR and ATR-FTIR spectroscopy. Elemental analysis was carried out by the Institute for Soil, Climate and Water, Pretoria, South Africa. Infrared-spectra were recorded on an ATR-FTIR Bruker Tensor 27. Absorption values are reported between 4000-550 cm^{-1}. The NMR spectra (chemical shift data in ppm) were recorded in $CDCl_3$ at ambient probe temperature using a Bruker Avance 300 (^1H, 300.13 MHz) spectrometer. DSC data were obtained on a Mettler-Toledo DSC822e calorimeter; each sample was recorded in the temperature range 100-250 ^oC under a N_2 atmosphere at a rate of 10^{o}C/min Thermogravimetric analysis (TGA) was performed using a Perkin-Elmer Pyris 1 TG analyzer at a heating rate 10 ^oC /min under either air or nitrogen atmospheres. TEM images were recorded on a Jeol JEM 100s electron microscope operating at 80 keV. Samples for analysis were prepared by spreading them on a holey carbon film supported on a copper grid. Raman spectra were obtained with a Jobin-Yvon T64000 Raman spectrometer operated in single spectrograph mode with either a 600 lines/mm grating or an 1800 lines/mm grating. The 514.5 nm line of an argon ion laser was used as the excitation source. Laser power at the sample was kept at 1.2 mW or less to minimize local heating. Laser plasma lines were removed from the incident beam using a narrow band pass interference filter and a Kaiser Optics holographic notch filter was used to remove the Rayleigh scattered light from the backscattered beam. Spectra accumulation time was 120 seconds and was collected using a liquid nitrogen-cooled CCD detector. Data was ued to measure the intensity of the D and G bands of the CNTs.

6.2.2 Synthesis of carbon nanotubes

6.2.2.1 Catalyst preparation for CNT synthesis [39]

A catalyst was prepared using a mixture of $Fe(NO_3)_3{\cdot}9H_2O$ and $Co(NO_3)_2{\cdot}6H_2O$, both purchased from Sigma Aldrich, as sources of Fe and Co respectively. A calculated amount of the Fe and Co salts were mixed, ground to a fine powder and dissolved in distilled water to make a 50:50 Fe-Co precursor solution (0.3 M). This solution (28 mL) was then added to $CaCO_3$ (10 g) and the suspension was left to age for 30 min while stirring. The mixture was then filtered and allowed to

dry at r.t., after which time it was further dried in an air oven at 120 °C for 12 h. The resulting course powder was then cooled to r.t., ground and finally screened through a 150 μm sieve. The fine catalyst powder was then calcined at 400 °C for 16 h.

6.2.2.2 Carbon nanotube synthesis [39]

MWNTs were synthesized by the decomposition of acetylene (C_2H_2), (Afrox) in a tubular quartz reactor (51 cm × 1.9 cm i.d.) that was placed horizontally in a furnace. The furnace was electronically controlled such that the heating rate, reaction temperature and gas flow rates could be accurately maintained as desired. The catalyst (0.2 g) was loaded into a quartz boat (120 mm × 15 mm) at r.t. and the boat was placed in the centre of the quartz tube. The furnace was then heated at 10 °C/min while N_2 was passed over the catalyst at 40 mL/min Once the temperature had reached 700 °C, the N_2 flow rate was set to 240 mL/min and C_2H_2 was introduced at a constant flow rate of 90 mL/min After 60 min of reaction time, the C_2H_2 flow was stopped and the furnace was left to cool to r.t. under a continuous flow of N_2 (40 mL/min). The boat was then removed from the reactor and the product (carbon deposit) that formed along with the catalyst was weighed.

6.2.2.3 Nitrogen doped multiwall carbon nanotubes

Synthesis of N-CNTs was carried out at a temperature at 800 °C, under 5 % H_2 in Ar (v/v) (AFROX) at atmospheric pressure. The flow rate of H_2 in Ar was kept constant at 200 mL/min A mixture of pyridine (2 g, 20 %) and ferrocene (1 g, 10 %) was dissolved in toluene (7 g, 70 %) (Merck chemicals) and the solution was placed in a 10 mL syringe driven by a SAGE syringe pump. The solution was injected at ~0.80 mL/min rate into a quartz tube reactor (800 × 28 mm i.d.) via a specially designed quartz reactor delivery tube, cooled by water. This designed tube enabled the solution to be injected directly into the high temperature region of the large quartz tube reactor. The carbon deposit that formed was scraped from the walls of the quartz tube and weighed.

6.2.3 Purification of carbon nanotubes

The synthesized nitrogen doped and undoped carbon nanotubes were purified by adding the carbon nanotubes to hydrochloric acid (35 %) which was heated at 80 ^{o}C for 24 h. After filtering and washing several times with distilled water and acetone (3 x 500 mL), the purified carbon nanotubes were finally heated in an oven under an inert atmosphere at 400 ^{o}C for 30 min

6.2.4 Functionalisation and polymerization of carbon nanotubes

6.2.4.1 Functionalisation of carbon nanotubes

In each of two round bottomed flasks an equal amount of N-doped and undoped carbon nanotubes (each 0.100 g) were suspended in 1,2-dichlorobenzene (50 mL) and sonicated for 30 min 5-Norbornene-2-carboxaldehyde (Sigma-Aldrchi) (0.12 g, 0.98 mmol) was then added to each CNT suspension. *N*-methylglycine (0.158 g, 1.9 mmol) was then added to each reaction mixture in small portions over 5 days (about 0.032 g per day) at 160 ^{o}C. The reaction mixtures were then left to cool to r.t. and the solid material filtered using 1 µm pore size membrane filter papers. The products were then washed with DMF (100 mL), ethanol (300 mL), 1:1 distilled water: acetone mixture (3 x 500 mL) and several times with acetone (500 mL). The black solid products were then dried at 45 ^{o}C under vacuum for 48 h to yield 0.157 g and 0.148 g of dark gray functionalized N-doped and undoped carbon nanotubes, respectively.

6.2.4.2 Ring opening metathesis and functionalization of CNTs with norbornene

In two round bottom flasks an equal amount of both functionalized N-doped and undoped CNTs (each 50 mg) were suspended in dried chloroform (25 mL) and sonicated for 2 h. Grubbs' second generation catalyst (30 mg, 40 µmol) was then added to the two suspensions and sonication was carried on for a further hour. Norbornene (bicyclo[2.2.1]hept-2-ene) (1.00 g, 10.4 mmol) was dissolved in dry chloroform (25 mL) and then added dropwise over 60 min to each reaction mixture. The reaction mixtures were then left to stir overnight at r.t. The polymerization reactions were then terminated by adding a few drops of ethylvinylether (4-5 drops). The mixtures were then poured into an excess of MeOH (50 mL), containing a few drops of 1 M HCl, to precipitate the crude polymers. The synthesized polymers were filtered using a filter paper and

dried under vacuum for 48 h to afford gray coloured polymers 0.977 g (93 % yield) and 0.875 g (82 % yield) for the N-doped and undoped CNTs, respectively.

6.3 Results and discussion

6.3.1 Synthesis of CNTs

As described in the experimental section the undoped CNTs were synthesized by the decomposition of acetylene at 700 ^{o}C for 1 h. No pre-reduction of the catalyst was necessary since the catalyst was reduced in-situ by the H_2 released from the decomposition of the feed stock gas (C_2H_2). $Fe(NO_3)_3.9H_2O$ and $Co(NO_3)_2.6H_2O$ were used as sources of Fe and Co respectively to give a Fe/Co on $CaCO_3$ catalyst that has been shown to efficiently give high yields of CNTs [39].

On the other hand, the N-CNTs were synthesized by the flotation catalyst methodology [40], using ferrocene as a catalyst and toluene as the carbon source. Pyridine was a source of both nitrogen and carbon for the formation of the N-CNTs [11]. The reaction temperature was carried out at 800 °C in a 5 % H_2 in Ar gas mixture and the synthesized N-CNTs were finally purified using concentrated hydrochloric acid under reflux for 24 h. After washing with distilled water and drying under vacuum, TEM images revealed that the synthesized N-CNTs contained were multiwalled (see section Figure **5.3.4.2**).

6.3.2 Functionalization reactions of CNTs

Functionalization of carbon nanotubes using azomethine ylides was first reported by Georgakilas *et al.* [35] The azomethine ylides were formed thermally *in situ* by the condensation of an *R*-amino acid and an aldehyde. The reagent was successfully added to the graphitic surface via a 1,3-dipolar cycloaddition reaction, forming pyrrolidine fused rings on the side wall of the CNTs. The 1,3-dipolar cycloaddition reaction of azomethine ylides with alkene or alkyne is a very effective method for the construction of pyrrolidine- and pyrrole-rings in the synthesis of pyrrolidine- and pyrrole-containing molecules. This procedure initially was developed for organic modification of C_{60} fullerenes [41] and has been termed the "Prato reaction".

In this study, the functionalisation of N-doped and undoped CNTs, by 5-norbornene-2-carboxaldehyde and *N*-methylglycine by way of the Prato reaction, was investigated. The norbornene-functionalized CNTs were obtained as a gray dark product for both the N-doped and undoped CNTs (see Scheme **6.1**). The increase in mass between 32-36 % after the reaction indicated that the side walls of the CNTs had organic functional groups attached to the CNTs. Furthermore, the TGA scan after functionalization indicated that the decomposition temperatures were lower than the pristine CNTs (see Figure **6.7a**).

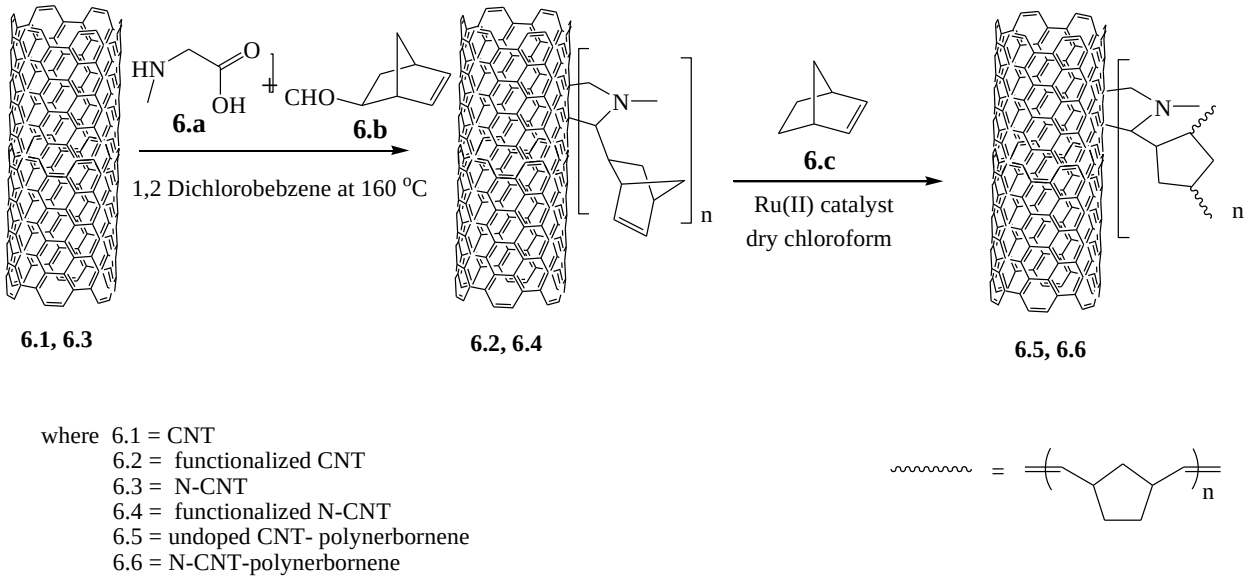

where 6.1 = CNT
6.2 = functionalized CNT
6.3 = N-CNT
6.4 = functionalized N-CNT
6.5 = undoped CNT- polynerbornene
6.6 = N-CNT-polynerbornene

Scheme **6.1** Functionalization and polymerization methodology for the carbon nanotubes.

6.3.3 Polymerization reactions of functionalized CNTs

Ring-opening metathesis polymerization (ROMP) using ruthenium alkylidene catalysts has attracted significant attention due to its versatility, effectiveness, and functional group tolerance, allowing for a variety of monomers bearing polar and charged functional groups to be successfully polymerized [42]. It has recently been shown that extremely narrow polydispersities and excellent control over polymer molecular weight and architecture can be achieved if appropriate ligands are utilized, where high ligand dissociation rates result in rapid initiation of polymerization [43,44]. Recently, Gomez *et al.* [45] have reported a successful ROMP from the surface of SWNTs, where the ruthenium alkylidene catalysts were physiosorbed on the nanotube surface using pyrene molecules as anchors. Similarly, Liu and Adronov [46] showed that

catalyst-functionalized nanotubes initiated effectively the ROMP of norbornene, resulting in rapid polymerization from the catalyst sites on the nanotube.

During the polymerization reactions in our work the Grubbs' second generation catalyst was used as a polymerization catalyst in chloroform under argon. The monomer, bicyclo[2.2.1]hept-2-ene, was added dropwise to the mixture of the functionalized CNTs and Grubbs' second generation catalyst at r.t. The reaction gave a dark gray spongy solid in good yield, which was recovered by precipitation in methanol and then purified by dissolving in chloroform and re-precipitation from methanol, followed by filtration. The polymers were found to be soluble in dichloromethane and chloroform. Their characterization will be described in the next sections.

6.3.4 Characterization of the synthesised products

6.3.4.1 Raman Spectroscopy of the synthesised products

Raman spectroscopy is a very useful tool to characterize CNTs [47]. Raman spectra were obtained with a Jobin-Yvon T64000 Raman spectrometer operated at 514.5 nm line of an argon ion laser excitation source. The Raman spectra of N-doped and undoped CNTs are shown in Figure **6.1.** The spectrum of N-doped unfunctionalized CNTs **6.1** (Figure **6.1** spectrum **A**) showed two bands. One band occurred at 1352 cm^{-1} (D band) which is attributed to disorder, or sp^3-hybridized carbons, in the hexagonal framework of the nanotube walls. The second band at 1585 cm^{-1}(G band) is associated with tangential modes. The spectrum of the functionalized N-doped material **6.2** gave the conventional bands at 1363 cm^{-1} and 1583 cm^{-1}, respectively (Figure **6.1** spectrum **B**). After functionalization, the G band slightly shifts up field by ~2 cm^{-1}, as compared with that of N-doped unfunctionalized CNTs **6.1**. This shift should be associated with organic functional group covalently attached to the nanotube surface [48]. The spectrum of undoped unfunctionalized CNTs **6.3** gave two bands at 1351 cm^{-1} and at 1583 cm^{-1} (Figure **6.1** spectrum **C**), however, the spectrum of the functionalized undoped **6.4** sample was dominated by fluorescence, i.e. no D and G bands were observable (Figure **6.1** spectrum **D**).

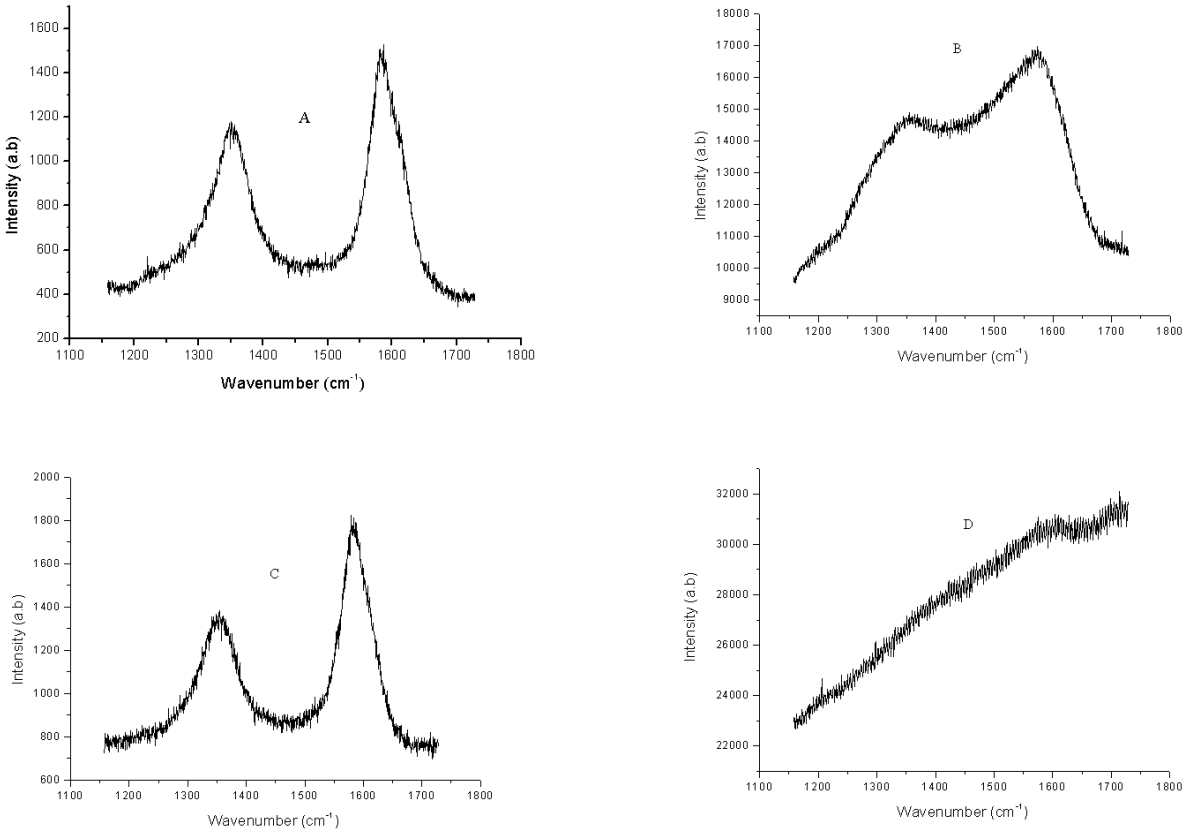

Figure **6.1** Raman spectra of A) unfunctionalized N-CNTs **6.3**; B) functionalized N-CNTs **6.4**; C) unfunctionalized CNTs **5.1**; D) functionalized CNTs **6.2**.

A comparison of the Raman spectra of the unfunctionalized CNTs (Figure **6.1** spectrum **A** vs **C**) reveals that the I_D/I_G value (0.78 for **6.1** and 0.75 for **6.3**) increased due to the doping with nitrogen. The I_D/I_G ratio appears to be even greater for the N doped material after functionalization, 0.88 for **6.4** and 0.78 for **6.1** (see Figure **6.1**). These values are distinctly larger than 0.78 for **6.1** and 0.75 for **6.3**, indicating the introduction of covalently bound moieties to the nanotube framework wherein significant amounts of the sp^2 carbons have been converted to sp^3 hybridization. Thus, both functionalized carbon nanotubes samples display similar modifications, but to different degrees.

6.3.4.2 Transmission electron microscopy (TEM)

Samples for transmission electron microscopy (TEM) analysis were prepared by sonication of the copolymeric materials in methanol, followed by placing a few drops of the resulting suspension onto a holey copper TEM grid for analysis. The results from such analyses offer the most direct evidence for the presence of carbon nanotubes in the samples.

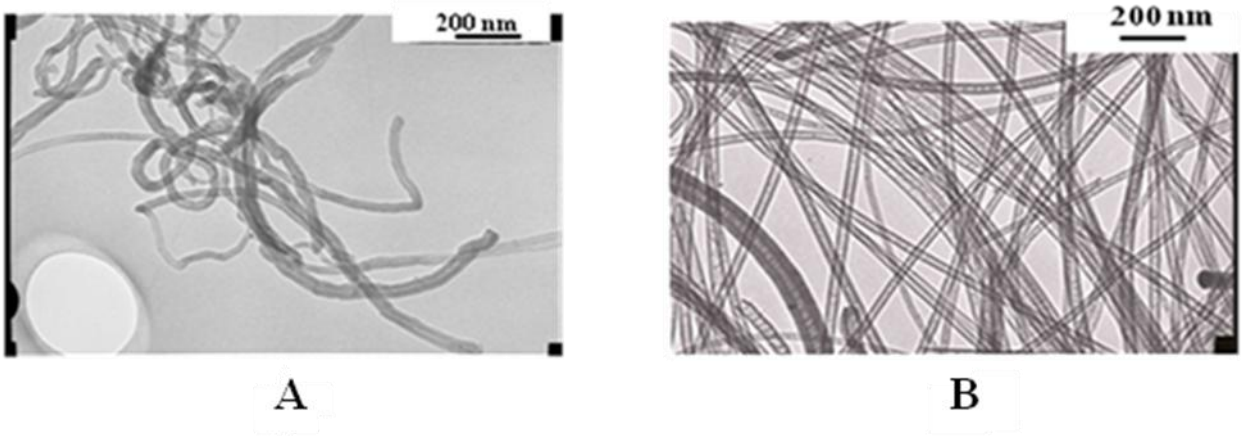

Figure **6.2** TEM image of A) undoped CNT **6.1**; B) N-CNTs **6.3**

The undoped CNTs **6.1**, with a diameter range of 25-30 nm, were clearly observed from the TEM analysis (Figure **6.2** image **A**). The outer diameter of the nanotubes ranged from 20-25 nm with the inner diameter ranging from 3-5 nm. Similarly, for the N-CNTs **6.3**, the diameters were measured to be in a range of 32-40 nm, with an overall wall thickness of 8 nm.

The CNTs grown from the mixture of pyridine and ferrocene in toluene, had a bamboo structure (Figure **6.2** image **B**), and this bamboo structure is known to be a characteristic of nitrogen-doped MWNTs [49]. The bamboo-like structure and distinctive compartment layers are probably due to the incorporation of nitrogen atoms such as pyridinic nitrogen or graphitic nitrogen [50-54] into the growing structure. Finally, elemental analysis indicated that indeed, nitrogen atoms had been doped into the N-CNTs with the nitrogen content being 3.4 %.

After the polymerizations reaction, the functionalized carbon nanotubes (both undoped **6.5** and N-doped **6.6**) were found to have much larger diameters (65-130 nm) than the pristine N-CNTs

(**6.3**) (32-40 nm) (see Figure **6.3**). This is due to the polymer that formed on the surface of the CNTs, i.e. the polynorbornene (see Scheme **6.3**). This polymerization was further substantiated by ^{1}H NMR, FT-IR and TGA studies (see Figure **6.5**, **6.6b**, **6.7b**).

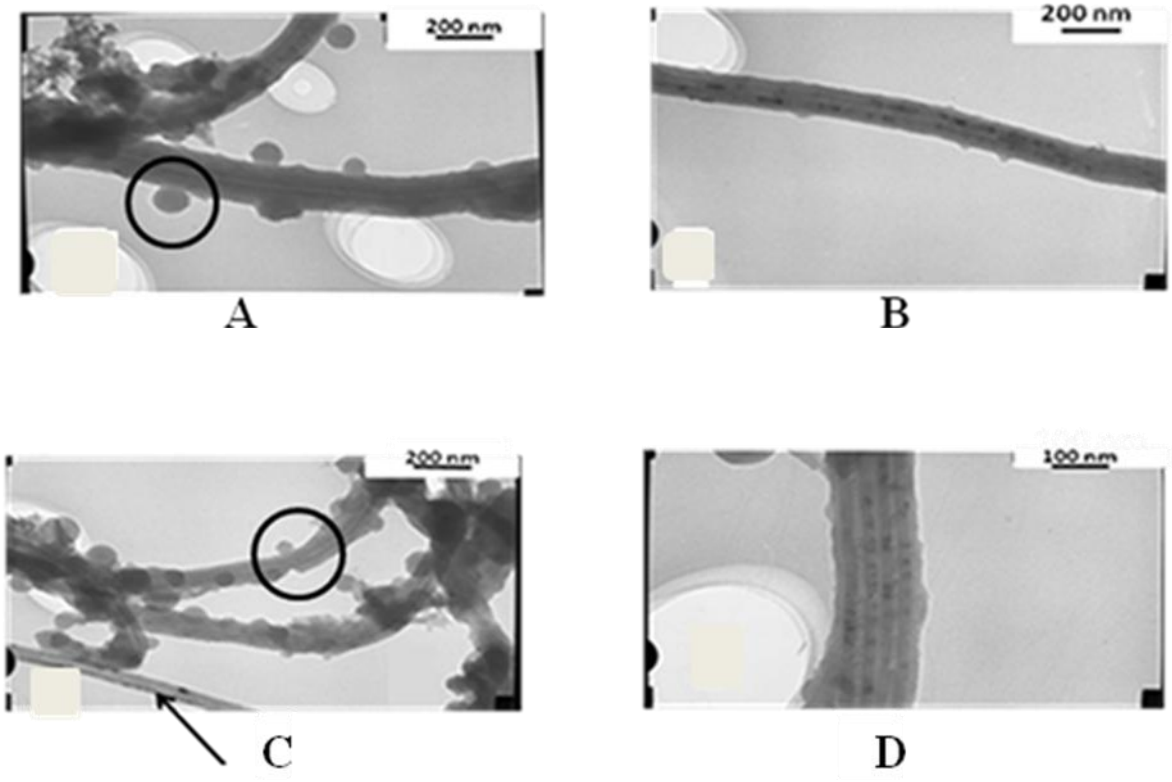

Figure **6.3** TEM images of A) and B) polymer attached CNTs **6.5**; C) and D) polymer attached N-CNTs **6.6**.

In Figure **6.3** TEM images of **A**, **B** and **C** show polymer formation on the surface of the nanotubes. The underlying tube can readily be seen in Figure **6.3,** image **C** in the circled region. In some instances some carbon nanotubes were not visibly covered by the polymers (see the arrow in Figure **6.3**, image **C**). This could be due to the N-CNTs **6.4** only being partially functionalized or inhomogeneous in the polymerization reaction. The polymerization is inhomogeneous, but in general polymer formation gives tube covered by polymer (Figure **6.3** image **B**). This inhomogeneous is readily seen in Figure **6.3** image **A**, where polymer "blobs" are seen attached to the polymer on the tubes. This inhomogeneity is independent of doping (Figure **6.3**, image **C**). The TEM in Figure **6.3**, image **D** shows two functionalized N-CNTs that were

zipped together during ROMP. This indicated that if two tubes are in closed proximity then a covalently linkage between the tubes is possible. The implication is that if tubes could be aligned after functionalization then a composite with high strength could be synthesised. In summary, the data revealed that while polymer coverage of both doped and undoped CNTs is possible, however the growth of the polymer still need to be optimized to ensure both total coverage of all tubes as well as constant growth on the tubes.

6.3.4.3 Spectroscopic studies on the copolymers synthesized

6.3.4.3.1 ^{1}H NMR studies of synthesized copolymers

The ^{1}H NMR spectrum of the polymer-attached CNTs are shown in Figure **6.5.** Both *cis* and *trans* resonances for the olefinic and the allylic protons [55] were observed in all the polymers obtained (see Figure **6.4** below). The *cis* and *trans* olefinic protons of the pure polynorbornene resonate at 5.21 and 5.35 ppm, respectively. The *cis:trans* ratio for pure polynorbornene (Figure **6.5**) was calculated by integration and found to be 59:41.

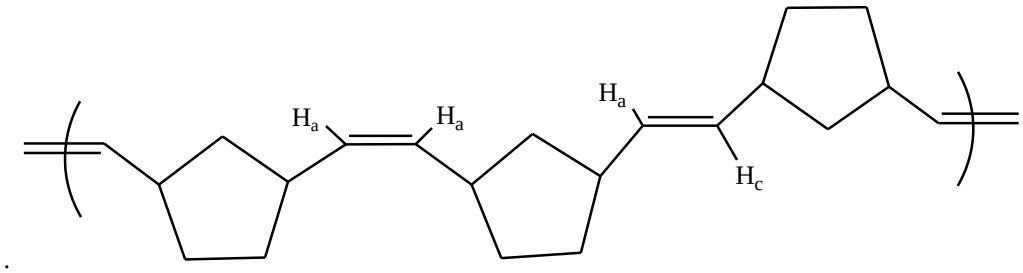

Figure **5.4** Schematic diagram of the *cis* and *trans* olefinic and allylic protons.

The *cis/trans* proton resonances for the polynorbornene formed in the presence both **6.5** and **6.6** were broader than those found for polynorbornene (See Figure **6.5**). The broadening of the signals is caused by the NMR nuclei spin-lattice (T_1) and spin-spin (T_2) relaxation time; they are associated with diamagnetic species of low mobility [56].

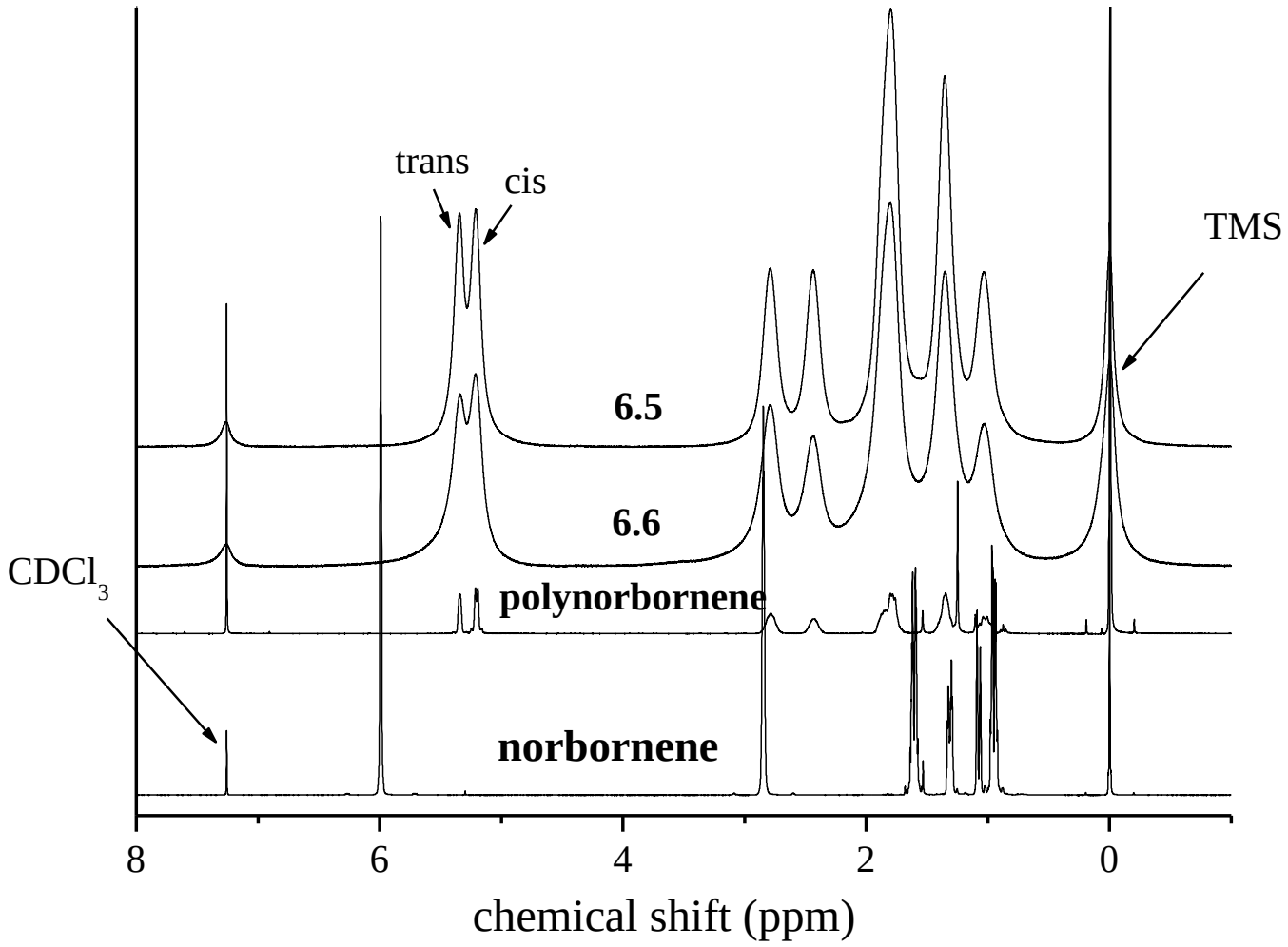

Figure **6.5** ^{1}H NMR spectra (in $CDCl_3$) of the monomer norbornene; polynorbornene; (**6.5**) copolymer from undoped CNT-polynorbornene and (**6.6**) copolymer from N-doped-polynorbornene copolymers.

In the case of the CNT-attached polymers, **6.5** and **6.6**, the ratios of *cis* and *trans* proton were estimated to be 52:48 and 44:56, respectively. From the spectra it is seen that both N-doped and undoped CNTs attached to the polynorbornene favored the *trans* isomer relative to the pure

polynorbornene. Further the N-doped CNT's gives a reversal of the isomers amount. While this might be an artifact of the broadened signals, it does suggest potential content of isomers ratio by controlling doping or functionalization of CNTs.

Table **6.1** Summary of *cis* and *trans* ratios of the polymer and functionalized copolymers.

Polymer	*cis*	*trans*
Polynorborene	59	41
6.5 (CNTs)	52	48
6.6 (N-CNTs)	44	56

6.3.4.3.2 FT-IR studies of synthesized copolymers

FT-IR spectroscopy was used to further characterize the synthesized polymers. As shown in figure **6.6a** new absorption bands were recorded for both functionalized carbon nanotubes (**6.2** and **6.4**), relative to the pristine CNTs. Absorption bands between 3074-2800 cm^{-1} were assigned to the C-H stretching bands. These arise from the norbornene and methylglycine functional groups in the Prato reaction precursors. The presence of an absorption band at 1050 cm^{-1} is indicative of the N-C stretching vibration [57] that is associated mainly with Prato products. Those were not observed in the unfunctionalized CNTs.

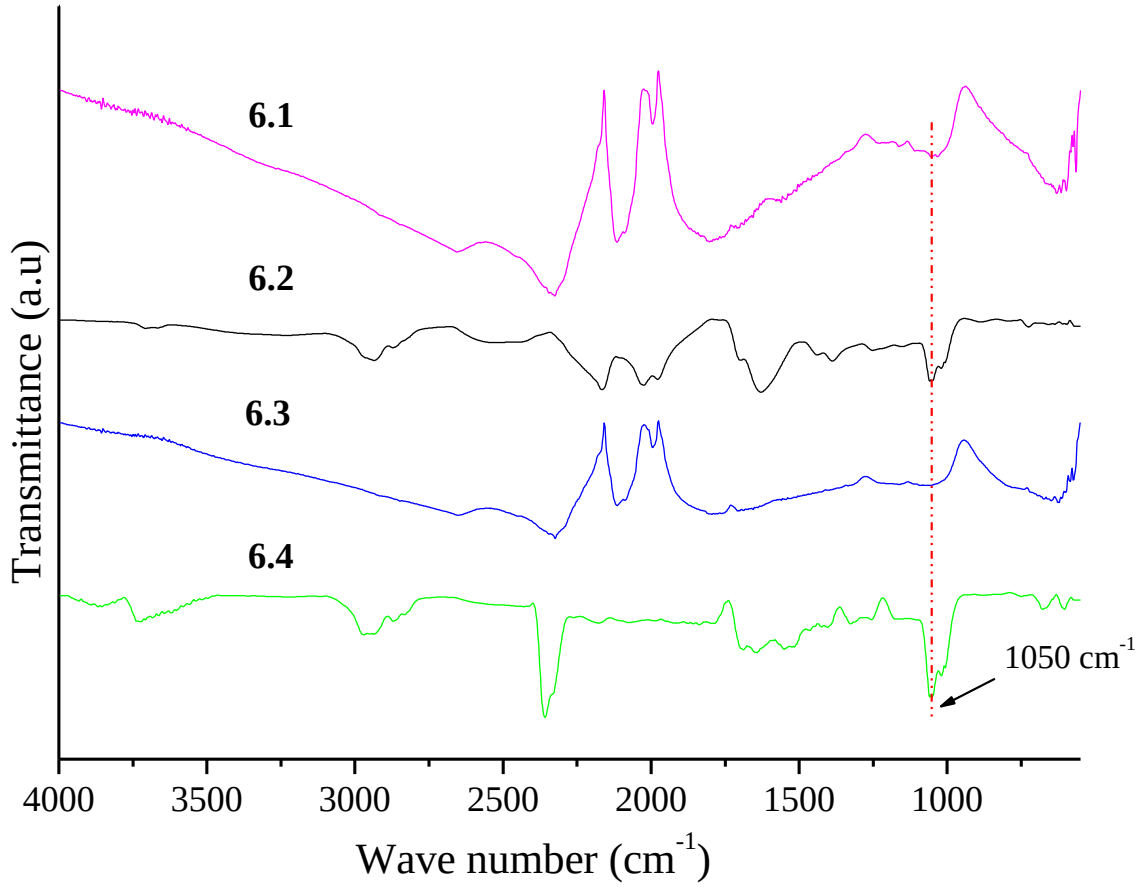

Figure **6.6a** FT-IR of Pristine undoped CNTs **6.1**; functionalized undoped CNTs **6.2**; pristine N-CNTs **6.3**; functionalized N-CNTs **6.4**.

After the ROMP, new absorption bands at 967 and 745 cm^{-1} were seen and these were associated with the norbornene-based polymer chain (Figure **6.6b**). In addition, the absorption bands between 3074-2800 cm^{-1} were more intense due to the increased contribution from the polynorbornene CH and CH_2 groups. In summary, the IR

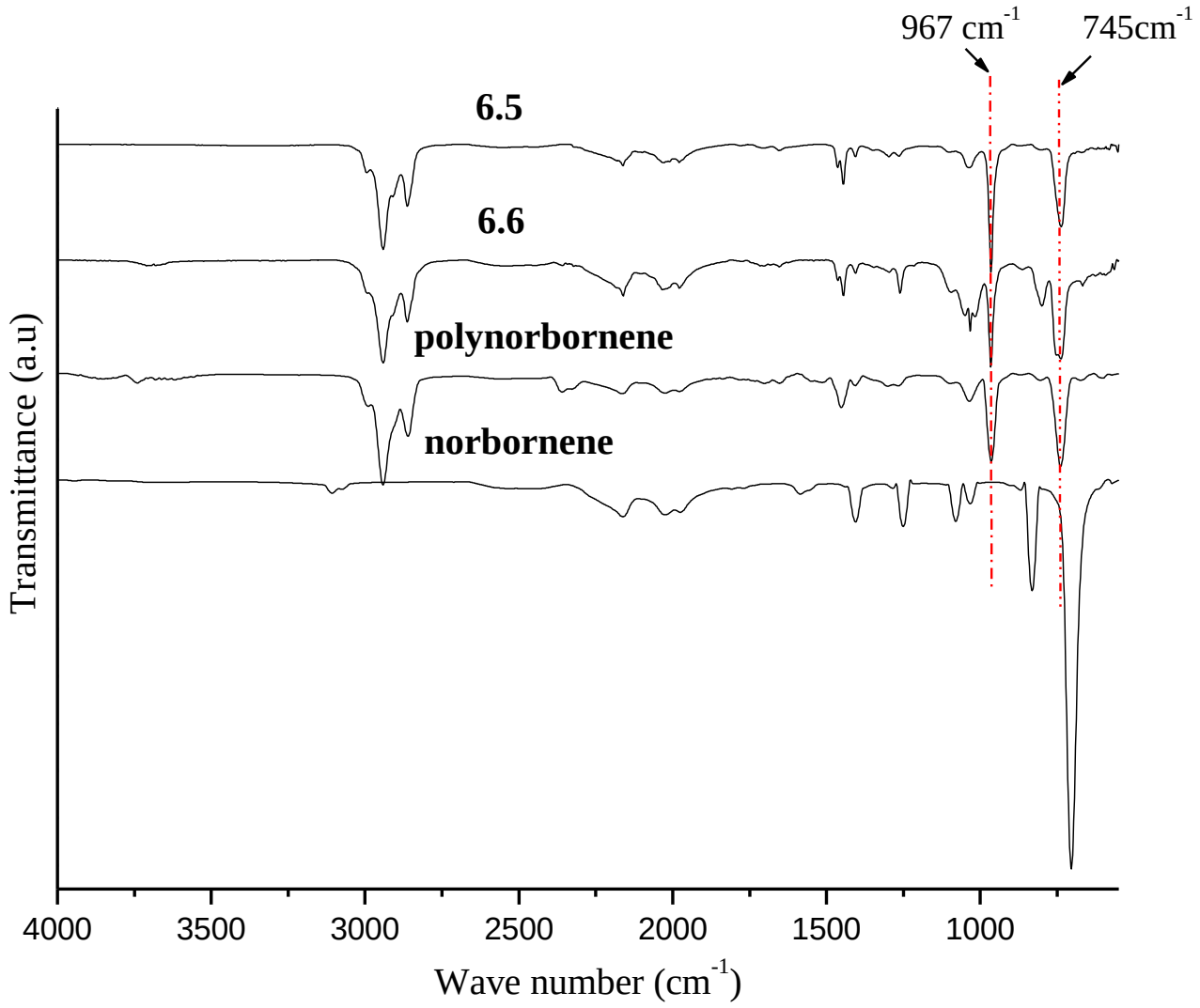

Figure **6.6b** FT-IR of polynorbornene-attached CNT **6.5**; polynorbornene-attached N-CNT **6.6**; polynorbornene and norbornene monomer.

Absorption bands at 745 cm^{-1} and 967 cm^{-1} were assigned to the *cis* and *trans* double bonds of the polymer, respectively; however, in the vinylcyclopentane units resulting from ROMP the *cis* and *trans* positions have been reported at lower wavenumbers 730 cm^{-1} and 960 cm^{-1} for *cis* and *trans* respectively [58].

6.3.5 Thermal analysis

6.3.5.1 Thermogravimetric Analysis (TGA) of the synthesized materials

TGA measurements on the materials synthesised in this chapter were also performed under air (see Figures **6.7a** and **b**). Both pristine N-doped **6.2** and undoped CNTs **6.1** showed a typical TGA profiles that indicated the graphitic nature of the CNTs; they decomposed at 519 and 508 ^{o}C, respectively. Functionalized N-CNTs **6.4** showed two stages of thermal decomposition at ~307 and 510 ^{o}C. Similarly, the functionalized CNTs **6.3** showed two stages of decomposition recorded at 241 ^{o}C and 403 ^{o}C (see Figure **6.7a**). During the first decomposition reactions 3 and 45 % mass losses were recorded for **6.3** and **6.4**, respectively**.** The first decomposition stages might be due to the de-attachment of organic functional groups from the side wall of CNTs and the second decomposition was due to the oxidation of the CNTs. These results would indicate that the N-CNTs were have highly functionalized than the non-doped CNTs.

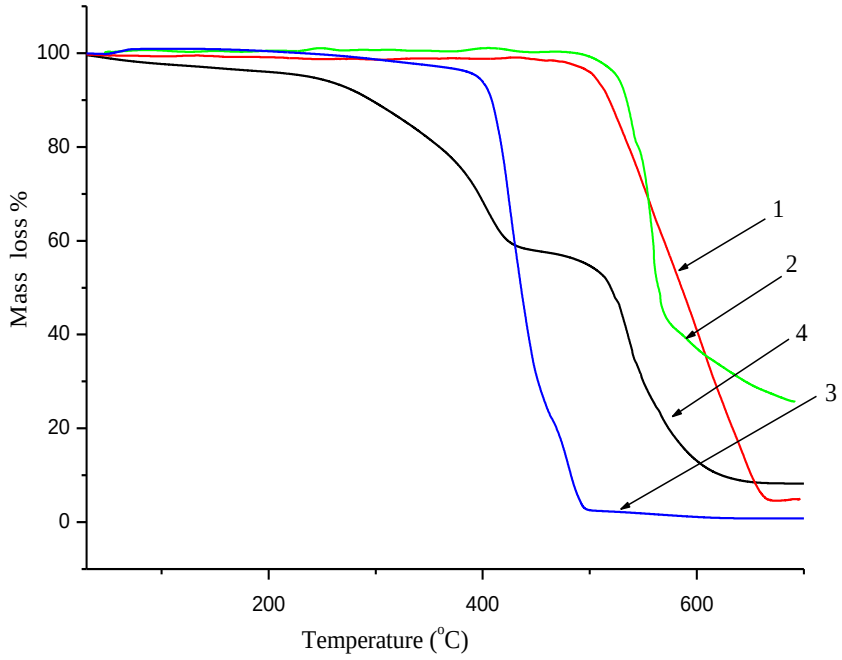

Figure **6.7a** TGA scan of **1**) pristine CNT **6.1**; **2**) pristine N-CNT **6.2**; **3**) functionalized CNT **6.3**; **4**) functionalized N-CNT **6.4**.

The TGA profile of the N-CNT containing polymer **6.6** was very similar to that of pure polynorbornene. Polynorbornene had only one decomposition temperature at 398 ^{o}C. The differentiate curve for **6.6** (not shown) revealed two decomposition reactions; at 387 ^{o}C (92 % mass loss) and at 527 ^{o}C (see Figure **6.7a**).

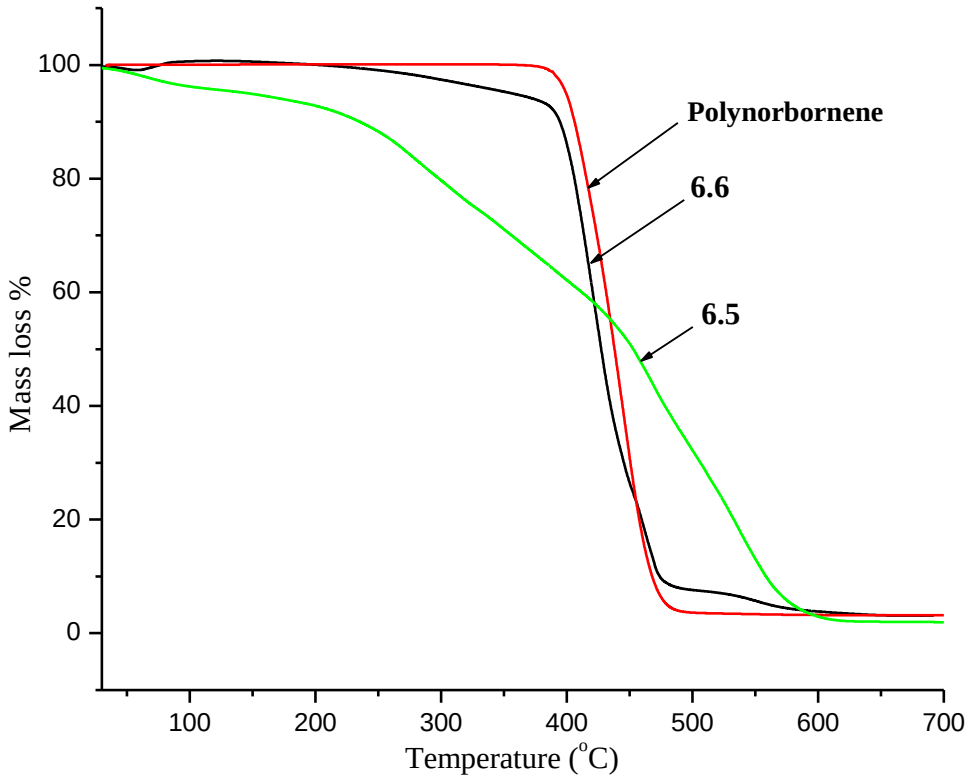

Figure **6.7b** TGA scan of polynorbornene-attached CNT **6.5**; polynorbornene-attached N-CNT **6.6**; and polynorbornene.

For **6.5** there was only one very visible decomposition temperature at 214 ^{o}C. From this result it appears that the copolymer decomposed over a broader range. The incorporation of the CNTs into polynorbornene did therefore not affect the thermal stability of the N-CNT/polymer contain.

6.3.5.2 Differential scanning calorimetry studies (DSC) of synthesized copolymers

The thermal stabilities of the synthesised polymers were also examined. DSC profiles of the samples were thus recorded under a nitrogen atmosphere using a 5 ^{o}C/min heating rate (Figure **6.8**). The Tg (glass transition) temperatures were found to be significantly affected by the incorporation of the carbon nanotubes. The two polymers attached to CNTs, **6.5** and **6.6**, were found to have approximately the same Tg at ca. 46 ^{o}C, while for pure polynorbornene polymer the Tg was recorded at 52 ^{o}C (see inserted graph in Figure **6.8**).

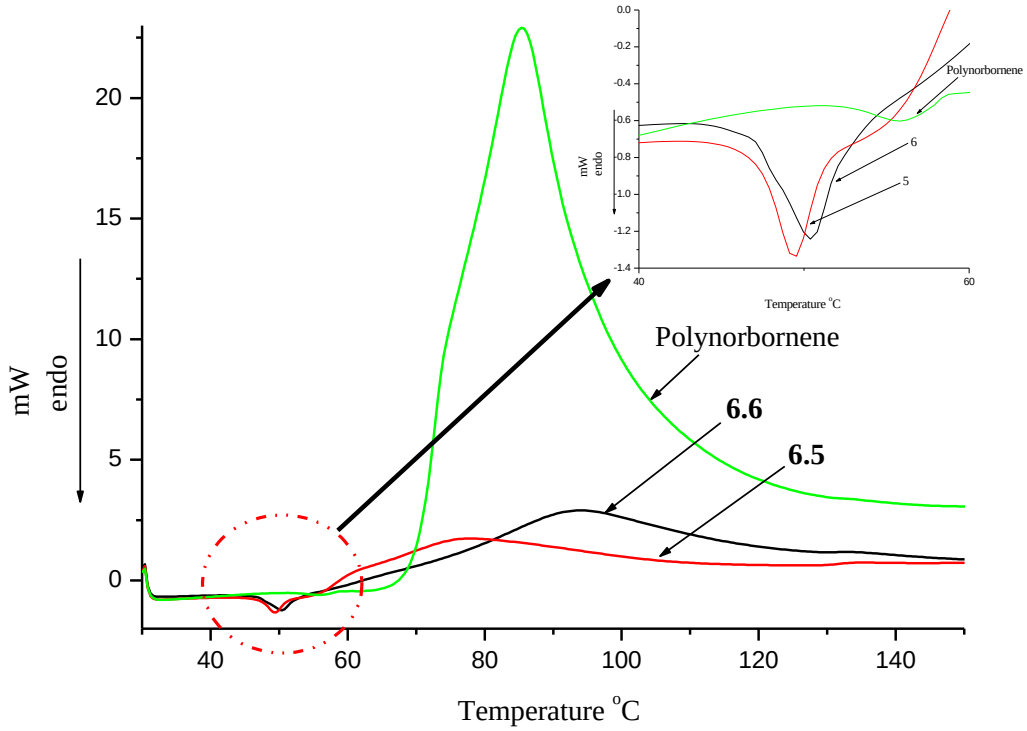

Figure **6.8** DSC scan of polynorbornene-attached CNT **6.5**; polynorbornene-attached N-CNT **6.6**; and polynorbornene run under N_2 at 5 ^{o}C/min heating rate.

Gao *et al*. [59] showed that the Tg of composites gives information on the mobility of molecular chain segments. In their report they furthermore indicated that the lower the Tg, the easier the motion of chain segments and that the Tg continued to decrease as the concentration of CNT in the polymer increased.

6.4 Conclusion

Functionalization of carbon nanotubes was achieved by using azomethine ylides that were generated *in situ* by the decarboxylation of immonium salts derived from thermal condensation of *N*-methylglycine and 5-norbornene-2-carboxaldehyde (the Prato reaction). ROMP on the side walls of the carbon nanotubes **6.2** and **6.4** using bicyclo[2.2.1]hept-2-ene as a co-monomer, was achieved using Grubbs' second generation catalyst. From the ^{1}H NMR evidence that *trans* resonances was favored for the olefinic and the allylic protons when CNTs incorporated in the copolymer. The TEM images revealed that the polymer-attached carbon nanotubes (both undoped and N-doped CNTs, **6.5** and **6.6** respectively) were found to have relatively larger diameters than the pristine CNTs; this is due to the polymers were attached on the side wall of the carbon nanotubes. It is also revealed that two functionalized N-CNTs were zipped together during ROMP. This indicated that if two tubes are in closed proximity then a covalently linkage between the tubes is possible. The implication is that if tubes could be aligned after functionalization then a composite with high strength could be synthesised. Generally, the incorporation of the CNT into polynorbornene did not improve the Tg and thermal stability.

6.5 References

1 S. Iijima, *Nature*, **1991**, 56, 354.

2 T. W. Ebbesen, H. J. Lezec, H. Hiura, J. W. Bennett, H. F. Ghaemi, T. Thio, *Nature*, **1996**, 382, 54.

3 N. H. Tai, M. K. Yeh, J. H. Liu, *Carbon*, **2004**, 42, 2774.

4 Z. H. Gan, Q. Zhao, Z. H. N. Gu, Q. K. Zhuang, *Anal. Chim. Acta*, **2004**, 511, 239.

5 S. Saito, *Science,* **1997**, 278, 77.

6 M. Terrones, N. Grobert, H. Terrones, *Carbon,* **2002**, 40, 1665.

7 (a) O. Stephan, P. M. Ajayan, C. Colliex, P. Redlich, J. M. Lambert, P. Bernier, P. Lefin, *Science,* **1994**, 266, 1683. (b) L. H. Chan, K. H. Hong, D. Q. Xiao, W. J. Hsieh, S. H. Lai, H. C. Shih, T. C. Lin, F. S. Shieu, K. J. Chen, H. C. Cheng, *Appl. Phys. Lett.*, **2003**, 82, 4334.

8 M. Terrones, P. M. Ajayan, F. Banhart, X. Blase, D. L. Carroll, J. C. Charlier, R. Crzerw, B. Foley, N. Grobert, R. Kamalakaran, P. Kohler-Redlich, M. Ruhle, T. Seeger, H. Terrones, *Appl. Phys. A*, **2002**, 74, 355.

9 Y. Miyamoto, M. L. Cohen, S. G. Louie, *Solid State Commun*., **1997**, 102, 605.

10 Y. Huang, J. Gao, R. Liu, *Synth. Met*., **2000**, 113, 251.

11 (a) C. M. Yang, M. El-Merraoui, H. Seki, K. Kaneko, *Langmuir*, **2001**, 17, 675. (b) R. Sen, B. C. Satishkumar, A. Govindaraj, K. R. Harikumar, M. K. Renganathan, C. N. R. Rao, *J. Mater. Chem.*, **1997**, 7, 2335. (c) M. Nath, B. C. Satishkumar, A. Govindaraj, C. P. Vinod, C. N. R. Rao, *Chem. Phys. Lett.*, **2000**, 322, 333. (d) R. Sen, B. C. Satishkumar, A. Govindaraj, K. R. Harikumar, G. Raina, J. P. Zhang, A. K. Cheetham, C. N. R. Rao, *Chem. Phys. Lett.*, **1998**, 287, 671. (e) J. W. Liu, S. Webster, D. L. Carroll, *J. Phys. Chem. B*, **2005**, 109, 15769.

12 (a) M. C. dos Santos, F. Alvarez; *Phys. Rev. B*, **1998**, 58, 13918. b) M. Terrones, P. Redlich, N. Grobert, S. Trasobares, W. K. Hsu, H. Terrones, Y. Q. Zhu, J. P. Hare, C. L. Reeves, A. K. Cheetham, M. Ruhle, H. W. Kroto, D. R. M, Walton, *Adv. Mater.*, **1999**, 11, 655. (c) A. G. Kudashov, A. V. Okotrub, L. G. Bulusheva, I. P. Asanov, Y. V. Shubin, N. F. Yudanov, L. I. Yudanova, V. S. Danilovich, O. G. Abrosimov, *J. Phys. Chem. B*, **2004**, 108, 9048.

(d) Y. T. Lee, N. S. Kim, S. Y. Bae, J. Park, S. C. Yu, H. Ryu, H. J. Lee, *J. Phys. Chem. B,* **2003**, 107, 12958.

13 (a) M. Terrones, H. Terrones, N. Grobert, W. K. Hsu, Y. Q. Zhu, J. P. Hare, H. W. Kroto, D. R. M. Walton, P. Kohler-Redlich, M. Ruhle, J. P. Zhang, A. K. Cheetham, *Appl. Phys. Lett.,* **1999**, 75, 3932. (b) M. Terrones, N. Grobert, J. Olivares, J. P. Zhang, H. Terrones, K. Kordatos, W. K. Hsu, J. P. Hare, P. D. Townsend, K. Prassides, A. K. Cheetham, H. W. Kroto, D. R. M. Walton, *Nature,* **1997**, 388, 52. (c) X. B. Wang, Y. Q. Liu, D. B. Zhu, L. Zhang, H. Z. Ma, N. Yao, B. L. Zhang, *J. Phys. Chem. B,* **2002**, 106, 2186. (d) H. C. Choi, S. Y. Bae, W. S. Jang, J. Park, H. J. Song, H. J. Shin, H. Jung, J. P. Ahn; *J. Phys. Chem. B,* **2005**, 109, 1683. (e) E. J. Liang, P. Ding, H. R. Zhang, X. Y. Guo, Z. L. Du, *Diamond Relat. Mater.*, **2004**, 13, 69. (f) C. Tang, Y. Bando, D. Golberg, F. Xu, *Carbon*, **2004**, 42, 2625.

14 (a) X. C. Ma, E. G. Wang, W. Z. Zhou, D. A. Jefferson, J. Chen, S. Z. Deng, N. S. Xu, J. Yuan, *Appl. Phys. Lett.*, **1999**, 75, 3105. (b) X. C. Ma, E. G. Wang, *Appl. Phys. Lett.*, **2001**, 78, 978. (c) C. J. Lee, S. C. Lyu, H. W. Kim J. H. Lee, K. I. Cho, *Chem. Phys. Lett.*, **2002**, 359, 115. (d) G. Y. Zhang, X. C. Ma, D. Y. Zhong, E. G. Wang, *J. Appl. Phys.*, **2002**, 91, 9324. (e) J. H. Yang, B. J. Kim, Y. H. Kim, Y. J. Lee, B. H. Ha, Y. S. Shin, S. Y. Park, H. S. Kim, C. Y. Park, C. W. Yang, J. B. Yoo, M. Kwon, H. K. Ihm, H. J. Song, T. H. Kang, H. J. Shin, Y. J. Park, J. M. Kim, *J. Vac. Sci. Technol. B,* **2005**, 23, 930. (f) T. Y. Kim, K. R. Lee, K. Y. Eun, K. H. Oh, *Chem. Phys. Lett.*, **2003**, 372, 603.

15 O. Lourie, H. D. Wagner, *Appl. Phys. Lett.*, **1998**, 73, 3527.

16 M. M. J. Treacy, T. W. Ebbesen, J. M. Gibson, *Nature,* **1996**, 381, 678.

17 M. Cadek, J. N. Coleman, K. P. Ryan, V. Nicolosi, G. Bister, A. Fonseca, J. B. Nagy, K. Szostak, F. Beguin, W. J. Blau, *Nano Lett.*, **2004**, 4, 353.

18 D. Qian, E. C. Dickey, R. Andrews, T. Rantell, *Appl. Phys. Lett*., **2000**, 76, 2868.

19 J. M. Benoit, B. Corraze, S. Lefrant, W. Blau, P. Bernier, O. Chauvet, *Synth. Met.*, **2001**, 121, 1215.

20 T. Kashiwagi, E. Grulke, J. Hilding, R. Harris, W. Awad, J. Douglas, *Macromol. Rapid Commun.*, **2002**, 23, 761.

21 R. Haggenmueller, H. H. Commans, A. G. Rinzler, J. E. Fischer, K. I. Winey, *Chem. Phys. Lett*., **2000**, 330, 219.

22 J. Hone, B. Batlogg, Z. Benes, M. C. Llaguno, N. M. Nemes, A. T. Johnson, J. E. Fischer, *Mater. Res. Soc. Symp. Proc.*, **2001**, 633,11.

23 P. M. Ajayan, L. S. Schadler, C. Giannaris, A. Rubio, *Adv. Mater.*, **2000**, 12, 750.

24 J. Chen, A. M. Rao, S. Lyuksyutov, M. E. Itkis, M. A. Hamon, H. Hu, R. W. Cohn, P. C. Eklund, D. T. Colbert, R. E. Smalley, R. C. Haddon, *J. Phys. Chem. B*, **2001**, 105, 2525.

25 J. E. Riggs, Z. Guo, D. L. Carroll, Y.-P. Sun, *J. Am. Chem. Soc.*, **2000**, 122, 5879.

26 J. E. Riggs, D. B. Walker, D. L. Carroll, Y.-P. Sun, *J. Phys. Chem. B*, **2000**, 104, 7071.

27 L. J. Bahr, J. M. Tour, *Chem. Mater.*, **2001**, 13, 3823.

28 S. Pekker, J.-P. Salvetata, E. Jakab, J.-M. Bonard, L. Forro, *J. Phys. Chem. B*, **2001**, 105, 7938.

29 E. T. Michelson, C. B. Huffman, A. G. Rinzler, R. E. Smalley, R. H. Hauge, J. L. Margrave, *Chem. Phys. Lett.*, **1998**, 296, 188.

30 J. Liu, A. G. Rinzler, H. Dai, J. H. Hafner, R. K. Bradley, P. J. Boul, A. Lu, T. Iverson, K. Shelimov, C. B. Huffman, F. Rodriguez-Macias, Y. S. Shon, T. R. Lee, D. T. Colbert, R. E. Smalley, *Science*, **1998**, 280, 1253.

31 M. A. Hamon, H. Hu, P. Bhowmik, S. Niyogi, B. Zhao, M. E. Itkis, R. C. Haddon, *Chem. Phys. Lett.*, **2001**, 347, 8.

32 S. Li, Y. Qin, J. Shi, Z.-X. Guo, Y. Li, D. Zhu, *Chem. Mater.*, **2005**, 17, 130.

33 E. Tamburri, S. Orladucci, M. L. Terranova, F. Valentín, G. Palleschi, A. Curulli, F. Brunetti, D. Passeri, A. Alippi, M. Rossi, *Carbon,* **2005**, 43, 1213.

34 L. Valentín, I. Armentano, D. Puglia, J. M. Kenny, *Carbon,* **2004**, 42, 323.

35 V. Georgakilas, K. Kordatos, M. Prato, D. M. Guldi, M. Holzinger, A. Hirsch, *J. Am. Chem. Soc.,* **2002**, 124, 760.

36 (a) V. Georgakilas, N. Tagmattarchis, D. Pantararotto, A. Bianco, J.-P. Briand, M. Prato, *Chem. Commun.*, **2002**, 3050. (b) Z. Yao, N. Braidy, G. A. Botton, *J. Am. Chem. Soc.*, **2003**, 125, 16015. (c) D. Pantarotto, C. D. Partidos, R. Graff, J. Hoebeke, J.-P. Briand, M. Prato, A. Bianco, *J. Am. Chem. Soc.*, **2002**, 124, 760.

37 R. Singh, D. Pantarotto, L. Lacerada, G. Pastorin, C. Klumpp, M. Prato, A. Bianco, K. Kostarelos, *Proc. Natl. Acad. Sci. U.S.A.,* **2006**, 103, 3357.

38 D. M. Guldi, G. M. A. Rahman, F. Zerbetto, M. Prato, *Acc. Chem. Res.,* **2005**, 38, 871.

39 S. D. Mhlanga**,** *Synthesis and Study of Carbon Nanotubes and Carbon Nanosphers*, **2009**, PhD thesis, submitted at University of the Witwatersrand, Johannesburg, South Africa.

40 M. S. Mohlala**,** *Organometallic iron complexes as catalysts for carbon nanotube synthesis* , **2006**, PhD thesis, submitted at University of the Witwatersrand, Johannesburg, South Africa.

41 M. Maggini, G. Scorrano, M. Prato, *J. Am. Chem. Soc*., **1993**, 115, 9798.

42 J. Louie, R. H. Grubbs, *Organometallics,* **2002**, 21, 2153.

43 J. A. Love, J. P. Morgan, T. M. Trnka, R. H. Grubbs, *Angew. Chem., Int. Ed.,* **2002**, 41, 4035.

44 T. L. Choi, R. H. Grubbs, *Angew. Chem., Int. Ed.,* **2003**, 42,1743.

45 F. J. Gomez, R. J. Chen, D. W. Wang, R. M. Waymouth, H. J. Dai, *Chem. Commun.,* **2003**, 190.

46 Y. Liu, A. Adronov, *Macromolecules*, **2004,** 37, 4755.

47 R. Czrew, M. Terrons, J. C. Charlier, X. Blase, B. Foley, R. Kamalakaran, N. Grobert, H. Terrones, D. Tekleab, P. M. Ajayan, W. Blau, M. Ruehle, D. L. Carroll. *Nano Lett*., **2001**, 1, 457.

48 H. Xu, X. Wang, Y. Zhang , S. Liu, *Chem. Mater*., **2006,** 18**,** 2929.

49 C. P. Ewels, C. P. Glerup, *J. Nanosci. Nanotech.,* **2005**, 5, 1345.

50 (a) M. Terrones, P. Redlich, N. Grobert, S. Trasobares, W. K. Hsu, H. Terrones, Y. Q. Zhu, J. P. Hare, C. L. Reeves, A. K. Cheetham, M. Ruhle, H. W. Kroto, D. R. M, Walton, *Ad*v. *Mater.,* **1999**, 11, 655. (b) A. G. Kudashov, A. V. Okotrub, L. G. Bulusheva, I. P. Asanov, Y. V. Shubin, N. F. Yudanov, L. I. Yudanova, V. S. Danilovich, O. G. Abrosimov, *J. Phys. Chem. B,* **2004**, 108, 9048.

51 X. B. Wang, Y. Q. Liu, D. B. Zhu, L. Zhang, H. Z. Ma, N. Yao, B. L. Zhang, *J. Phys. Chem. B,* **2002**, 106, 2186.

52 (a) C. M. Yang, M. El-Merraoui, H. Seki, K. Kaneko, *Langmuir*, **2001**, 17, 675. (b) R. Sen, B. C. Satishkumar, A. Govindaraj, K. R. Harikumar, M. K. Renganathan, C. N. R. Rao, *J.*

Mater. Chem., **1997**, 7, 2335. (c) M. Nath, B. C. Satishkumar, A. Govindaraj, C. P. Vinod, C. N. R. Rao, *Chem. Phys. Lett.*, **2000**, 322, 333. (d) R. Sen, B. C. Satishkumar, A. Govindaraj, K. R. Harikumar, G. Raina, J. P. Zhang, A. K. Cheetham, C. N. R. Rao, *Chem. Phys. Lett.*, **1998**, 287, 671. (e) J. W. Liu, S. Webster, D. L. Carroll, *J. Phys. Chem. B*, **2005**, 109, 15769.

53 (a) G. Y. Zhang, X. C. Ma, D. Y. Zhong, E. G. Wang, *J. Appl. Phys.*, **2002**, 91, 9324. (b) T. Y. Kim, K. R. Lee, K. Y. Eun, K. H. Oh, *Chem. Phys. Lett.*, **2003**, 372, 603.

54 I. Shimoyama, G. Wu, T. Sekiguchi, Y. Baba, *J. Electron Spectrosc. Relat. Phenom.*, **2001**, 114, 84.

55 L. Delaude, A. Demonceau, A. F. Noels, *Macromolecules*, **2003,** 36, 1446.

56 Y.-P. Sun, W. Huang, Y. Lin, K. Fu, A. Kitaygorodskiy, L. A. Riddle, Y. J. Yu, D. L. Carroll, *Chem. Mater.*, **2001**, 13, 2864.

57 H. C. Choi, S. Y. Bae, J. Park, K. Seo, C. Kim, B. Kim, H. J. Song, H.-J. Shin, *Appl. Phys. Lett*.**, 2004**, 85, 5742.

58 (a) X. Mi, D. Xu, W. Yan, C. Guo, Y. Ke, Y. Hu, *Polym. Bullet.*, **2002**, 47, 521. (b) T. Tsujino, T. Saeguss, J. Furukawa, *Die Makromolekulare Chemie*, **1965**, 85, 71 (c) T. Saegusa, T. Tsujino, J. Furukawa, *Makromol. Chem.*, **1964**, 78, 231.

59 Y. Gao, Y. Wang, J. Shi, H. Bai, B. Song, *Polymer Testing*, **2008**, 27, 179.

Chapter 7

Synthesis of polythiophene covalently liked to nitrogen doped and undoped carbon nanotubes

7.1 Introduction

The discovery of carbon nanotubes (CNTs) has attracted the attention of a number of research groups with the prospect of developing novel carbon-based nanomaterials due to their unique structure-dependent electronic and mechanical properties [1-4]. Carbon nanotubes (CNTs) are believed to a potential alternative to silicon for development of carbon-based nanoscale diodes or transistors, and has therefore become one of the main topics of research for CNT-based nanoelectronics [5]. CNTs can readily accept electrons, which can then be transported under nearly ideal conditions along the tubular axis. The fact that CNTs appear in structurally defined semiconductive or conductive forms turns the CNTs into ideal components for various electronic applications [6]. On account of the large number of concentric cylindrical graphitic tubes present in MWNTs, they are considered even more suitable in electron-donor–acceptor ensembles than SWNTs [7]. CNTs can be doped with heteroatoms, such as nitrogen, which is a promising method to tailor the electronic property of CNTs [8]. Doping with nitrogen and boron leads to the formation of electron-excess *n*-type and electron-deficient *p*-type semiconducting nanotubes, respectively [5,6 ,9,10]. The application of CNTs in devices has become a significant challenge since CNTs tend to be insoluble in most common solvents. However, dispersion of CNTs into polymers has been improved by either mixing the materials in a conical twin-screw extruder [11], using surfactants as processing aids [12], by appropriate functionalization [13] or by *in situ* polymerization [14]. Composites based on polymers and nanotubes have the potential to make an impact on a variety of applications ranging from general low-cost circuits and displays to power devices, micro electromechanical systems, super capacitors, solar call sensors, and displays [15,16].

Successful covalent functionalisation of both SWNTs and MWNTs has been reported by many researchers [17]. For example, Georgakilas *et al.* [18] have demonstrated the functionalisation of the sidewalls of SWNTs using a 1,3-dipolar cycloaddition of azomethine ylides, generated by condensation of an amino acid with an aldehyde (i.e. the Prato reaction).

The combination of CNTs with electron donors has also signified an innovative concept to harvest solar energy and to convert it into electricity, and like C_{60}, CNTs have been introduced into conjugated polymers to produce organic photovoltaic devices [19]. Electrical and photoelectrical properties of CNT/conjugated polymer composites and interfaces have been investigated since the mid 1990s [20-25]. For example, bulk heterojunction solar cells based on conjugated polymers blended with MWNT [26] and SWNTs [27-29] have been reported. In addition, Kumakis *et al*. [28] have reported a high value of 0.75 V for V*oc* by using 1 % SWNT/poly-3-octyl-thiophene (P3OT) in bulk heterojunction solar cells. In addition, they have claimed that this achievement was due to the HOMO–LUMO band gaps that could be associated with the P3OT and SWNT interactions. Improvement of the light absorption has also been achieved by using dye (naphthalocyanine, NaPc) coated CNTs blended with P3OT in a bulk heterojunction configuration [30]. For the same purpose, Jin and Dai suggested a cell that, instead of using CNTs randomly mixing with polymers, could contain a network of vertically aligned CNTs separated by vertical polymer layers [31].

Pradhan *et al*. [32] have demonstrated that physically blended MWNTs with polyhexythiophene (P3HT) provides extra dissociation sites and assists hole transportation in a P3HT-MWNT/C_{60} double layer device. However, power conversion efficiency under white light illumination was low. Similarly, MWNT sheets have been used as the hole collecting electrode in polymer solar cells with P3HT as the donor material and PCBM as the acceptor material [33]. Recently, Reyes *et al*. [34] have studied and compared nitrogen doped to undoped carbon nanotubes in a photovoltaic cell that was fabricated using a P3OT polymer blended with undoped CNTs and N-doped CNTs. Their results indicated that N-doped CNTs enhanced the efficiency of the P3OT solar cells in comparison with the undoped CNTs.

In this work, we report a new approach for the functionalization of N-doped and undoped CNTs using a 1,3-dipolar cycloaddition of azomethine ylides and a subsequent *in situ* polymerization

with thiophene. The resulting polymers were characterized and their thermal and electronic properties studied and the results described in this Chapter.

7.2 Experimental

7.2.1 General procedures

The general procedures used in this Chapter were the same as those used in Chapter 5.

7.2.2 Synthesis and purification of carbon nanotubes

The procedures used for the synthesis of both N-doped and undoped carbon nanotubes were the same as those used in Chapter 6. Similarly, the purification methods used in this Chapter were also the same as those stated in Chapter 6.

7.2.3 Functionalization of 7.1 and 7.3 [18]

The functionalization methodology used to prepare **7.2** and **7.4** was the same as that used in Chapter 6, Section 6.*2.3.1*. However, 2-thiophenecarboxaldehyde was used instead of 5-norbornene-2-carboxaldehyde in the Prato reaction. Purified dark brown solids of functionalized CNTs **7.2** and **7.4** were obtained in amounts of 0.131 g and 0.150 g, respectively.

7.2.4 Polymerization reactions

7.2.4.1 Preparation of copolymers 7.5 and 7.6

The same procedure was followed as described in Chapter 5, Section, *5.2.3.3*. In two separate round bottomed flasks functionalized N-doped and undoped CNTs (each 0.050 g) were suspended in pre-dried chloroform (~25 mL). The reaction mixtures were subsequently sonicated for 2 h. $FeCl_3$ (~5.2 g, 32 mmol) was then added to each CNT suspension and then the mixtures were left to sonicate for a further 1 h. 3-Hexylthiophene (1.00 g, 5.9 mmol) in chloroform (~25 mL) was then added dropwise over 60 min, under constant stirring, to each reaction mixture. The reactions mixtures were then left to stir overnight. The polymerization reactions were terminated by pouring each of the reaction mixtures into an excess of MeOH (~50 mL) to precipitate the crude polymers. The synthesised polymers were then obtained by filtration using membrane

filter papers (1 μm). Both the products were washed with ethanol (~100 mL), with a 1:1 distilled water and acetone mixture (500 mL) and finally twice with acetone (500 mL). The resultant brown solid products were then dried under vacuum for 48 h to give dark brown spongy solids of **7.5** (0.977 g, 93 % yield) and **7.6** (0.917 g, 87 % yield), respectively.

7.2.4.2 Preparation of copolymers 7.7 and 7.8

The same procedure was followed as above to synthesis copolymers **7.7** and **7.8**. In this case unsubstituted thiophene (1.00 g, 12 mmol) and either functionalized N-doped (**7.4**) or functionalized undoped CNTs (**7.2**) (each 0.050 mg) were used. After the reactions were complete the products were purified and dried as before to give brown solid products of copolymer **7.7** (0.658 g, 86 % yield) and **7.8** (0.470 g, 58 % yield), respectively.

7.2.4.3 Preparation of 7.11

The same procedure was adopted as above (Section *7.2.4.4*) to polymerize the composite. In this case unfunctionalized N-CNTs (0.050 g) and thiophene (1.00 g, 12 mmol) were used to make the polymer composite. At the end of the reaction purifying and drying gave (0.500 g, 48 % yield) a brown solid product.

7.2.4.4 Preparation of 7.9 and 7.10 [35]

The polymerization reaction was done in the same manner as that reported in Chapter 5, Section *5.2.3.1*. At the end of the reaction the products were purified and dried to give brick red solid polythiophene (0.658 g, 86 % yield) and polymer **7.9** as a dark brown spongy solid (0.855 g, 86 % yield), respectively.

7.3 Results and discussion

7.3.1 Functionalization reactions of CNTs

The functionalization of the N-doped and undoped CNTs was achieved when 2-thiophenecarboxaldehyde **7.a** and *N*-methylglycine **7.b** were used as the precursors for the Prato reaction. The functionalized CNTs were obtained as a dark gray product for both the N-doped and undoped CNTs. The increase in mass, by 50 mg and 31 mg for N-doped and undoped CNTs respectively, of the product indicated that the side walls of the CNTs contained organic functional groups attached to the CNTs (see Scheme **7.1**).

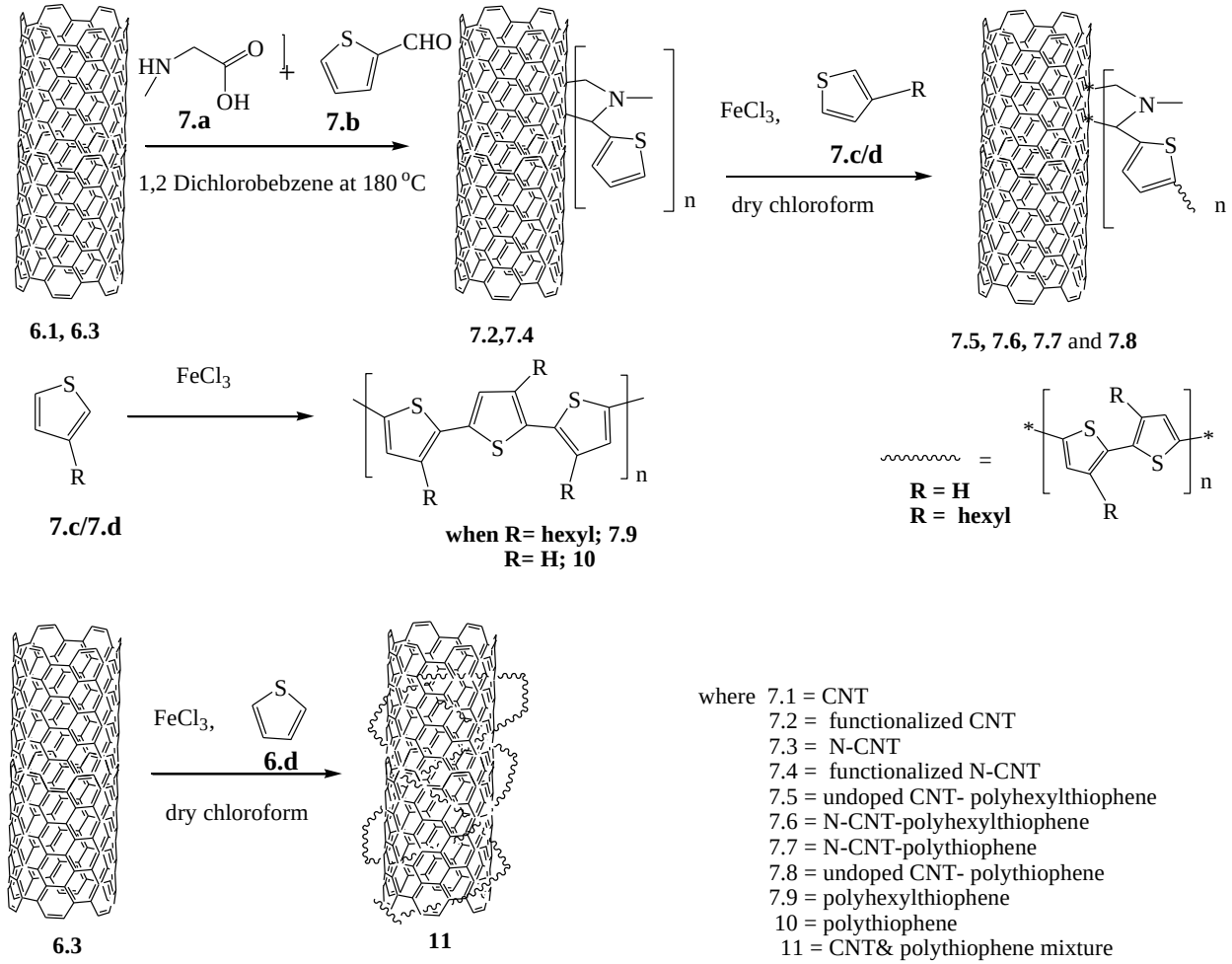

Scheme **7.1** Functionalization and polymerization methodology used to make polymer carbon nanotubes/polymer composite.

7.3.2 Polymerization reactions

In this study, $FeCl_3$ was used as a polymerization initiator to polymerize thiophene in chloroform under argon. The monomers, either thiophene **7.c** or 3-hexylthiophene **7.d**, were added dropwise to the $FeCl_3$ mixture at r.t. [36-39]. The resulting brick red and dark brown spongy solids were recovered by filtration in good yields from both monomers respectively. Figure **7.2** shows the synthesized polymers dissolved in THF.

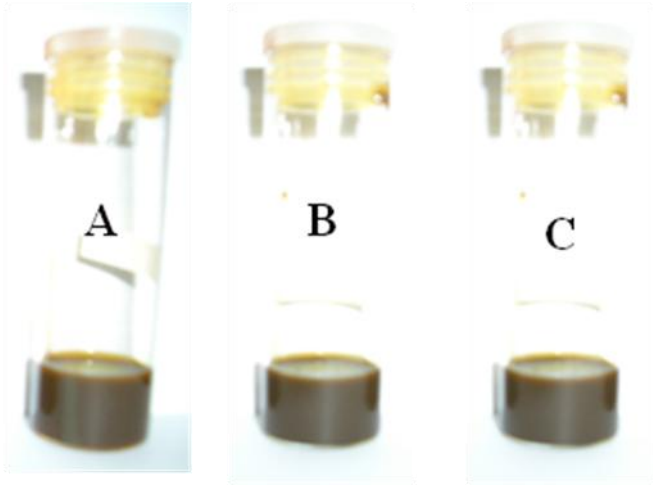

Figure **7.1** A) Poly(3-hexylthiophene) **7.9**; B) undoped CNT-poly(3-hexylthiophene) **7.5**; C) N-doped CNT-poly(3-hexylthiophene) **7.6**.

7.3.3 Characterization of functionalized CNTs and copolymers

7.3.3.1 Raman Spectroscopy of functionalized CNTs

Raman spectroscopy has been shown to be a useful technique to characterize the crystallinity of CNTs [40]. The Raman spectrum of undoped **6.1** (Figure **6.3** spectrum **A**) and N-doped CNTs **6.3** (Figure **6.3** spectrum **C**) are shown. The spectrum of N-doped unfunctionalized CNTs showed the D band at 1352 cm^{-1} and a G band at 1585 cm^{-1} (Figure **7.3** spectrum **C**), while the functionalized N-doped **7.4** material displayed the conventional bands at 1358 cm^{-1} and 1573 cm^{-}

[1], respectively. Similarly the undoped unfunctionalized CNTs **6.1** (Figure **7.3** spectrum **A**) gave two bands at 1351 cm^{-1} and at 1583 cm^{-1} while the functionalized undoped CNTs **6.2** gave bands at 1346 cm^{-1} and 1582 cm^{-1} (Figure **7.3** spectrum **B**).

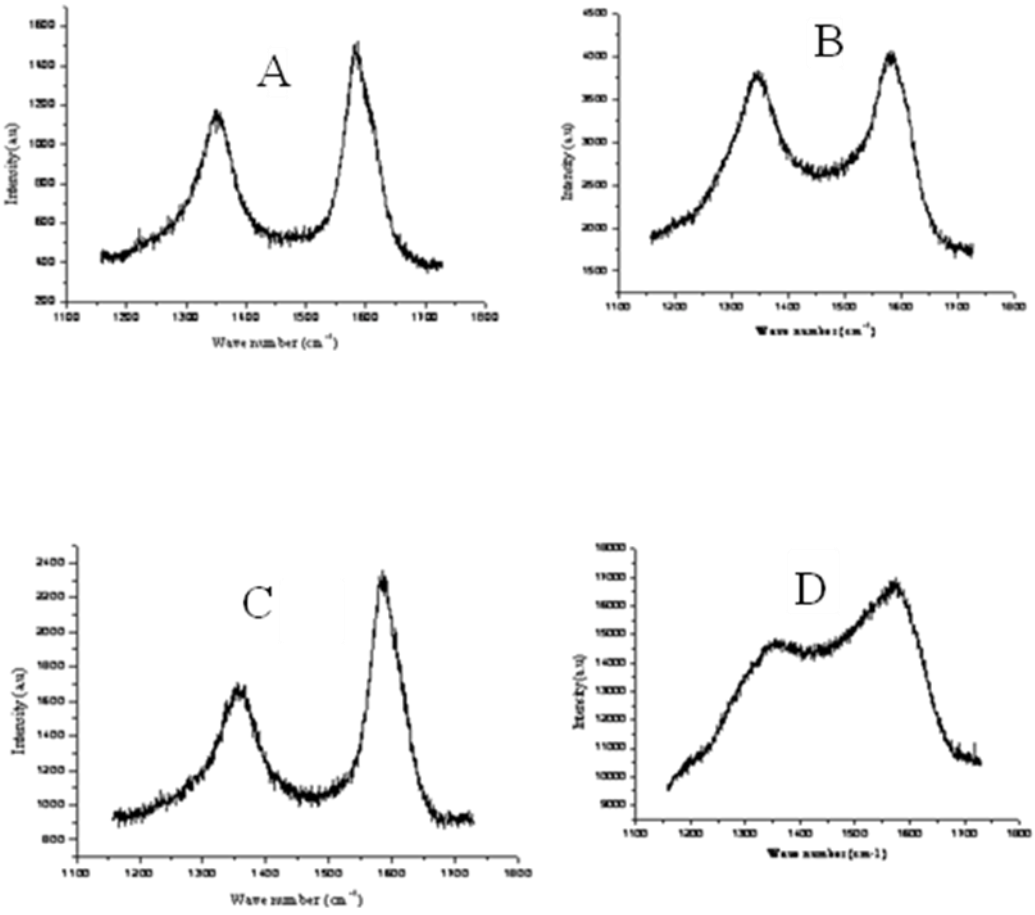

Figure **7.2** Raman spectra of **A**) unfunctionalized CNTs **6.1**; B) functionalized CNTs **7.2**; **C**) unfunctionalized N-CNTs **7.3**; **D**) functionalized N-CNTs **7.4**.

The relative intensities of the I_D/I_G values increased in pristine N-doped CNTs relative to the undoped CNTs. Furthermore, the I_D/I_G ratios increased in the functionalized CNTs this is indicates the introduction of covalently bound moieties to the nanotube framework wherein significant amounts of the sp^2 carbons have been converted to sp^3 hybridization after the functionalization process. The I_D/I_G ratios of **7.2** found to be larger than **7.4**, this could be the

side wall of the undoped CNTs after functionalization became highly disordered than N-doped CNTs (the see Figure **7.3** and Table **7.1**).

Table **7.1** intensity ratios of the D and G Raman bands

Sample	Pristine I_D/I_G ratio	After functionalization I_D/I_G ratio
Undoped CNTs	0.72	0.94
N-doped CNTs	0.78	0.88

7.3.3.2 Transmission Electron Microscopy (TEM)

The polymer attached CNTs in solution could be readily deposited directly onto a surface for various microscopy analyses and the TEM images offered the most direct evidence for the presence of carbon nanotubes in the samples.

The synthesized CNTs (both undoped CNTs **7.1** and N-CNT **7.3**) were purified by heating then reflux in concentrated hydrochloric acid to remove impurities. The TEM images also confirmed that multi-walled CNTs had been synthesized and that the CNTs were relatively pure. In the case of the nitrogen doped CNTs, they were found to have defective bamboo-like structures and distinctive compartment layers due to the incorporation of nitrogen atoms into the CNTs, either as pyridinic nitrogen or graphitic nitrogen.

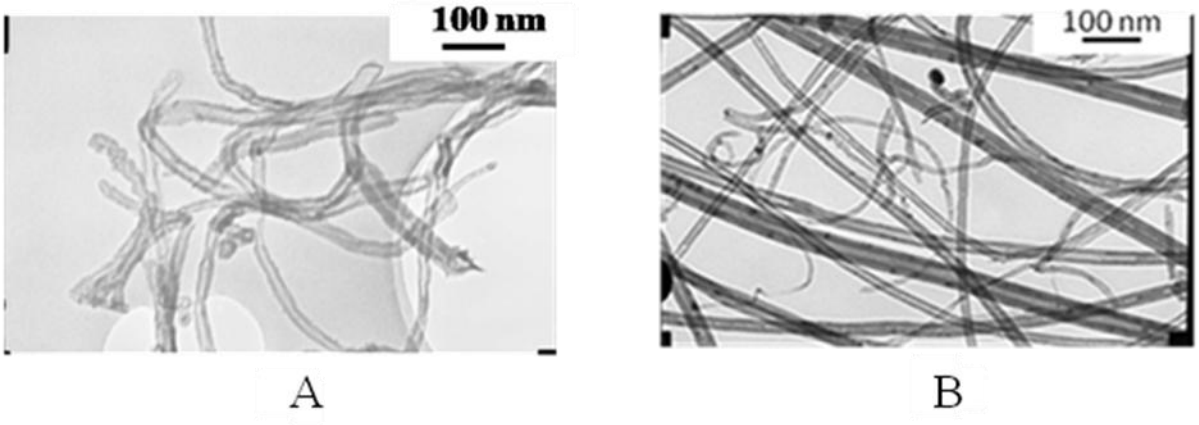

Figure **7.3** TEM images of A) CNTs **7.1** and B) N-CNTs **7.3**.

After functionalization of the CNTs **7.4**, the side walls became rougher (shown in Figure **7.4**) than the pristine CNTs (as shown in Figure **7.3**).

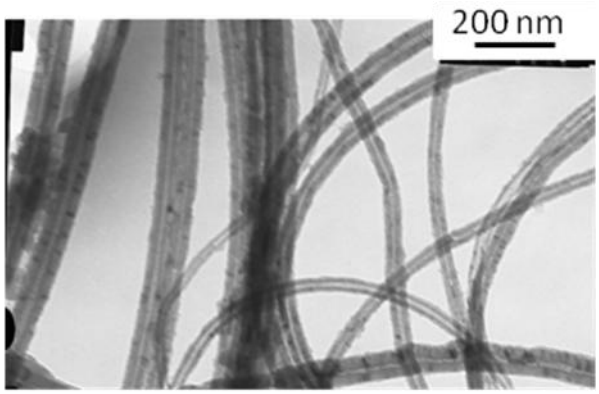

Figure **7.4** TEM images of functionalized N-CNTs **7.4**

Figure **7.5a-c** shows the TEM images of **7.5**, **7.6**, and **7.7** and **7.8**. From the TEM images the CNTs were seen to be covered with poly(3-hexylthiophene) and polythiophene respectively. This was further substantiated by ^{1}H NMR, FT-IR and UV-visible studies (Section *7.3.3.3-7.3.3.5*). The morphology of the two classes of thiophenes will be discussed separately below.

7.3.3.2.1 Poly(3-hexylthiophene)/CNT composite

The poly(3-hexylthiophene)-attached CNTs (both nitrogen doped **7.6** and undoped CNTs **7.5**) were covered with polymer. The CNTs can readily be seen embedded in the polymer. The TEM images (Figure **7.5a**), revealed that the N-CNTs were not covered uniformly with polymers. In the case of the undoped CNTs, the CNTs were more or less uniformly covered by the polymer. The average overall thickness of **7.5** (shown in Figure **7.5a,** image **A** and **B**) was measured to be about 85 nm. Similarly for N-CNTs **7.6** (shown in Figure **7.5a** image **C** and **D**) the average diameter was found to be about 130 nm.

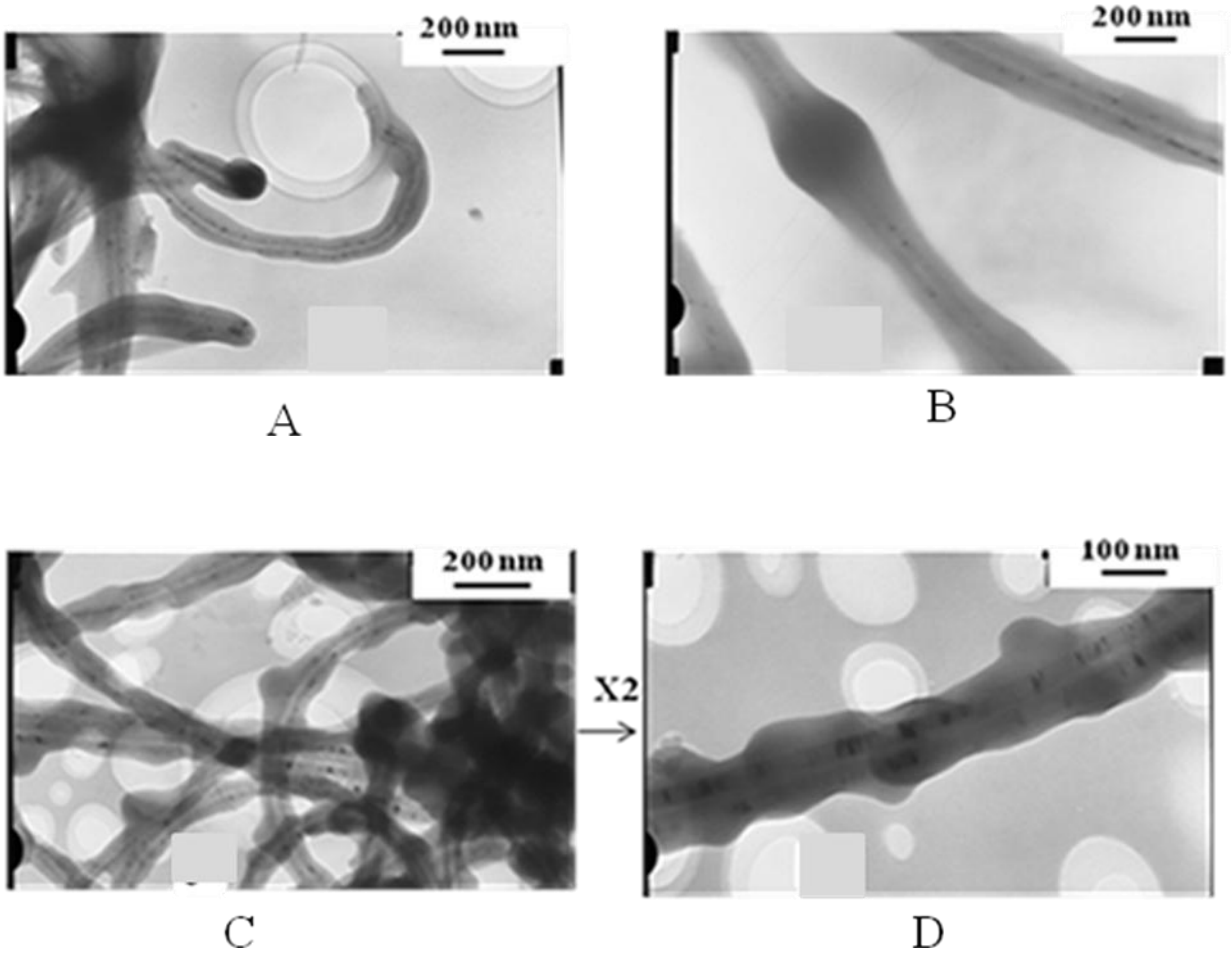

Figure **7.5a** TEM images of **A** and **B** are for poly(3-hexylthiophene) attached undoped CNTs **7.5 ; C** and **D** for poly(3-hexylthiophene) attached N-CNTs **7.6**.

7.3.3.2.2 Polythiophene/CNT composite

The morphology of the polythiophene polymer attached CNTs (both N-CNT and undoped) was found to be different from that of poly(3-hexylthiophene) attached to CNTs. The TEM images revealed that, when using polythiophene, the CNTs were covered by a rough and bumpy polymer (Figure **7.5b**). The average overall thicknes of the polymer covered N-CNTs **7.7** (as shown in Figure **7.5b A** and **B**) was about 126 nm. Similarly, for the undoped polymer attached CNTs **7.8** (as seen in Figure **7.5b C**) was mesured about 69 nm.

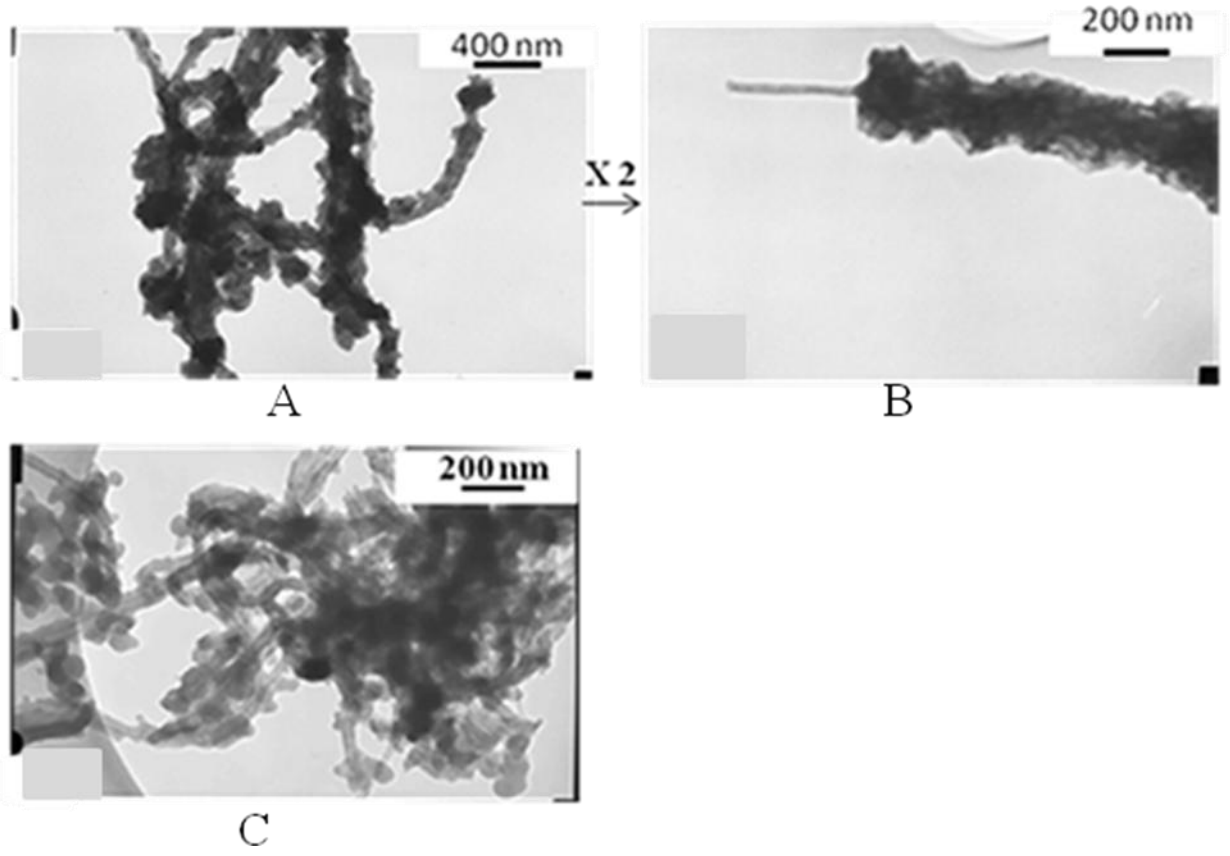

Figure **7.5 b** TEM images of **A** and **B,** and **C** polythiophene attached N-CNTs **7.7** and undoped CNTs **7.8**, respectively.

On other hand, for comparison purpose, a composite of pristine N-CNTs (not reacted with a Prato reagent) and polythiophene was synthesized using pristine N-CNTs and thiophene in the presence of $FeCl_3$ under inert atmosphere. The TEM images show a clear difference between the product produced by polymerisation with functionalised N-CNTs (Figure **7.5b** image **A** and **B**) and the product produced by mixing pristine N-CNTs with the thiophene (Figure **7.5c**). The new product shows that the CNTs and the "roses" polythiophene existed separately, i.e there was little interaction between the two reactants. This substantiate that the two reactants had only physical interactions, as a result the surface of the N-CNTs was smoothly coated with polymers. It is thus clear that the functionalization process leads to a new type of compounds.

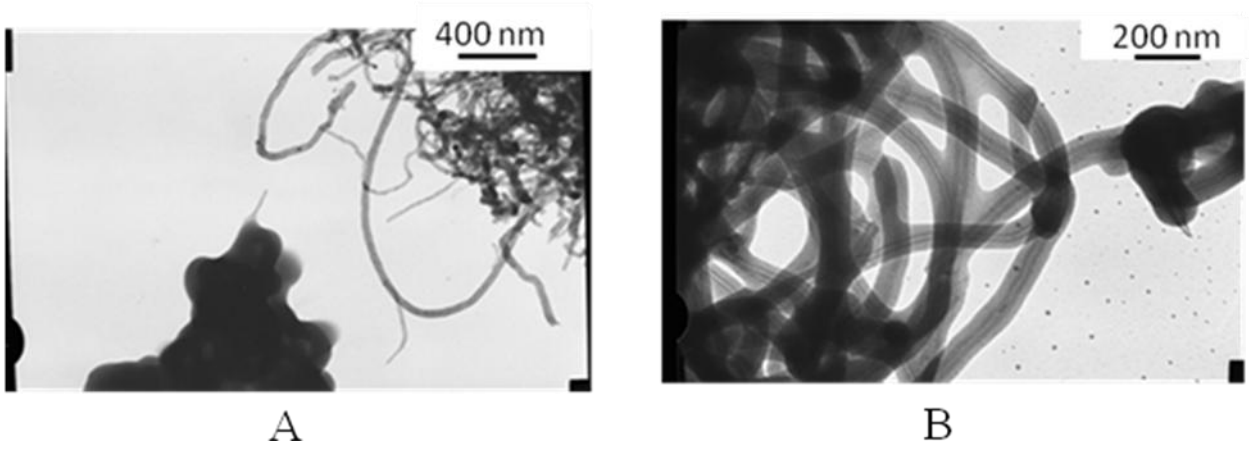

Figure **7.5c** TEM images for unfunctionalized CNT and polythiophene mixed **7.11**.

7.3.3.3 ^{1}H NMR spectroscopic studies of the synthesized materials

In a study by Leclerc *et al.* [41] it was found that π-electron delocalization and solubility of the polymers was largely affected by the substitution pattern of the polymer chain. In addition, Maior *et al*. [42] and Sato *et al*. [43] have reported that ^{1}H NMR spectroscopy studies provides important information on the substitution pattern in a polymer backbone. The NMR spectra of **7.5**, **7.6** and **7.9** were thus measured to provide information of the polymer backbone geometry.

The relative chemical shifts and the peak assignments of the poly(3-hexylthiophene) and 3-hexylthiophene materials were discussed in detailed in Chapter 5, Section *5.3.3.1*. The peaks found in the spectra of both **7.5** and **7.6**, had the same chemical shifts at 7 ppm as those for the pure poly(3-hexylthiophene). The peaks were broad in all those cases (see Figure **7.6**). This broadening effect was also observed in the case of C_{60} incorporation in to the poly(3-hexylthiophene) (Chapter 5). Results from the determination of the NMR nuclei spin-lattice (T_1) and spin-spin (T_2) relaxation time suggest that the broadened proton signals are associated with diamagnetic species of low mobility [44], namely, the nanotube-attached poly(3-hexylthiophene) moieties.

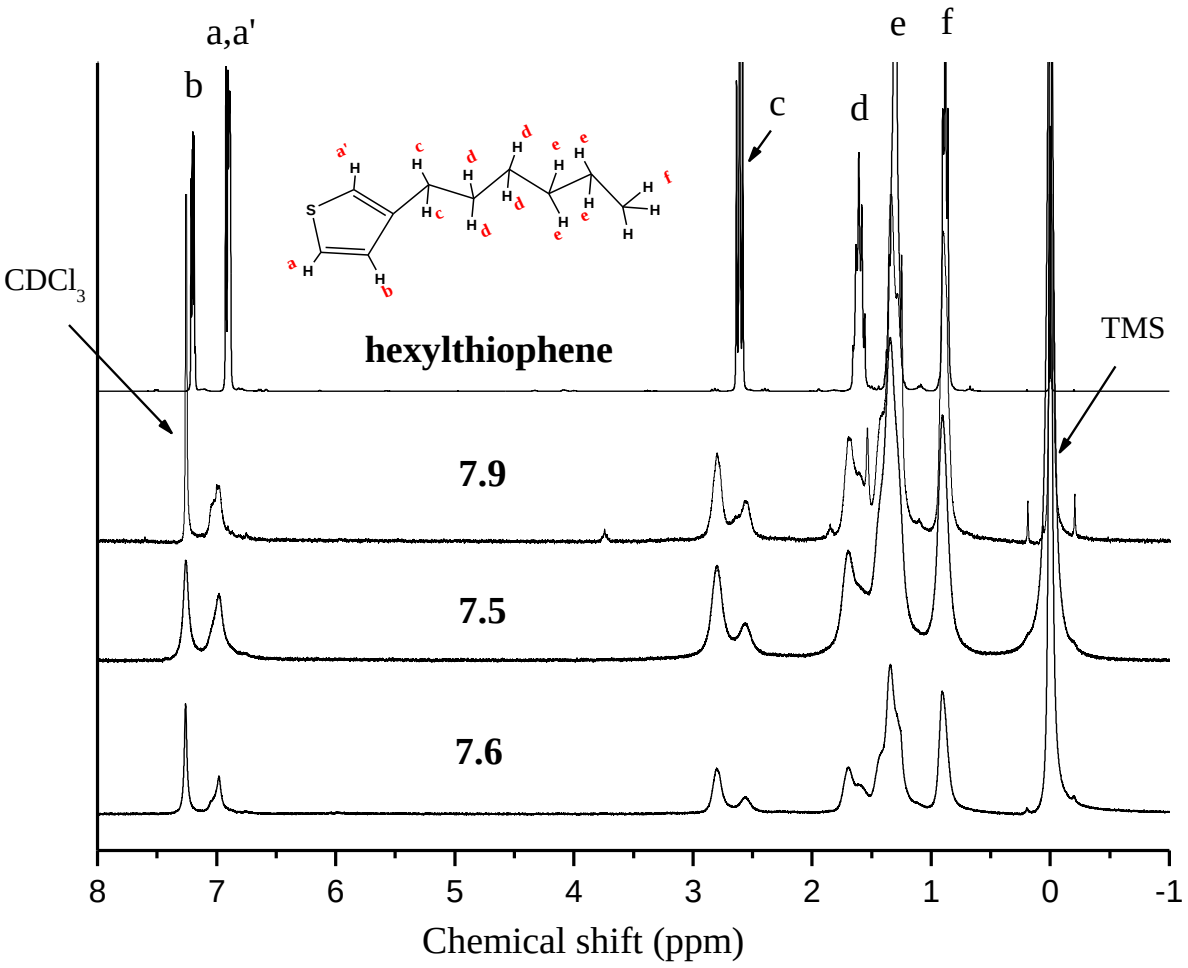

Figure **7.6** ^{1}H NMR spectra of the monomer and copolymers ($CDCl_3$), Poly(3-hexylthiophene) **7.9**; undoped CNT poly(3-hexylthiophene) **7.5**; N-doped poly(3-hexylthiophene) **7.6**.

The HT:HH ratio of the pure poly(3-hexylthiophene) was found to be 60:40. The HT:HH ratio deduced from the ^{1}H NMR spectrum for copolymers **7.5** and **7.6** were 69:31 and 70:30, respectively. The copolymers **7.5** and **7.6** were found to be more regioregular than poly(3-hexylthiophene) **7.9**. Similarly, at high concentrations of C_{60} derivative in poly(3-hexylthiophene) the HT:HH ratio found to be more regioregular (see Chapter 5, Section *5.3.3.1*).

The presence of CNT during a polymerization reaction influences the HT orientation less preferential. Similar results were reported by Saini *et al.* [45].

7.3.3.4 FT-IR studies of the synthesized materials

The FT-IR spectra of the synthesized polymers are shown in Figure **7.7** and a summary of FT-IR band positions and their assignments is given in Table **7.2**. The IR bands and assignments of the thiophene, 3-hexylthiophene, polythiophene and poly(3-hexylthiophene) were discussed in detail in Chapter 5, Section *5.3.3.2* and will not be repeated here.

No significant peaks were noticed after functionalization of the CNTs (see Figure **7.7**), since the CNT carbon atoms were more dominant than the added organic functional groups (see TGA profiles Figure **7.11**). However, after polymerization of the functionalized CNTs, new and distinctive peaks were recorded. The positions of those peaks were found to be similar to those found for polythiophene and poly(3-hexylthiophene) (see Figure **7.8a** and **b**). However, for polymer **7.5**, the band at 1507 cm^{-1} was difficult to identify as it was overshadowed by a very broad band in the same region.

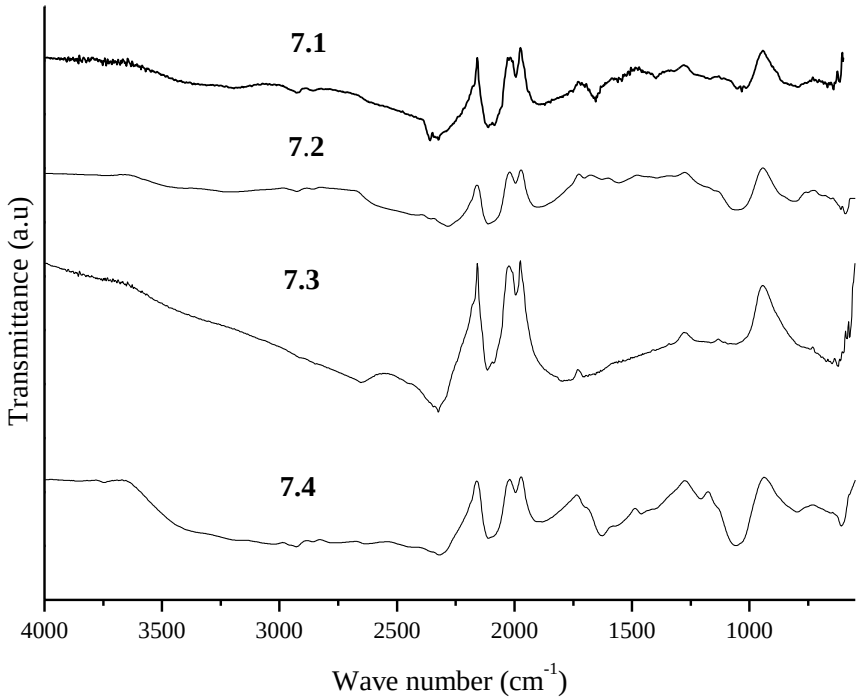

Figure **7.7** FT-IR of unfunctionalized undoped CNTs **7.1**; functionalized undoped CNTs **7.2**; unfunctionalized N-CNTs **7.3**; functionalized N-CNTs **7.4**.

Table **7.2** Summary of FT-IR of the monomer, poly(3-hexylthiophene) and CNT attached polymers (values in cm^{-1}). *

Sample	Ar C-H str.	C-H str.	Ring str.	Ar C-H out of plane
3-hexythiophene	3095 (vw)	2823 -2714 (br. m)		660 (s)
7.5	3053 (vw)	2955-2850 (br. s)	1456 (w)	817 (s), 670 (w)
7.6	3053 (vw)	2955-2855 (br. s)	1507 (vw), 1456 (m)	824 (s), 670 (w)
7.7, 7.8, Polythiophene		2927-2856 (br. s)	1438 (m)	795(m), 689(s)
7.9	3053 (vw)	2955-2855 (br. s)	1507 (vw), 1456 (m)	822 (s), 670 (w)

Ar = Aromatic; *vw = very weak, w = weak, m = medium, s = strong, br. s = broad and strong

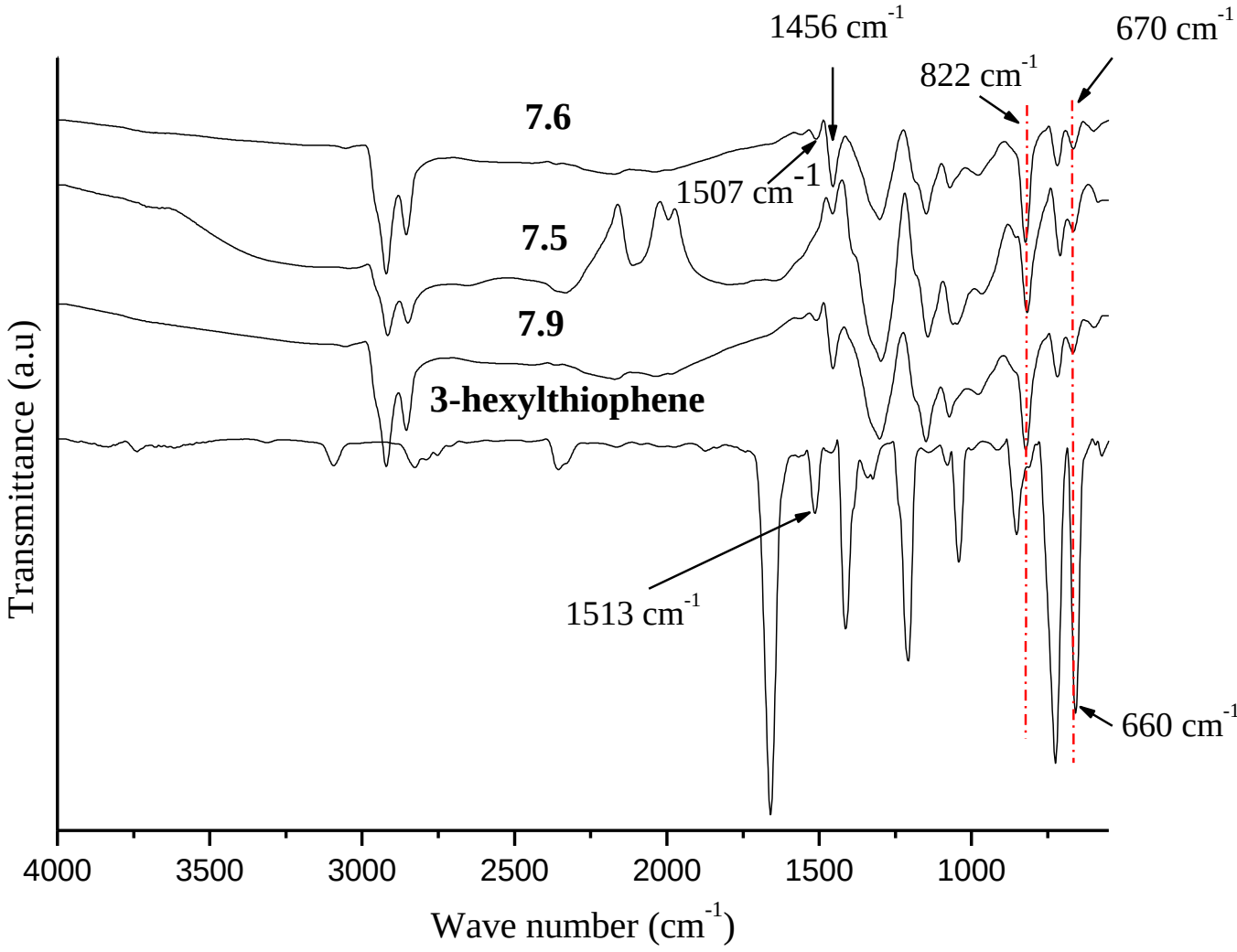

Figure **7.8a** FT-IR spectra of 3-hexylthiophene; poly(3-hexylthiophene) **7.9**; poly(3-hexylthiophene) attached to N-CNTs **7.5** and poly(3-hexylthiophene) attached to undoped CNTs **7.6**.

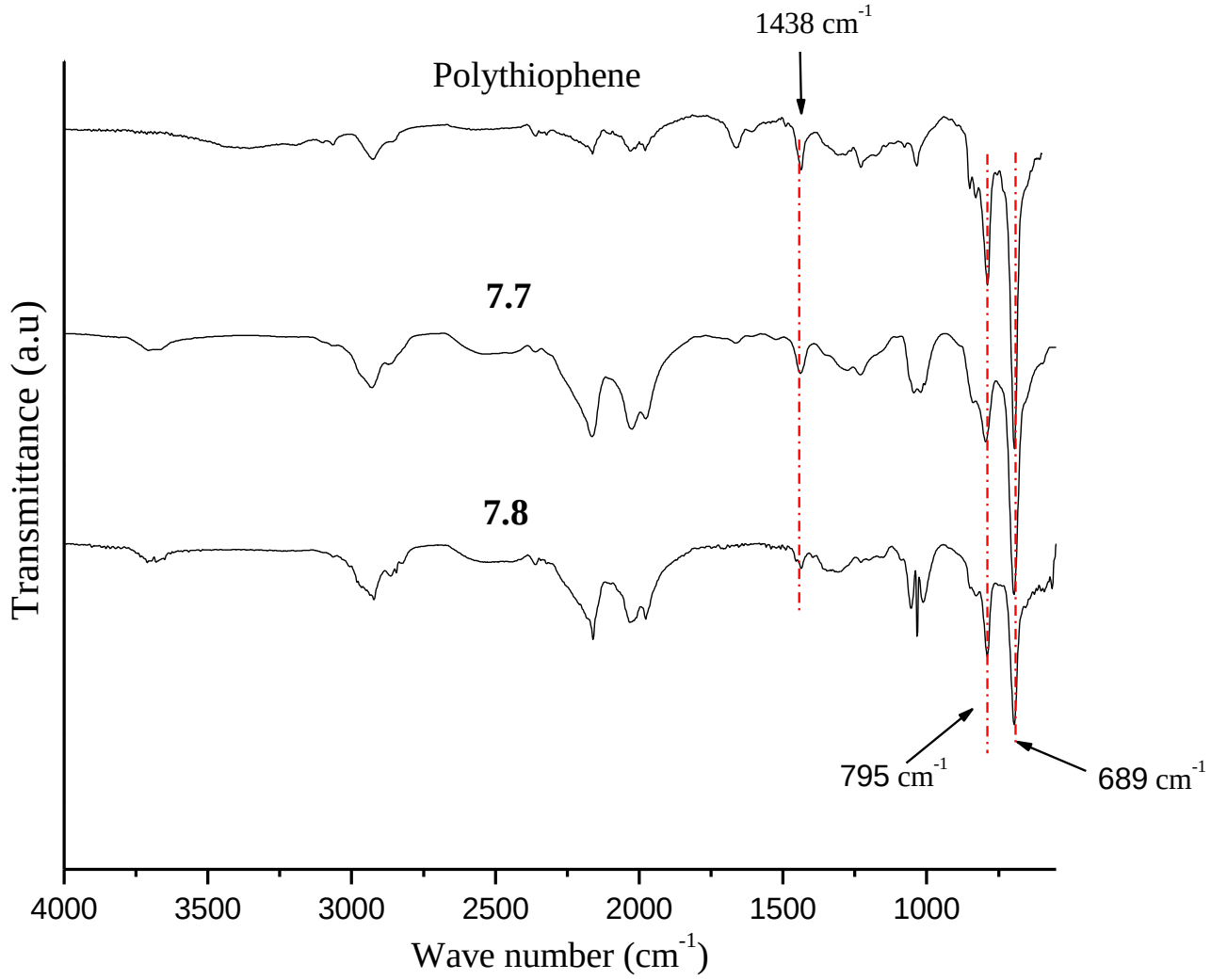

Figure **7.8b** FT-IR spectra of polythiophene attached to N-CNT **7.7**; polythiophene attached to undoped CNT **7.8** and polythiophene **7.9**.

7.3.3.5 UV-visible and photoluminescence spectra of the synthesized materials

UV-vis absorption spectra of **7.5**, **7.6** and **7.9** are shown in Figure **7.9** and a summary of the absorption bands are given in Table **7.2**. Pure polymer **7.9** showed an absorption band at 428 nm which corresponds to the π-π* transition of its conjugated segments [46]. In polymer **7.5** and **7.6**

this particular band shifted slightly to the red region. Similarly, the red shift was also noted in the C_{60} copolymers (see Chapter 5 Section *5.3.3.3*). Although the absorption band shift to the red region has been observed in some instances [47], this is contrary to the usual blue shift observed for poly(3-hexylthiophene)/clay mixtures [48].

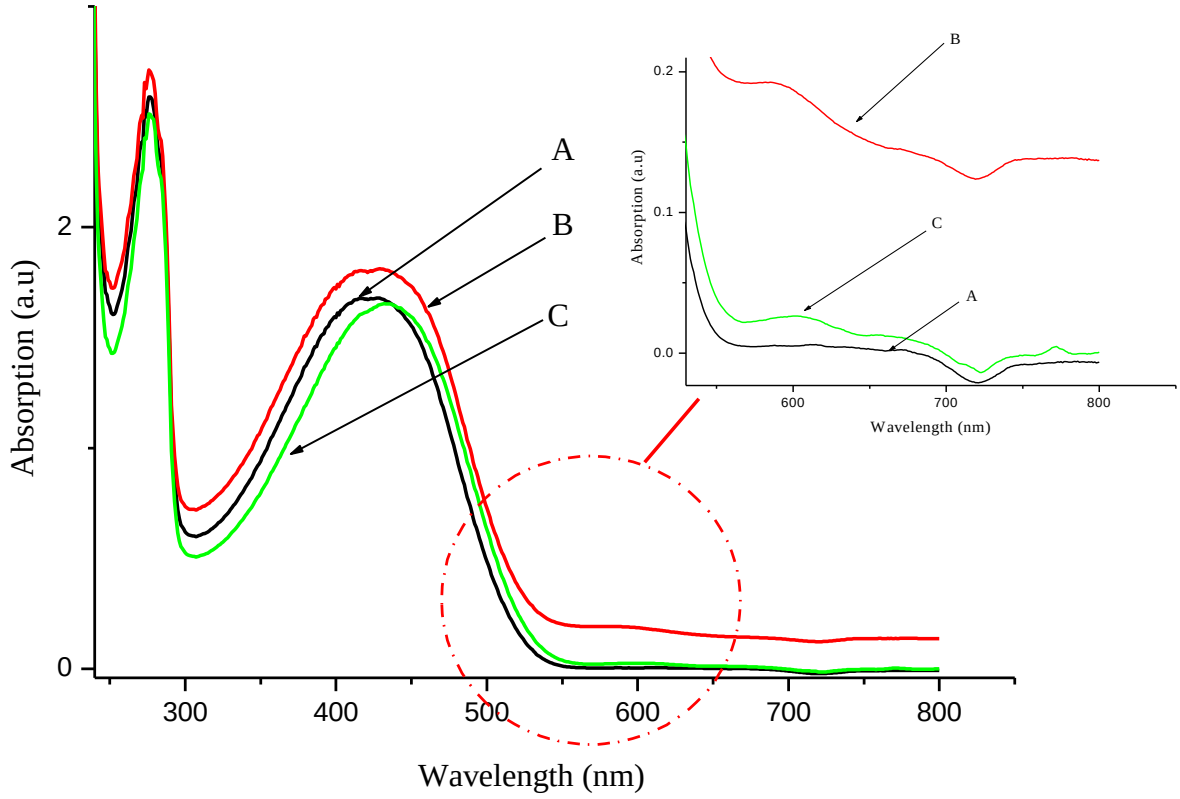

Figure **7.9** UV-vis absorption spectra in THF of A) poly(3-hexylthiophene) **7.9** ; B) polymer attached to undoped CNTs **7.5**; C) polymer attached to N-doped CNTs **7.6**.

The photoluminescence spectra of **7.5, 7.6** and **7.9** are shown in Figure **7.10**. Studies have indicated that poly(3-hexylthiophene) has photoluminescence properties [46]. The photoluminescence of **7.5, 7.6** and **7.9** were recorded at 500 nm excitation wavelength and showed emissions at 578, 577 and 574 nm, respectively (see Table **7.3**). In addition a small red shift relative to the poly(3-hexylthiophene) photoluminescence emissions were observed in both CNT derivatives.

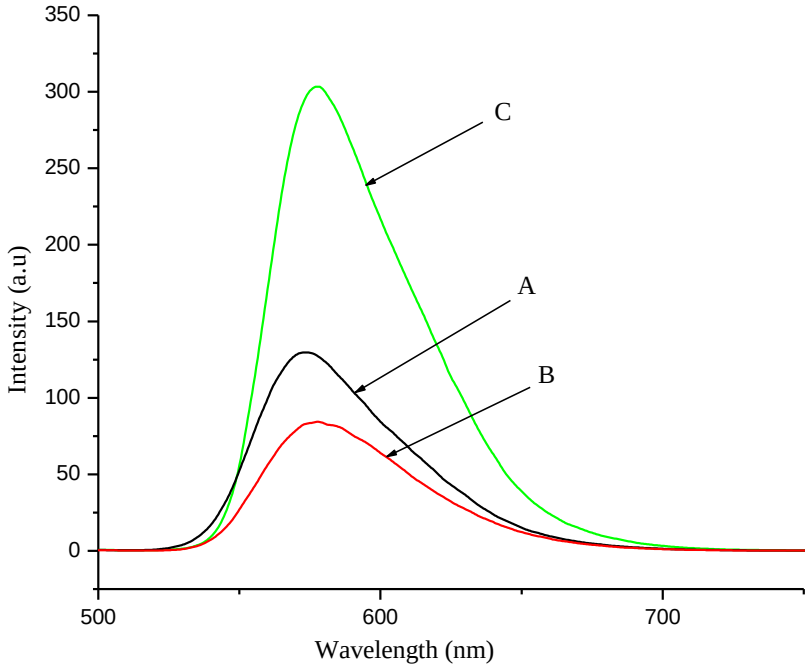

Figure **7.10** Photoluminescence at 500 nm excitation wavelength in THF of A) poly(3-hexylthiophene) **7.9**; B) polymer attached undoped CNTs **7.5**; C) polymer attached N-CNT **7.6**.

Table **7.3** Summary of the Photoluminescence and UV-visible spectra maximum in THF.

Sample	Photoluminescence Max centered (nm)	UV-visible max centered (nm)
7.9	574	276, 428
7.5	577	276, 431, 585
7.6	578	276, 435, 603, 771

7.3.4 Thermal analysis

7.3.4.1 Thermogravimentric analysis (TGA)

TGA of the samples was performed under air for the polymers prepared in this chapter (see Figures **7.11** and **7.12a** and **b**). Functionalized CNTs display two stages of thermal decomposition at ~ 200 and 494, and 250 and 516 ^{o}C for **7.2** and **7.4**, respectively (see Figure **7.11**). During the first decomposition reaction 5 and 37 % mass losses were recorded for **7.2** and **7.4** respectively. These results indicated that N-CNTs were more functionalized than the undoped CNTs. Similar results were recorded for functionalized N-CNTs and undoped CNTs in Chapter 5 (see Chapter 6, Section *6.3.4.4*).

The TGA profiles of **7.5, 7.6** and **7.9** were all similar (see Figure 6.12a). Polymer **7.9** underwent a single stage of decomposition at 330 ^{o}C, while **7.5** and **7.6** decomposed at lower temperatures of 252 and 262 ^{o}C.

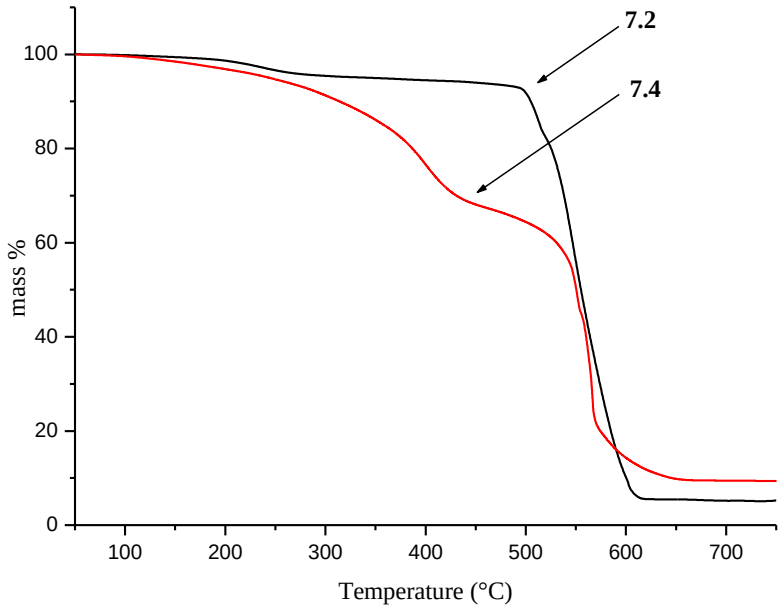

Figure **7.11** TGA profile of functionalized CNTs **7.2** and **7.4**.

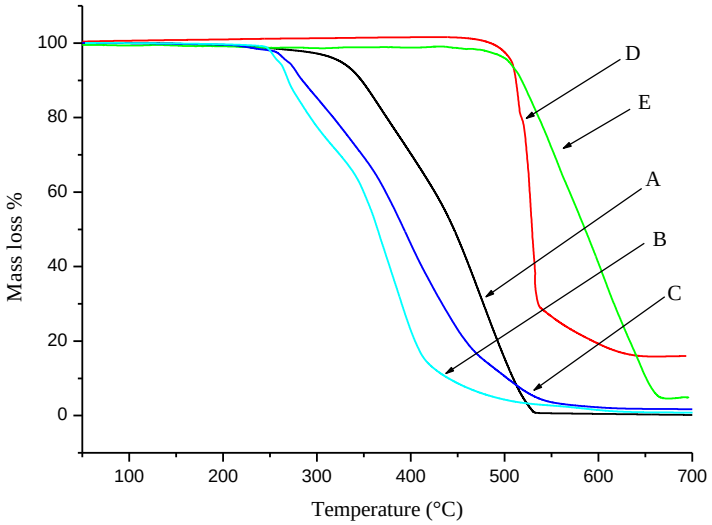

Figure **7.12a** TGA profile of A) poly(3-hexylthiophene) **7.9**; B) polymer attached undoped CNTs **7.5**; C) polymer attached N-doped CNTs **7.6**; D) unfunctionalized undoped CNTs **7.1**; E) unfunctionalized N-doped CNTs **7.3**.

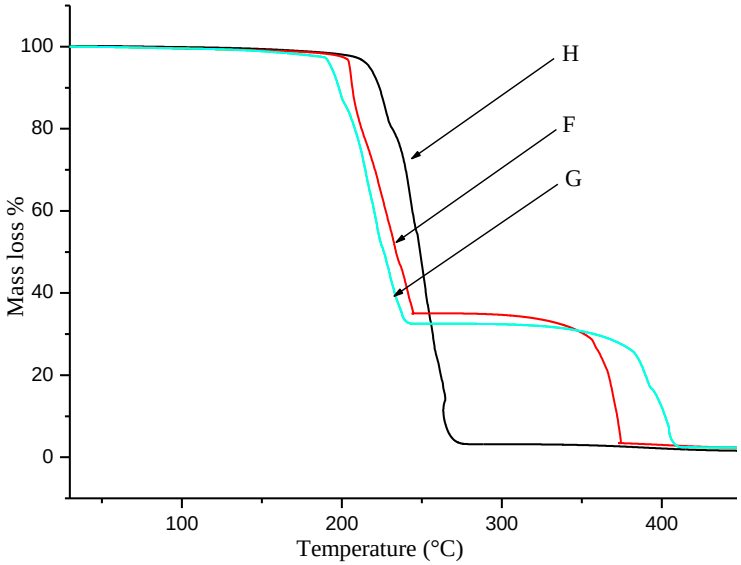

Figure **7.12 b** TGA profile of F) polymer attached N-CNTs **7.7**; G) polymer attached undoped CNTs **7.8**; H) polythiophene **7.10**.

For **7.5** the first decomposition was at 263 ^{o}C; however the second decomposition could not precisely be identified. Similarly for **7.6**, the first thermal decomposition was at 263 ^{o}C. The second thermal decomposition was recorded at 350 ^{o}C (33 % of mass loss).

In the case of copolymers formed from unsubstituted thiophene monomer, the TGA profiles revealed that the first decomposition reactions were found to be generally occurred at a lower temperature than observed for the substituted thiophenes. The first decomposition temperature for the copolymer **7.8** was approximately at ~ 190 ^{o}C, while for **7.7** and polythiophene the values were 204 and 215 ^{o}C, respectively (Figure **7.12b**). During the first stage of decomposition 66, 70, and 100 % mass losses were recorded for **7.7**, **7.8** and polythiophene (**7.10**), respectively. The second decomposition temperatures were noted at ~ 356 and 383 ^{o}C for **7.7** and **7.8**, respectively.

7.3.4.2 Differential scanning calorimetry studies

The glass transition (Tg) temperature measurements of the polymers synthesized were performed under a dynamic nitrogen flow in all cases. From the Differential Scanning Calorimetry (DSC) measurements, the Tg value were taken as the midpoint of the transition region (see Figure **6.13**).

DSC scans for **7.7**, **7.8** and **7.10** did not give results that correlated with their structure. All the polymers synthesized from 3-hexylthiophene showed a single Tg, indicating the absence of a mixture of homopolymers or the formation of a block copolymer [49]. The Tg of pure poly(3-hexylthiophene) **7.9** was found to be at 137 ^{o}C and for the polymer attached to carbon nanotubes the Tg occurred at 150 ^{o}C and 154 ^{o}C for **7.5** and **7.6**, respectively. Increases in Tg due to the incorporation of both N-doped and undoped CNTs indicates a decrease in the chain mobility of the polymer. This result is contrary to those recently reported by Gao *et al*. [50].No explanation for this founding can be suggested at present.

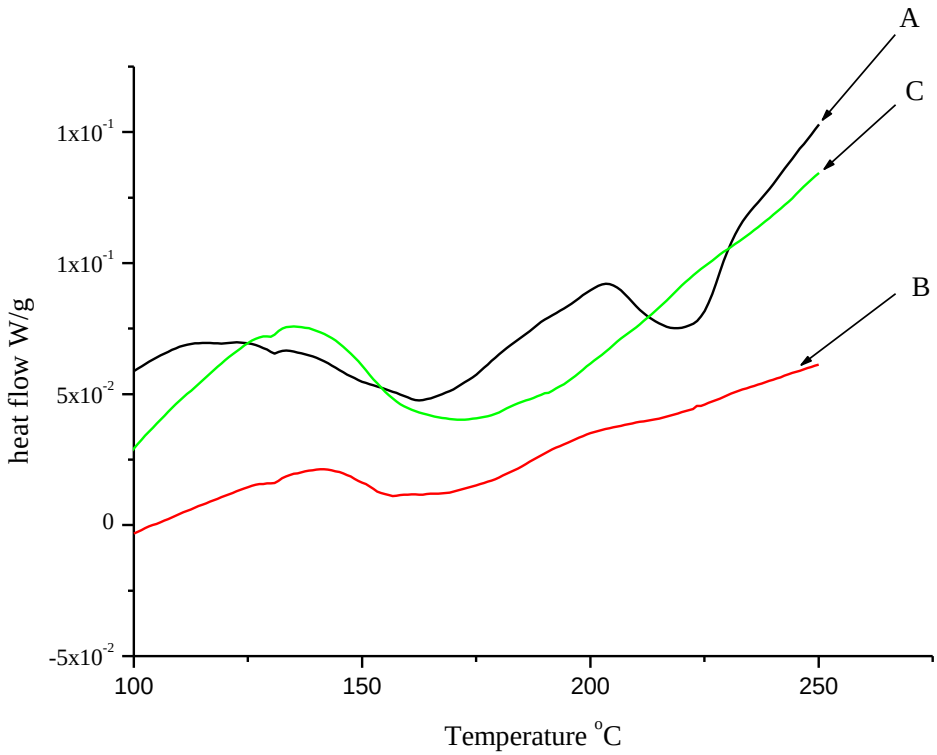

Figure **7.13** DSC scan of the synthesized of A) poly(3-hexylthiophene) **7.9**; B) polymer attached undoped CNTs **7.5**; C) polymer attached N-CNTs **7.6**.

7.4 Conclusions

Undoped CNTs were synthesized by the decomposition of acetylene at high temperature. The nitrogen doped CNTs (3.4 %) were synthesized by the floating catalyst methodology using ferrocene as a catalyst, pyridine as a source of nitrogen and toluene as the carbon sources. Attachment of organic functional groups on the side wall of the carbon nanotubes was achieved through a 1,3-dipolar cycloaddition reaction by forming pyrrolidine fused rings on the side wall of the CNTs. TEM images and Raman spectra were used to confirm that the organic groups were attached to the side wall of the carbon nanotubes. Further covalent attachment of the thiophene backbone was then accomplished by a $FeCl_3$ mediated oxidative polymerization. A high HT/HH ratio was noted after incorporation of CNT into the copolymers and the copolymers **7.5** and **7.6**

were found to be more regioregular than pure poly(3-hexylthiophene) **7.9**. Finally an increase in the Tg of the copolymers was observed as the CNTs were incorporated into the copolymers.

7.5 References

1 S. Iijima, *Nature*, **1991**, 56, 354.

2 T. W. Ebbesen, H. J. Lezec, H. Hiura, J. W. Bennett, H. F. Ghaemi, T. Thio, *Nature*, **1996**, 382, 54.

3 N. H. Tai, M. K. Yeh, J. H. Liu, *Carbon*, **2004**, 42, 2774.

4 Z. H. Gan, Q. Zhao, Z. H. N. Gu, Q. K. Zhuang, *Anal. Chim. Acta*, **2004**, 511, 239.

5 S. Saito, *Science,* **1997**, 278, 77.

6 M. Terrones, N. Grobert, H. Terrones, *Carbon,* **2002**, 40, 1665.

7 Y. Miyamoto, M. L. Cohen, S. G. Louie, *Solid State Commun*., **1997**, 102, 605.

8 (a) O. Stephan, P. M. Ajayan, C. Colliex, P. Redlich, J. M. Lambert, P. Bernier, P. Lefin, *Science,* **1994**, 266, 1683. (b) L. H. Chan, K. H. Hong, D. Q. Xiao, W. J. Hsieh, S. H. Lai, H. C. Shih, T. C. Lin, F. S. Shieu, K. J. Chen, H. C. Cheng, *Appl. Phys. Lett.*, **2003**, 82, 4334

9 M. Terrones, P. M. Ajayan, F. Banhart, X. Blase, D. L. Carroll, J. C. Charlier, R. Crzerw, B. Foley, N. Grobert, R. Kamalakaran, P. Kohler-Redlich, M. Ruhle, T. Seeger, H. Terrones, *Appl. Phys. A*, **2002**, 74, 355.

10 Y. Huang, J. Gao, R. Liu, *Synth. Met*., **2000**, 113, 251.

11 M. Sennett, E. Welsh, J. B. Wright, *Materials Research Society Symposium Proceedings*, **2002**, 706, 97.

12 X. Gong, J. Liu, S. Baskaran, R. D. Voise, J. S. Young, *Chem. Mater.*, **2000**, 12, 1049.

13 V. Georgakilas, K. Kordatos, M. Prato, D. M. Guldi, M. Hoizinger, A. Hirsch, *J. Am. Chem. Soc.*, **2002**, 124, 760.

14 Z. Tang, H. Xu, *Macromolecules*, **1999**, 32, 2569.

15 O. A. Williams, M. D. Whitfield, R. B. Jackman, J. S. Foord, J. E. Butler, C. E. Nebel, *Appl. Phys. Lett.*, **2001**, 78, 3460.

16 B. Kleinsorge, A. C. Ferrari, J. Robertson, W. I. Milne, *J. Appl. Phys.*, **2000**, 88, 1149.

17 (a) J. Chen, A. M. Rao, S. Lyuksyutov, M. E. Itkis, M. A. Hamon, H. Hu, R. W. Cohn, P. C. Eklund, D. T. Colbert, R. E. Smalley, R. C. Haddon, *J. Phys. Chem. B*, **2001**, 105, 2525. (b) J. E. Riggs, Z. Guo, D. L. Carroll, Y.-P. Sun, *J. Am. Chem. Soc.*, **2000**, 122, 5879. (c) J. E. Riggs, D. B. Walker, D. L. Carroll, Y.-P. Sun, *J. Phys. Chem. B*, **2000**, 104, 7071. (d) L. J. Bahr, J. M. Tour, *Chem. Mater.*, **2001**, 13, 3823. (e) S. Pekker, J.-P. Salvetata, E. Jakab, J.-

M. Bonard, L. Forro, *J. Phys. Chem. B*, **2001**, 105, 7938. (f) E. T. Michelson, C. B. Huffman, A. G. Rinzler, R. E. Smalley, R. H. Hauge, J. L. Margrave, *Chem. Phys. Lett.*, **1998**, 296, 188. (g) J. Liu, A. G. Rinzler, H. Dai, J. H. Hafner, R. K. Bradley, P. J. Boul, A. Lu, T. Iverson, K. Shelimov, C. B. Huffman, F. Rodriguez-Macias, Y. S. Shon, T. R. Lee, D. T. Colbert, R. E. Smalley, *Science*, **1998**, 280, 1253. (h) M. A. Hamon, H. Hu, P. Bhowmik, S. Niyogi, B. Zhao, M. E. Itkis, R. C. Haddon, *Chem. Phys. Lett.*, **2001**, 347, 8.

18 V. Georgakilas, K. Kordatos, M. Prato, D. M. Guldi, M. Holzinger, A. Hirsch, *J. Am. Chem. Soc.*, **2002**, 124, 760.

19 E. Kymakis, G. A. J. Amaratunga, *Appl. Phys. Lett.*, **2002,** 80, 112.

20 D. B. Romero, M. Carrard, W. de Heer, L. Zuppiroli, *Adv. Mater*., **1996**, 8, 899.

21 K. Yoshino, H. Kajii, H. Araki, T. Sonoda, H. Take, S. Lee, *Full. Sci. Tech*., **1999**, 695.

22 H. Ago, M. S. P. Shaffer, D. S. Ginger, A. H. Windle, R. H. Friend, *Phys. Rev. B*, **2000**, 61 2286.

23 S. B. Lee, T. Katayama, H. Kajii, H. Araki, K. Yoshino, *Synth. Met*., **2001**, 121, 1591.

24 H. S. Woo, R. Czerw, S. Webster, D. L. Carroll, J. W. Park, J. H. Lee, *Synth. Met.*, **2001**, 116, 369.

25 L. M. Dai, A. W. H. Mau, *Adv. Mater*., **2001**, 13, 899.

26 H. Ago, K. Pettrish, M. S. P. Shaffer, A. H. Windle, R. H. Friend, *Adv. Mater.*, **1999**, 11 1281.

27 E. Kumakis, G. A. J. Amaratunga, *Appl. Phys. Lett*., **2002**, 80, 112.

28 E. Kumakis, I. Alexandrou, G. A. J. Amaratunga, *J. Appl. Phys*., **2003**, 93, 1764.

29 B. J. Landi, R. P. Raffaelle, S. L. Castro, S. G. Bailey, *Prog. Photovolt: Res. Appl.*, **2005**, 13 165.

30 E. Kumakis, G. A. J. Amaratunga, *Sol. Energ. Mater. Sol. Cells*, **2003**, 80, 465.

31 M. H.-C. Jin, L. Dai, in "*Organic Photovoltaics: Mechanisms, Materials and Devices*" (S.-S. Sun and N. S. Sariciftci, Ed.), pp. 579–598, Taylor & Francis, Boca Raton, London, **2005**.

32 B. Pradhan, S. K. Batabyal, A. J. Pal, *Appl. Phys. Lett*., **2006,** 88, 093106.

33 R. Ulbricht, X. Jiang, S. Lee, K. Inoue, M. Zhang, S. Fang, R. Baughman, A. Zakhidov, *Phys. Stat. Sol., B*, **2006**, 13, 243.

34 M. Reyes-Reyes, R. Lopez-Sandoval, J. Liu, D. L. Carroll, *Sol. Energ. Mater. Sol. Cells*, **2007**, 91, 1478.

35 R. Sugimoto, S. Takeda, H. B. Gu, K. Yoshino, *Chem. Express*, **1986**, 1, 635.

36 T.-A. Chan, X. Wu, R. D. Rieke, *J. Am. Chem. Soc.,* **1995**, 117, 233.

37 F. Andreani, E. Salatelli, M. Lanzi, F. Bertinelli, A. M. Fichera, M. Gazzano, *Polymer*, **2000**, 41, 3147.

38 R. K. Singh, J. Kumar, R. Singh, R. Kant, S. Chan, V. Kumar, *Materials Chem. Phy.,* **2007,** 104, 390.

39 M. R. Karim, K. T. Lim, C. J. Lee, M. S. Lee, *Synth. Met*., **2007**, 157, 1008.

40 R. Czrew, M. Terrons, J. C. Charlier, X. Blase, B. Foley, R. Kamalakaran, N. Grobert, H. Terrones, D. Tekleab, P. M. Ajayan, W. Blau, M. Ruehle, D. L. Carroll, *Nano Lett*., **2001**, 1, 457.

41 M. Leclerc, F. M. Diaz, G. Wegner, *Makromol. Chem*., **1989**, 190, 3105.

42 R. M. S. Maior, K. Hinkelmann, H. Eckert, F. Wudl, *Macromolecules,* **1990**, 23, 1268.

43 (a) M.-A. Sato, H. Morii, *Macromolecules,* **1991**, 24, 1196. (b) M.-A. Sato, H. Morii, *Polym. Commun.*, **1991**, 32, 42. (c) G. Barbarella, A. Bongini, M. Zambianchi, *Macromolecules*, **1994**, 27, 3039.

44 Y.-P. Sun, W. Huang, Y. Lin, K. Fu, A. Kitaygorodskiy, L. A. Riddle, Y. J. Yu, D. L. Carroll, *Chem. Mater*., **2001**, 13, 2864.

45 V. Saini, Z. Li, S. Bourdo, E. Dervishi, Y. Xu, X. Ma, V. P. Kunets, G. J. Salamo, T. Viswanathan, A. R. Biris, D. Saini, A. S. Biris, *J. Phys. Chem. C,* **2009,** 113, 8023.

46 S. Hotta, S. D. D. V. Rughooputh, A. J. Heeger, F. Wudl, *Macromolecules*, **1987**, 20, 212.

47 B. K. Kuila, S. Malik, S. K. Batabyal, A. K. Nandi, *Macromolecules*, **2007**, 40, 278.

48 (a) B. K. Kuila, A. K. Nandi, *Macromolecules,* **2004**, 37, 8577. (b) B. K. Kuila, A. K. Nandi, *J. Phys. Chem. B*, **2006**, 110, 1621.

49 A. Delibas, C. Soykan, *J. Appl. Poly. Sci.*, **2008**, 104, 364.

50 Y. Gao, Y. Wang, J. Shi, H. Bai, B. Song, *Polymer testing*, **2008**, 27, 179.

Chapter 8

Application of 3-hexylthiophene functionalized C_{60} and carbon nanotubes in solar cells

8.1 Introduction

Diamond and graphite have long been the only known forms of carbon, thus the unexpected discovery of fullerene, a new carbon allotrope, has fascinated the scientific community. Indeed since the discovery of C_{60}, intensive research activities have been focused on the properties of fullerenes [1]. As a result, novel properties associated with functionalized fullerenes that have been reported by various researchers include superconductivity, ferromagnetism, and optical nonlinearity [2]. The synthesis of fullerene containing polymers has also been of interest from the viewpoint of both basic research and practical applications and these novel polymers could contribute to the development of processable fullerene-based specialty materials [3].

The interaction of C_{60} with photons has also attracted considerable interest and numerous research articles have reported on the exploration of applications related to photophysical, photochemical and photoinduced charge transfer properties of C_{60}-derivatives. The unique electrochemical properties of fullerene with six reversible single-electron reduction waves [4], and its photophysical properties [5], make C_{60} and its derivatives interesting complexes to study photo-driven redox phenomena. Photoinduced electron and energy transfer processes are of great significance and a large number of studies have reported on the construction of C_{60}-based molecular structures as artificial photosynthetic systems [6].

The use of electron-accepting fullerenes in combination with π-conjugated systems, as sacrificial electron donors, offers several attractive features. In particular, fullerene, due to its low reorganization energy in electron-transfer reactions, accelerates charge separation and decelerates charge recombination, compared to two dimensional, planar electron acceptors [7]. This is beneficial for stabilizing the charge-separated state in C_{60}-based materials, as required in

artificial electron transfer systems. Sariciftci *et al.* [8] demonstrated that a *n*-conjugated polymer was able to efficiently transfer electrons to a C_{60} core giving rise to long-lived charge-separated states. Since then, intensive research programs have focused on the utilization of fullerene derivatives acting as electron acceptors in both organic and dye sensitized solar cells.

In typical organic solar cells, the solid-state heterojunctions consist of p-type donor (D) and n-type acceptor (A) semiconductors. Organic C_{60}-based solar cells can be fabricated by inserting (or sandwiching) the p-type and n-type materials between two different electrodes. One of the electrodes must be (semi-) transparent; the electrode is often indium tin oxide (ITO), but a thin metal layer can also be used.

In donor-acceptor-linked molecules, the fullerene acts as an electron acceptor and the donor can be made of dyad molecules such as aniline [9], carotenoid [10], porphyrin [10b,11,12], pyrazine [13], or tetrathiophene [14]. In these molecules, the quantum yields of the charge-separation processes were close to unity and the lifetimes of the charge-separated states were on the order of sub nanoseconds. Imahori *et al*. [12b] reported that the reorganization energy of the dyad molecule, including the fullerene acceptor, is small compared with other reported electron acceptors. This feature has been one of the advantages of the fullerene-containing dyad molecules, the use of which is aimed at attaining a long-lived charge-separated state with high quantum yield for application in energy-storage systems or other sensitized reactions. As for the donor moiety of the dyad molecule, several candidates have been proposed, in addition to those listed above, because many examples of photoinduced electron transfer reactions between fullerene and donors have been reported [15-18].

The application of carbon nanotubes in both organic and dye sensitized solar cells have been investigated. A bulk heterojunction solar cell based on conjugated polymers blended with multi-walled carbon nanotubes (MWNTs) [19] and single-walled carbon nanotubes (SWNTs) [20-22] has been reported. For 1 % SWNT/ poly-3-octylthiophene (P3OT) bulk heterojunction solar cells, high values of Voc (0.75 V) were achieved and this was reasonably well explained in terms of the HOMO–LUMO electronic structures of P3OT and SWNTs [21].

MWNTs exhibit metallic or semiconducting properties, which depend solely on their outermost shell. On account of the large number of concentric cylindrical graphitic tubes present in MWNTs, they are considered even more suitable in electron-donor–acceptor ensembles than SWCNTs [23].

In dye sensitized solar cells (DSSC), the maximum current density is determined by how well the absorption window of the dye overlaps the solar spectrum. The poor absorption of low-energy photons by many dyes is consistent with the low performance of the cells. As a result, considerable effort has been made to develop dyes and dye mixtures that absorb better at long wavelengths [24-26].

In this study we report on the photovoltaic performance of both DSSC and organic solar cells. Cells with different concentrations of derivatized C_{60} in C_{60}-poly(3-hexylthiophene) mixtures were studied. The poly(3-hexylthiophene) was attached to both N-doped and undoped carbon nanotubes with and without ruthenium dye impregnated TiO_2, and those mixtures were then investigated. In addition to this, the effects on the solar cells, of physically mixing the copolymers with TiO_2 prior to deposition on the dye impregnated TiO_2 was also investigated.

8.2 Experimental

8.2.1 Assembly of the DSSC

TiO_2 nanoparticles powder (3.0 g, Degussa P25), acetylacetone (0.10 mL), polyethylene glycol (1.2062 g, F.W. 20,000), distilled water (5 mL) and Triton X-100 (0.025 mL) were added into a mortar and ground to form a slurry. The mixture was then transferred to a container with a tight stopper and left to stir for 48 h at r.t. A TiO_2 nanoporous film was prepared from the mixture by a doctor blading technique, by spreading the slurry onto SnO_2:F conducting glass (FTO, fluorine-doped SnO_2, sheet resistance 8-10 Ω/cm^2, Hartford Glass Co.). After the substrate was allowed to dry at r.t., it was heated to 450 ^oC for 30 min and cooled down to r.t. The TiO_2 thin film electrode was then immersed in a 1.5×10^{-3} mol L^{-1} solution of the sensitizer, *cis*-bis(isothiocyanato)bis(2,2'-bipyridyl-4,4'-dicarboxylate)-ruthenium(II) (N719) in EtOH for 20 h at r.t.

A liquid electrolyte was prepared from LiI (0.10 mol L^{-1}), I_2 (0.05 mol L^{-1}), tetrabutylammonium iodide (0.80 mol L^{-1}), and 4-tertbutylpyridine (0.50 mol L^{-1}) in 50 % acetonitrile–50 % 3-methoxypropionitrile.

The copolymers, with and without TiO_2, were suspended in chlorobenzene and stirred at r.t. for 48 h. Two drops of the suspension were deposited on the surface, with and without dye impregnated TiO_2. A sandwich-type cell with active area 0.25 cm^2 made from a TiO_2 thin films electrode, with and without a dye was impregnated into an ionic liquid electrolyte. A Pt-coated FTO counter electrode was also prepared.

8.2.2 Assembly of the organic solar cell

A film of poly(3,4-ethylenedioxythiophene):poly(styrenesulfonate) (PEDOT:PSS) solution (Bayer) was spin coated (1500 rpm) on indium-SnO_2 (ITO), followed by heating for 10 min at 120 ^oC in air. A C_{60}-copolymer:P3HT 1:1 mixture (25 mg mL^{-1} in chlorobenzene) was stirred for 3 days at r.t. The solution was then spincoated on PEDOT (acceleration 800 rpm/s, 40 s). The solar cells were fabricated by thermally evaporating and deposited aluminum metal (10^{-6} Torr) on top of the polymer film with 70 nm thickness.

The cell performance characterization was carried out by measuring the current-voltage (*I-V*) characteristics in the dark and under AM 1.5G spectral distribution, which was obtained using a 150 W Oriel solar simulator plus filters. The samples were illuminated through the glass substrate, and the radiance was controlled using neutral filters. The radiance was determined using a calibrated silicon photo-detector.

8.3 Results and discussion

8.3.1 Synthesis of the copolymers

Prato [27] has developed a powerful procedure for the functionalization of C_{60}. The Prato reagent is made by adding an aldehyde and a glycine to C_{60}. The reagents form azomethine ylides at high temperature that react by way of a 1,3 dipolar cycloaddition with C_{60}, to give functionalized fullerenes. The same method has also been used by Georgakilas *et al*. [28] to functionalise CNTs. This procedure allows the synthesis of a wide range of substituted fullerenes and CNTs by variation of the aldehyde and glycine functional groups.

This procedure was used to make variants of the Prato reagent by specifically mixing C_{60} with 3-thiophenecarboxaldehyde and *N*-methylglycine. The reaction gave the product **5.3,** a thiophene containing moiety covalently bonded to C_{60}. Complex **5.3** was reacted with 3-hexylthiophene by using a varied 2:3-hexylthiophene ratio [1:10 (**5.3a**), 1:500 (**5.3b**) and 1:1000 (**5.3c**)] in the presence of $FeCl_3$. Similarly a reaction between either **7.1** or **7.3** and the Prato reagent gave products **7.2** and **7.4**. Polymerization was achieved by varying the ratio of either **7.2** or **7.4** to 3-hexylthiophene (**7.d**) (1:20) in the presence of $FeCl_3$ to give either **7.5** or **7.6** (Scheme **8.1** and **8.3**; see details in Chapters 5 and 7 section *7.3.1*).

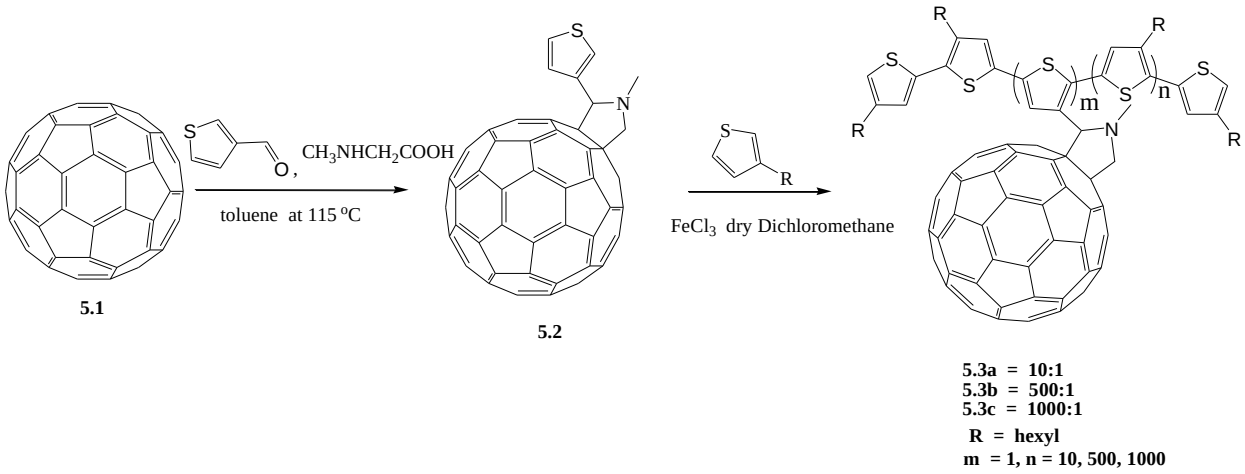

Scheme **8.1** Functionalization and polymerization methodology used for the synthesis of C_{60}-copolymers.

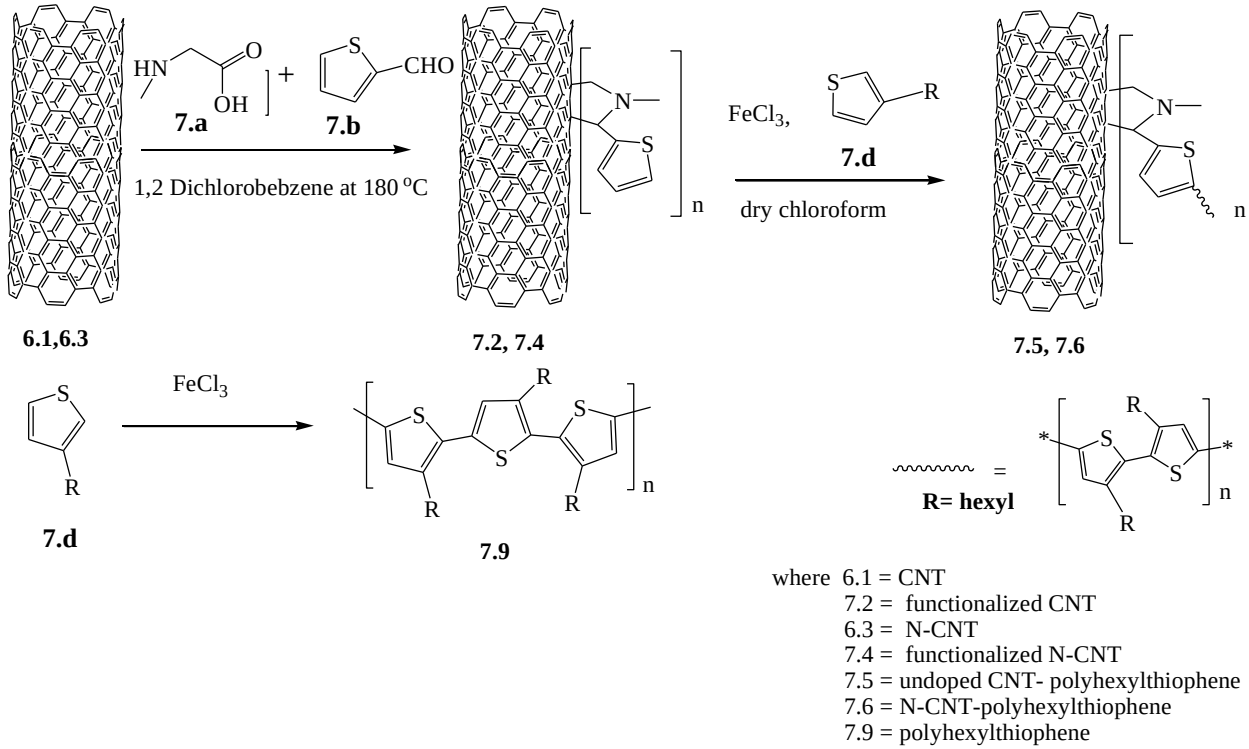

Scheme **8.2.** Functionalization and polymerization methodology used for the synthesis of polymer-carbon nanotube copolymers.

8.3.2 Application of copolymers in dye-sensitized solar cells (DSSCs)

8.3.2.1 Current-Voltage Characteristics

8.3.2.1.1 C_{60}-copolymers 5.3a, 5.3b and 5.3c in DSSC

The charge recombination between conduction band electrons of TiO_2 and triiodide ions, I_3^-, of the electrolyte decreases the open-circuit voltage (*V*oc) of a dye-sensitized solar cell (DSSC). In order to reduce the recombination, attempts have been made to introduce a metal oxide blocking layer on a TiO_2 surface [29] this was achieved by using a composite semiconductor oxide film of TiO_2 and SiO_2, Al_2O_3, or ZrO_2 [30] that form an insulating film of poly(methylsiloxane) on parts of the TiO_2 [31], or by attaching long alkyl chains to the bipyridine rings of ruthenium dyes [32]. Lim *et al*. [33] were the first to incorporate C_{60} into a DSSC with a ruthenium dye as the sensitizer. In this particular study, C_{60} was covalently linked to the N3 dye [*cis*-bis(4,4'-dicarboxy-2,2'-bipyridine)dithiocyanate ruthenium(II)] via diaminohydrocarbon linkers with different carbon chain lengths. A device was prepared by dipping a TiO_2 film into a solution of the modified dye. The authors [33] made the claim that the short-circuit photocurrent density (*J*sc) of the dye-sensitized solar cells (DSSCs) using the fullerene-attached sensitizers varied markedly with on the chain length of the linker this may be correlated with the amount of total sensitizer adsorbed on the surface of the TiO_2 film, which was determined by absorption spectra for each TiO_2 film with a relatively large area. For example, for the linker 1,6-diaminohexane, the *J*sc, *V*oc and conversion efficiency of the pertaining cell were 11.75 mA cm^{-2}, 0.70 V and 4.5 %, respectively, as against the values of 10.55 mA cm^{-2}, 0.68 V and 4.0 %, respectively, for a DSSC containing ordinary N3 dye.

The photoelectrochemical cells used in this study were assembled using the previously prepared C_{60}-copolymers **5.3a-c** and TiO_2 nanoparticles mixtures. The copolymers **5.3a-c** and TiO_2 were mixed in a 1:1 mass ratio in chlorobenzene and two drops of the suspension were deposited on the surface of the TiO_2-FTO glass. The architecture of this device is shown in Figure **8.1a**. The cartoon, Figure **8.1b**, (not to scale) shows the mixture of the C_{60}-copolymers mixed with TiO_2 nanoparticles deposited on the surface of the TiO_2 pasted FTO glass. The overall thickness on top of the FTO glass was measured to be about 6 µm.

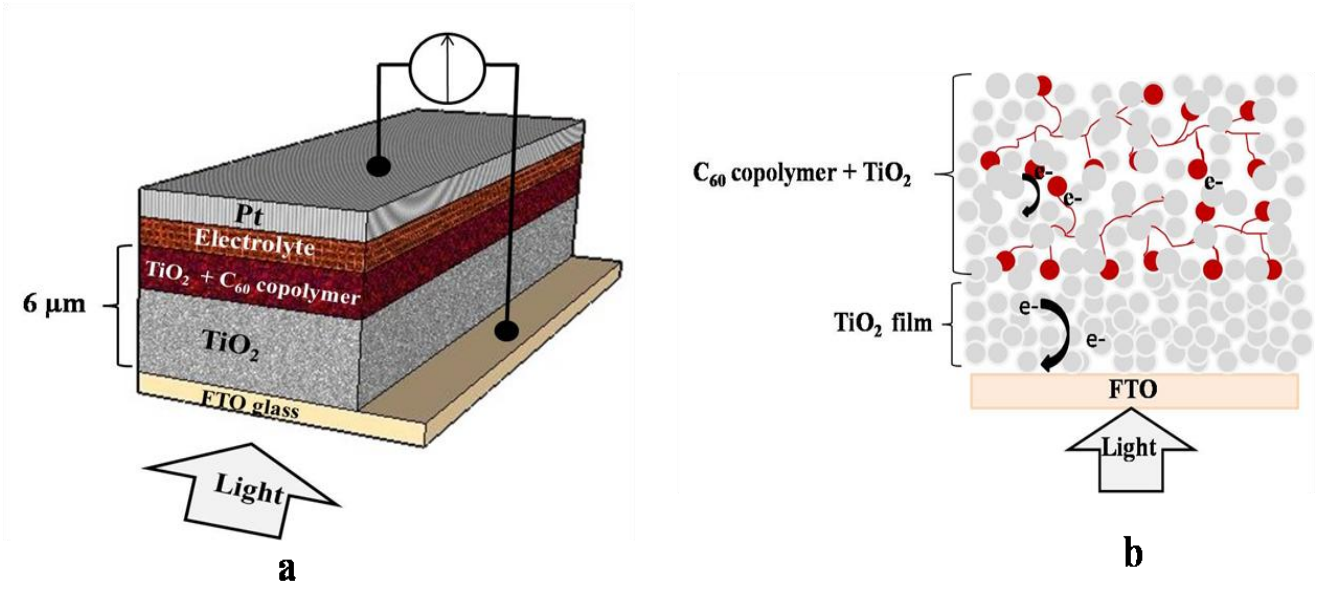

Figure **8.1**. Schematic representation of: (a) a DSSC with the FTO/TiO_2/C_{60}-containing copolymer +TiO_2/ electrolyte/Pt; (b) microscopic representation of the TiO_2 and C_{60}-copolymer interaction on FTO glass. (Note: the representations are not drawn to scale.)

Figure **8.2** shows the current voltage (I-V) curves for the devices assembled with **5.3a-c**. The current density appears to be dependent on the concentration of C_{60} in the copolymers, following the order **5.3a** (0.9 mA cm^{-2}) > **5.3b** (0.6 mA cm^{-2}) > **5.3c** (0.5 mA cm^{-2}). The C_{60} in such devices is thought to act as an electron acceptor for the system [8]. The open circuit voltage values (V_{oc}) were observed to give the same trend, i.e. the sample with more C_{60} moieties was the one that gave rise to the higher photovoltage, with **5.3a** (0.63 V) > **5.3b** (0.57 V) > **5.3c** (0.47 V). The decrease in efficiency (η) could be due to the decrease in the photocurrent density (J_{sc}), the open circuit potential (V_{oc}) or the fill factor (FF) [34]. According to the UV-visible spectra in Figure **5.4**, the copolymer **5.3c** demonstrates higher light absorption than copolymer **5.3a** and it would be expected that copolymers can also absorb light, increasing light-harvesting, and this should improve Jsc. However, the solar cells performed better with copolymer **5.3a**. This might result from a reduction in the recombination effect (from the C_{60} contribution) being more effective than the "dye effect", possibly because the polyhexylthiophene polymer does not have carboxylic groups to chemically attach to the TiO_2 as the sensitizers usually do [35].

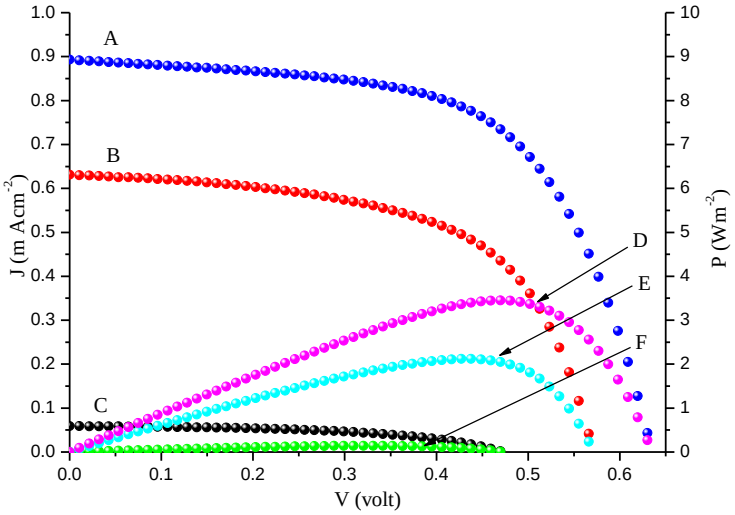

Figure **8.2** DSSC current-voltage curves (100 mW cm^{-2} incident light) for the TiO_2/C_{60}-copolymer + TiO_2/electrolyte/Pt system: A) **5.3a**; B) **5.3b**; C) **5.3c**. Power-voltage curves: D) **5.3a**; E) **5.3b**; F) **5.3c**.

The dark current was measured at 1.9 and 2.6 µA cm^{-2} for the photocells made from the **5.3b** and **5.3c** copolymers, respectively (Figure **8.3**). This implies that, the back-electron-transfer process, corresponding to the reaction between the conduction-band electrons in the TiO_2 and I_3^- ion in the electrolyte under dark condition [36], occurs more easily in the cell based on **5.3c**, than on the **5.3a** copolymers. A predominant back-electron-transfer process would directly act to lower the V_{oc} of cell made from **5.3c** copolymers, compared to the **5.3a** copolymers. The results also confirm that with a higher concentration of C_{60} in the copolymer the photocell behaves like a diode (see Figure **8.3**). This is in agreement with the functionalized C_{60} in the polymer acting to accelerate charge separation and decelerate charge recombination due to the low reorganization energy in the electron-transfer reaction [8,37].

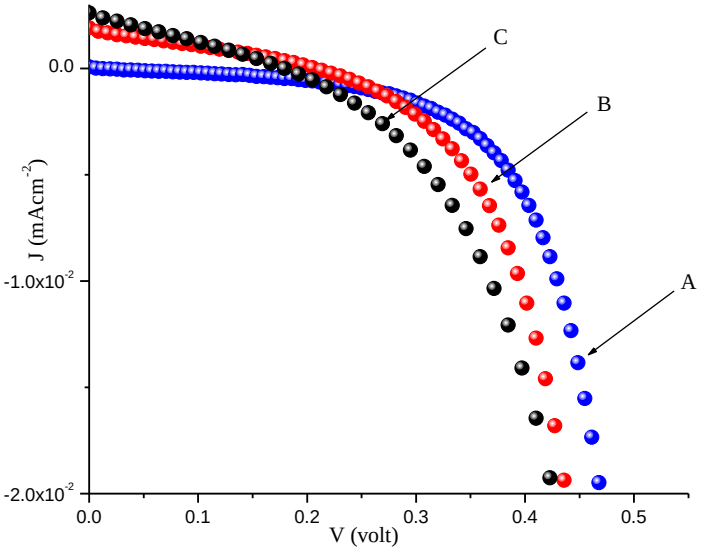

Figure **8.3** DSSC current density vs voltage (vs Pt counter electrode) curves obtained under dark conditions for the cells assembled with A) 10:1 mole ratio (**5.3a**); B) 500:1 mole ratio (**5.3b**) and C) 1000:1 mole ratio (**5.3c**) C_{60}:hexylthiophene copolymer.

Table **8.1** Photovoltaic performance of the DSSCs based on TiO_2/C_{60}-copolymer + TiO_2 /electrolyte/Pt.

Mole ratio of polymer to C_{60}	incident light (P_{in}) (mW cm^{-2})	η (%)	FF	V_{oc} (Volt)	J (mA cm^{-2})	output P_{max} (W m^{-2})
1000:1 (**5.3c**)	100	0.18	0.63	0.59	0. 49	0.15
	10	0.08	0.45	0.45	0.04	
500:1 (**5.3b**)	100	0.21	0.59	0.57	0.63	2.1
	10	0.06	0.46	0.40	0.03	
10:1 (**5.3a**)	100	0.34	0.61	0.63	0.89	3.4
	10	0.27	0.64	0.53	0.08	

A further investigation was performed by incorporating the synthesized copolymers with the well known ruthenium(II) dye N719, [*cis*-bis(isothiocyanato)bis(2,2'-bipyridyl-4,4'-dicarboxylate)-

ruthenium(II)]. The effect of mixing C_{60}-copolymer with TiO_2 nanoparticles was also investigated (Figure **8.4b**).

The schematic diagrams below show devices that were assembled with the 10:1 mole ratio (**5.3a**) copolymer without (in Figure **8.4a**) and with (Figure **8.4b**) TiO_2 mixtures deposited on the surface of dye impregnated TiO_2. The cartoon, figure **8.4c**, (not drawn to scale) shows the mixture of the C_{60}-copolymers with TiO_2 nanoparticles deposited on the surface of dye impregnated TiO_2 pasted FTO glass. The total thickness of the component was measured to be about 6 µm.

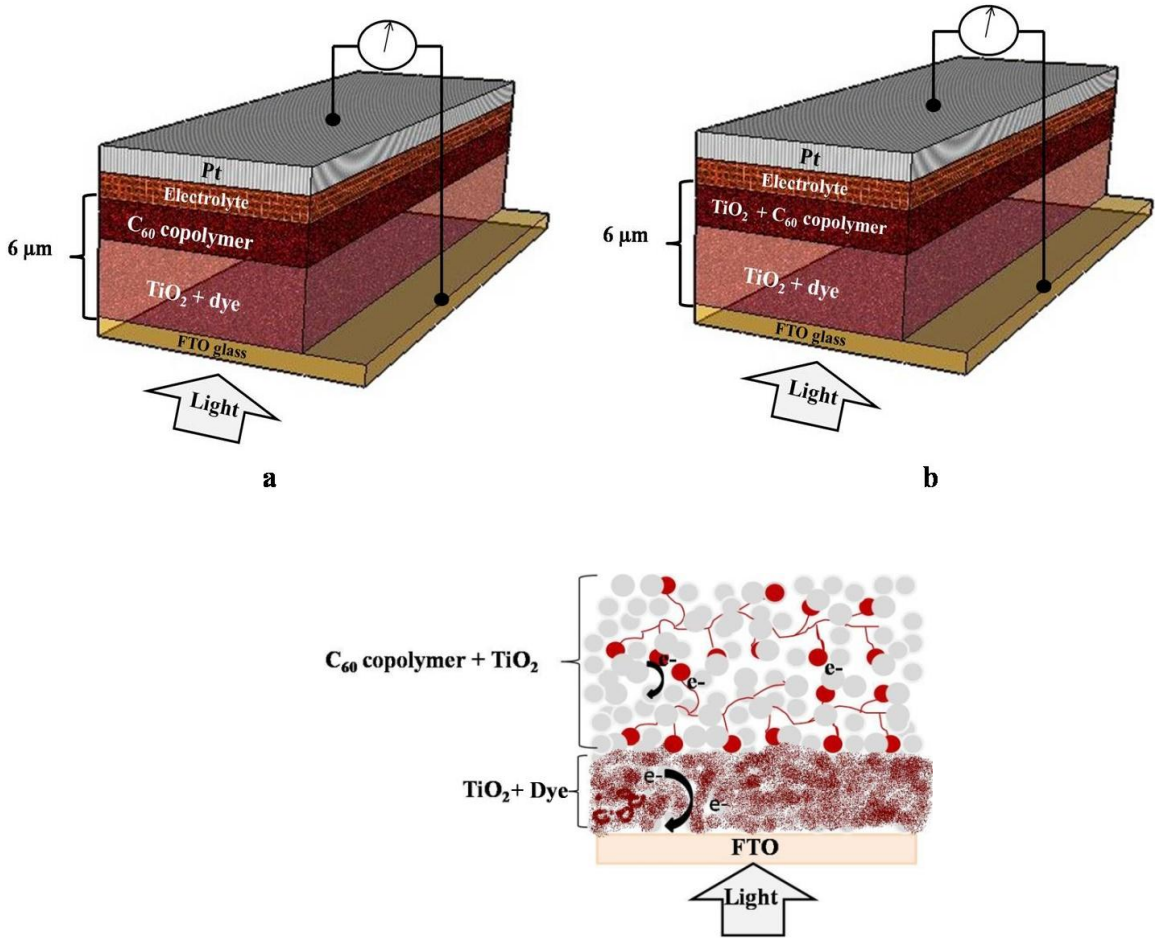

Figure **8.4**. Schematic representation of a DSSC with: a) the glass-FTO/TiO_2/dye/**5.3a** copolymer/electrolyte/Pt; b) the glass-FTO/TiO_2/dye/**5.3a** copolymer + TiO_2/electrolyte/Pt; c)

microscopic representation of the TiO_2+dye and **5.3a** copolymer + TiO_2 interaction on FTO glass. (Note: the schematic representations are not drawn to scale.)

The results from the current–voltage measurements showed that the current density and the V_{oc} of the TiO_2 mixed sample (**B**) increased as compared to the sample without TiO_2 (**A**) (see figure **8.5**). This might be due to the mixing of the copolymers with the TiO_2 nanoparticles creating better contacts between the C_{60}-copolymer molecules and the electron transporter TiO_2 nanoparticles. In other words, electrons from an electron acceptor, C_{60}, are transported to the TiO_2 more readily. In both cases, **A** and **B**, the addition of C_{60}-copolymer to the dye impregnated TiO_2 enhanced the overall performance of the cell as compared to the solar cell that had been assembled without the C_{60}-copolymer (**C**).

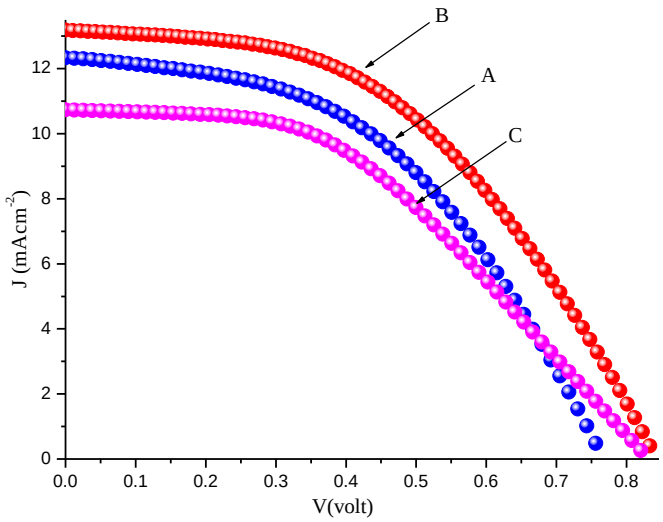

Figure **8.5**. DSSC current-voltage curves (100 mW cm^{-2} incident light): A) **5.3a** copolymer without TiO_2; B) **5.3a** copolymer with TiO_2; C) only with N719 dye.

The current–voltage curves under dark conditions were also measured for photocells made from a **5.3a** copolymer with and without TiO_2 nanoparticles. According to the results, the photo cell made with TiO_2 (**A**) showed more diodic behavior than the sample without TiO_2 (**B**) (see Figure **8.6**).

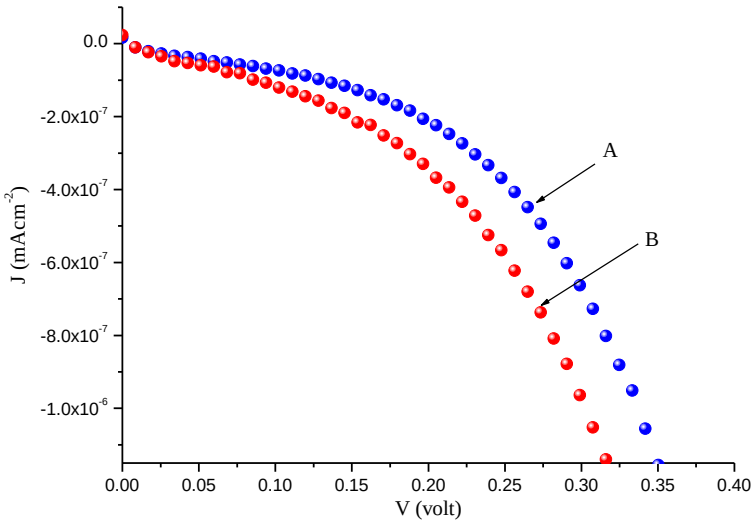

Figure **8.6** Current density - voltage (I-V) curves obtained under dark conditions with DSSCs based on **5.3a** copolymer: A) mixed with TiO_2; B) without TiO_2.

The concentration of the C_{60} derivatives in the copolymer mixed with TiO_2 nanoparticles was also investigated. As shown in Figure **8.7** and Table **8.2,** the concentration of the C_{60}-derivatives in the copolymer has pronounced effects on the current densities and V_{oc}. The increase in the amount of functionalized C_{60} in the sample led to an increase in the efficiency of the cell; 5.2 % for the **5.3a** as compared to 2.1 % for the **5.3c** (100 mW cm^{-2} light intensity). This would suggest that a high concentration of C_{60} in the copolymer creates less chance of electron recombination.

The cell efficiency was found to increase at low incident light (Table **8.2**). This is due to the fact that the mechanism of charge transport in the cells includes the diffusion of ionic species in the electrolyte inside the nanoporous TiO_2. Under high incident light radiation a large number of charge carriers would be generated as a result of electrons being injected from the excited dye to the conduction bands of TiO_2 nanoparticles. This process occurs faster than the regeneration of the dye by the electrolyte. This leads to an increase in the recombination of the injected electrons and as a result the short circuit current and efficiency of the cell is reduced [38].

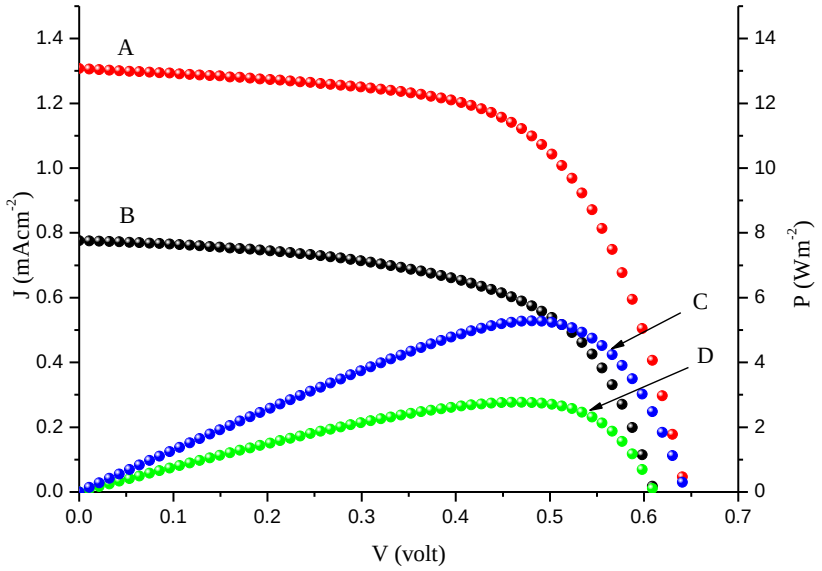

Figure **8.7**. DSSC current-voltage curves (100 mW cm^{-2} incident light) for the TiO_2/dye/C_{60}-copolymer + TiO_2/electrolyte/Pt system: A) **5.3a**; B) **5.3b**; C) **5.3c**. Power-voltage curves are also shown: D) **5.3a**; E) **5.3b**; F) **5.3c**.

At a low concentration of C_{60} in the copolymers the current density and V_{oc} of the cell is suppressed as compared to the results for the solar cell assembled only with N719 dye. Decreases in the open-circuit voltage can be explained as being due to the recombination of photo-injected electrons with I_3^- [29-32].

Table **8.2** Photovoltaic performance of the DSSCs based on glass-FTO/TiO_2/dye/C_{60}-copolymer + TiO_2 /electrolyte/Pt

Sample mole ratio	incident light (P_{in}) ($mWcm^{-2}$)	η (%)	FF	V_{oc} (volt)	J ($mAcm^{-2}$)	Output P_{max} (Wm^{-2})
1000:1 **(5.3c)**	100	2.1	0.58	0.72	5,0	21.2
	10	1.6	0.61	0.61	0.43	
500:1 (**5.3b**)	100	2.7	0.56	0.74	6.5	27.6
	10	2.1	0.66	0.64	0.5	
10:1 (**5.3a**)	100	5.2	0.47	0.84	13.18	52.2
	10	6.8	0.70	0.76	1.28	
Only N719 dye	100	3.9	0.44	0.83	10.7	39.0
	10	5.0	0.86	0.74	1.0	

Finally, the current–voltage curves under dark conditions, indicate that the photocell made from the **5.3a** copolymer with TiO_2 nanoparticles (A) exhibits a less pronounced dark current than the **5.3b** (B) and **5.3c** (C) copolymers (see Figure **8.8**).

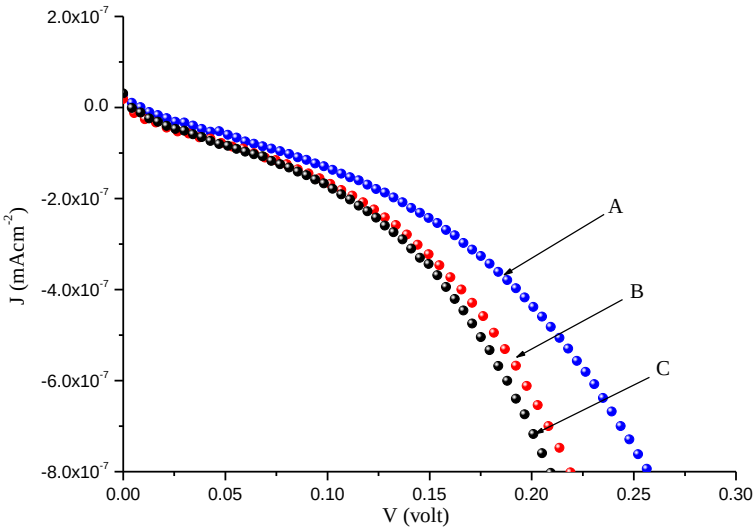

Figure **8.8.** DSSC current-voltage curves generated under dark conditions for the cells made from TiO_2/dye/C_{60} copolymer + TiO_2/electrolyte/Pt system: (A) 10:1 mole ratio (**5.3a**); (B) 500:1 mole ratio (**5.3b**); (C) 1000:1 mole ratio (**5.3c**).

8.3.2.1.2 Solar cell assembled with functionalized carbon nanotubes

The incorporation of CNTs, either functionalized or pristine into conjugated polymers in photocells has been reported by various groups [19-21] and the performance of the cells was found to increase when functionalized CNTs were used [39,40]. Kumakis *et al.* [20] have proposed that the photovoltaic response of their devices was based on the introduction of internal polymer/nanotube junctions within the polymer matrix. This is due to a photoinduced electron transfer from the polymer to the nanotube that contributed to enhanced charge separation and collection.

The photocells assembled in this study were assembled with N-doped and undoped carbon nanotube-copolymer and TiO_2 nanoparticles mixtures. The N-doped and undoped carbon nanotube-copolymers with TiO_2 were mixed in chlorobenzene to give a 1:1 mass ratio respectively, and two drops of the suspension were deposited on the surface of TiO_2 pasted FTO glass (see Figure **8.9**). As shown in Figure **8.10** and Table **8.3** the current density and V_{oc} of the N-CNT copolymer was found to be higher than the (undoped) CNT copolymer. This might be due to (i) the additional electrons contributed by the nitrogen atoms that can provide electron carriers for the conduction band [23] and or (ii) the creation of a narrower energy gap [23,41].

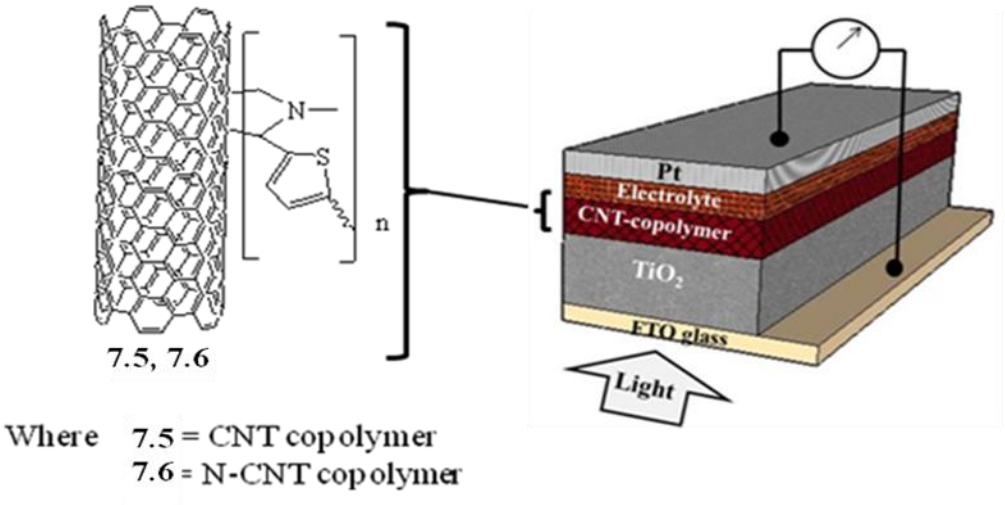

Figure **8.9.** Schematic representation of the DSSC solar cell with the glass-FTO/TiO_2/CNT-copolymer + TiO_2 / electrolyte/ Pt. (Note: the schematic representation is not drawn to scale)

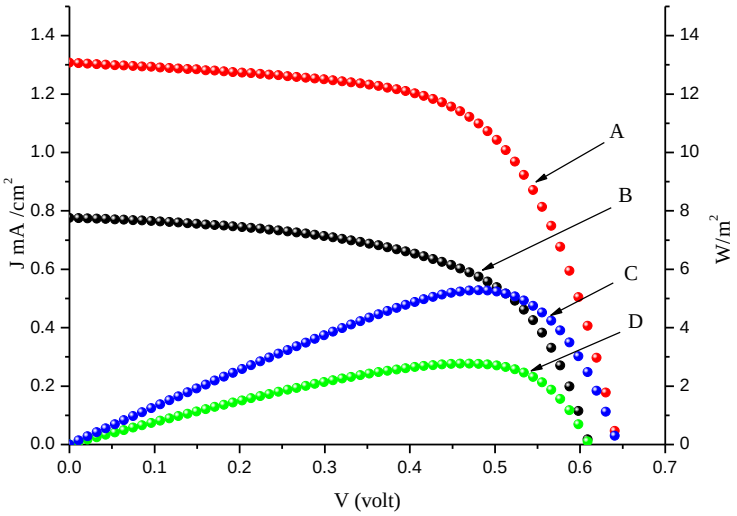

Figure **8.10**. DSSC current-voltage curves (100 mW cm^{-2} incident light) for the TiO_2/CNT-copolymer + TiO_2/ electrolyte/ Pt system: A) N-CNT copolymer **7.6**; B) CNT copolymer **7.5**. Power-voltage curves are also shown: C) N-CNT copolymer **7.6**; D) CNT-copolymer **7.5**.

The current-voltage curves under dark condition showed that the photocell made from CNT-copolymer **7.5** had more diodic behavior than the one made from the N-CNT copolymer **7.6** (see Figure **8.11**). This might be due to the N-doped CNTs showing more metallic behavior than the undoped CNTs since they are narrow energy gap semiconductors [23,41].

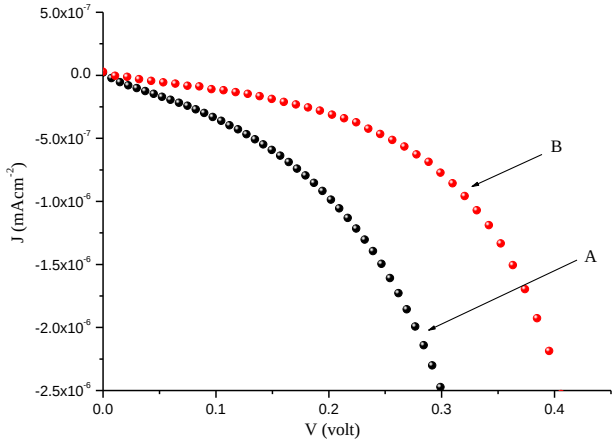

Figure **8.11** Current-voltage curves under condition dark for A) N-CNT copolymer **7.6**; B) CNT copolymer **7.5**.

Table **8.3** Photovoltaic performance of the DSSCs made from glass-FTO/TiO_2/CNT copolymer + TiO_2 /electrolyte/Pt

Sample	incident light (P_{in}) (mW cm^{-2})	η (%)	FF	V_{oc} (Volt)	J (mA cm^{-2})	Output P_{max} (W m^{-2})
N-CNT copolymer **7.6**	100	0.53	0.63	0.64	1.31	5.3
	10	0.39	0.63	0.54	0.11	
CNT copolymer **7.5**	100	0.28	0.59	0.61	0.77	2.8
	10	0.12	0.48	0.45	0.06	

The N-CNT copolymer **7.6** and CNT copolymer **7.5** with TiO_2 were mixed in chlorobenzene to give a 1:1 mass ratio respectively, and two drops of the suspension were deposited on surface of dye impregnated TiO_2 FTO glass (see Figure **8.12** for architectural arrangements). Here, unlike in the previous investigation, incorporation of both carbon nanotube-copolymers with ruthenium dye revealed that the current density and V_{oc} showed better performance for the CNT copolymer (**7.5**) than for the N-CNT copolymer (**7.6**) (see Figure **8.13** and Table **8.4**).

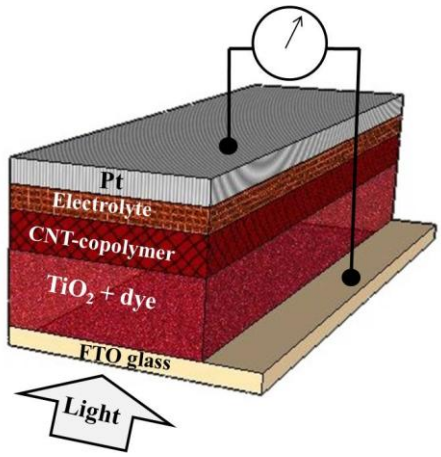

Figure **8.12.** Schematic representation of the DSSC made from glass-FTO/TiO_2/dye/CNT copolymer / electrolyte/ Pt. (the schematic representation is not to scale)

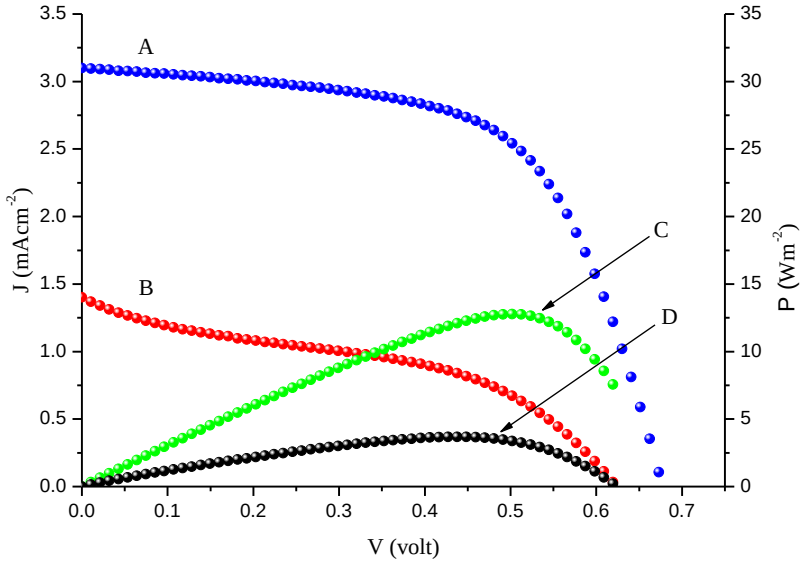

Figure **8.13**. DSSC current-voltage curves (100 mW cm^{-2} incident light) of the glass-FTO / TiO_2 / dye/CNT + TiO_2/electrolyte/Pt system: A) CNT copolymer **7.5**; B) N-CNT copolymer **7.6**. Power-voltage curves are also shown: C) CNT copolymer **7.5**; E) N-CNT copolymer **7.6**.

Table **8.4**. Photovoltaic performance of the DSSCs based on glass-FTO/TiO_2/dye/CNT-copolymer + TiO_2 /electrolyte/Pt

Sample	incident light (P_{in}) (mW m^{-2})	η (%)	FF	V_{oc} (Volt)	J (mA cm^{-2})
N-CNT copolymer **7.6**	100	0.37	0.42	0.62	1.4
	10	0.48	0.51	0.55	0.18
CNT copolymer **7.5**	100	1.28	0.61	0.68	3.1
	10	0.51	0.53	0.54	0.18
Dye N719	100	3.9	0.44	0.83	10.7
	10	5.0	0.86	0.74	1.0

The V_{oc} and J_{sc} were found to increase with increasing P_{in} at lower light intensities (from 10 mW cm^{-2} to 100 mW cm^{-2}) in all cases. This dependence of J_{sc} on the incident light power indicates that the photocurrent production is not limited by the diffusion kinetics of I_3^-/ I^- ions. This is due to the rapid regeneration of the photo-oxidized dye molecules. However, in case of N-CNT

copolymer **7.6** and Dye N719 at high P_{in} value (100 mW cm^{-2}) the diffusion of I_3^-/I^- is too slow to efficiently regenerate the oxidized dye molecules resulting in a decrease in the photocurrent. This effect coupled with possible ohmic losses in the TCO support leads to the observed decrease in the fill factor at higher light intensities (100 mW cm^{-2}) [42]. These loss processes have the effect of modulating the power conversion efficiencies of the cells at higher P_{in}.

8.3.3 Organic solar cells

Photovoltaic devices have also been fabricated by blending C_{60} with conducting polymers. Yu *et al*. [43] have developed new conducting polymer composites that contain an electron-donating species and an electron accepting species in a bi-continuous network. These photovoltaic systems were based on the mechanism of photoinduced charge separation. The electron donor phase utilized a soluble poly(phenylene vinylene) (PPV) derivative and poly(2-methoxy-5-(2'-ethylhexyloxy) l,4-phenylvinylene), more commonly known as MEH-PPV. The acceptor phase used one of two soluble forms of C_{60} known as [6,6] PCBM and [5,6] PCBM.

In this study, C_{60} covalently attached to poly(3-hexylthiophene) in a pearl necklace manner on the polymer back bone was utilized (see Scheme **8.1**). In this donor-acceptor-linked molecule, the fullerene acted as an electron acceptor and poly(3-hexylthiophene) as a donor.

A film of poly(3,4-ethylenedioxythiophene):poly(styrenesulfonate) (PEDOT:PSS) solution was spin coated (1500 rpm) onto indium-SnO_2 (ITO), followed by heating for 10 min at 120 ^oC in air. A C_{60}-copolymer:P3HT 1:1 mixture (25 mg mL^{-1} chlorbenzene) solution was spincoated onto PEDOT (acceleration 800 rpm/s, 40 s). The solar cells were fabricated by thermally evaporating and depositing aluminum metal (10^{-6} Torr) of 70 nm thickness on top of the polymer film (see Figure **8.14** for architectural arrangements).

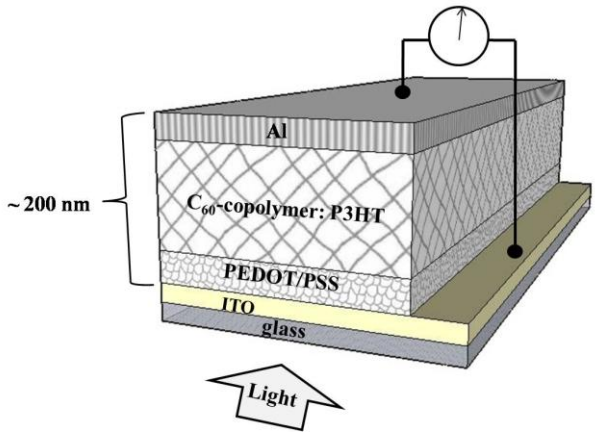

Figure **8.14** Schematic representation of the organic solar cell with the ITO/PEDOT-PSS/P3HT:C_{60}-copolymer/Al device. (Note: the schematic representation is not drawn to scale).

Attempt to get I-V measurements of the devices fabricated using the functionalized CNT-poly(3-hexylthiophene) and the **5.3c (**1000:1 mole ratio) C_{60} copolymer was not successful. However, the devices fabricated using the **5.3a** (10:1 mole ratio) and **5.3b** (500:1 mole ratio) C_{60} copolymer will be discussed below.

Due to low solubility of the **5.3a** in chlorobenzene, the initial attempt to get current voltage measurement was unsuccessful. However a 1:1 mixture of poly(3-hexylthiophene) to **5.3a** in chlorobenzene, gave a better film during spincoating. The **5.3b** C_{60} copolymer spincoated without the addition of poly(3-hexylthiophene).

The efficiencies of the solar cells were much lower than that reported in the literature for [6,6] PCBM devices [44]. For the **5.3a** C_{60} copolymer the efficiency was only 0.001 %; a value much lower than the 2.5 % previously reported for a PDOT/PSS:MDMO-PPV:PCBM system [44]. In addition, the current densities obtained in this study were significantly lower (see Figure **8.14** and Table **8.5**). The open circuit potential was about 0.91 V while the literature reported values of 0.6 V for PDOT:MDMO-PPV:PCBM [45] and 0.8 V for PDOT/PSS:MDMO-PPV:PCBM [44] containing photo cells.

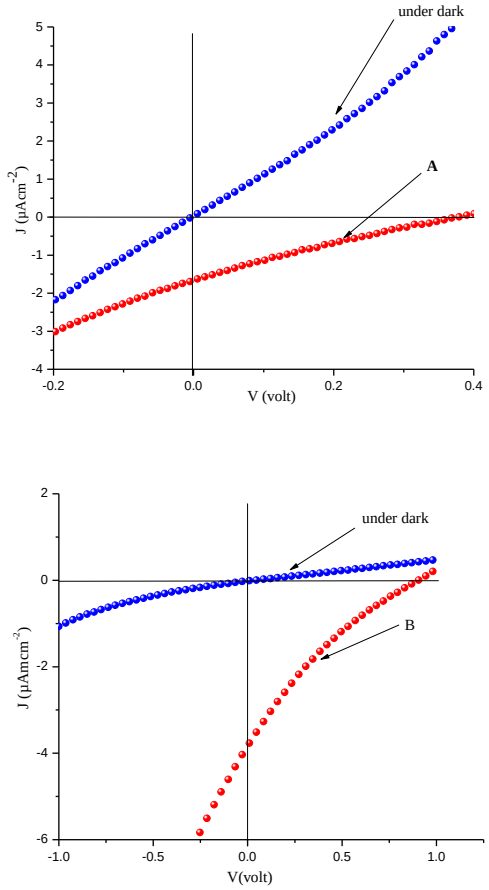

Figure **8.15** Current-voltage curves of organic solar cells based on: a) glass-ITO/PEDOT-PSS/P3HT: **5.3a** (10:1 mole ratio C_{60}-copolymer)/Al; b) glass-ITO/PEDOT-PSS/**5.3b** (500:1mole ratio C_{60}-copolymer) /Al (both under dark conditions and 60 mW cm^{-2} irradiation.)

Table **8.5** Photovoltaic performance of organic solar cell based on glass-ITO/PEDOT-PSS/C_{60}-copolymer /Al.

Sample	V_{oc} (Volt)	J_{cs} (μ Am cm^{-2})	FF (%)	P_{max} (mW cm^{-2})	Efficiency x 10^{-3} η (%)
500:1mole ratio (**5.3b)**	0.372	1.6	23	0.14	0.23
10:1 mole ratio (**5.3a**)(1:1 P3HT)	0.91	3.78	19	0.66	1.1

The source of the lower efficiencies can be related to the relatively low concentration of C_{60} in the composite; in the report using [6,6]PCBM system the C_{60} content in the polymer was about 63 % [44] while in our cell it is about 4 %. Moreover, our synthesized poly(3-hexylthiophene)

has regioregularites in a 60:40 ratio of HT:HH (see Chapter 4 section *4.3.3.1*). Studies have indicated that high regio-irregularitiy contributes to a decrease in π-electron delocalization [46].

8.4 Conclusions

Dye sensitized solar cells (DSSC) were assembled in diverse configurations with varying concentrations of C_{60} in the copolymer; **5.3a** was found to be more efficient than cells made with **5.3c**. Incorporation of a higher concentration of the functionalized C_{60} in the polymer, led to a better charge separation and this prevented charge recombination due to a lower reorganization energy in the electron-transfer reaction. As a result, the photocurrent density (*J*), the open circuit potential (V_{oc}) and the fill factor (FF) increased. As a consequence this effect led to an increase in efficiency (η). In all cases the C_{60}-copolymer showed photovoltaic activity. Prior mixing of TiO_2 nanoparticles with the C_{60}-copolymer before deposition on the dye impregnated TiO_2, further improved the overall efficiency of the solar cells.

Similarly, the polymer attached CNTs (**7.5** and **7.6**) were found to be photovoltaic active. The *I–V* curves under dark conditions revealed that the N-doped CNT copolymer **7.6** was found to be less conducting than the CNT copolymer **7.5**. This was suggested to be due to the incorporation of nitrogen atoms into the CNT structures that contribute additional electrons to the structure. Finally, the organic solar cells were found to be less efficient than that made with the [6,6]PCBM. This might be due to a relatively low concentration (4 %) of C_{60} in the copolymer used when compared to the C_{60} content (63 %) in the [6,6]PCBM. In addition to this, the synthesized poly(3-hexylthiophene) has more regioregularites which also contributes to a decrease to a π-electron delocalization.

8.5 References

1 (a) *Recent Advances in the Chemistry and Physics of Fullerenes and Related Materials*, K. M. Kadish, R. S. Ruoff, Eds., Electrochemical Society, Pennington, NJ, **1997**, Vol. 4. (b) *Organic Materials and Fullerenes*, D. Bloor, Ed., Elsevier, Amsterdam, **1996**.

2 (a) L. W. Tutt, A. Kost, *Nature*, **1992**, 356, 225. (b) A. F. Hebard, M. J. Rosesernsky, R. C. Haddon, D. W. Murphy, S. H. Glarum, T. T. M. Palstra, A. P. Ramirez, A. R. Kortan, *Nature*, **1991**, 350, 600. (c) P.-M. Allemand, K. C. Khemani, A. Koch, F. Wudl, K. Holczer, S. Donovan, G. Gruner, J. D. Thompson, *Science*, **1991**, 253, 301.

3 (a) A. O. Patil, In *Polymeric Materials Encyclopedia*; J. C. Salamone, Ed., CRC Press: Boca Raton, FL, **1996**; Vol. 4, 2603. (b) *The Chemistry of the Fullerenes*, R. Taylor, Ed., World Scientific: Hong Kong, **1995**.

4 Q. Xie, E. Perez-Cordero, L. Echegoyen, *J. Am. Chem. Soc*., **1992**, 114, 3978.

5 (a) C. S. Foote, in *Topics in Current Chemistry; Photophysical and Photochemical Properties of Fullerenes*, J. Matty, (eds), Springer Berlin, **1994**, 169, 347. (b) Y.-P. Sun, in *Molecular and Supermolecular Photochemistry; Photophysics and Photochemistry of Fullerene Materials*, V. Ramamurthy, K. S. Schanze (eds), Marcel Dekker, New York, **1997**, 1, 325. (c) D. M. Guldi, P. V. Kamat, in *Fullerenes, Chemistry, Physics, and Technology*, (K. M. Kadish, R. S. Ruoff (Ed), Wiley, New York, **2000**, 5, 225).

6 (a) H. Imahori, Y. Sakata, *Adv. Mater.*, **1997**, 9, 537. (b) H. Imahori, *Org. Biomol. Chem.*, **2004**, 2, 1425.

7 G. Yu, Y. Gao, J. C. Hummelen, F. Wudl, A. J. Heeger, *Science*, **1995**, 270, 1789.

8 N. S. Sariciftci, L. Smilowitz, A. J. Heeger, F. Wudl, *Science*, **1992**, 258, 1474.

9 R. M. Williams, J. M. Zwier, J. W. Verhoeven, *J. Am. Chem. Soc.*, **1995**, 117, 4093.

10 (a) H. Imahori, S. Cardoso, D. Tatman, S. Lin, L. Noss, G. R. Seely, L. Sereno, C. Silber, T. A. Moore, A. L. Moore, D. Gust, *Photochem. Photobiol.*, **1995**, 62, 1009. (b) D. Gust, T. A. Moore, A. L. Moore, *Res. Chem. Intermed.*, **1997**, 23, 621.

11 D. Kuciauskas, S. Lin, G. R. Seely, A. L. Moore, T. A. Moore, D. Gust, T. Drovetskaya, C. A. Reed, P. D. W. Boyd, *J. Phys. Chem.*, **1996**, 100, 15926.

12 (a) H. Imahori, K. Hagiwara, M. Aoki, T. Akiyama, S. Taniguchi, T. Okada, M. Shirakawa, Y. Sakata, *J. Am. Chem. Soc.,* **1996**, 118, 11771. (b) H. Imahori, K. Hagiwara, T. Akiyama, M. Aoki, S. S. Taniguchi, T. Okada, M. Shirakawa, Y. Sakata, *Chem. Phys. Lett.,* **1996**, 263, 545.

13 D. M. Guldi, G. Torres-Garscia, J. Mattay, *J. Phys. Chem. A,* **1998**, 102, 9679.

14 M. Fujitsuka, O. Ito, T. Yamashiro, Y. Aso, T. Otsubo, *J. Phys. Chem. A,* **2000,** 104, 4876.

15 (a) R. J. Senssion, C. M. Phillips, A. Z. Szarka, W. J. Romanow, A. R. McGhie, J. P. McCauley, A. B. Smith, R. M. Hochstrasser, *J. Phys. Chem.,* **1991**, 95, 6075. (b) N. M. Dimitrijevic, P. V. Kamat, *J. Phys. Chem.,* **1992**, 96, 4811. (c) D. K. Palit, A. V. Sapre, J. P. Mittal, C. N. R. Rao, *Chem. Phys. Lett.,* **1992**, 195, 1.

16 (a) J. W. Arbogast, C. S. Foote, *J. Am. Chem. Soc.,* **1991**, 113, 8886. (b) J. W. Arbogast, C. S. Foote, M. Kao, *J. Am. Chem. Soc.,* **1992**, 114, 2277. (c) S. Nonell, J. W. Arbogast, C. S. Foote, *J. Phys. Chem.,* **1992**, 96, 4169. (d) X. Zhang, C. S. Foote, *J. Am. Chem. Soc.,* **1995**, 117, 4271. (e) X. Zhang, A. Fan, C. S. Foote, *J. Org. Chem.,* **1996**, 61, 5465. (f) R. Bernstein, F. Prat, C. S. Foote, *J. Am. Chem. Soc.,* **1999**, 121, 464.

17 (a) D. M. Guldi, H. Hungerbuhler, K.-D. Asmus, *J. Phys. Chem.,* **1995**, 99, 9380. (b) D. M. Guldi, H. Hungerbuhler, K.-D. Asmus, *J. Phys. Chem.,* **1995**, 99, 13487. (c) D. M. Guldi, H. Hungerbuhler, K.-D. Asmus, *J. Phys. Chem. A,* **1997**, 101, 1783. (d) D. M. Guldi, *J. Phys. Chem. A,* **1997**, 101, 3895. (e) K. G. Thomas, V. Biju, M. V. George, D. M. Guldi, P. V. Kamat, *J. Phys. Chem. A,* **1998**, 102, 5341. (f) D. M. Guldi, H. Hungerbuhler, K. D. Asmus, *J. Phys. Chem. B.,* **1999**, 103, 1444. (g) A. Polese, S. Mondini, A. Bianco, C. Toniolo, G. Scorrano, D. M. Guldi, M. Maggini, *J. Am. Chem. Soc.,* **1999**, 121, 3446.

18 (a) Y. Sasaki, M. Fujitsuka, A. Watanabe, O. Ito, *J. Chem. Soc., Faraday Trans.,* **1997**, *93,* 4275. (b) T. Nojiri, M. M. Alam, H. Konami, A. Watanabe, O. Ito, *J. Phys. Chem. A,* **1997**, 101, 7943. (c) T. Nojiri, A. Watanabe, O. Ito, *J. Phys. Chem. A,* **1998**, 102, 5215. (d) M. M. Alam, M. Sato, A. Watanabe, T. Akasaka, O. Ito, *J. Phys. Chem. A,* **1998**, 102, 7447. (e) C. P. Luo, M. Fujitsuka, C. H. Huang, O. Ito, *J. Phys. Chem. A,* **1998**, *102,* 8716. (f) M. El-Kemary, M. Fujitsuka, O. Ito, *J. Phys. Chem., A,* **1999**, 103, 1329. (g) T. Akasaka, T. Suzuki, Y. Maeda, M. Ara, T. Wakahara, K. Kobayashi, S. Nagase, M. Kako, Y. Nakadaira, M. Fujitsuka, O. Ito, *J. Org. Chem.,* **1999**, 64, 566.

19 H. Ago, K. Pettrish, M. S. P. Shaffer, A. H. Windle, R. H. Friend, *Adv. Mater.*, **1999**, 11 1281.

20 E. Kumakis, G. A. J. Amaratunga, *Appl. Phys. Lett*., **2002**, 80, 112.

21 E. Kumakis, I. Alexandrou, G. A. J. Amaratunga, *J. Appl. Phys*., **2003**, 93 1764.

22 B. J. Landi, R. P. Raffaelle, S. L. Castro, S. G. Bailey, *Prog. Photovolt: Res. Appl.*, **2005**, 13 165.

23 Y. Miyamoto, M. L. Cohen, S. G. Louie, *Solid State Commun*., **1997**, 102, 605.

24 A. J. Frank, N. Kopidakis, J. van de Lagemaat, *Coord. Chem. Rev*., **2004**, 248**,** 1165.

25 T. Renouard, R.-A. Fallahpour, Md. K. Nazeeruddin, R. Humphry-Baker, S. I. Gorelsky, A. B. P. Lever, and M. Grätzel, *Inorg. Chem*., **2002**, 41**,** 367.

26 K. Hara, M. Kurashige, Y. Dan-oh, C. Kasada, A. Shinpo, S. Suga, K. Sayamaa, H. Arakawa, *New J. Chem*., **2003**, 27**,** 783.

27 M. Maggini, G. Scorrano, M. Prato, *J. Am. Chem. Soc*., **1993**, 115, 9798.

28 V. Georgakilas, K. Kordatos, M. Prato, D. M. Guldi, M. Holzinger, A. Hirsch, *J. Am. Chem. Soc.*, **2002**, 124, 760.

29 E. Palomares, J. N. Clifford, S. A. Haque, T. Lutz, J. R. Durrant, *J. Am. Chem. Soc.*, **2003**,125, 475.

30 K. Tennkone, G. R. R. A. Kumara, I. R. M. Kottegoda, V. P. S. Perera, *Chem. Commun.*, **1999**, 1, 15.

31 B. A. Gregg, F. Pichot, S. Ferrere, C. L. Fieldes, *J. Phys. Chem. B*, **2001**, 105, 1422.

32 J.-J. Lagref, M. K. Nazeeruddin, M. Grätzel, *Synth. Met.*, **2003**, 138. 333.

33 M. K. Lim, S.-R. Jang, R. Vittal, J. Lee, K.-J. Kim, *J. Photochem. Photobio. A, Chem.* **2007**, 190, 128.

34 M. K. Nazeeruddin, R. Humphry-Baker, P. Liska, M. Grätzel, *J. Phys. Chem. B*, **2003**, 107 , 8981.

35 S. Yanagida, G. K. R. Senadeera, K. Nakamura, T. Kitamura, Y. Wada, *J. Photochem. Photobiol. A, Chem*, 2004, **166**, 75-80

36 M. K. Nazeeruddin, A. Kay, I. Rodicio, R. Humphry-Baker, E. Müller, P. Liska, N. Vlachopoulos, M. Grätzel, *J. Am. Chem. Soc.*, **1993**, 115, 6388.

37 (a) N. S. Sariciftci, *Prog. Quantum Electro.* **1995**, 19, 131. (b) N. S. Sariciftci, A. J. Heeger, In *Handbook of Organic Conductive Molecules and Polymers*; H. S. Nalwa, Ed.; Wiley: New York, **1996**.

38 M. K. Nazeruddin, A. Kay, I. Rodicio, R. Humphry-Baker, M. Grätzel, *J. Am. Chem. Soc*., **1993**, 115, 6382.

39 B. J. Landi, R. P. Raffaelle, S. L. Castro, S. G. Bailey, *Prog. Photovolt: Res. Appl.,* **2005**, 13, 165.

40 A. F. Nogueira, B. S. Lomba, M. A. Soto-Oviedo, C. R. D. Correia, P. Corio, C. A. Furtado, I. A. Hummelgen, *J. Phys. Chem. C,* **2007**, 111, 18431.

41 Y. Huang, J. Gao, R. Liu, *Synth. Met*., **2000**, 113, 251.

42 (a) F. S. Freitas, J. N. de Freitas, B. I. Ito, M.-A. De Paoli, A. F. Nogueira, *Applied Materials and interface*, **2009**, 1, 2870. (b) H. Kim, G. P. Kushto, C. B. Arnold, Z. H. Kafafi, A. Piqué , *Appl. Phys. Lett.*, **2004**, 85, 464.

43 (a) I. Yoo, M. Lee, C. Lee, D.-W. Kim, I. S. Moon, D.-H. Hwang, *Synth. Met.*, **2005**, 153, 97. (b) G. Yu, A. J. Heeger, *J. Appl. Phys.*, **1995**, 78, 4510.

44 S. E. Shaheen, C. J. Brabec, N. S. Sariciftci, *Appl. Phys. Lett.*, **2001**, 78, 841.

45 T. Fromherz, F. Padinger, D. Gebeyehu, C. Brabec, J. C. Hummelen, N. S. Sariciftci, *Sol. Energ. Mater. Sol. Cells*, **2000**, 63, 61.

46 M. Leclerc, F. M. Diaz, G. Wegner, *Makromol. Chem*., **1989**, 190, 3105.

Chapter 9

9.1 Conclusions and future work

9.1.1 Conclusions

Addition and reduction reactions are among the most important reactions for the functionalization of C_{60} and carbon nanotubes. In this thesis we have explored cycloaddition reactions to functionalize both C_{60} and carbon nanotubes. The products were further copolymerized with appropriate monomers and in most cases used to make photovoltaic devices.

In chapter 3 and 4, C_{60}-cyclopentadiene was synthesized by a Diels-Alder reaction between C_{60} and cyclopentadiene. The functionalized C_{60} was further copolymerized either with norbornene or *N*-(cycloheptyl)-*exo*-norbornene-5,6-dicarboximide using ROMP in the presence of the Grubbs second-generation catalyst. Various C_{60}/monomer ratios were used. However the *N*-(cycloheptyl)-*exo*-norbornene-5,6-dicarboximide was found to give more soluble polymers than those produced from the norbornene. Spectroscopic evaluation revealed that incorporation of the fullerene into the polymers had occurred and that the relative amount of C_{60} affected the polymer thermal properties by increasing both the decomposition and the glass transition temperatures, relative to the pure polynorbornenes.

In chapter 5, functionalization of C_{60} was achieved by using the Prato's reagent. The structure of the two C_{60} derivatives (**5.2** and **5.3**) were confirmed by mass spectrometric (*m/z* 860 [M+1] at 2.6 %) and UV-visible spectral analysis. In addition, the overall yield was significantly improved when compared to literature reports, by increasing the reaction time to five days. Furthermore, covalent attachment either with thiophene or 3-hexylthiophene in varying ratios was accomplished by a $FeCl_3$ oxidative polymerization reaction. Incorporation of C_{60} derivatives into the thiophene backbone was confirmed by UV-visible and FT-IR spectra. Finally, the copolymers were also characterized by ^1H NMR spectroscopy and TGA.

In chapter 6, nitrogen-doped carbon nanotubes (N-CNTs) **6.3** were also synthesized by the floating catalyst methodology using ferrocene as catalyst, pyridine as a source of nitrogen and

toluene as the carbon source. Undoped CNTs **6.1** was synthesized by the decomposition of acetylene. The doping of nitrogen into carbon nanotubes were confirmed by elemental analysis. Functionalization of the N-doped **6.3** and undoped carbon nanotubes **6.1** was achieved by using azomethine ylides that were generated *in situ* by decarboxylation of immonium salts derived from thermal condensation of *N*-methylglycine and 5-norbornene-2-carboxaldehyde. Polymerization from the side wall of functionalized carbon nanotubes (**6.2** and **6.4**) with bicyclo[2.2.1]hept-2-ene **6.c** as a monomer was then possible using the Grubb's second generation catalyst. After the polymerization reactions, TEM images showed that the polymer-attached carbon nanotubes (**6.5** and **6.6**) were found to have enlarged diameters relative to the pristine CNTs (**6.1** and **6.3**). In subsequent NMR studies the N-doped CNTs/polymer was found to have more *trans* isomer than the undoped CNT/polymer material. Finally, the glass transition (Tg) temperatures were found to have decreased by the incorporation of carbon nanotubes.

In chapter 7, different organic functional groups were attached to the side walls of carbon nanotubes using the same methodology as that used in chapters 5 and 6. A reactive intermediate, that was generated *in situ* by decarboxylation of immonium salts derived from thermal condensation of N-methylglycine **7.a** and 2-thiophenecarboxaldehyde **7.b** gave the products. The functionalized carbon nanotubes (**7.2** and **7.4**) together with either thiophene **7.c** or 3-hexylthiophene **7.d** were then used in copolymerization reactions which were initiated by $FeCl_3$. TEM images clearly indicated that the polymers were attached to the side wall of the carbon nanotubes. NMR spectroscopy revealed that **7.5** and **7.6** were more regioregular than that of pure poly(3-hexylthiophene) **7.9**. The thermal properties of the synthesized copolymers were also examined. Copolymers **7.5**, **7.6** and poly(3-hexylthiophene) **7.9** all revealed single Tg temperatures. Furthermore, the synthesised CNTs and the CNT/polymer were characterised by elemental analysis, thermogravimentric analysis (TGA), as well as Raman and FT-IR, UV visible and photoluminescence spectroscopy.

Potential applications of the synthesized C_{60}-thiophene copolymer and the CNT-thiophene copolymer were also studied.

Dye sensitized solar cells (DSSC) were assembled in diverse configurations with varying concentrations of C_{60} in copolymers; when the mixture contained larger concentration of C_{60} (**5.3a**) the DSSC was more efficient than when low concentrations of C_{60} were used (**5.3c**). Incorporation of more functionalized C_{60} into the polymer, led to a better charge separation as this prevented charge recombination due to a lower reorganization energy in the electron-transfer reaction. As a result, the photocurrent density (J_{SC}), the open circuit potential (V_{OC}) and the fill factor (FF) increased. As a consequence this effect led to an increase in efficiency (η) that reached 0.34 % for the configuration: glass–FTO/TiO_2/C_{60}-copolymer + TiO_2/electrolyte/Pt layers. Furthermore, prior mixing of the TiO_2 nanoparticles with the C_{60}-copolymer, before it was deposited on the dye impregnated TiO_2, improved the overall efficiency of the solar cells. Similarly, the polymer-attached CNTs (**7.5** and **7.6**) were found to be photovoltaic active. The polymer-attached N-doped CNTs **7.6** performed better than polymer attached undoped CNTs **7.5**. However, the *I–V* curves under dark conditions revealed that the N-doped CNT copolymer **7.6** was found to be less of a semiconductor than the CNT copolymer **7.6**. This is probably due to the incorporation of nitrogen atoms into the CNT structures that contributes additional electrons to the structure. Finally, the organic solar cells were found to be less efficient than [6,6]PCBM. This might be due to a relatively low concentration of C_{60} in the copolymers used.

9.1.2 Future work and recommendations

9.1.2.1 Functionalization of carbonaceous materials

In this study, functionalization of carbonaceous materials was achieved using a well known procedure, based on the Prato reagent. In the particular of CNTs, the Prato reaction has been demonstrated to be an efficient method for functionalization of CNTs. The degree of functionalization on the side wall of CNTs has been estimated from the TGA profile. In this project however, we noted that not all the CNTs were equally functionalized; some CNTs were only partially functionalized. This had an effect during the polymerization reactions leading to

CNTs that were either not covered or only partially covered by polymer. Therefore, controlling the degree of functionalization is a crucial step in making the composites. Inhomogeneous reactivity and nucleation effects had thus occurred during the polymerization reaction. This could be due to a combination of the high reactivity of the reactants and poor dispersibility of the functionalized CNTs in a solvent leading to CNTs not uniformly covered by polymer. Control of the thickness of the polymer on the side walls needs to investigated. Thus it is recommended that control of the amount of functional groups on the side walls of the CNTs, and dispersibility after functionalization be investigated in detailed. This could be studied by varying the degree of CNT sidewall coverage and the use of shorter length CNTs.

9.1.2.2 Photovoltaic Device applications

In this study, the potential application of the synthesized C_{60}-thiophene copolymers and the CNT-thiophene copolymers were explored in DSSC and organic solar cells. As a result, the photocurrent density (J_{SC}), the open circuit potential (V_{OC}) and efficiency (η) of the cell were measured on the synthesized materials to determine if the synthesized materials were photovoltaically active. Improving the efficiency of the devices is still possible by further manipulating of the existing molecular structures.

The DSSC is regarded as the next generation photovoltaic device due to its attractive features of high power conversion efficiency (>10 %) and low production cost [1-6]. Among the photosensitizers that have been investigated and used in DSSC, Ru(II)-based complexes are the most efficient. Since this type of photosensitizer has an intense absorption in the visible region, as well as a strong adsorption onto the semiconductor surface and efficient electron injection into the conduction band of the semiconductor. Moreover, complexes of Ru(II) with 2,2'-bipyridine ligands have long-lived metal-to-ligand-charge-transfer (MLCT) excited states. Their potential in supramolecular architectures has been widely exploited for future photoinduced energy- and electron-transfer processes [7, 8]. In this regard, Ru(II) complexes have a marked reducing character that makes them ideal partners for C_{60} and CNT oxidants in the construction of donor-acceptor arrays for photoinduced electron transfer devices. For instance, the use of a covalently

linked electron acceptor, either modified C_{60} or CNTs, which bonded to the Ru(II)-based dye could lead to a new class of supramolecular molecules. A photocell made from such materials could be expected to give enhanced activity. It is recommended that the electronic properties and utilization of Ru(II)-based dyes covalently linked to carbonaceouses materials in photovoltaic devices be explored in detailed.

9.2 Reference

1. M. K. Nazeerudin, F. De Angetis, S. Fantacci, A. Selloni, G. Viscardi, P. Liska, S. Ito, T. Bessho, M. Gratzel, *J. Am. Chem. Soc.*, **2005**, 127, 16835.
2. M. Gratzel, *Chem. Lett.*, **2005,** 34, 8.
3. M. Gratzel, *Nature*, **2001**, 414, 338.
4. M. Wang, X. R. Xiano, X. W. Zhou, X. P. Li, Y. Lin, *Sol. Energy Mater. Sol. Cells*, **2007**, 91, 785.
5. D. B. Kuang, C. Klen, H. J. Snaith, J. E. Moser, R. Humphry-Baker, P. Campte, S. M. Zakeeruddin, M. Gratzel, *Nano Lett*., **2006**, 6, 769.
6. M. K. Nazeerudin, A. Kay, I. Rodicio, R. Humphry-Baker, E. Muller, P. Liska, N. Viachopoulos, M. Gratzel, *J. Am. Chem. Soc.*, **1993,** 115, 6382.
7. A. Juris, V. Balzani, F. Barigelletti, S. Campagna, P. Belser and A. von Zelewsky, *Coord. Chem. Rev*., **1988**, 84, 85.
8. F. Barigelletti, L. Flamigni, *Chem. Soc. Rev*., **2000**, 29, 1.